D 2023

U.PORTO

FEUP FACULDADE DE ENGENHARIA
UNIVERSIDADE DO PORTO

NETWORK-SECURE PARTICIPATION OF AGGREGATORS OF MULTI-ENERGY SYSTEMS IN MULTI-ENERGY MARKETS

ANTÓNIO COELHO

THESIS SUBMITTED TO THE FACULTY OF ENGINEERING OF UNIVERSITY OF PORTO
IN PARTIAL FULFILLMENT OF THE REQUIREMENTS FOR THE DEGREE OF
DOCTOR OF PHILOSOPHY IN SUSTAINABLE ENERGY SYSTEMS

FEUP FACULDADE DE ENGENHARIA
UNIVERSIDADE DO PORTO

NETWORK-SECURE PARTICIPATION OF AGGREGATORS OF MULTI-ENERGY SYSTEMS IN MULTI-ENERGY MARKETS

ANTÓNIO COELHO

ACADEMIC DISSERTATION IN SUSTAINABLE ENERGY SYSTEMS

Dissertation submitted to the Faculty of Engineering of University of Porto in partial fulfillment of the requirements for the degree of Doctor of Philosophy.

Faculty of Engineering,
University of Porto

Porto, January 2023

Supervisor

Filipe Joel Soares, Ph.D.,
Senior researcher
Center of Power and Energy Systems
INESC TEC
Porto, Portugal

Co-supervisor João Abel Peças Lopes, Ph.D.,
Full Professor
Faculty of Engineering
University of Porto
Porto, Portugal

Co-supervisor José Pedro Barreira Iria, Ph.D.,
Lecturer and researcher
College of Engineering, Computing & Cybernetics
Australian National University
Canberra, Australia

This PhD thesis was supported by Fundação para a Ciência e a Tecnologia (Portuguese Foundation for Science and Technology) through the grant PD/BD/142811/2018 and by the Centre for Power and Energy Systems of INESC TEC (https://www.inesctec.pt/).

Fundação
para a Ciência
e a Tecnologia

This PhD thesis was developed under the framework of the MIT Portugal program (https://www.mitportugal.org/).

This PhD thesis was also supported by the ATTEST project (https://attest-project.eu/). The ATTEST project was funded by the European Union's Horizon 2020 research and innovation programme under grant agreement No 864298.

“See the animal in his cage that you built
Are you sure what side you're on?
Better not look him too closely in the eye
Are you sure what side of the glass you are on?
See the safety of the life you have built
Everything where it belongs
Feel the hollowness inside of your heart
And it's all
Right where it belongs

What if everything around you
Isn't quite as it seems?
What if all the world you think you know
Is an elaborate dream?
And if you look at your reflection
Is it all you want it to be?
What if you could look right through the cracks?
Would you find yourself
Find yourself afraid to see?

What if all the world's inside of your head
Just creations of your own?
Your devils and your gods
All the living and the dead
And you're really all alone?
You can live in this illusion
You can choose to believe
You keep looking but you can't find the woods
While you're hiding in the trees

What if everything around you
Isn't quite as it seems?
What if all the world you used to know
Is an elaborate dream?
And if you look at your reflection
Is it all you want it to be?
What if you could look right through the cracks?
Would you find yourself
Find yourself afraid to see?”

Trent Reznor

Right Where It Belongs a song from *Nine Inch Nails*

Acknowledgment

The work carried out in this Ph.D. thesis was done over several years. A lot of things happened, and a lot of things changed during this time. I was on a lot of adventures, met a lot of people, and made several friends. All became part of this intellectual challenge and emotional rollercoaster. So here, I would like to give a note of appreciation and acknowledge the role of my family, friends, and colleagues, that were part of this journey and made it possible to finish this work.

First of all, I would like to thank my supervisor Filipe Joel Soares and co-supervisors Professor João Peças Lopes and José Iria, for accepting to supervise my thesis. The discussions we had and the suggestions they gave allowed me to improve and enhance the quality of my work. Their guidance was crucial to finish this thesis.

A special thanks to Filipe Joel Soares, as he was the one who gave the first ideas to develop this work and was the main guidance during this journey. He always kept a positive attitude and support that helped me get through the hardest times. He always trusted me and my work and always gave me the flexibility to work independently and in my own rhythm.

Another special thanks to José Iria, as he was the one who worked more closely with me during the last few years. His knowledge, vision, and hard-working and detailed-oriented skills helped me develop a work that would not be possible without him. His passion for scientific research and work excellency became an inspiration. I learned a lot from him: mathematical optimization topics, power system topics, how to write quality papers, how to write well-organized mathematical formulations, and more. All this contributed to a much better work and made me a better scientific researcher overall. Although he was in a much different time zone (Australia), he always made the effort to meet with me to clarify my doubts.

I thank Miguel Heleno, for allowing me to stay at the Lawrence Berkeley National Laboratory which became one of the greatest adventures of my life. During my stay, I was able to learn a lot from him, especially in the energy area. He was also very helpful and facilitated my integration to the maximum, which I will never forget. I also would like to thank all my other colleagues from there, which helped me grow up as a person and learn a lot about the world. They also made this brief stay much more fun, interesting, and inspiring than what I was envisioning.

I would also like to thank my colleagues from INESC TEC that helped me improve the quality of this thesis by clarifying some of my doubts and giving me helpful insights. Moreover, they all allowed for the creation of an excellent environment facilitating the day-to-day work. All those activities like the fun and exciting dinners at Almada or Paraíso, the epic moments at Portinho or Rendevouz, the beginning-of-summer paintball-barbecue, and the liberating "sextas-feiras loucas" were very much appreciated and will forever be treasured. Also, a special thanks to Paula Castro who also contributed to the creation of a good work environment and helped me with the more bureaucratic stuff.

Family and friends are one of the essential things a person can have. Without their support, directly or indirectly, this work could never be done.

I thank my parents, for their support and I acknowledge the sacrifices they made to give me a proper education and a good living. I also thank my sister for her support, especially during the years we lived together, for helping me take care of the day-to-day things. Without them, I would not be the person I am today and would not be able to have done any of this work. I also thank all my uncles and cousins for their care and affection.

I thank all my friends, for their support in helping me live life as best as I can. Without their company, life would not have the same flavor. They make me feel good, have fun, challenge myself, see the world from another perspective, and make me more cultured, allowing me to grow and be a better human being. To all those who accompanied me in travels, festivals, concerts, cinema sessions, Virtudes, night outs, dinners, sports events, and many other entertaining activities, a very big thank you.

Sports are a big part of my life and they helped me grow up as a person, showing me the benefits of hard work, perseverance, and trusting “the process”. During these years I was able to integrate different sports groups. I thank my teammates and coaches from the swimming team Clube Natação de Valongo. This has definitely been a great source of joy and well-being during the most critical moments of this thesis. I thank the basketball team Matosinhos Basket for allowing me to join their team and participate in their basketball league. I thank Gonçalo Cardoso, and the rest of my teammates, for allowing me to play in the indoor soccer tournament during my stay at Berkeley. This really facilitated my integration there. And finally, I thank my padel partners for helping me get into this sport, which has been providing me with so much fun.

So, to finalize, thank you all so much!

Porto, 24th January 2023

António Coelho

António Coelho

Abstract

The replacement of fossil fuel power plants by variable renewable energy sources is reducing the flexibility of energy systems, which puts at risk its security. Exploiting the flexibility of distributed multi-energy resources through aggregators presents a solution for this problem.

Under this scope, this thesis presents a set of optimization tools for aggregators to use to participate in multi-energy markets. Each tool considers a different market stage (i.e. day-ahead or real-time):

- **Network-secure bidding optimization framework –** this tool assists aggregators of multi-energy systems in calculating day-ahead electricity (energy and reserve), natural gas, green hydrogen, and carbon bids, considering multi-energy network constraints. This strategy is a distributed approach based on the alternating direction method of multipliers, where the aggregator collaborates with the operators of electricity, gas, and heat networks to calculate network-secure bids.

- **Real-time network-secure optimization framework –** a new hierarchical model predictive control framework to assist multi-energy aggregators in the network-secure delivery of multi-energy services traded in electricity, natural gas, green hydrogen, and carbon markets. This framework complements the network-secure bidding optimization framework – it closes the cycle of aggregators' participation in multi-energy markets, i.e. day-ahead bidding and real-time activation of flexibility services. This new model predictive control framework uses the alternating direction method of multipliers on a rolling horizon to negotiate the network-secure delivery of multi-energy services between aggregators and distribution system operators of electricity, gas, and heat networks.

At the end of this thesis, an economic and environmental analysis of the aggregator's performance under different decarbonization policies and future low-carbon scenarios is presented.

Resumo

A substituição de centrais de fontes não renováveis (combustíveis fósseis) por fontes de energia renováveis tem vindo a reduzir a flexibilidade dos sistemas de energia, pondo em risco a sua segurança. A exploração da flexibilidade de recursos distribuídos multi-energia através de agregadores é considerada como uma das potenciais soluções para este problema.

Neste contexto, esta tese apresenta um conjunto de ferramentas de otimização para agregadores de forma a participarem em mercados multi-energia. Cada ferramenta considera um estágio de mercado diferente (i.e., dia seguinte ou tempo real):

- **Esquema de otimização de ofertas de mercado seguro para as redes** – esta ferramenta ajuda os agregadores de sistemas multi-energia a calcular ofertas de mercado para o dia seguinte nos mercados de eletricidade (energia e reservas), gás natural, hidrogénio verde e carbono, considerando as restrições das redes de energia. Esta estratégia consiste numa abordagem distribuída baseada no método *alternating direction method of multipliers*, onde o agregador colabora com os operadores das redes de distribuição de eletricidade, gás e calor para calcular ofertas de mercado seguras do ponto de vista técnico das redes de energia.

- **Esquema de otimização em tempo real seguro para as redes** – é um novo modelo de controlo preditivo hierárquico que pretende auxiliar os agregadores multi-energia na entrega de serviços negociados previamente nos mercados de eletricidade, gás natural, hidrogénio verde e carbono de forma segura do ponto de vista técnico das redes. Este esquema complementa o esquema de otimização de ofertas de mercado anterior – fecha o ciclo de participação dos agregadores em mercados multi-energia, ou seja, ofertas para o dia seguinte e ativação em tempo real de serviços de flexibilidade. Este novo modelo de controlo preditivo usa o método *alternating direction method of multipliers* num horizonte contínuo, de forma a negociar entre agregadores e os operadores das redes de distribuição de eletricidade, gás e calor a entrega segura de serviços.

No final da tese, é apresentada uma análise económica e ambiental do desempenho do agregador sob diferentes políticas de descarbonização e cenários futuros de baixo carbono.

Table of contents

List of figures

List of tables

List of Acronyms and Abbreviations

AC	Air conditioner
ADMM	Alternating direction method of multipliers
AGC	Automatic generation control
AS	Ancillary services
CHP	Combined heat and power
DA	Day-ahead
DER	Distributed energy resource
DMER	Distributed multi-energy system resources
DR	Demand response
DSO	Distribution system operator
EMS	Energy management system
ENTSO-E	European Association for the Cooperation of Transmission System Operators for Electricity
ENTSO-G	European Network for Transmission System Operators for Gas
ESS	Energy storage system
ETS	Emission trading system
EU	European Union
EV	Electric vehicle
FC	Fuel cell
FCAS	Frequency containment ancillary services
GB	Gas boiler
GHG	Greenhouse gas
GO	Guarantee of origin
HHV	Higher heating value
HP	Heat pump
HSS	Hydrogen storage system
HV	High voltage
ICEV	Internal combustion engine vehicle
ISO	Independent system operator
LCS	Low-carbon scenario
LNG	Liquefied natural gas
LV	Low voltage
MARI	Manually Activated Reserves Initiative
MES	Multi-energy system
MIBEL	Iberian Electricity Market
MIBGAS	Iberian Gas Market
MO	Market operator
MPC	Model predictive control
M-NF	Multi-energy and network-free strategy
M-NS	Multi-energy and network-secure strategy
NF	Network-free

NS	Network-secure
NF-NF	Day-ahead network-free and real-time network-free strategy
NF-NS	Day-ahead network-free and real-time network-secure strategy
NS-NF	Day-ahead network-secure and real-time network-free strategy
NS-NS	Day-ahead network-secure and real-time network-secure strategy
PICASSO	Platform for the International Coordination of Automated Frequency Restoration and Stable System Operation
PV	Photovoltaic
P2G	Electrolyzer
RES	Renewable energy source
RT	Real-time
RTO	Regional transmission organization
SOC	State-of-charge
S-NF	Single-energy and network-free strategy
TCL	Thermostatically controlled loads
TERRE	Trans European Replacement Reserves Exchange
TSO	Transmission system operator
UK	United Kingdom
US	United States
VPP	Virtual power plant
VTP	Virtual trading point
WI	Wobbe index

Nomenclature

Indices and sets

$d \in \{E, G, H, H2\}$	Energy vectors
$a \in \{S, R\}$	Supply and return networks
$j \in J$	Clients
$J_n \subset J$	Clients at bus n
k	ADMM iteration
$m, n, i, j \in N^E, N^G, N^H$	Buses/nodes of electricity, gas, and heat networks
$(m, n), (i, j) \in B^E, B^G, B^H$	Lines/pipelines from bus m to bus n for electricity, gas, and heat networks
$N^{NG} \subset N^G$	Gas nodes with natural gas injection
$N^{GL} \subset N^G$	Gas nodes with natural gas loads
$N^{H2} \subset N^G$	Gas nodes with hydrogen resources
$s \in \{En, U, D\}$	Delivery scenarios per energy vector
$t, y \in T$	Time intervals
$v \in \{E, G, H2, H2O, O2, C\}$	Markets/products

Superscripts

Abs	Absolute tolerance
Amb	Ambient temperature of pipelines' surroundings
AGC	Automatic generation control
B	Electricity reserve band bid
C	Carbon market
CFA	Free allowances of carbon market
CHP	Combined heat and power
CO_2	Carbon dioxide
D	Downward reserve
DA	Day-ahead
DH	District heating
$Dual$	Dual residual
E	Electricity
EH	Heat pump
En	Energy
End	End of pipeline
F	Power flow
G	Gas
GL	Natural gas loads
GO	Guarantees of origin
H	Heat
HLG	Heat loads and generators
HV	Hydrogen vehicles
H_2	Hydrogen
H_2O	Water

IL	Inflexible load
In	Input flow
Mix	Gas mixture
Net	Network injection
NG	Natural gas injection
O	Outdoor temperature
Ot	Outlet temperature
Out	Output flow
$O2$	Oxygen
$Primal$	Primal residual
PV	Photovoltaic system
$P2G$	Power-to-gas (or electrolyzers)
R	Return temperature
RT	Real-time
S	Supply temperature
St	Standard conditions of temperature and pressure
$Start$	Start of pipeline
Sto	Energy storage system
U	Upward reserve
$+, -$	Charging, discharging of electric storage systems or positive, negative
$\bar{\ }, \underline{\ }$	Maximum, minimum
^	DSOs replicated values

Parameters

c	Conversion factors
CP	Water specific heat (J/kg.°C)
$CSCF$	Cross-sector correction factor
d	Diameter of pipeline (mm)
e	Efficiency factor
FA	Free allowances (tCO_2)
h	Heat transfer coefficient (W/°C.m)
HAL	Historical activity level
HBM	Heat benchmark
k	Coefficient of pressure loss in water pipelines
K	Resistance pipeline coefficient
L	Length of pipeline (m)
LHV	Low heating value (kWh/kg)
NCL	Carbon leakage factor
r	Resistance of power lines (p.u.)
R	Resistance of thermal buildings (°C/kW)
SB	Base power (kVA)
x	Reactance of power lines (p.u.)
Δt	Length of the time interval t (h)
β	Thermal constant
η	Efficiency/coefficient of performance
γ	Hydrogen storage energy dissipation rate (%)

λ	Price (€/kWh, €/kW, €/tCO_2, €/L or €/kg)
μ	Parameter of response of CHPs
ϕ	Ratio of secondary reserves activation
ρ	Penalty of the augmented Lagrangian (€/kW^2)
τ	Residual
ϑ	Heat gains and losses not modeled explicitly (℃)
α	Parameter that converts MWh of natural gas to tonnes of CO_2
μ	Parameter of response of CHPs
ϵ	Residual tolerance
Variables	
A	Allowances (tCO_2)
b	Binary variable
D	Downward band (kW)
E	Energy bid (kWh)
HHV	Higher heating value (MJ/m^3)
ℓ	Square of the current magnitude (p.u.)
m	Mass flow of pipelines (kg/s)
mq	Mass flows of heat loads and generators (kg/s)
p	Pressure (gas: bar, heat: Pa)
P	Power (kW)
q	Gas flows (m^3/h)
Q	Reactive power (p.u.)
S	Specific gas gravity
SOC	State-of-charge (kWh)
U	Upward band (kW)
v	Square of the voltage magnitude (p.u.)
w	Hydrogen fraction
WI	Wobbe index (MJ/m^3)
X	Internal variables of the aggregator problem
Y	Internal variables of the energy DSO problem
φ	Auxiliary binary variable
π	Dual variables of the augmented Lagrangian (€/kW)
θ	Temperature (gas network: °K, other: ℃)

Chapter 1
Introduction

1.1. Motivation for the Thesis

Around the world, there is an increasing awareness of the environmental impacts of human activity. These impacts are caused by overpopulation, deforestation, burning fossil fuels, and deforestation. This ended up triggering climate change, which is being fought worldwide through different policies, like the Paris Agreement. The Paris Agreement is an international treaty signed in 2016 with, currently, 194 parties involved. With this treaty, countries worldwide have agreed on making efforts to keep the rising of global temperature below 2°C.

To achieve this goal, the European Union (EU) has set several ambitious goals:

- decrease CO_2 emissions by at least 55% by 2030 [1];
- being the first climate-neutral continent by 2050.

One of the ways to decrease CO_2 emissions is through decarbonization policies of energy systems.

Decarbonization policies

The decarbonization of the energy system is seen as the first step to achieve the EU's climate goals. The measures adopted by the EU are mainly focused on energy and climate actions and include the integration of renewable energy sources (RES), energy efficiency, energy systems integration, and the implementation of an EU emission trading system (ETS), generally known as the EU carbon market.

The introduction of the Renewable Energy Directive (2009/28/EC) [2] in 2009, allowed RES to have priority access to the electricity networks. Since then, the deployment of RES has increased over the years, reaching more than 22% in 2020. In 2018 [3] and 2021 [4], the Directive was revised, and new targets were proposed that included rules to:

- ensure the uptake of renewables in the transport sector;
- ensure the uptake of renewables in heating and cooling systems;

- definition of common principles and rules for renewables support schemes;
- the rights to produce and consume renewable energy and to establish renewable energy communities.

With the new revisions, the Directive also sets a new target of 45% for the amount of renewable energy in the total energy consumption by 2030. Figure 1.1 presents the evolution of renewable energy targets imposed by the EU over the years. The directives focus on various types of RES including solar energy, onshore and offshore wind energy, bioenergy, and hydropower. They also introduce specific provisions to speed up the extension of renewables in heating and cooling [3].

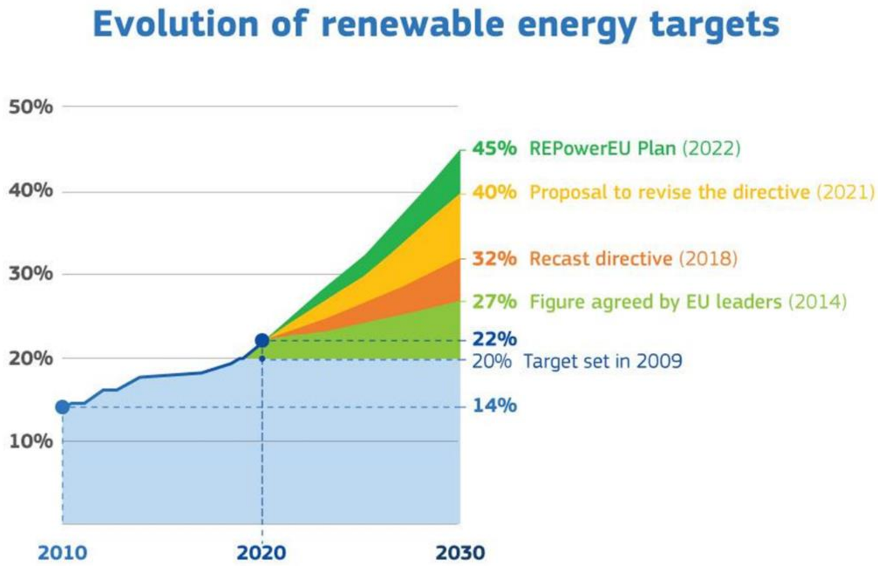

Figure 1.1 – Evolution of renewable energy targets set by the European Union (from [5]).

The EU also promotes energy efficiency as an overall principle of the EU energy policy. The newest policies set new targets like an additional reduction of energy consumption of 9% by 2030, compared with 2020 values [6]. With the increasing pressure of the EU to reach energy independence, this target was increased to 13%, as per the new REPowerEU plan [7] presented in 2022. Other measures of energy efficiency pass by the reduction of 1.7% of the annual energy consumption that englobe a wide range of public sectors including buildings, transport, water, and street lighting.

The integration of energy systems (also known as multi-energy systems (MES)[1]) is also one of the focuses of energy policies from the EU [8]. Nowadays, each energy vector (i.e. electricity, gas, heat, water, etc.) is operated and planned independently. Market rules are also very specific to each different sector. The integration of energy systems proposes a global coordinated operation and planning of several energy vectors, across multiple energy carriers, infrastructures, and consumption sectors (Figure 1.2). This means that different energy carriers

[1] In this thesis, an energy vector refers to a single system (i.e. or electricity, or gas, or heat, or water, etc); an energy system refers to a system with several energy vectors with or without integration; multi-energy systems or integration of energy systems refer to a system with several energy vectors integrated (i.e. connected and optimized all together).

(i.e. electricity, gas, heat, cold, liquid fuels, etc.) are linked among each other and with end-use sectors, like buildings, industry, or transport. Linking sectors allows for global optimization of the entire energy system improving the cost-effective decarbonization process of energy systems. The pillars for the integrated energy systems identified are a more circular energy system, with "energy-efficiency-first" at its core; accelerating the electrification of energy demand, buildings on a largely renewable-based power system; promoting renewable and low-carbon fuels, including hydrogen; making energy markets fit for decarbonization and distributed resources; a more integrated energy infrastructure; and finally, a digitalized energy system.

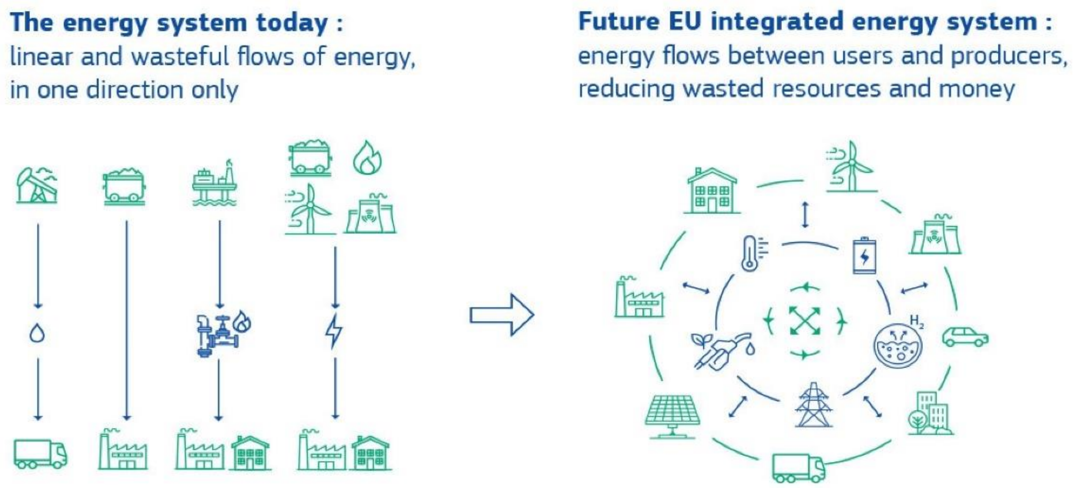

Figure 1.2 - Integration of energy systems (adapted from [10]).

Another important step in the decarbonization process of the European Union was the implementation of the EU ETS. The EU ETS is seen as "the cornerstone of the Union's climate policy" and it is the main instrument to achieve the emissions reduction target [9]. Set up in 2005, the EU ETS is the world's first international emissions trading system. The sectors covered by the EU ETS must reduce their emissions by 43% compared to 2005 levels. This market has been through several phases: Phase 1 (2005-2007), Phase 2 (2008-2012), and Phase 3 (2013-2020). It is currently in its 4th phase which, compared to the previous phases, will be more demanding to participants as they will have more pressure to reduce emissions.

The EU also sets new rules and legislation for markets and consumers [11] focusing on electricity and gas market designs (considering the decarbonization of the gas sector through hydrogen), protecting energy consumers, energy communities, capacity mechanisms, and energy taxation. Another topic is related with research and technology [12]. Within it, the EU sets new directives focusing on the integration of energy storage systems (ESSs), the digitalization of the energy sector, flexibility markets, fusion energy, smart cities, and competitiveness over clean energy.

Impact of decarbonization policies on energy systems

Following the several measures being implemented, the decarbonization of energy systems impacted their functioning and operation. Electricity, gas, or heat systems are some of the cases that were affected by these changes.

The electricity system started to be decarbonized several years ago through the integration of RES, such as wind or photovoltaic (PV) farms. This changed the traditional organization of power systems, which was based on large central generation units connected to consumers through high voltage transmission networks. These generation units were installed with overcapacity to ensure the security of supply. RES are now integrated into any part of the network, from high voltage transmission networks to low voltage distribution networks and their uncertainty is spread through all voltage levels. This way, the organization and coordination of the electricity networks are much more complex and require more advanced control tools to operate and plan the networks in a safely manner.

The natural gas systems, such as gas networks, are planning to be partially decarbonized through the injection of green hydrogen[2] and biogas. Green hydrogen can also be seen as a storage solution for the excess of electricity produced by RES, since it can be stored, and later converted into electricity through fuel cells (FCs). Moreover, the use of green hydrogen in transportation is also gaining traction which will likely increase the number of hydrogen resources connected to the electricity network.

Heating systems powered by fossil fuels are planned to be replaced by high-efficiency electric heating systems, such as heat pumps. Nonetheless, high efficiency combined heat and power (CHP) systems may also play an important role in the transition period.

The deployment of these low-carbon emission technologies has contributed to the reduction of CO_2 emissions. Nonetheless, despite the benefits they bring, it is now proven that they are increasing uncertainty and may jeopardize the secure operation of energy systems due to their variability and lack of flexibility.

New strategies to counteract the impact of decarbonization policies

To counteract this, new strategies are being developed. One of these strategies is using prosumers' flexibility through demand response (DR) programs that are managed by aggregators. Another strategy is using MES as they can provide more flexibility due to the possibility to optimize different energy networks or energy resources.

DR focus on operating prosumers' distributed energy resources (DER) to optimize their flexibility. In turn, this flexibility can be turned into market products. This can help to reduce peak demands, increase the integration of RES, postpone network investments, increase market competition, and improve the operation of electricity networks. DR is addressed in different directives including the 2012/27/EU [13]. In this directive it is stated that member states should ensure proper regulatory frameworks to encourage demand side resources to participate in energy markets; for network operators (i.e., transmission system operators (TSOs) and distribution system operators (DSOs)) to consider DR providers, including aggregators, in their operations; and to promote access of DR to market services (i.e., balancing, reserves, or other).

To meet the EU's carbon-neutral goals in 2050, DR is expected to grow in the following years. Figure 1.3 presents the DR availability at times of highest flexibility needs and share in total

[2] Green hydrogen is produced through electrolyzers with renewable energy, making it carbon-free.

flexibility provision in the years 2020 and 2030. The capacity of DR is made available through the installation of DERs. Table 1.1 presents the expected growth of some of these technologies.

In relation to the use of MES, in the last years, the scientific community started exploiting synergies between energy vectors and distributed MES resources (DMER) in order to make them more efficient and to help the integration of RES. As recent studies show, it is expected that MES bring advantages to the global system by delivering cost-effective and reliable energy services, and reducing the environmental impacts. These energy vectors can be interpreted at different levels, from buildings to cities and regions, and are dependent on local resources, policies, and capital available [14]. MES can help to increase the penetration of energy from RES due to the possibility of switching between energy sources and large-scale heat and gas storage systems, which is an eventually cheaper option when compared with electric storage systems like batteries. This extra flexibility would help to mitigate the problems that arise from the uncertainty and variability of RES.

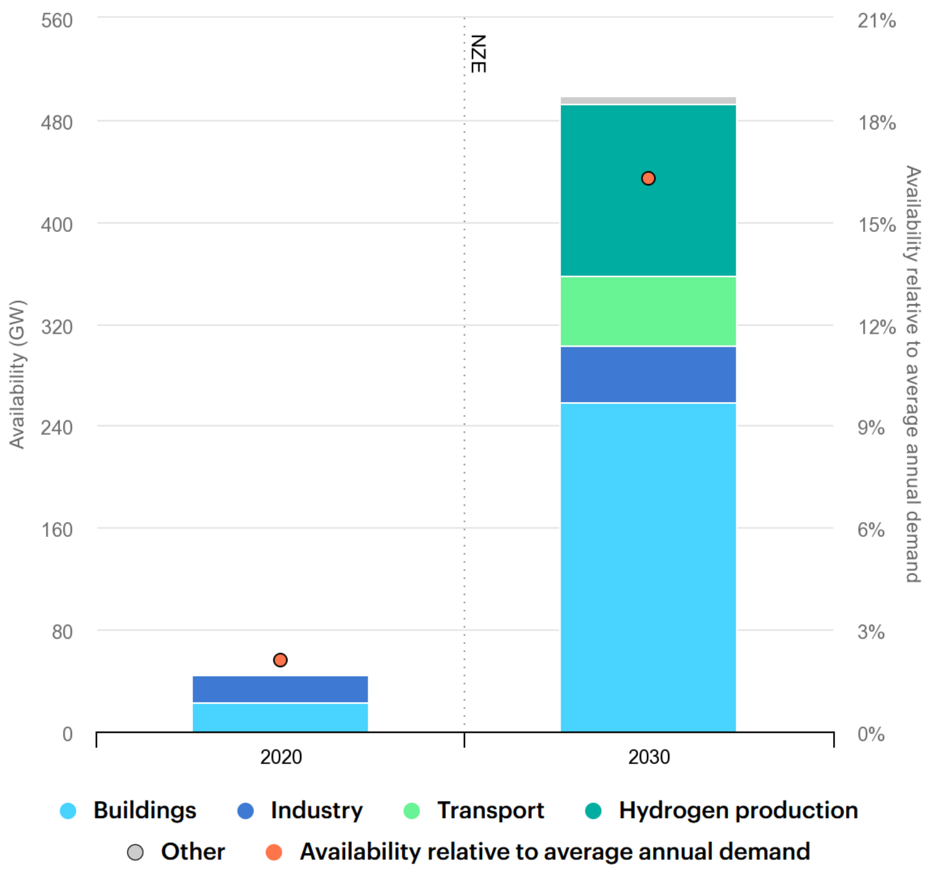

Figure 1.3 - Demand response availability at times of highest flexibility needs and share in total flexibility provision, 2020 and 2030 (adapted from [15]).

Table 1.1 - DMERs deployment for 2020 and 2030 (adapted from [16]).

Technology	2020 deployment status	2030 deployment
Commercial and residential energy storage systems	3.7 GW	510 GW
Smart thermostats	30.4 million	231.5 million
Home energy management systems	4 million	32.7 million
Residential air conditioners	1.9 billion	2.6 billion
Heat pumps	180 million	600 million

Residential electric vehicle smart chargers	117 000	28.7 million

In this context, aggregators provide a technological solution to transform the flexibility of DMERs into multi-energy market services, which can be used to compensate for the variability of RES. These DMERs are usually installed in buildings with smart technologies, such as sensors, smart appliances, and devices that allow aggregators to control them. They can also be installed on premises built exclusively for their use. The DMERs can include thermostatically controlled loads (TCLs), PVs, ESSs, electric vehicles (EVs), heat pumps (HPs), gas boilers (GBs), CHPs, electrolyzers (P2G), FCs, or hydrogen storage systems (HSSs). This way, smart building technologies allow prosumers to be the center of energy systems transforming them into smart citizen-centered energy systems.

However, these new measures and strategies also pose new challenges to aggregators and distribution network operators. These challenges are related with technical problems of the energy networks, data privacy, independence of roles, and computational complexity. For example, these challenges can encompass a situation where it is needed to ensure that the energy services traded by aggregators in multi-energy markets can be delivered without violating the constraints of multi-energy networks, while also ensuring the privacy of any of the energy stakeholders involved.

This thesis contributes with a set of new optimization tools to address the described challenges faced by aggregators and distribution network operators. The main research questions that this work aims to answer are the following:

- How can the aggregator safely participate in multi-energy markets without jeopardizing the secure operation of multi-energy networks?
- How can the aggregator optimize its portfolio of DMERs without incurring in wholesale market penalties?
- How can the aggregator ensure the data privacy of its prosumers?
- What are the economic and environmental benefits provided by a multi-energy aggregator?

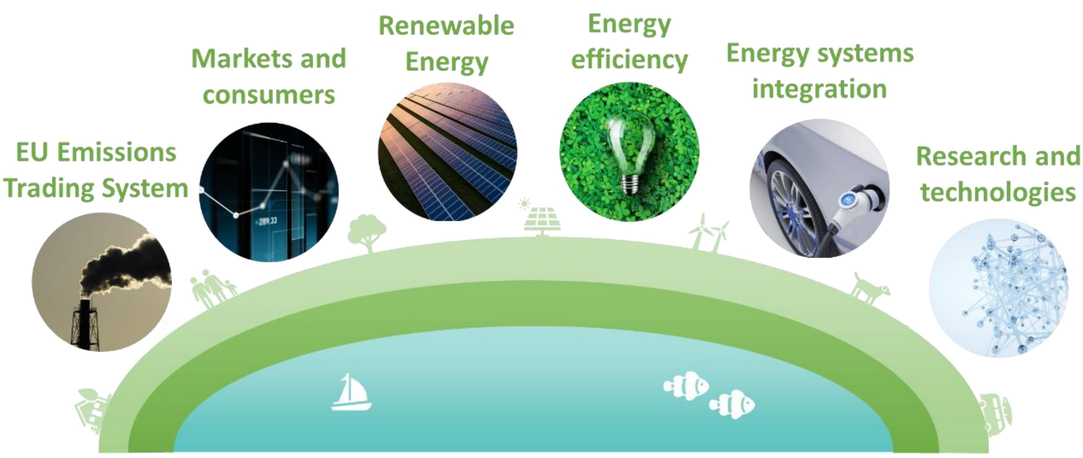

Figure 1.4 - Energy and climate topics covered in this thesis.

In a last note, taking into consideration the importance of following EU policies, this thesis focuses on and explores several energy and climate topics decreed by the EU, including renewable energy, energy efficiency, the EU emissions trading system, integration of energy systems, markets and consumers, and finally, research and technologies (Figure 1.4).

1.2. Objective of the Thesis

The work developed in this thesis encompasses the development of tools to optimize the participation of aggregators in multi-energy markets. The multi-energy markets considered are the electricity (energy and secondary reserves), natural gas, green hydrogen, and carbon markets. The aggregator is able to exploit a different set of DMERs including HPs, GBs, CHPs, PVs, ESSs, EVs, P2Gs, FCs, and HSSs.

Therefore, the main objectives of this thesis are the following:

- **Definition of a network-secure aggregator's framework** – this framework considers the relevant optimization algorithms used by the aggregator, the smart technologies installed at the buildings/resources level, the necessary flows of communications and information, and commercial contracts between the different actors (aggregators, prosumers, DSOs) participating in the different energy markets.

- **Development of a day-ahead network-secure bidding optimization framework** – this framework is a bidding optimization framework used by aggregators of prosumers to participate in day-ahead multi-energy markets in a network-secure way. Using this framework, the aggregator is able to submit bids to the day-ahead (DA) electricity (energy and reserves), natural gas, green hydrogen, and carbon markets. This framework computes network-secure bids, i.e., bids that do not violate any energy network constraints. This is done by including negotiations between aggregators and electricity, heat, and gas DSOs into the framework. This way, the bids are computed to satisfy the constraints of multi-energy markets, DMERs, and multi-energy networks. This strategy is a distributed approach based on the alternating direction method of multipliers (ADMM).

- **Development of a real-time network-secure optimization framework** – a new hierarchical model predictive control (MPC) framework is proposed to support aggregators in the real-time (RT) delivery of network-secure and multi-energy services. The aim is to ensure that aggregators deliver the multi-energy services traded in DA electricity, gas, green hydrogen, and carbon markets. The MPC framework uses the ADMM on a rolling horizon to negotiate the network-secure delivery of multi-energy services between aggregators and multi-energy DSOs. The multi-energy services include electricity (energy and reserves), natural gas, green hydrogen, and carbon allowances, which result from the RT optimization of the multi-energy resources managed by aggregators. This framework builds upon the DA bidding optimization framework, extending it and completing the participation cycle of aggregators in multi-energy markets.

- **Analysis of the aggregator's performance under different decarbonization policies and future low-carbon scenarios** – this consists in the economic and environmental analysis of the aggregator's performance considering different decarbonization policies and low-carbon scenarios (LCSs). Decarbonization policies are focused on carbon and green hydrogen prices. LCSs are focused on the replacement of resources with a higher carbon footprint with low-carbon resources like HPs, PVs, ESSs, or EVs.

1.3. Contributions of the Thesis

This section is divided into three subsections: research and innovations (1.3.1), publications (1.3.2), and research and development projects (1.3.3).

1.3.1. Research and innovation

This thesis addresses the challenges identified in section 1.1 and improves the current state-of-the-art in three main points:

- **Conceptual contribution** – this thesis proposes the transformation of the capabilities of buildings' technologies into multi-energy market products with the following features:
    - These market products are traded by aggregators in different energy markets like the electricity (energy and reserve), natural gas, green hydrogen, and carbon markets;
    - The participation in multi-energy markets considers the constraints of the multi-energy networks (electricity, gas, and heat) making the market bids network-secure, i.e. without violating network constraints.
- **Mathematical modeling contributions** – this thesis proposes two different tools that can be used by aggregators: a DA network-secure bidding optimization framework and a RT network-secure optimization framework.
    - The DA network-secure bidding optimization framework computes multi-energy (electricity, natural gas, green hydrogen, and CO2) bids considering the constraints of electricity, gas, and heat networks. It exploits distributed optimization (i.e. ADMM) to decompose a complex problem (i.e., a mixed-integer nonlinear problem) into smaller sub-problems (e.g., smaller mixed-inter linear problems and nonlinear problems), and to preserve the independent roles of energy operators and the data privacy of the aggregator's clients and DSOs;
    - The RT network-secure optimization framework guarantees that aggregators deliver cost-effectively and safely the multi-energy services traded previously in day-ahead electricity, gas, green hydrogen, and carbon markets. This tool is based on a MPC tool that uses the ADMM on a rolling horizon to negotiate the network-secure delivery of multi-energy services between aggregators and multi-energy DSOs. It considers the non-convex constraints of electricity, gas (with blending of natural gas and hydrogen), and heat networks guaranteeing the network-secure delivery of multi-energy services.

- **Societal contributions** – this thesis estimates the economic and environmental impacts from the optimal participation of aggregators in multi-energy markets considering different decarbonization policies and future LCSs.

1.3.2. Publications

From the work developed in this thesis, 5 journal and 4 conference papers were developed.

Journal:

1. **A. Coelho**, N. Neyestani, F. Soares, and J. P. Lopes, "Wind variability mitigation using multi-energy systems," *Int. J. Electr. Power Energy Syst.*, vol. 118, p. 105755, Jun. 2020, doi: 10.1016/J.IJEPES.2019.105755.

2. **A. Coelho**, F. Soares, and J. Peças Lopes, "Flexibility Assessment of Multi-Energy Residential and Commercial Buildings," *Energies*, vol. 13, no. 11, p. 2704, May 2020, doi: 10.3390/en13112704.

3. **A. Coelho**, J. Iria, and F. Soares, "Network-secure bidding optimization of aggregators of multi-energy systems in electricity, gas, and carbon markets," *Appl. Energy*, vol. 301, p. 117460, Nov. 2021, doi: 10.1016/J.APENERGY.2021.117460.

4. J. Iria, **A. Coelho**, and F. Soares, "Network-secure bidding strategy for aggregators under uncertainty," *Sustain. Energy, Grids Networks*, vol. 30, p. 100666, Jun. 2022, doi: 10.1016/J.SEGAN.2022.100666.

5. **A. Coelho**, J. Iria, F. Soares, and J. P. Lopes, "Real-time management of distributed multi-energy resources in multi-energy networks," Sustain. Energy, Grids Networks, vol. 34, p. 101022, Jun. 2023, doi: 10.1016/J.SEGAN.2023.101022.

Conference:

1. N. Neyestani, **A. Coelho**, and F. Soares, "Strategic Trade of Multi-Energy Aggregators with Local Multi-Energy Systems while Participating in Energy and Reserve Markets," Int. Conf. Eur. Energy Mark. EEM, vol. 2019-September, Sep. 2019, doi: 10.1109/EEM.2019.8916369.

2. **A. Coelho**, J. Iria, F. Soares, and J. P. Lopes, "Evaluation of the economic, technical, and environmental impacts of multi-energy system frameworks in distribution networks", IEEE PowerTech, Jun. 2023

3. N. Fonseca, J. Iria, F. Soares, **A. Coelho**, "DSO framework to handle high participation of DER in electricity markets", 2023 19th International Conference on the European Energy Market, Jul. 2023, doi: 10.1109/EEM58374.2023.10161794

4. J. Fountoura, F. Soares, **A. Coelho**, Z. Mourão, "Optimal Operation of Gas Networks with Multiple Injections of Green Hydrogen", 6th International Conference on Smart Energy Systems and Technologies, Sep. 2023

1.3.3. Research and development projects

The work developed in this thesis contributed to the elaboration and development of the ATTEST project. ATTEST is a R&D project that received funding from the European Union's Horizon 2020 research and innovation program under grant agreement No 864298 ([Online] Available: https://attest-project.eu/about-us/).

1.4. Structure of the Thesis

This thesis is organized into seven chapters and one appendix.

Chapter 1 (current chapter) presents an introduction to the theme explored in this thesis. It also describes the objectives and contributions of the thesis.

Chapter 2 presents a review of the state-of-the-art focusing on frameworks of electricity, natural gas, hydrogen, ETSs and guarantees of origin (GO) markets from different parts of the world, TSO-DSO coordination mechanisms, and finally, multi-energy aggregators and the decision-support optimization tools developed that consider aggregator's participation in multi-energy markets.

Chapter 3 describes the framework for a multi-energy aggregator to participate in electricity, natural gas, green hydrogen, and carbon markets. It also details the relevant interactions of the aggregator with TSOs, electricity, gas, and heat DSOs, market operators, and prosumers with multi-energy resources.

Chapter 4 presents the mathematical formulation of the aggregator subproblem (i.e. the bidding optimization model), the formulation of the DSOs' subproblems (i.e. the multi-energy flow optimization models), the case study used to analyze the framework developed, the results obtained and the analyzes of the newly developed framework, and finally, the conclusions of this chapter.

Chapter 5 presents the hierarchical MPC framework, the formulation of the aggregator's sub-problem (i.e. the aggregator's RT optimization model), the formulation of the DSO's sub-problems (i.e. the distribution system operators' flow optimization models), the case study used to analyze the framework developed, the results obtained and the analyzes of the newly developed framework, and finally, the conclusions of the chapter.

Chapter 6 presents two sensibility studies covering the impact that carbon prices and green hydrogen policies have on the aggregator's performance, discusses the economic and environmental impacts of different LCSs from the perspective of the aggregator, and finally, presents the conclusions of this chapter.

Chapter 7 discusses the main contributions provided by the work from this thesis, focusing on the main conclusions and findings obtained from this work. It also outlines prospects for future work.

Annex A presents the case study used to evaluate the strategies presented in Chapter 4 and Chapter 5. It presents the network, DMERs, buildings, market, weather, and inflexible load data.

Chapter 2
Background and State-of-the-Art

2.1. Introduction

This chapter presents the literature review about multi-energy markets, TSO-DSO coordination mechanisms, and multi-energy aggregators. Section 2.2 presents the frameworks of electricity, natural gas, ETSs, hydrogen, and GO markets. The description of the markets covers different parts of the world including Europe, the United States (US), Australia, and New Zealand. Section 2.3 presents the 5 major TSO-DSO coordination mechanisms described in the literature. Section 2.4 gives a background about multi-energy aggregators and the decision-support optimization tools developed that consider aggregators' participation in multi-energy markets.

2.2. Multi-energy markets

This section presents frameworks of the electricity (2.2.1), natural gas (2.2.2), ETSs (2.2.3), hydrogen (2.2.4), and GOs (2.2.5) markets. The rules of each energy market are defined considering the different characteristics of the energy networks they are representing.

2.2.1. Electricity spot markets

Electricity markets can be divided into spot and future markets. Future markets negotiate products to be delivered in the long term. They can be weekly, monthly, quarterly, or annual products. In spot markets, market players trade electricity to be consumed or generated in the short term, i.e., in the following days or hours. Figure 2.1 presents a general framework of an electricity market.

In electricity markets, energy is traded through market pools or bilateral contracts and ancillary services (AS) through market pools, bilateral contracts, or tenders. Market pools are auctions where buyers and sellers can buy or sell energy or AS respectively; bilateral contracts are independent agreements between two parties for the delivery of energy or other products; tenders are contracts for the delivery of AS for a certain period.

This subsection describes the European, US, and Australian spot electricity markets. It provides details about the DA, intraday, and RT energy and AS markets and respective settlements.

2.2.1.1. European spot markets

This subsection presents the main European electricity market architectures. These markets are usually divided into energy (DA and intraday) and AS markets.

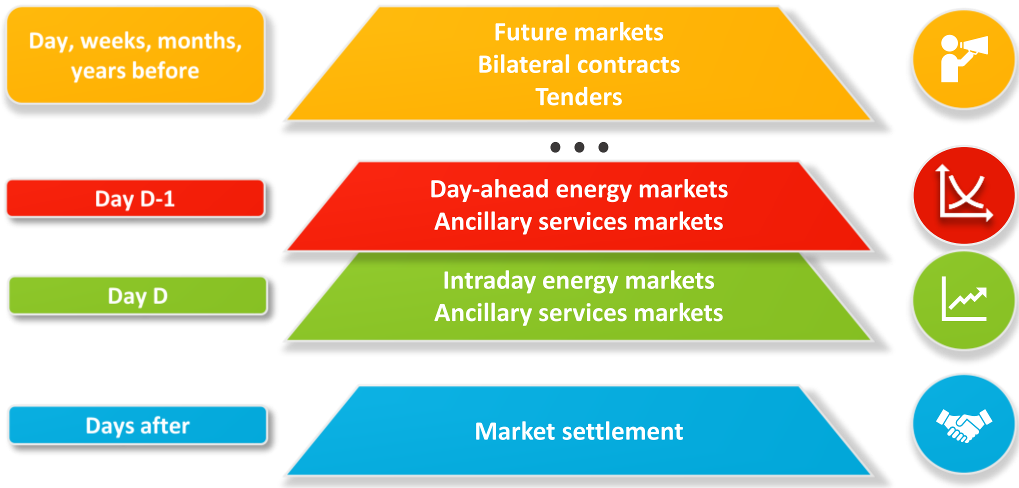

Figure 2.1 - General framework of an electricity market (adapted from [17][18]).

Energy markets

Market operators are responsible for the economic management of the DA and intraday markets. They manage market operations, which include receiving buying and selling bids, matching them, and settling all transactions made. They also exchange information with system operators regarding bilateral contracts.

The DA market is a single auction session where bids are sold and bought for each hour of the following day. The market operator gathers all the bids and matches them using the Euphemia algorithm [19]. The EUPHEMIA clears the bids such that social welfare is maximized and the power flows between the European control areas do not exceed the capacity of the transmission interconnectors [20]. The first step of the matching process is to order the bids for each period: buying bids are ordered by descending price (demand curve) and selling bids are ordered by ascending price (supply curve). The point of intersection of the demand and supply curves defines the clearing price.

Afterwards, the TSO of each control area adds the physical bilateral contracts to the clearing offers and performs congestion management [21] to compute viable energy schedules. In this process, the TSO only considers the transmission network constraints of its area. In case of detected transmission network problems, the TSO can use market-based approaches (e.g., market-splitting) or technical-based methods (e.g., adjusting transformer taps) to solve the problems. In short, the EUPHEMIA and congestion management ensure that the energy bids do not violate any transmission network constraints between and within the European control areas.

The hourly DA market bids can be simple or complex. Simple bids are bids with a price (€/MWh) and an amount of power (MWh). Complex bids can include many other types of bids. They can include bids with additional complex terms that must be considered in the matching process like conditions of indivisibility, minimum income, schedule stop and production capacity variation, load gradient conditions, among others.

The electricity market operators present in the EUPHEMIA platform are the CROP EX, EPEX SPOT, EXAA, GME, HEnEx, HUPX, IBEX, Nord Pool, OKTE, OMIE, OPCOM, OTE, SEMOpx and South Pool [22] covering the electricity markets in Austria, Belgium, Czech Republic, Denmark, Estonia, Finland, France, Germany, Hungary, Ireland, Italy, Latvia, Lithuania, Luxembourg, the Netherlands, North Ireland, Norway, Poland, Portugal, Romania, Slovakia, Slovenia, Spain, and Sweden. Figure 2.2 presents the EUPHEMIA participants.

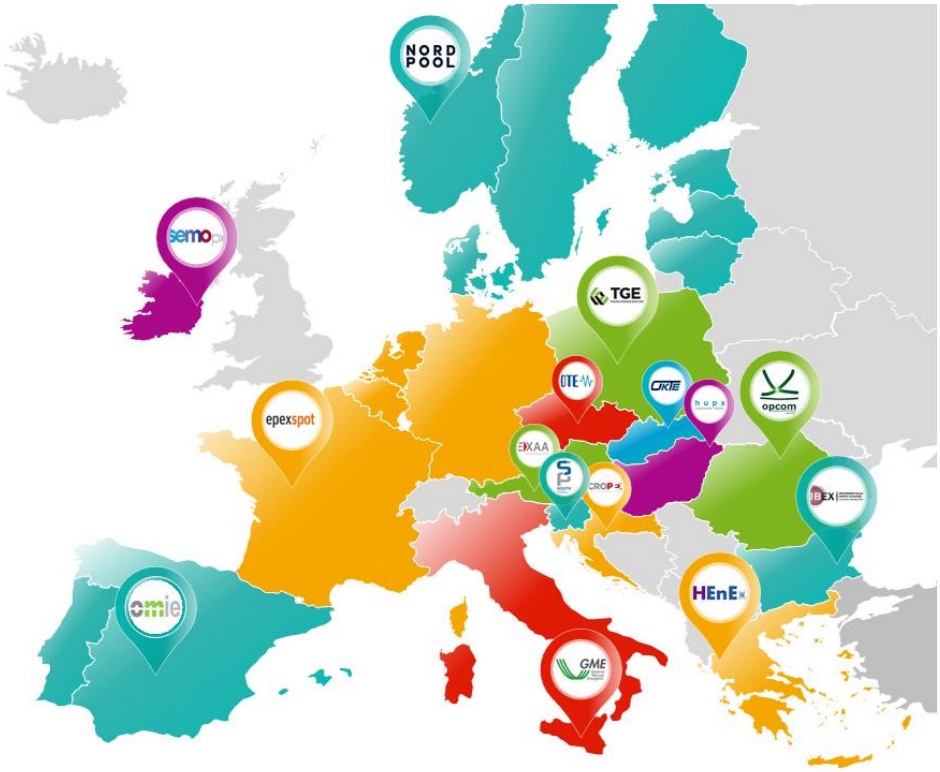

Figure 2.2 - EUPHEMIA participants.

The intraday market has the purpose of attending energy purchases and sales which may occur in the following hours after the closure of the DA market sessions. Its structure is similar to the DA market. In this market, the market agents can correct the bids previously accepted in the DA market or previous intraday sessions. It can encompass different discrete auction sessions or a continuous auction session. The discrete sessions occur in established schedule periods with the delivery of products one hour after the session's closure. The continuous auction session starts after the DA market and closes one hour before the delivery of products.

To create a single pan European cross zonal intraday market in Europe and increase the efficiency of intraday trading, the XBID project was implemented [23]. This project provides an intraday coupling algorithm to calculate intraday prices in different regions of Europe. The electricity market operators that participate in this project are EPEX SPOT, GME, NordPool, OMIE, and the North Western European and Baltic TSOs. The countries coupled with this algorithm are Austria, Belgium, Bulgaria, Croatia, Czech Republic, Denmark, Estonia, Finland, France, Germany, Hungary, Italy, Latvia, Lithuania, Luxembourg, Netherlands, Norway, Poland, Portugal, Romania, Slovenia, Spain, and Sweden [24].

Ancillary services

AS are essential for ensuring power systems' security and reliability by maintaining the balance between load and generation. They mitigate frequency and voltage deviations that could lead to system failure. These services are constituted by frequency reserves (primary, secondary, and tertiary), congestion management, voltage, and black start services.

The frequency reserve services act on loads and generators that can increase or decrease their generation/consumption as necessary. The TSO is responsible for procuring and managing reserves in the respective markets. The three types of reserves mentioned are defined as [25]:

- Primary reserve: automatically activated when frequency deviations occur to stabilize the system frequency. It increases or decreases the output of the generating units according to its speed-droop characteristic. It must be activated within 15s for frequency variations lower than 100 mHz and linearly up to 30s for frequencies up to 200 mHz;

- Secondary reserve: it starts after the primary reserve is activated and runs in parallel with it. Its purpose is to bring the system frequency back to the nominal value by maintaining the balance between generation and consumption within the synchronous area. It makes use of an automatic generation control (AGC) that controls the resources' output within the time frame of seconds up to 15 min;

- Tertiary reserve: manually activated to replace the secondary reserve in order to clear it for other eventual occurrences. The resources participating in this reserve must increase or decrease their power output within 15 min and sustain it for at least 2h.

The classification of reserves was recently reviewed by the European Association for the Cooperation of Transmission System Operators for Electricity (ENTSO-E) [26]. In general, the use of reserves and their classifications is similar in Europe, with the exceptions of the Nord Pool and the UK. Figure 2.3 presents the differences between the classic ENTSO-E, new ENTSO-E, Nord Pool, and UK classification of reserves.

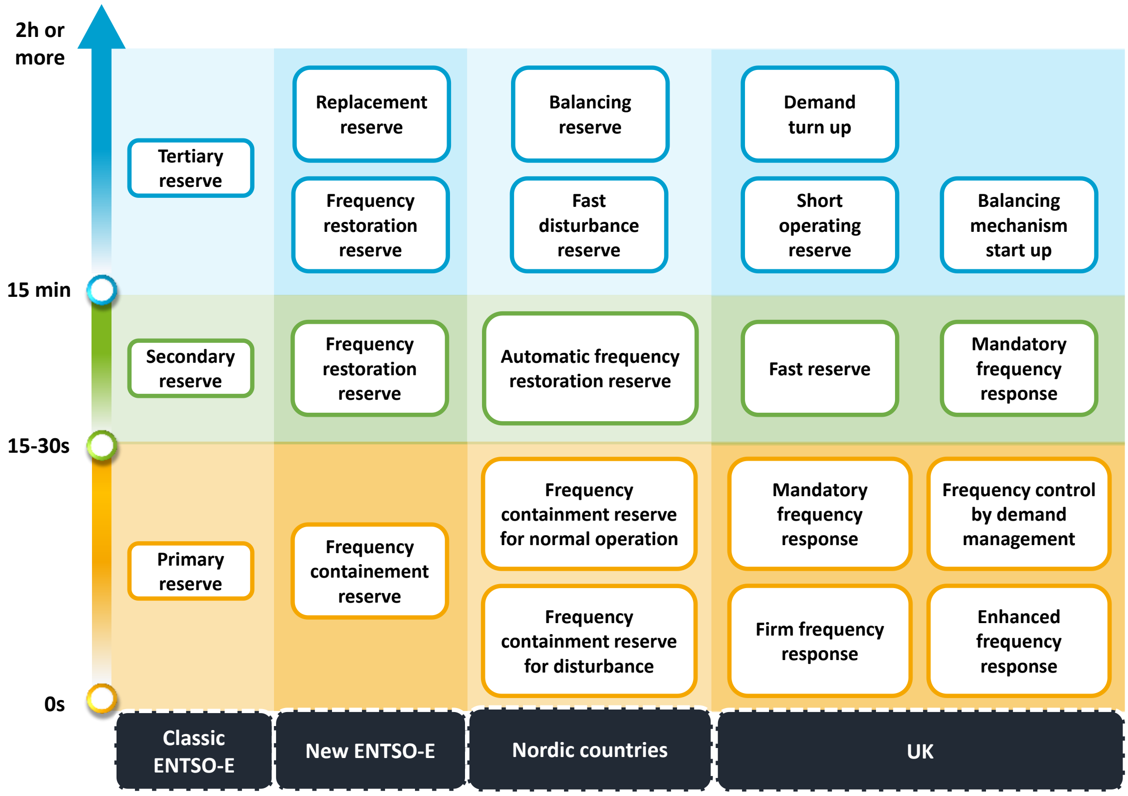

Figure 2.3 - Reserve classifications in Europe [17].

There are different types of mechanisms used by TSOs for procuring reserves which differ from country to country. These mechanisms can be the following [27]:

- Mandatory offer – where generators must offer the remaining capacity available;
- Mandatory provision – where generators must reserve a certain amount of capacity remunerated for a fixed price or for free;
- Mandatory provision without reservation – where generators must provide balancing services without any reservation of capacity;
- Bilateral markets – where TSOs and grid users negotiate the contracts according to their terms
- Organized markets – where grid users are free to offer reserves to the markets according to their will.

In Portugal and Spain, the primary reserve is mandatory and non-remunerated. The secondary reserve is traded in DA markets that begin after the congestion management phase. Market participants trade for upward and downward reserves that later are activated by the AGC. These bids are presented between 19h and 19h45. The TSO buys secondary reserve under the form of a band (MW), taking into account the constraints of the transmission network of its control area [28]. They are remunerated in the form of availability (€/MW) and utilization (€/MWh). The price of band availability is set by the secondary reserve market, while the price of utilization is defined by the tertiary reserve market [21]. The tertiary reserve market begins after the closing of the secondary reserve market. The bids are presented in form of power (MW) and an associated price (€/MWh) and they are remunerated in the form of utilization (€/MWh). During operation, market agents can modify their bids 1h (in Portugal) or 45 min (in Spain) before delivery.

In Italy, the primary reserve is mandatory and non-remunerated. The secondary and tertiary reserves are traded in DA markets. They are remunerated at the offered price (i.e., pay-as-bid).

In Germany, the primary reserve is purchased in weekly markets and remunerated through availability terms [13][29]. The secondary reserve is also purchased in weekly markets and remunerated by availability and utilization terms. The tertiary reserves are purchased in daily markets and remunerated through availability and utilization.

In Nordic countries, primary reserves are purchased in hourly market pools and tenders and they are remunerated through availability terms [30]. Secondary reserves and fast disturbance reserves are purchased through hourly market pools, bilateral contracts, and tenders and they are remunerated through availability and utilization terms. The balancing reserve (i.e. tertiary reserve) is dispatched and purchased based on an economic merit order of submitted hourly bids. The remuneration is set by the marginal price.

In 2017, the European Commission published the Commission Regulation (EU) 2017/2195 establishing a guideline on the European Union electricity balancing markets. These markets are integrated into common European platforms for “operating the imbalance netting process and enabling the exchange of balancing energy from frequency restoration reserves and replacement reserves” [31]. There are four platforms:

- Trans European Replacement Reserves Exchange (TERRE) – in this platform it occurs the exchange of balancing energy from replacement reserves (tertiary reserves) [32]. The members of this project consist of 11 TSOs from France, Czech Republic, Great Britain, Italy, Poland, Portugal, Spain, and Switzerland. This project is still in its implementation phase which consists of the development of the common European replacement reserves platform, local implementation, preparation for the parallel testing, and the Go-live;

- Manually Activated Reserves Initiative (MARI) - in this platform it occurs the exchange of balancing energy from frequency restoration reserves with manual activation [33]. Currently, there are 30 TSOs as members of this platform from Austria, Belgium, Croatia, Czech Republic, Denmark, Estonia, Finland, France, Germany, Great Britain, Greece, Hungary, Italy, Latvia, Lithuania, Luxembourg, the Netherlands, Norway, Poland, Portugal, Romania, Slovak Republic, Slovenia, Spain, Sweden, and Switzerland. This project is still in its implementation phase;

- Platform for the International Coordination of Automated Frequency Restoration and Stable System Operation (PICASSO) - in this platform it occurs the exchange of balancing energy from frequency restoration reserves (secondary reserves) with automatic activation [34]. This project includes 26 TSOs from Austria, Belgium, Bulgaria, Croatia, Czech Republic, Denmark, Finland, France, Germany, Greece, Hungary, Italy, Luxembourg, the Netherlands, Norway, Poland, Portugal, Romania, Slovak Republic, Slovenia, Spain, Sweden, and Switzerland. It became operational in June 2022;

- International Grid Control Cooperation (IGCC) - in this platform it occurs the imbalance netting process [35]. The members of this platform must maintain the balance between electricity consumption and generation in their respective load-frequency control areas, at all times. There are 21 operational TSOs from Austria, Belgium, Croatia, Czech Republic, Denmark, France, Germany, Greece, Hungary, Italy, the Netherlands, Poland, Portugal, Romania, Slovak Republic, Slovenia, Spain, and Switzerland. It became operational in June 2021.

Market settlement

Market settlements may occur days after the operational day, and they are handled by the TSO and/or the market operator. Market participants are charged or paid for the energy and ancillary services bought or sold. If energy imbalances occur, i.e. differences between the energy delivered and the DA bids or intraday positions, the market participants are charged or paid at an imbalance price. The imbalance prices vary according to their direction. If the AS previously negotiated are not provided, the market participants incur in heavy penalties or even expulsion from the markets.

2.2.1.2. United States spot markets

The US electricity markets are divided by regions as seen in Figure 2.4: California (CAISO), Texas (ERCOT), New England (ISO-NE), Midwest (MISO), Northwest, New York (NYISO), Maryland (PJM), Southeast, Southwest and Southwest (SPP). The Southeast, Southwest, and Northwest markets are traditional wholesale electricity markets. They are vertically integrated with utilities owning generation, transmission, and distribution. Physical power is usually traded through bilateral contracts. The other regions have more competitive wholesale electricity markets operated by independent system operators (ISOs) with energy (DA and RT), capacity, and AS markets.

Figure 2.4 - US electricity market regions (from [36]).

Energy market

Energy markets are divided into DA and RT markets. The DA markets are spot markets where prices are cleared for each hour of the next day. In RT markets, electricity prices are cleared every 5 minutes [37]. These prices are calculated based on locational marginal pricing [38][39], reflecting the buying and selling offers, transmission congestion costs, and marginal losses. This mechanism makes electricity prices vary according to their location. These markets use a market-clearing mechanism that co-optimizes them with the frequency reserve markets, contrary to the European markets. This way, this mechanism defines the clearing bids and prices of both energy and reserves. Through co-optimization, it is possible to obtain more efficient dispatches from an economic point of view. Nonetheless, the auctions are more complex as it needs to consider the more complex technical constraints of resources, like ramp rates or minimum start-up times.

Ancillary services: frequency reserve services

The frequency reserve services in the US are divided into four services [40][41]:

- Regulation reserve – constant and automatic services used to correct small fluctuations of the system balance (i.e. supply and demand balance). Providers must respond to the AGC in the order of one to several seconds;

- Spinning reserve – services used to rapidly respond to forced outages or any other contingency events. Providers must be online at the moment of contingency, be fully available for 10 to 15 minutes, and maintain their services for 2 hours. These services can be provided through DR;

- Non-spinning reserve - services used to help the system recover from contingencies. These services are provided by offline resources that can start and change their output according to the system needs between 10 to 30 minutes. Online units with enough capabilities can also provide these services.

- Replacement reserve – services used to replace other reserves in order to reduce costs and guarantee the security of the system by making the faster replaced reserves available for other possible contingency events. These services must be supplied within 30 minutes.

Figure 2.5 presents a general comparison between the classic ENTSO-E reserves and US reserves.

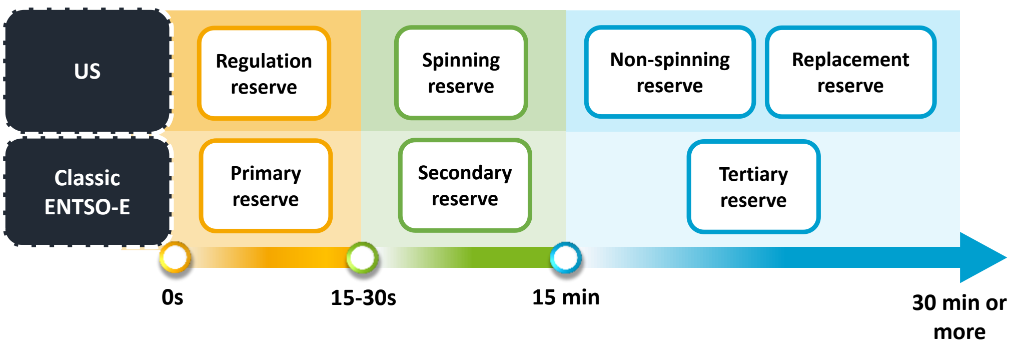

Figure 2.5 – General comparison between classic ENTSO-E and US reserves (based on [38]).

As these reserves are co-optimized with the energy markets, they typically use the same market-clearing mechanisms. Frequency reserves can be remunerated by three components: utilization, availability, and pay-as-performance. Pay-as-performance is only applied to regulation services and they consider the actual mileage, mileage price, and performance score of the service provided to calculate prices [42].

Settlement

Settlements use the clearing prices of the DA and RT markets to calculate the final payments to the service providers. Regulation services can also be remunerated through the prices from the pay-as-performance mechanism.

2.2.1.3. Australian spot markets

The National Electricity Market in Australia covers New South Wales, the Australian Capital Territory, Queensland, South Australia, Tasmania, and Victoria. It is a RT market, where eligible bidders bid to supply energy and AS. The Australian energy market operator is responsible for buying energy and AS to ensure the secure operation of the power system. It co-optimizes energy and frequency reserve services, named by frequency containment AS (FCAS) [43][44].

Energy market

The energy market is a RT one-sided spot market where supply and demand are matched and dispatched every 5 minutes. The marginal price results from matching the supply bids with the forecasted demand.

Ancillary services

AS in Australia are composed of FCAS, network support control AS, and blackstart AS [43].

FCAS are used to maintain the frequency of the power systems close to the predefined value of fifty cycles per second [43]. These services can be found in the RT FCAS market which is co-optimized with the energy market every 5 minutes. FCAS can be divided into 2 sets of services [43]:

- Regulation – services used to correct minor changes in the frequency of the system, i.e. small differences between supply and demand, and maintain its balance. They are provided by generators through the AGC in order to maintain the frequency between 49.85 Hz and 50.15 Hz;

- Contingency – services used to correct the system frequency when there is a major contingency event. The system should return to its normal operating state within 5 minutes. Some technologies able to provide these services are the generator governor response, load shedding, rapid generation (starting of fast generators), and rapid unit unloading (reduction of generators' output).

There are 8 markets for the delivery of FCAS: two for the regulation services and 6 for the contingency services. The regulation service markets are divided into raise and lower markets.

The contingency service markets are divided into 6 markets: fast raise (6 seconds), fast lower (6 seconds), slow raise (60 seconds), slow lower (60 seconds), delayed raise (5 minutes), and delayed lower (5 minutes). 6-second services are used for services to arrest a fast change in the power system's frequency; 60-second services are used to stabilize the power system's frequency; 5-minute services are used to restore the power system's frequency to its nominal value [43]. In each market, the bids are ordered by merit order of cost, and the marginal price is set by the highest cost offer enabled.

Figure 2.6 presents a general comparison between the classic ENTSO-E and Australian reserves.

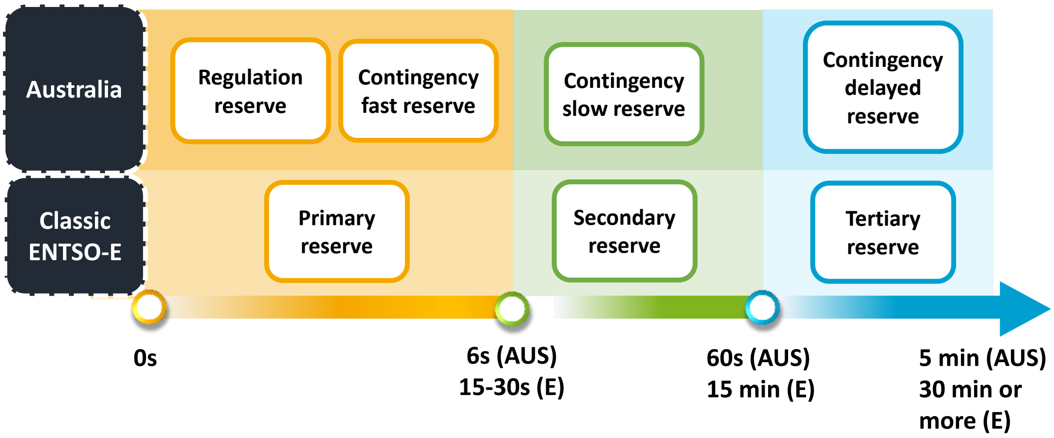

Figure 2.6 - General comparison between classic ENTSO-E (E) and Australian (AUS) reserves.

The National Electricity Market can purchase the network support control AS and system restart AS under independent arrangements with service providers [43]. Network support control AS are used to control the voltage, the flow on inter-connectors, and transients of the system. System restart AS are used in case of major supply disruption or when the power system must be restarted.

Bid submission

On the previous day, participants submit 5-min energy and reserve bids to the 288 intervals of the following day. Services providers can submit bids, indicating the amount of energy (MWs) they can add/take to/from the system [45]. The bids must be submitted by 12h30 of the previous day. This stage is known as a pre-dispatch which allows the market operator to plan for possible contingencies in the networks.

During the operating day, participants can update the quantity of their bids, although the prices must remain the same.

Settlement

Settlements use the clearing prices of the energy and FCAS market to calculate the final payments to the energy buyers and sellers and market services providers [43]. The payments are aggregated and expressed in 5-minute payments.

2.2.2. Natural gas markets

This subsection describes the European and US natural gas markets. In general, the natural gas supply chain of these countries is similar. The supply chain starts with the gas reserves being explored and extracted of natural gas or with imported gas via pipelines or through liquefied natural gas (LNG) from other markets. Then, this gas is supplied to the wholesale markets where buyers and sellers can trade for it. After this, the gas is moved through pipelines or to storage systems. Pipeline capacity rights to move gas through the transportation networks are bought and sold by market agents. Gas TSOs are responsible for the balance of the entire gas network. Finally, the gas is received by retailers that sell gas to consumers through pipelines. Figure 2.7 presents a typical natural gas supply chain.

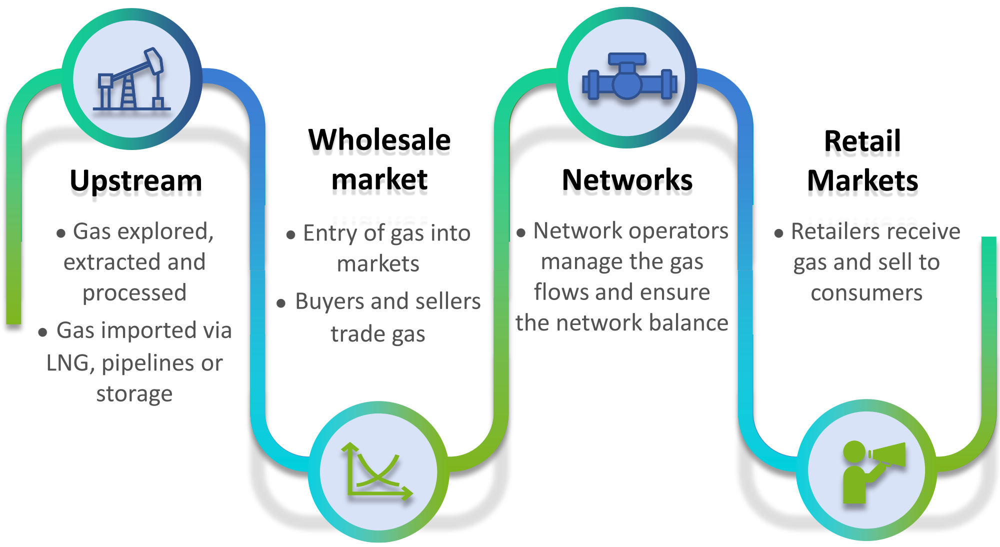

Figure 2.7 - Traditional gas supply chain (based on [46]).

Natural gas markets are usually represented by hubs which differ depending on characteristics like the supply structure or the level of infrastructure development. These hubs can be physical hubs, like the Henry Hub in the US, or virtual (balancing) trading hubs, like the Punto Virtual de Balance in Spain or the Trading Hub Europe in Germany. A physical hub is a physical point where different pipelines converge and where buyers and sellers can trade for natural gas. A virtual trading hub, also known as virtual trading point (VTP), is a platform present in an entry-exit system that allows the trade of gas between network users. The VTPs are not related to pipeline intersections but rather abstract places representing entire infrastructures.

An entry-exit system can represent a country or a regional zone and it is defined by a pipeline grid and all its entry and exit points. These models are usually used by countries with a high dependency on imports (as is the case for most European countries). As seen in Figure 2.8, these systems have entry (N) and exit (X) points [47]:

- Natural gas can enter the system at cross-border entry points (via pipelines or LNG terminals) or local entry points from domestic production or storage.
- Natural gas can exit the system at cross-border exits, at local exit points (customers at the transmission level or storage), or to distribution networks.

In a full entry-exit system, gas brought into the system at any entry point can be made available at any exit point, without restrictions [47]. This way, market players have access to any entry or exit point within the system and can purchase entry and exit capacity (buy or sell natural gas) through the VTP and irrespectively of its actual physical location. Thus, VTPs within this type of system can facilitate the operation of a functional wholesale gas market [47].

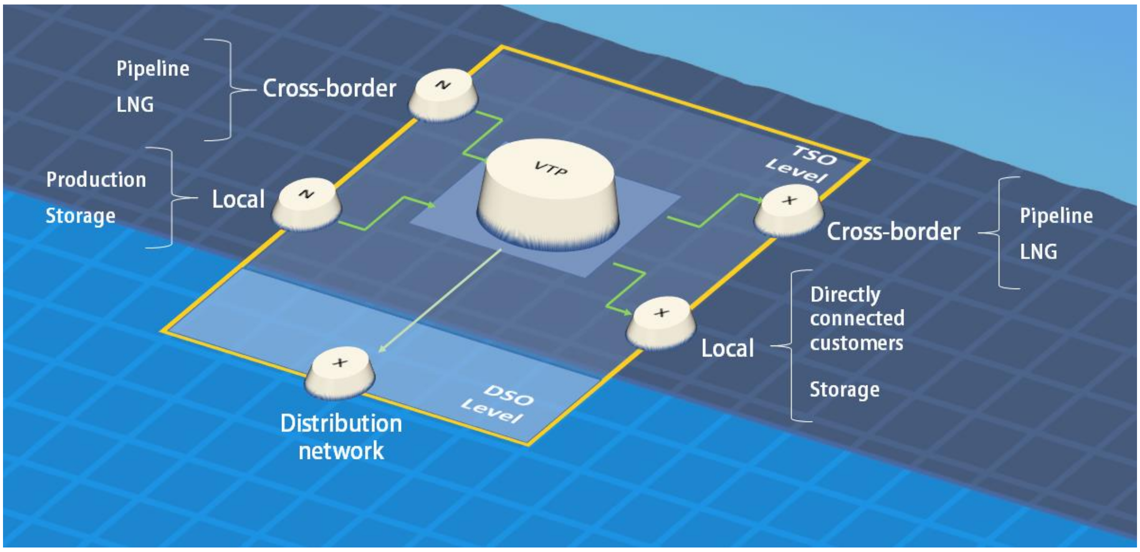

Figure 2.8 – Virtual trading point scheme (based on [47]).

2.2.2.1. Europe

The European gas market has gone through several changes in the last few years. These changes are mainly driven by the EU's goals of decarbonizing energy systems and phasing out coal by switching it to natural gas. Moreover, as most of the natural gas consumed in the EU is imported from other countries (pipeline natural gas mainly from Russia, Norway, and Algeria, and LNG mainly from USA, Qatar, and Nigeria [48]), a well-designed gas market structure is mandatory to create a market environment that is more competitive and fairer toward market participants.

With the "Third energy package" [49], enacted on September 2009, the EU introduced new structural changes in the wholesale gas markets. These changes broke and unbundled the vertically-integrated system which separated the operation of gas networks from the business of providing gas. With these changes, the EU aimed to guarantee non-discriminatory access to gas networks and efficient competition between market players. As the EU gas market has a cross-border nature, this package also aimed to ensure that natural gas was effectively transported through national pipelines and grids. This was ensured through the European Network for Transmission System Operators for Gas (ENTSO-G) which facilitates and enhances cooperation between national gas TSOs throughout Europe. A newer legislation, the "Clean energy for all Europeans package" [50], was adopted in 2019 that aims at updating and reinforcing the legislation imposed by the "Third energy package". With these regulations, the EU is taking efforts at transforming the various national gas markets into a single, pan-European market, with common market mechanisms to form similar prices.

In the European natural gas markets, there are usually two different types of market: spot and forward/future markets. Different products are traded inside them [51]. In spot markets, the products traded are short term which can range from hourly products to multi-day products like weekend or balance-of-the-month products. In forward or futures markets, the products traded can be medium or long-term. Medium-term products can range from one calendar month to one quarter; long-term products can range from season products (Summer, Winter) to one or more calendar years.

The European natural gas markets are composed of entry-exit models [52] with VTPs. These VTPs are also interconnected with other European VTPs or with international networks. Nonetheless, as the EU regulations are relatively recent, not all EU countries have established VTPs yet. The countries with VTPs already established are Austria, Belgium, Czechoslovakia, Denmark, France, Germany, Hungary, Ireland, Italy, Netherlands, Poland, Portugal, Serbia, Slovakia, Spain, Romania, and the UK, although not all of them are in the same phase of development [47][53]. Figure 2.9 presents the advanced and fully established VTPs in Europe [48][54].

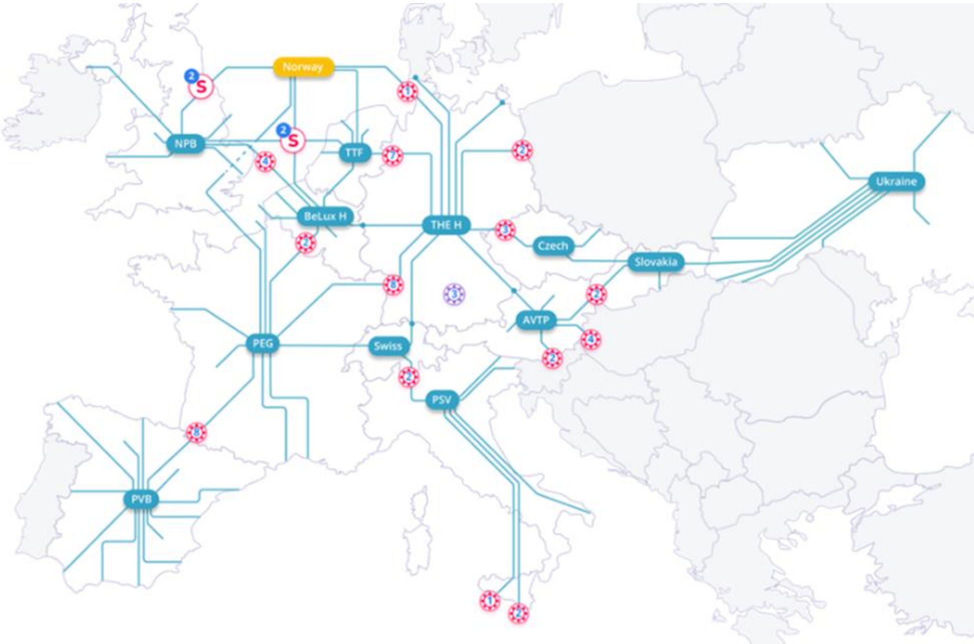

Figure 2.9 - European advanced and fully established VTPs (from [54]).

Within each VTP, there is a wholesale natural gas market in which different products can be bought: gas energy and transmission capacity. Gas energy is the quantity of gas, expressed in kWh in terms of the higher heating value (HHV). Transmission capacity is the right of an agent to transit gas energy through the transmission network, expressed in kWh/h. Participants need to buy capacity from the TSOs to access the wholesale energy natural gas markets and to transmit the required gas energy [55][56]: suppliers of natural gas need to buy entry capacity while buyers of natural gas need to buy exit capacity. Then, traders of capacity must submit nominations to the TSOs indicating the gas energy to be transmitted within the capacity bought. After the nominations, TSOs in each VTP perform balancing operations to ensure the balance of the system and they can restrict the amount of capacity sold in case of necessity [57][58]. Market agents are responsible for their own natural gas balance, i.e. the scheduled gas energy indicated to the TSOs and the actual natural gas consumed must be equal. They can participate in the intraday wholesale natural gas energy markets to ensure the natural gas balance.

This way, the European organized wholesale gas markets have several core concepts in common including [59]:

- Possibility to trade gas at Virtual Balancing Points or other points;
- Possibility to independently contract capacity for inputs or outputs on the network;
- Daily balancing operations with the gas TSO involvement in order to guarantee the necessary supply and a secure operation
- Firm trades, i.e. actors commit to deliver the negotiated products;

Nonetheless, each European wholesale natural gas market has its own specific set of rules related with market schedules, products, and other particular constraints. This section only presents in more detail the rules of one wholesale energy natural gas market, the Iberian Gas Market (MIBGAS), i.e. the Portuguese and Spanish gas market.

MIBGAS - Wholesale natural gas energy market of the Iberian Peninsula

The wholesale natural gas energy market of the Iberian Peninsula has a platform that allows for trading natural gas at different local points and performing daily balancing operations. The gas TSO guarantees the secure operation of the transmission networks. A market operator is responsible for managing this market.

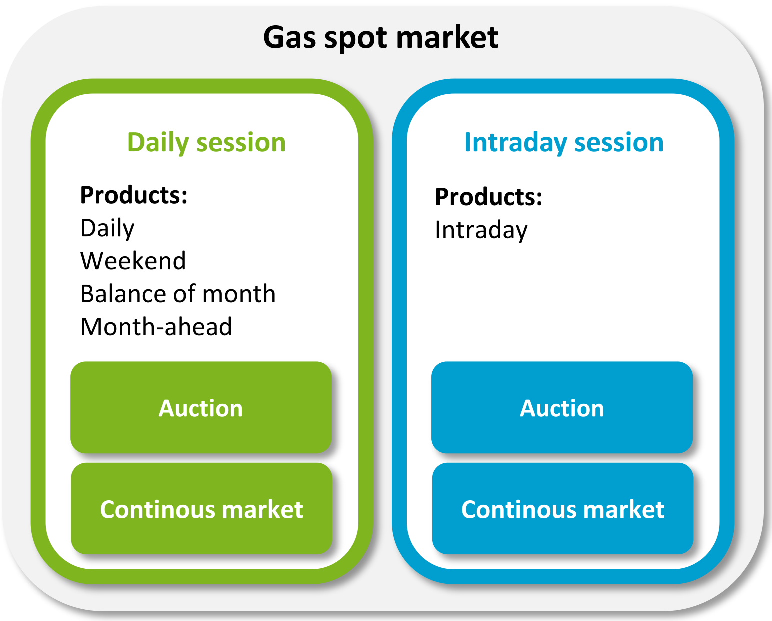

Figure 2.10 - MIBGAS wholesale natural gas energy market structure.

MIBGAS is constituted by two trading sessions: daily and intraday (Figure 2.10). The products offered in these sessions are the following [60][61]:

- **Intraday –** negotiated and delivered during day D;
- **Daily –** negotiated between day D-1 and D-3 and delivered during day D;
- **Weekend –** negotiated between the previous Monday and day D-1 with delivery during day D (Saturday) and D+1 (Sunday);

- **Balance of month –** negotiated between the first day of the month being negotiated (M) and the fifth day before the start of the following month (M+1). Delivered between the following day of the negotiating day and the last day of the month M;

- **Month-ahead –** negotiated between the first and last days of the previous month (M-1) and delivered during month M.

The daily, weekend, balance-of-the-month, and month-ahead spot products are offered in the daily session. The intraday spot products are delivered in the intraday session.

Both daily and intraday markets are divided into an auction and a continuous market [62]. The auction starts at 8h30 and closes at 9h30. The continuous market starts at 9h35 and closes at 18h for the DA market and 21h30 for the intraday market.

In the auctions, the market participants can offer buying or selling bids for a certain product. When the auction session closes, the market operator gathers all the bids and obtains the aggregated buying and selling curves for each product. The intersection of the curves defines the clearing price of the auction session. The bids are simple, i.e. without complex conditions, and indicate the price (€/MWh) and daily quantity (MWh/day) of natural gas to be bought. Each auction session considers the bids presented in this session, bids from previous future products, and bids from the previous auction sessions that were not selected. The auction occurs before the continuous market and the products negotiated serve as a reference for it.

The continuous market occurs after the auction whose products' prices serve as a reference. Here, market participants can also offer buying and selling bids. Contrary to the auction sessions, in this market, it is also possible to offer complex bids. This way, these bids indicate the price (€/MWh), the daily quantity (MWh/day) of natural gas to be bought, and the respective complex conditions. New bids are processed as they are offered. If the new bids are competitive with other pre-existing bids in the continuous market, i.e. higher or similar prices for buying bids or lower or similar prices for selling bids, they are accepted and matched with those orders.

After the closure of the markets, the market agents inform the TSO about the quantity and direction of flow of gas to be deployed and the TSO validates them according to the technical constraints of the transmission gas network [63].

The market operator is responsible for calculating the market's economic results, invoicing, collection, and payment processes.

2.2.2.2. United States

Historically, the US had most of its natural gas needs satisfied by its own natural gas production, although part of it was still imported (mainly from Canada). Nonetheless, its production has recently increased substantially due to the advancements in the technologies of horizontal drilling and hydraulic fracturing which allows them to be a net exporter of natural gas [64]. This trend is leading to the development of projects for pipeline exports and LNG. Its natural gas supply structure is similar to other ones worldwide with the primary activities being exploration and production, processing, transportation, storage, local distribution, and LNG [64].

The gas markets in the US are divided into gas transportation markets and physical commodity markets (wholesale natural gas markets) [65]. Market participants like producers, distribution companies, large end-users, and marketers can trade for gas capacity in the gas transportation markets and trade for gas energy in the wholesale natural gas markets. Pipeline companies operate the transportation networks and sell gas capacity in the gas transportation markets [66] [67]. The main natural gas markets in the US are placed at trading points for physical delivery, meaning that they are physical hubs. Figure 2.11 presents the major gas hubs in the US. The Henry Hub is the most known hub which serves as the pricing reference point for virtually the US natural gas market.

Figure 2.11 - Main North American gas trading locations (from [64]).

In the gas transportation markets, distribution companies, large end-users, and marketers usually take long-term contracts for capacity [65]. On the contrary, producers usually take short-term contracts as they are dependent on their demand which varies cyclically according to daily and seasonal conditions of the wholesale gas market. Capacity contracts can be bought in primary markets, at regulated prices, or secondary markets, at unregulated prices [68]. Agents that hold capacity rights, i.e. shippers, must notify pipeline companies on a daily basis about the receipt and delivery points and the daily scheduled quantity of gas flowing there [65]. Shippers can incur in imbalances penalties in case they have gas flow imbalances. During the gas day, shippers can adjust their schedule values to match the actual gas flows in intraday markets. Intraday markets have a minimum of three intraday sessions, which are required by the Federal Energy Regulatory Commission.

Market agents can buy or sell natural gas on a “spot” basis every day. Transactions are made through independent negotiations between buyers and sellers. This is the process chosen because this way, sellers can incorporate their costs of the natural gas and capacity rights, which differ according to the receipt and delivery points. This way, buyers and sellers agree on the price and the quantities of natural gas to be delivered at a specific location. There is also the possibility to negotiate monthly spot transactions, which happens on the last five business days of each month [64]. With these transactions, market agents negotiate the purchase and sale of gas to be delivered during the coming month. Buyers can also purchase gas under longer-term contracts, futures, and options in financial gas markets [69].

2.2.3. Emission trading systems

ETSs are market-based mechanisms that set emission caps in different sectors to incentivize the reduction of harmful emissions, like carbon. Identified emitters in these ETS are exposed to the external costs of emissions and must comply with the respective ETS caps and rules. Over the last years, several ETS were implemented while others already in activity were reformed and restructured with the new market mechanisms. Figure 2.12 presents the current state of ETS around the world. This subsection presents some of the ETSs already implemented including the EU, California, and New Zeeland ETS.

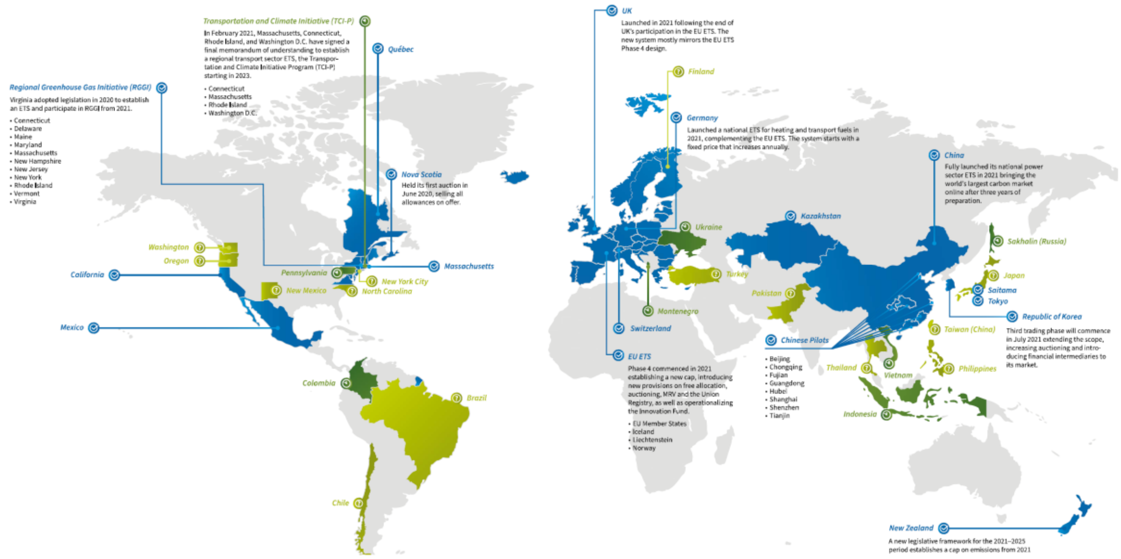

Figure 2.12 - Emissions trading systems worldwide (from [70]).

2.2.3.1. European Union

The EU ETS [3] was created in 2005 and it was the world's first international emissions trading system. It has been following different phases of development and in the current year, it entered in its 4th phase (2021-2030). This phase will be more demanding to participants as they will have more pressure to reduce their emissions. This system is seen as "the cornerstone of the Union's climate policy" and it is the main instrument to achieve the emissions reduction target [4].

The EU ETS is a 'cap and trade' system, which works by capping emissions [3]. A limited amount of emission allowances is issued per year by the EU to the Member States. An emission allowance is a right to emit an average greenhouse gas (GHG) equivalent to a tonne of CO_2. Companies must buy allowances and are taxed if they produce higher emissions than their allowances permit. This market covers electricity and heat generation, energy-intensive industries sectors, and aviation. In the actual regulatory system, 43% of total allowances are given for free to some participants, to avoid carbon leakage, and the other 57% are auctioned.

The auction format is a single-round, sealed bid and uniform price auction that occurs three times per week. They are run in a common platform, the European Energy Exchange, although some countries have their own platforms. Market participants can participate in any of these platforms. Member States act as auctioneers and ETS operators, aviation operators, or other eligible entity act as bidders. Small and medium size enterprises and small emitters can also participate in these markets and may do it through intermediaries as it can decrease market costs and ensure they have a minimum number of allowances to participate (500 allowances). The bidders can place any number of bids, specifying the number of allowances they want to buy at a given price (€/tCO_2). The clearing price is the price at which the sum of volumes matches or exceeds the volume of allowances auctioned. The auctions have a reserve price to ensure a minimum price. Market participants can also trade allowances between themselves. Figure 2.13 presents the EU cap and trade scheme.

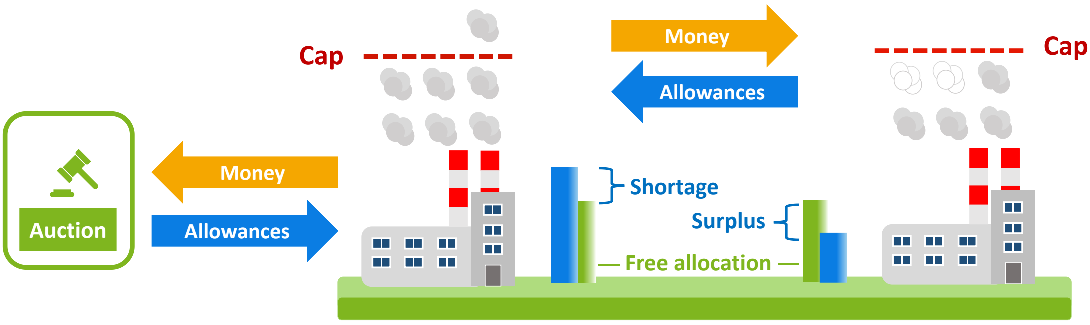

Figure 2.13 – European cap and trade scheme.

The participants that can apply for free allowances are identified in [9]. This list includes district heating providers and excludes generators of electricity, for example. The determination of the number of free allowances is done through 54 benchmarks. Each benchmark is calculated according to the GHG emissions of the best performing 10% of the installations producing that product.

Some installations can be excluded from this system if their yearly emissions are lower than 25 000 tonnes of CO_2 and if they have a thermal power lower than 35 MW in case they are identified in [9] and hospitals. Nonetheless, these installations must ensure equivalent measures of CO_2 reduction, unless their yearly emissions are lower than 2 500 tonnes of CO_2.

2.2.3.2. California

The California ETS was implemented in 2012. This system is a “cap-and-trade” program with allocation, auction distribution, and trading of instruments [71][70]. It covers 80% of the state’s GHG emissions, covering the power, industry, transport, and buildings sectors. Around 400 entities have compliance obligations. The compliance period started in 2013, with a cap of 162.8 MtCO_2e, and it has suffered several modifications over the years. Presently, it is in its fourth phase and its cap declines around 4% per year in order to reach 200.5 MtCO_2 in 2030 [70].

The installations included in this system must present allowances covering their yearly GHG emissions. Allowances can be distributed via free allocation, allocation with consignment, and auctions [70]. The free allowances are distributed to industrial facilities through specific benchmarks, production volumes, and adjustment factors. The total amount of free allowances declines over the years. Free allowances are distributed to industrial facilities, generators, public wholesale water entities, public service facilities, universities, and waste-to-energy facilities. Electrical distribution utilities and natural gas suppliers receive free allowances with consignment, i.e., on behalf of their ratepayers. These utilities must use their allowances and sell them in auctions to benefit ratepayers and reduce emissions [72]. Other entities that want to buy allowances can do it in quarterly state auctions or the private secondary market [72]. There is a reserve price, i.e. a minimum price per allowance, which increases annually by 5%. The allowances distributed in auctions represented 58% of the total California allowances issued in 2020. There is also a price containment reserve to protect entities against sudden price spikes, covering a certain percentage of the allowances under the cap [72].

Entities covered by the California ETS must present allowances covering 30 % of the emissions verified in the previous year (year i-1) by November 1 (year i) [70]. The remaining emissions of that previous year (year i-1) are covered by allowances presented until November 1 of the following year (year i+1). Emitters with more 10 000 tCO_2e per year must report their emissions through internal audits. If they fail to comply with covering their emissions, these entities are obliged to surrender the allowances covering the yearly emissions plus three additional allowances for each allowance failed to surrender. Ultimately, if they fail these obligations, they incur in substantial financial penalties.

The revenues from the auctions are returned directly to ratepayers or go to the Greenhouse Gas Reduction Fund which invests mainly in projects for reducing GHG emissions in low-income and disadvantaged communities [72].

2.2.3.3. New Zealand

The New Zealand ETS was implemented in 2008 and it is also a “cap-and-trade” system. It covers different sectors including power, industry, domestic aviation, transport, buildings, waste, forestry, and agriculture [70][73]. The agriculture sector only has the obligation of reporting and not acquiring emission allowances, although their emissions will be priced from 2025 onwards. This system has gone through several changes and the new regulatory framework for the 2021-2025 period implemented, for the first time, a cap on emissions [74]. This cap limits the units to be supplied to the ETS system.

Emitters must present allowances covering their yearly GHG emissions. Allowances can be distributed via free allocation and auctions [70]. Industrial activities can receive free allowances based on different benchmarks. Activities with high emissions can receive up to 90% free allocation while activities with moderate emissions can receive up to 60%. During the 2021-2030 period, there will be a phase-down for the number of free allowances allocated to the industrial sector, at an annual rate of 1% [73]. Auctions only started in 2021. They have a reserve price which acts as a price floor and also price control regulations which allow the release of more allowances to counteract high prices. Auctions are operated by the New Zealand Exchange and the European Exchange [70].

Most of the sectors (except the agricultural sector) covered by the New Zealand ETS must comply with their yearly emissions. If any entity does not provide enough allowances to cover their yearly emissions they must pay a penalty of three times the value of the current market price for the allowances not presented in due time [70].

2.2.4. Hydrogen market

Currently, there are not any hydrogen markets implemented worldwide. Nonetheless, several entities are working on developing this type of market. The EU, through its Hydrogen Strategy [75], is one of these entities. Within this strategy, several action points were implemented and delivered, in which one of them was to "design enabling market rules to the deployment of hydrogen" [76]. This strategy aims at removing barriers that hamper the development of hydrogen markets and infrastructures. This way, through this action, it proposed a regulation on the internal markets for hydrogen [77] covering hydrogen infrastructure, access to hydrogen markets, and the integrity of the market. This regulation addresses the access of hydrogen to gas infrastructures, like the VTPs and LNG terminals. This way, hydrogen may use the same infrastructure as natural gas, bringing cost savings and improving the decarbonization process of the gas sector. This proposal also introduces a European Network of Network Operators for Hydrogen which ensures the proper operation of the EU hydrogen network, facilitating the trade and supply of hydrogen. Another important point brought by this strategy is related with the gas quality: it allows blending in the natural gas up to 5% hydrogen.

2.2.5. Guarantees of origin market

GO are electronic certificates requested by energy producers that provide guaranteed information about the origin of products [78][3]. Usually, it is used as proof of the electricity generated from RES. There are four main types of GO worldwide: GOs from the EU (issued by the European Emission Certificate System), Renewable Energy GOs from the UK (issued by the Office of Gas and Electricity Market), renewable energy certificates from North America (issued by Green-e) and international renewable energy certificates worldwide (issued by the International Renewable Energy Certificate Standard Foundation). There are also other national systems like Australia [79], Japan, and Poland. This subsection describes the GO market from the European Union.

2.2.5.1. European Union market

In order to increase the dynamics and promote the integration of renewable generation there is a need for new products that increase energy markets' liquidity. This way, the EU proposed the creation of markets for GOs [78]. These markets create greater environmental awareness and offer consumers the chance to signal the energy markets for greener options. The European RES Directive (2018/2001/EC) [3] also supports these markets as it determines that the Member States should ensure that the origin of energy from RES can be guaranteed.

The GOs encompass different products such as electricity, heating, cooling, or hydrogen generated from RES or electricity generated from high-efficient cogeneration. These certificates indicate the source of the energy; the product (electricity, heating or cooling, hydrogen); the energy (in MWh); the dates when it was produced; the identity, location, type, and capacity of the production facility; if the installation benefited from any support scheme; the date when the installation became operational and the date and country of issue. They can be traded between agents from different countries in Europe as they are recognized by all Member States.

Figure 2.14 presents a typical scheme for the emission of GO for electricity generated from RES.

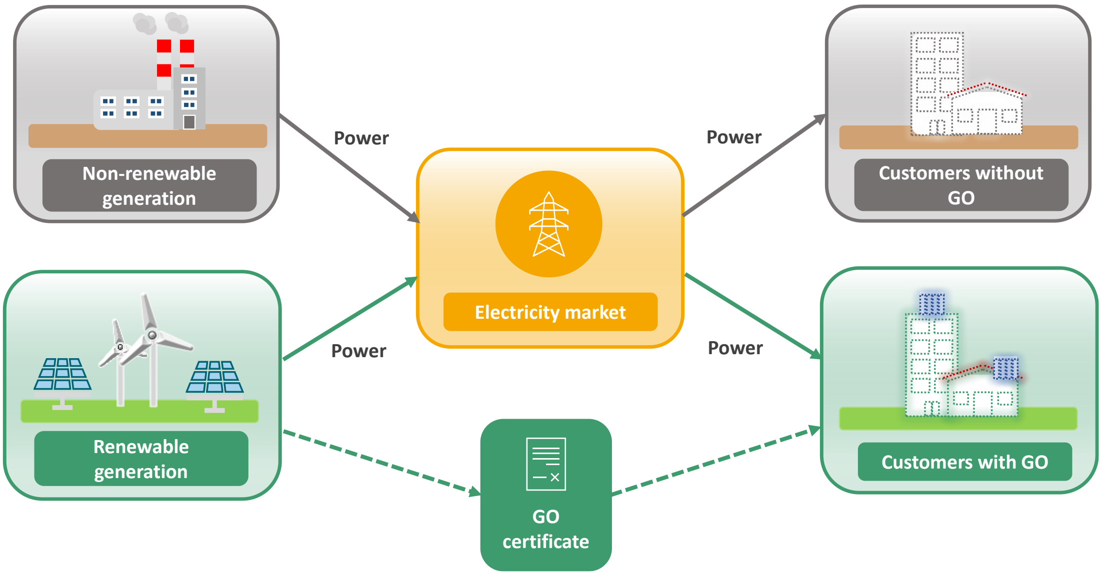

Figure 2.14 – Guarantees of origin (GOs) for electricity generated from renewable energy sources.

In relation to the GOs for the production of renewable hydrogen, there are additional rules that must be applied [80][81]. These rules are related to the temporal and geographical correlation between electricity production and fuel production units. This is done to incentivize the deployment of new renewable generation capacity (principle of additionality). The electricity can come from a RES directly connected to the production unit or from the grid. In case the electricity comes from the grid, in order to fully account for hydrogen as fully renewable, it must meet one of the following conditions:

- If it is produced in the same calendar hour as the generation of renewable electricity and there is not any electricity congestion in the grid between the installations producing hydrogen and generating electricity;
- if more renewable electricity is being produced in the bidding zone than on average;
- if the electricity prices are so low that the increased demand does not trigger additional generation from non-RES.

The GOs are sold and bought in auctions [78][3]. There is a reserve price which indicates the minimum price of the GOs. The marginal price of the auction is calculated through the intersection of the buying and selling curves. The auction is managed by the electricity market operator. It is foreseen that it exists at least one auction each month.

2.3. TSO/DSO-Aggregator coordination mechanisms

With the increase in the integration of DERs into the electricity distribution networks, there is an increase in the procurement of flexible services (i.e. frequency control, voltage control, or congestion management). The flexibility provided by DERs can be turned into flexible services through aggregators. This new source of flexibility can benefit both TSOs and DSO in the operation of their respective networks.

At the moment, there is an imposed separation between transmission and distribution networks. The coordination between TSOs and DSOs is very small or even inexistent in some regions. Usually, the TSO contracts resources from distribution grids without any DSO involvement. As local markets are still not a reality, the DSOs end up not having many options in procuring market services to operate their networks efficiently. This way, and in order to maximize the benefits that DERs can offer through AS markets to the global electricity system, there is a need to create better coordination mechanisms between the TSO, DSO, and aggregators. Coordination is important and necessary for an efficient and cost-effective operation of the networks, to avoid conflicted actions between the TSO and DSO, and to increase network observability.

2.3.1. Coordination schemes

Having this in mind, in the literature, different coordination schemes can be found [82][83]. The main ones are the centralized markets, local markets, shared balancing responsibility markets, common TSO-DSO markets, and integrated flexibility markets. These coordination schemes can be further simplified into three common approaches, as suggested in [84]: TSO centralized markets, local markets, and local (DSO) and global (TSO) markets.

2.3.1.1. Centralized market scheme

In the centralized market (Figure 2.15), the TSO/market operator (MO) are the only buyers. Resources from both the transmission and distribution networks (possibly through aggregators) participate in this market. The role of the DSO is very small as the TSO/MO contracts all resources directly. The only possible role of the DSO is when a prequalification process is implemented. This pre-qualification process is done before the market clearing and its purpose is to ensure that the TSO/MO management of DERs does not violate distribution network constraints. This step can be seen as a pre-congestion management step.

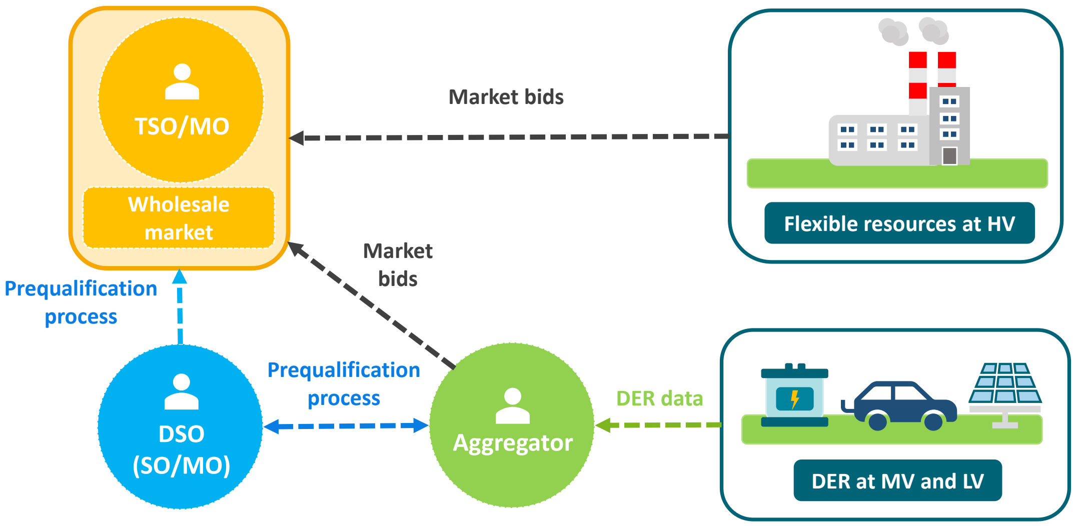

Figure 2.15 - Centralized reserves market scheme.

2.3.1.2. Local market scheme

In the local market (Figure 2.16), there is a wholesale market operated by the TSO/MO and a local market operated by the DSO. The local market is run before the wholesale market. The aggregators offer their bids first to the local market. The DSO clears the local market and the remaining non-used market bids from the aggregators are transferred to the wholesale market. The DSO is able to ensure that only distribution network-secure market bids are selected in the local market or transferred to the wholesale market. It can also be able to select bids that fit the TSO/MO's products requirements. To avoid imbalances within the transmission network, the TSO/MO can make corrective actions.

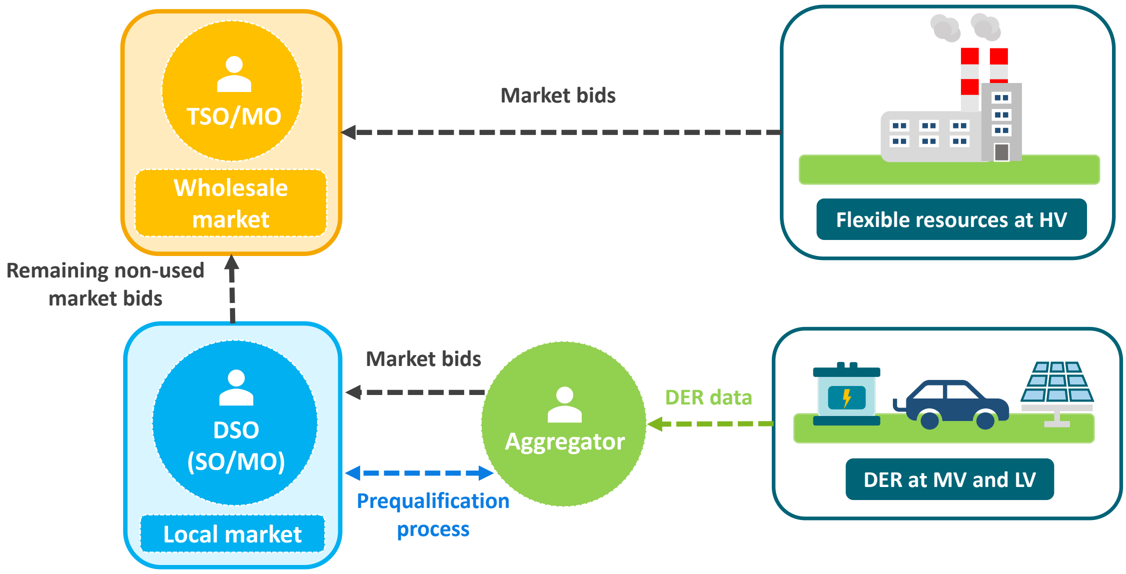

Figure 2.16 - Local reserves market scheme.

2.3.1.3. Shared balancing responsibility market scheme

In the shared balancing responsibility market (Figure 2.17), there is a wholesale market operated by the TSO/MO and a local market operated by the DSO. The aggregators of DER can only participate in local markets. There is a schedule balancing setpoint agreed upon between the TSO/MO and DSO for the entire DSO area or each individual TSO-DSO interconnection point. This way, the TSO/MO are responsible for maintaining the balance of the transmission grid and the DSO is responsible for keeping the scheduled balancing point, solving local congestions, and local balancing in the distribution grid at the same time.

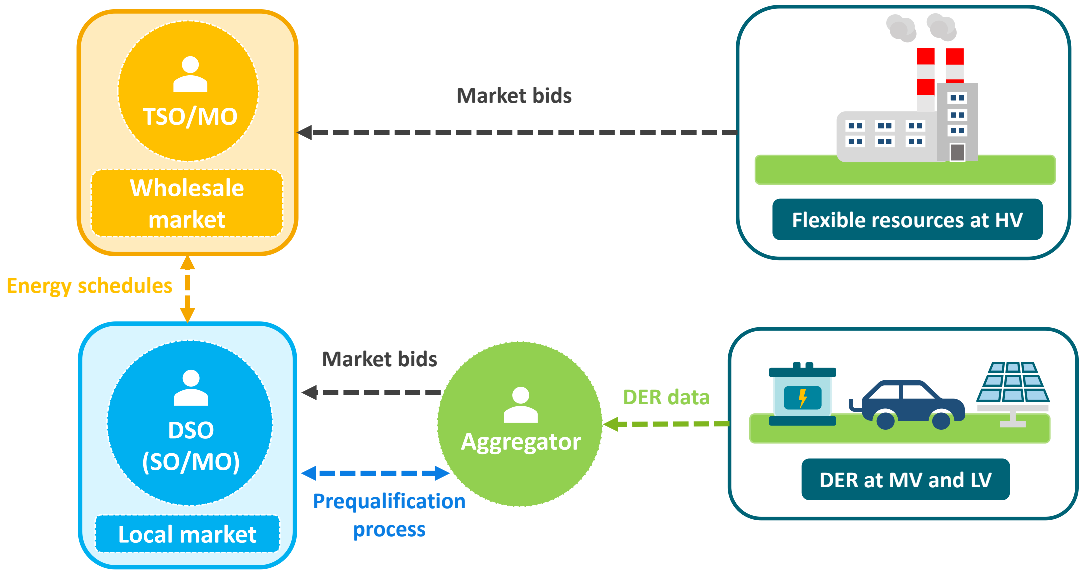

Figure 2.17 - Shared balancing responsibility market scheme.

2.3.1.4. Common TSO-DSO market scheme

In the common TSO-DSO market scheme (Figure 2.18), both TSO/MO and DSO participate and operate the wholesale market. Both transmission and distribution resources participate in this market. There is no priority in this market and the flexibility is allocated accordingly to the highest needs of the operators, taking into account social welfare. This market can be implemented through two variants:

- In the first one, all bids are cleared in one market session considering both transmission and distribution network constraints. The computational process can be very heavy in this variant due to the high quantity of constraints that represent all resources and networks.

- In the second variant, a local market run by the DSO with only distribution resources is implemented. First, the DSO clears this market, without any formal commitments. Then, it transmits the results to the TSO/MO which are integrated into the clearing process of the global market. When the global market is cleared, the TSO/MO informs the DSO of the selected bids from the local market.

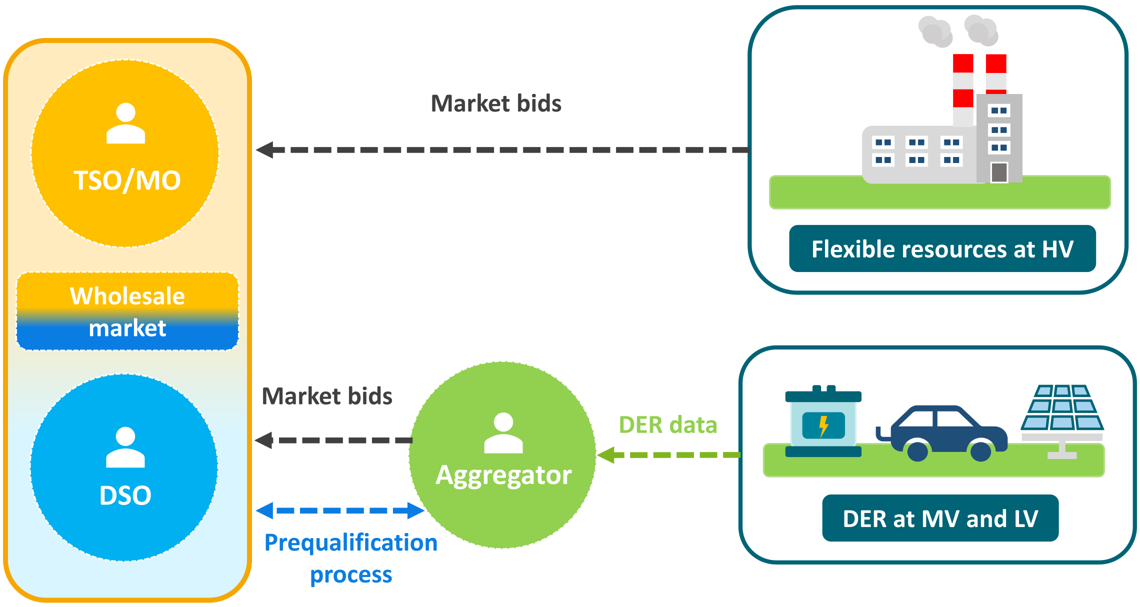

Figure 2.18 - Common TSO-DSO reserves market scheme.

2.3.1.5. Integrated flexibility market

In the integrated flexibility market (Figure 2.19), the wholesale market is run by an independent operator. This occurs because regulated (i.e. TSO/MO and DSO) and non-regulated agents participate in this market. The independent operator ensures the neutrality of the market operation. There is no priority in this market and flexibility is allocated according to the highest needs of the operators. The market bids of both transmission and distribution resources are offered to the wholesale market.

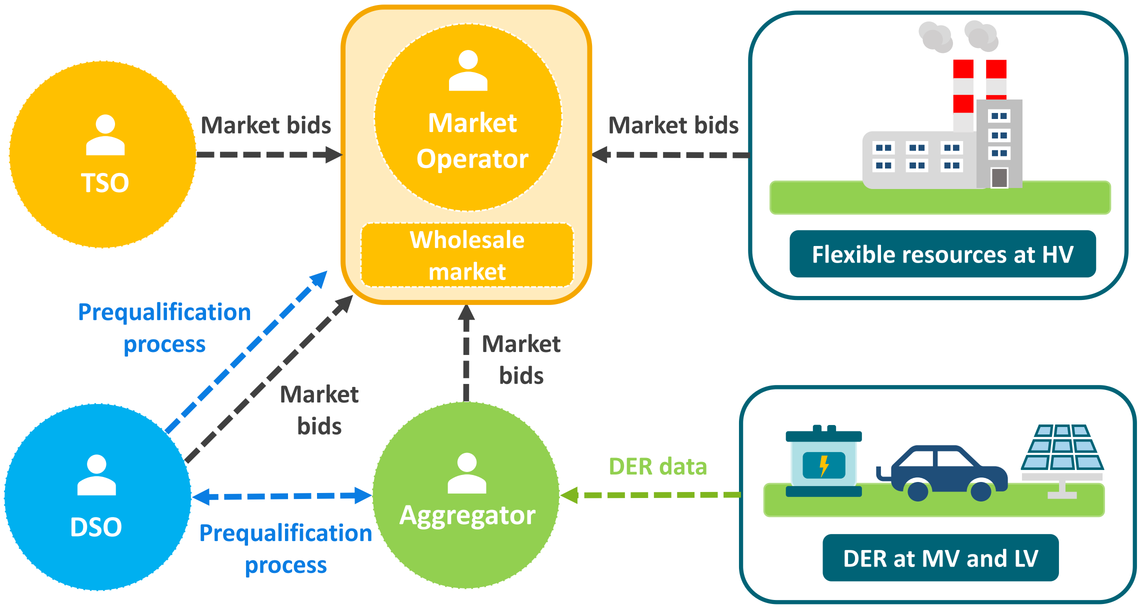

Figure 2.19 - Integrated flexibility market.

2.3.2. Overview of the coordination market schemes

Table 2.1 presents an overview of the five coordination market schemes presented in the previous subsection. This table indicates the operator of the wholesale market, the existence of local markets and its operator, the role of the DSO, and who can use distribution resources.

Table 2.1 - Overview of the coordination market schemes.

Coordination scheme	Wholesale market	Local market	Role of DSO	Use of distribution resources
Centralized market	Operated by TSO/MO	Nonexistent	Prequalification process / congestion management	Only by TSO/MO
Local market	Operated by TSO/MO	Operated by DSO	Market operator Congestion management	First by DSO, and then by TSO/MO
Shared responsibility balancing market	Operated by TSO/MO	Operated by DSO	Market operator Congestion and balancing management	Only by DSO
Common TSO-DSO market	Two options: 1. Operated by TSO/MO and DSO 2. Operated by TSO/MO	Two options: 1. Nonexistent 2. Operated by DSO	Market operator Congestion management	By TSO/MO and DSO
Integrated flexibility market	Operated by the independent market operator	Nonexistent	Congestion management	By TSO/MO and DSO

The roles of the TSO/MO and DSO differ among the coordination market schemes. Nonetheless, an expansion of the role of the DSO is clearly seen in most of the market schemes, as it will become a more active player in the markets. The DSO's presence will enable the consideration of the distribution network constraints in the market process. This can be done by a prequalification of the bids, by integrating the distribution network constraints directly in the market clearing process, or by an iterative process with post-qualification of the bids after the market clearing. Moreover, the DSO will also become an active buyer of reserves and be responsible for local or even the wholesale market (in pair with the TSO/MO) in some of the coordination schemes.

In terms of advantages and disadvantages of each market scheme, the following can be found:

- The centralized market can benefit from its easy implementation and low-cost operation, not requiring extensive regulation changes. The role of the DSO in this market is still not very active as they are not able to acquire services in competitive auctions. Nonetheless, if these markets consider a pre-qualification of the bids, the DSO is able to guarantee the feasibility of the bids considering the distribution networks constraints;

- The local and shared balancing responsibility markets already consider a more active role of the DSO and the consideration of distribution network constraints. Nonetheless, in case local markets are small, the illiquidity of the markets may occur. Moreover, they require significative regulation changes, and the coordination tasks are harder to implement;

- The common TSO-DSO and the integrated flexibility markets address the liquidity problem of the previous two market schemes. Nonetheless, the necessary communications between TSO/MO, DSO, and aggregators increase the complexity of these markets and computational efforts, and difficult its optimal operation. Moreover, it also requires significant regulatory changes.

In terms of implementation feasibility, the centralized market is the most promising one taking into account the actual regulatory framework. Nonetheless, a new organization of regulatory frameworks can be adopted to integrate other coordination market mechanisms.

2.4. Multi-energy aggregators

The transition toward cleaner energy systems is driving its development into a more integrated system [10]. This means that TSOs, DSOs, and other stakeholders will have new roles with more collaborative tasks among themselves. Moreover, it is foreseen the market participation of small prosumers. To better use prosumers' flexibility and to optimize their participation in wholesale markets, the concept of aggregators was developed. Aggregators are able to control and optimize prosumers' resources to maximize profits when participating in wholesale markets by using bidding strategies.

In this subsection, we describe the concept and role of aggregators (2.4.1), the regulatory framework related with aggregators in different parts of the world (2.4.2), their structure (2.4.3) and value (2.4.4), some real-world projects (2.4.5) and finally, DA bidding and RT control strategies described in the literature (2.4.6).

2.4.1. Concept and role

The role of the aggregator is defined in the (EU) 2019/944 Directive [85] as the "function performed by a natural or legal person who combines multiple customer loads or generated electricity for sale, purchase or auction in any electricity market". This role can be extended to the participation in other wholesale markets, including natural gas [86][87], thermal [88][89], hydrogen [90], or other markets. They may have the responsibility of supplying energy to costumers or only be responsible for flexibility contracts and respective activation. This way, aggregators facilitate the participation of small prosumers who could find their participation in muti-energy markets very hard due to market complexities, lack of know-how, and high costs related with market participation.

2.4.2. Regulatory framework

The regulatory frameworks of energy markets around the world have seen recent updates to incorporate the concept of aggregators. This can be seen in Europe, the USA, and Australia.

In Europe, the (EU) 2019/943 Electricity Regulation [91] and (EU) 2019/944 Directive [85] revise the rules and principles that electricity markets will undergo to adjust to the decarbonization of energy systems and the integration of RES. The driving forces of these regulations are enabling markets to allow the improvement of energy efficiency and facilitation of RES' integration; non-discriminatory market access of individual participants or through aggregation; and an effective and transparent market. In particular, this regulation emphasizes the market participation of generation and loads of small customers through aggregation. It mentions the participation and bidding of small market products in the order of 500 kW or less, promoting the participation of smaller agents and benefitting the aggregation of DMERs. The installation of smart meters in consumers' premises also incentivizes energy efficiency and facilitates the participation of small consumers in energy markets.

In the USA, the Federal Energy Regulatory Commission released Order No. 2222 in September 2020 [92]. This order imposes on the ISO and regional transmission organization (RTO) the development of a wholesale market to integrate the participation of DERs and DR through aggregators. This is done so DERs and DR providers can provide and be compensated for market services This order identifies the importance of creating new market mechanisms that increase networks' observability and cooperation between ISO, RTOs, and aggregators in order to preserve its safety, reliability, and resilience. It foresees the development of new roles for the different parties, tools, technologies, and protocols in order to facilitate the convergence of the wholesale market functions (ISO/RTO dispatch and aggregators bidding) and the distribution system operation. RTOs and ISOs shall revise their tariff systems to allow aggregators to offer energy, capacity, and AS to the respective markets. It also states that a DER is "any resource located on the distribution system, any subsystem thereof or behind a customer meter." Some of the identified DMERs were ESSs, EVs, intermittent or distributed generation, and thermal storage. It requires aggregators to have a minimum size of 100 kW and to specify how much of the total flexibility offered comes from each node.

In Australia, aggregators of small generating units were already able to participate in electricity markets since 2013 [93]. In 2016, a rule was proposed to allow the participation of the demand side in the FCAS markets [94]. This way, DR loads can participate in these markets individually or through aggregators to reduce their load according to the market needs. In 2018, a new rule proposed a wholesale DR mechanism [95]. Under this rule, consumers can sell DR in the wholesale market directly or through aggregators. They are able to bid in the wholesale market indicating the prices and energy to be consumed. This rule is directed to large consumers (industrial, commercial) although it states the importance of developing a two-sided market to include small consumers (residential). Nonetheless, the electricity markets did not recognize the capability of some resources to have bi-directional flows. This meant that aggregators with ESS or other hybrid systems had to differentiate their participation in electricity markets as consumers or as generators. They had to bid separately for generation and load and could not combine it into a single bid. ESSs lower than 5 MW were only seen as generators and were included in the portfolio of small generator aggregators. Their load side was not recognized and could not participate in market services. In 2021, a new rule was proposed to create a new category to consider bi-directional resources called integrated resource provider [96]. This category recognizes participants that consume and provide energy, like battery storage and other hybrid systems, and their participation in AS markets. This way, aggregators can now combine both load and generation tranches in the same bid and provide AS from load and generation. This creates the opportunity for better returns of investment for aggregators.

2.4.3. Aggregator frameworks

This subsection presents typical architectures of aggregators, portfolios of clients and resources, the home/building energy management systems (EMSs), and DR programs that are usually implemented.

2.4.3.1. Architecture

Typically, the architecture of aggregators has the purpose of facilitating its participation in energy and AS markets. They usually interact with downstream parties (prosumers) and a diverse range of upstream parties (DSO, TSO, market operator) according to the market schemes. Usually, the first step of the aggregator is to optimize its portfolio of resources. With the flexibility available, it calculates the bids to be offered in the DA multi-energy and AS markets. The aggregator can also sell AS directly to the TSO or DSO. Then, during the RT operation, the aggregators can activate the services offered in the DA markets through automatic or manual control [97][98] or price-volume signals (€/kWh) [99][100]. These signals depend on the contracts agreed between the aggregator and consumer and are explored in more detail in section 2.4.3.4.

Figure 2.20 presents a typical architecture of aggregators.

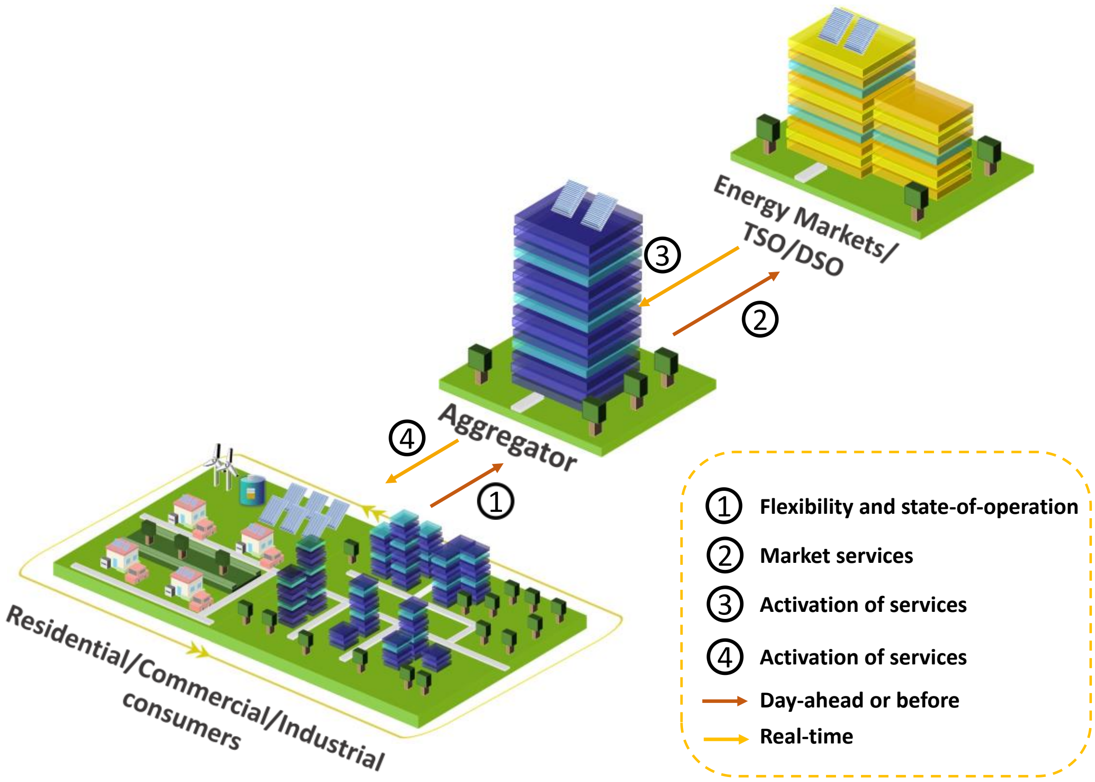

Figure 2.20 - Typical architecture of aggregators.

2.4.3.2. Portfolio of aggregators

The portfolio of aggregators can include residential [101][102], commercial [103], or industrial [104] customers. Aggregators have the capability of controlling a vast range of DMERs connected to the electricity, gas, and heat distribution networks. The DMERs usually explored by aggregators can include continuous loads like ACs [105], CHPs [106], ESSs [107], electrolyzers [90], EVs [101][102][108][109], FCs [110], HPs [111], hydrogen storage [90], PVs [101][102], thermal loads (heating and cooling) [101][102][112], etc, and shiftable loads [113] like fridges, ovens, washing machines, etc. These resources can be a source of demand and/or generation electricity flexibility (Table 2.2). The aggregators may also be responsible for supplying energy to prosumers, satisfying the needs of their inflexible electricity, gas, and heat loads.

Table 2.2 - Sources of demand and generation flexibility.

Sources of demand flexibility	Sources of generation flexibility
Air conditioners	Combined heat and power
Energy storage systems	Energy storage systems
Electrolyzers	Fuel cells
Heat pumps	PVs
Shiftable loads	
Thermal loads	

2.4.3.3. Home/building energy management systems

The aggregator usually communicates with prosumers and controls these resources through EMSs. EMSs are smart metering platforms that incorporate a set of capabilities providing control over DMERs [85][17][114][115]. These capabilities include submetering of local resources; monitoring and acquiring the resources' state-of-operation; prosumers' ability to configure their own settings according to their needs and other engagement functionalities; controlling the devices through set-points; energy management; communication between prosumers and agents like aggregators, retailers, DSOs, TSOs and weather service providers; visualization tools and security functionalities to secure the privacy of data and communications. Several EMSs are already available in the market including the ones from EDP [116], IBM [117], and Samsung [118]. Figure 2.21 presents an EMS scheme.

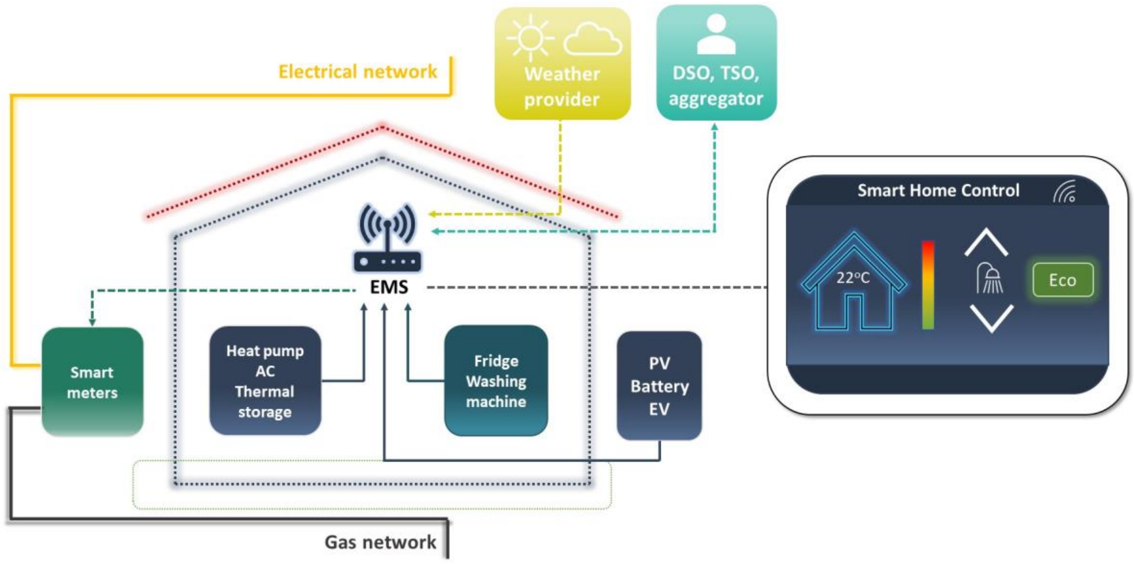

Figure 2.21 – Energy management scheme.

2.4.3.4. Demand response programs

Consumers allow aggregators to explore the flexibility of their multi-energy resources according to the DR contract agreed upon. There are five DR contracts that are usually considered [119][120][121]: time of use pricing, dynamic pricing, fixed load capping, dynamic load capping, and direct load control. The elected contract is usually related to the resources available for exploration.

The aggregators activate the requested services through a DR signal. The DR signal varies with the contract chosen and they can be based on prices (through tariffs) or volume (i.e. electric power consumption/generation). The signals can also be static (long notice and extended intervals) or dynamic (short notice and shorter intervals). Dynamic signals have the benefit of being better adapted to the reality of the wholesale markets. There is also a control-based contract in which the consumer's resources are directly controlled by the aggregator or other controlling agent.

In each of these contracts, there are different levels of risk related with prices, volume, complexity, loss of autonomy or privacy, and financial compensation. The price risk is related with the uncertainty of the consumer's prices and consumers might end up with higher costs in case they do not respond to the price signal accordingly. The volume risk is related with the uncertainty of power available for consumers which might be less or more than what they would want to consume at the moment. Complexity is related with the difficulties that consumers might find in understating what is expected from them to comply with the DR signals. The loss of autonomy and privacy is related to the fact that in some contracts the consumer's resources are controlled by other entities. This can limit the use of their own resources and expose personal information regarding resources use practices. The financial compensation risk is related with higher or lower compensation that may be available to consumers.

Table 2.3 identifies the characteristics of each DR contract [119].

Table 2.3 - Demand response contracts characteristics [119].

Contract	Signal form	Signal volatility	Financial compensation	Price risk	Volume risk	Complexity	Autonomy / Privacy
Time of use	Price	Static	Limited	Low	None	Low	None
Dynamic pricing	Price	Dynamic	Hight	High	None	High	None
Fixed load capping	Volume	Static	Limited	None	Low	High	Limited
Dynamic load capping	Volume	Dynamic	High	None	High	High	Limited
Direct load control	Control	Pre-defined	Limited/ High	None	None	None	High

The contracts just explained need the intermediaries to be active along the different phases of writing, agreement, activation, and settlement of contracts. With a higher volume of DERs and prosumers, and correspondingly a higher volume of contracts, the contract processes can become very laborious and with complications, especially in the settlement phase. This way, it is important to note the existence of a new type of contract that can facilitate the activation of DR programs: smart contracts. Smart contracts are self-executing programs integrated into a blockchain technology [122]. These contracts are automated peer-to-peer contracts that are executed when a specific set of pre-determined conditions are met. They do not require the active participation of the different intermediaries. They can bring benefits to the energy sector as they allow transactions between different parties with increased automation, security, transparency, and reduced transaction costs. This way, they are prone to incentivize the implementation of a decentralized system that facilitates the participation of small prosumers in energy markets and their interactions with other parties, like aggregators or system operators. As they can include DR options [123], the response in RT to the reserve market services can be much faster and facilitated, bringing benefits to the energy system operation and management. They also facilitate the settlement process as it is automated and based on the values directly read by the smart meters. Nonetheless, these contracts are still in the phase of research, proof-of concept, or being implemented in demonstration projects.

2.4.4. The value of aggregators

Aggregators can add value to energy systems and markets. These values can be divided into intrinsic or transitory values [124]. Intrinsic values are values that are inherent to aggregators and do not depend so much on actual regulatory frameworks or the level of technology of the power networks; they should be perceived as permanent values. Transitory values are values that depend on actual regulatory frameworks or other aspects and may improve with time due to new developments and innovation.

In relation to intrinsic values, it is possible to identify capitalization on economies of scale, management of uncertainty and price risks, and improving competition and innovation. The capitalization on economies of scale is related with the fact that the aggregator aggregates all the costs related with market participation, energy transactions, and technology infrastructure required to exercise its activity [125]. This way, the total costs are intrinsically minimized [126][127]. In relation to the managing of uncertainty and price risks, an aggregator with a large and diversified portfolio of consumers and resources is able to mitigate that uncertainty and risks due to aggregation. With the rise of aggregators, there will be more competition among themselves and retailers or other market entities [128]. This can stimulate more competitive prices, the integration of DERs, the creation of other customized market products, and technology innovations.

Regarding beneficial regulatory and market frameworks, aggregators can create and unlock value related with market complexities, information gaps, agent engagement, and coordination market mechanisms. Aggregators can help consumers by providing them with the necessary information to optimize the selection and management of their resources and technologies, their market participation [126] and above all, optimize their energy costs. With more detailed information on downstream resources, aggregators may also help system operators in their operational and planning tasks. Moreover, the existence of aggregators can facilitate the coordination between different market and system agents and the implementation of certain market mechanisms [125] (as described in section 2.3).

Focusing on the consumer's benefits, in the literature it is possible to find a vast range of works that quantify the value that aggregators bring to consumers. Among those works are the following: in [129], savings in the order of 40-106$/year due to the aggregation of 800 houses with space heating and cooling systems are presented; in [130], revenues of 73€/year are presented due to the aggregation of 1500 residential consumers and the optimal participation of their TCLs in the tertiary reserve market; in [131], savings of 22-233 $/year per TCL and 182-193 $/year per EV are presented; in [132], savings of 12.8-57.6 €/year per house are presented for the aggregation of 1000 households.

Figure 2.22 presents the values identified in this subsection.

Figure 2.22 - The value of aggregators.

2.4.5. Current real-world aggregators

There is already a diverse range of aggregators or entities with similar roles (i.e. virtual power plants (VPP)) to participate in energy markets [133][134]. These companies already provide flexibility or DR services to the markets or system operators and control a vast range of resources and different types of consumers. Most of these companies are based in the USA, Germany, the UK, or Australia. A few examples are mentioned below.

In the Netherlands, the Eneco utility company started CrowdNett [135], a VPP composed of a network of batteries. These batteries are installed in prosumers' homes and have the purpose of improving self-consumption (in pair with PVs) and providing AS to the markets. In Germany, the sonnenCommunity [136] is an aggregator composed of around 10 000 customers. It is able to manage its customer's battery storage and PV systems to provide frequency regulation. Fluence [137], a provider of storage solutions and digital applications provides market bidding services to several entities, including an energy community with 10 MW ESS in California, the Pacific Gas and Electric company with 182.5 MW ESS in California, among other projects, including some in Australia. Ecotricity [138] is an aggregator with RES, ESSs, and residential customers that participates in DA energy markets. It has a portfolio with 87.2 MW of wind generation and 1 MW of solar generation. Energy2market [139] from Germany, is a VPP that aggregates 3 185 MW of generation including wind, PV, CHP, hydroelectric power stations, and

CCGT, thousands of consumers through DR programs and ESS participating in energy and reserve markets. Enel X [140], is a company based in the USA (and also present in 19 other countries) that offers solutions for electric mobility and industrial and commercial consumers to participate in energy and reserve markets. It expects to aggregate 10.6 GW of DR by 2023. Flexitricity [141] is a DR aggregator based in the UK with 500 MW of flexible assets that participates in the energy and reserve markets. Sunrun [142], based in the USA, aggregates residential solar and ESSs to provide frequency regulation and spinning reserves. Energy Australia [143] has an aggregation business, which manages industrial and commercial consumers, in order to optimize their flexibility and sell it as services in wholesale markets.

2.4.6. Decision-support optimization tools for multi-energy aggregators

This subsection describes the literature about decision-support optimization tools for multi-energy aggregators. These tools transform the flexibility of DMERs into different multi-energy market services. These market services can be traded in multi-energy markets like electricity (energy and reserves), natural gas, thermal, or hydrogen markets.

There are two major groups of decision-support optimization tools which are presented in the following subsections:

1. **Day-ahead:** optimization models for aggregators to compute bids for DA markets (section 2.4.6.1);

2. **Real-time:** optimization approaches for aggregators to deliver services traded in DA markets (section 2.4.6.2).

2.4.6.1. Day-ahead

Aggregators use DA decision-support tools to compute bids for multi-energy DA markets. These tools are also known as bidding optimization models or strategies. In this regard, the literature presents a wide range of DA decision-support tools.

In [144], the authors developed a deterministic optimization model to consider the participation in the DA energy and tertiary market of the Iberian Electricity Market (MIBEL). The optimization model optimizes the charging of EVs by considering point forecasts for the DA energy prices and driving patterns. The same authors developed a similar model but considering the participation in DA energy and secondary reserves market of MIBEL [145].

To better account for the uncertainty of different aspects of the bidding process, some works developed stochastic optimization models. In [101], the authors developed a two-stage stochastic optimization model that calculates bids to participate in the DA electricity energy and secondary reserves markets. This optimization model optimizes the prosumer's resources to minimize the costs of purchasing and selling energy and secondary reserves in the DA electricity markets. It models the uncertainties of renewable generation, energy consumption, house occupancy, and outdoor temperature through a set of scenarios. The same authors also developed other similar stochastic optimization models that consider the participation solely in the energy market [146][147][148] and also in the tertiary market [102]. In [146], the authors compared the two-stage stochastic optimization model with a single-stage deterministic model and concluded that the first model outperformed the second model by 2%.

Another approach for considering uncertainty is through robust optimization. Reference [103] proposed a robust optimization model that considers the participation of commercial buildings in DA energy and secondary reserves markets. The model developed in [149] is also a robust optimization model to determine the aggregated scheduling of ESS and wind generation resources and optimize their participation in energy and secondary reserve markets.

As we can see, the works found in the literature consider different optimization models like deterministic [144][145], stochastic [101][102][148], or robust optimization models [103]. The models can also consider the participation in various electricity markets. Some works only considered the participation in electricity energy markets [148] while others also considered the participation in secondary [145][101] or tertiary [102] reserve markets.

Works related with bidding models for multi-energy aggregators that participate in multi-energy markets are scarcer. However, some works considered the participation in multiple markets including the natural gas [86][87], thermal [88][89], and hydrogen [90] markets.

In [86] and [87], a bi-level programming framework for aggregators was developed. In this model, the aggregators trade electricity and natural gas in the respective DA markets and with local energy networks equipped with resources participating through DR programs. Ref. [88] proposes a stochastic model for aggregators to participate in DA electricity and thermal markets. In [89], the authors developed an adaptive robust bidding model to participate in DA electricity and thermal energy markets, considering the uncertainty of loads and energy prices. In [90], the authors proposed a scenario-based stochastic method to optimize the participation of a wind-electrolytic HSS in electricity and hydrogen energy markets.

The optimization bidding models from [86]-[89][101]-[103][144]-[148][150] are network-free. This means that they do not consider network constraints in the bidding optimization process. Therefore, they may compute network-infeasible bids, which violate the physical limits of multi-energy networks [150][107]. This situation is especially prone to happen in scenarios of high DMER integration. The costs of operating distribution networks may increase as DSOs may need to procure and purchase market services to solve possible congestion and voltage problems. DSOs may also need to curtail load or generation. In this regard, aggregators may see their market bids curtailed by DSOs and their market services may not be fully delivered. In this situation, aggregators are penalized by paying fines for the services not delivered. In extreme situations, they may be even expelled from the markets.

To counteract the mentioned problems, several works in the literature developed optimization bidding models that consider electricity network constraints. These models provide better observability over the distribution networks, which may benefit their secure and optimal operation.

The work developed in [151] presents a multi-stage scenario based optimal power flow for the operation of a multi-energy VPP. With this model, the VPPs are able to participate in multiple markets, including in electricity (energy and reserve) and hydrogen markets, while considering local network constraints. To alleviate the non-linearity of the original problem, this framework decomposes the problem using linearization techniques. In [152], another optimization framework for VPPs to participate in multiple markets, including in energy, reserve, DR, and hedging contracts markets, was developed. This model considers electricity network constraints and uses a linear approximation of the active and reactive power constraints. The authors in [153] developed an optimization model that optimizes the market participation of a price-maker energy service provider through a Stackelberg game. This model also considers the electricity network constraints using the linearized DistFlow equations.

The network-constrained bidding models [151][152][153] are centralized, as they consider the joint optimization of bidding (aggregator) and network (DSO) problems. These models force the sharing of electricity DSO's network data (e.g. network characteristics and topology) with the aggregator and thus, the DSO's data privacy is not preserved. This may become a legal problem in regions where jurisdictions do not allow the sharing of network data. On the other hand, distributed approaches solve the aggregator and network problems separately and in a distributed manner. This way, the data privacy of aggregators (e.g. habit patterns and DER data) and DSOs is secured. These distributed approaches, usually use the ADMM to solve the aggregator and network problems and to compute network-secure bids [150][154]. The model developed in [150], calculates network-secure bids to participate in the electricity energy and reserves markets using the ADMM. Thus, the bids calculated do not violate any electricity network constraints while also maintaining the data privacy of both the DSO and aggregator. Also in [154], the authors presented a similar distributed optimization framework but now considering the uncertainty of the inflexible load, EV requirements, and PV generation through a set of scenarios.

Another advantage of the distributed approaches is that they are able to divide the original problem into smaller and less complex problems. This is important because, as we could see from the centralized approaches from [151][152][153], in order to consider the electricity network constraints, the authors had to use linearization techniques. These linearization techniques along with other simplifications turn the non-convex solution space of the network problems into a convex space which may reduce the feasible space [155], or even expand the original solution space to infeasible areas. In practice, linear network models are prone to compute network infeasible solutions in scenarios of low voltages [156][157]. This way, distributed approaches are able to solve the original problem without relying on simplified network models, which improves the feasibility of the original optimization problem.

Table 2.4 presents the DA bidding strategies identified in this subsection. It identifies the bidding strategies used (centralized or distributed), the uncertainty modeling (deterministic, stochastic, or robust), the energy and reserve markets considered, the regions of the markets and case study, and if they consider network constraints.

Table 2.4 - Day-ahead bidding strategies.

Paper	Bidding strategy	Uncertainty modeling	Markets	Region	Network constraints
[144]	Centralized	Deterministic	Energy	Europe	-

			Tertiary		
[145]	Centralized	Deterministic	Energy Secondary	Europe	-
[101]	Centralized	Stochastic	Energy Secondary	Europe	-
[102]	Centralized	Stochastic	Energy Tertiary	Europe	-
[146][147][148]	Centralized	Stochastic	Energy	Europe	-
[103]	Centralized	Robust	Energy Secondary	Europe	
[149]	Centralized	Robust	Energy Secondary	USA	
[86][87]	Centralized	Deterministic	Energy Gas	-	-
[88]	Centralized	Stochastic	Energy Thermal	-	
[89]	Centralized	Robust	Energy Thermal	Iran	-
[90]	Centralized	Stochastic	Energy Hydrogen	Europe	
[151]	Centralized	Stochastic	Energy FCAS Hydrogen	Australia	Electricity
[152]	Centralized	Deterministic	Energy FCAS	Australia	Electricity
[153]	Centralized	Deterministic	Energy	Europe	Electricity
[150]	Distributed	Deterministic	Energy Secondary	Europe	Electricity
[107]	Distributed	Deterministic	Energy FCAS	Australia	Electricity
[154]	Distributed	Stochastic	Energy Secondary	Europe	Electricity

2.4.6.2. Real-time

In relation to the first group of decision-support optimization tools, the second group is not as common in the literature. This group encompasses RT decision-support optimization tools used by aggregators to deliver the market services traded in the DA markets.

The RT decision-support optimization tools used by aggregators optimize the operation of DMERs so that they can deliver market services that comply with DA market commitments. In the literature, it is possible to find a vast range of algorithms that consider the delivery of market services, such as energy [108][109][112][144][105][111] and reserves [144] [105][111].

The authors in [108] and [109] present a bidding optimization framework for an aggregator of EVs to participate in the DA energy market. They propose a MPC framework, which uses a deterministic model to minimize the deviation costs between DA bids and RT operation costs. In [112], a two-level framework for an aggregator of thermal loads was proposed. This framework schedules the flexibility available through the thermal loads to participate in intraday electricity markets. The upper level of this framework uses a MPC to minimize the energy and capacity imbalance costs while the lower-level controls the thermostatically controlled loads.

The work developed in [144] also presents an operation algorithm that coordinates the charging of an EV fleet that mitigates forecast errors. This algorithm can track the AGC signal and is run in continuous mode. The authors in [105] proposed a three-level hierarchical control to deliver secondary reserve within a building aggregation. In level 1, the daily optimal reserve capacity is determined; in level 2, an MPC is used to minimize energy consumption while taking into account the reserve needs; in level 3, a controller modifies the operation of the resources to follow the AGC signal. In [111], the authors developed a hierarchical MPC to deliver market services taking into account the DA energy and secondary reserve bids offered in the DA markets. This MPC has two levels: level 1 is a deterministic optimization model that determines the operating points and bands of the flexible resources to minimize the net cost of delivering the market services; level 2 is a controller that adjusts the operating points of the flexible resources according to the band defined in level 1 and the AGC signal received. This model can optimize the operation of thermal loads, EVs and PVs.

The authors in [158] developed and MPC to provide near RT balancing services for an aggregator of micro-CHPs. The aggregator participates in the electricity and natural gas markets. In this model, an optimization for the entire time horizon (24h) is performed. This horizon is divided into 15 min time steps and only the first time slot is implemented. This procedure is repeated during the rest of the time horizon. In [159], a stochastic MPC scheme was proposed to optimize a VPP comprising PVs, P2Gs, FCs, and HSSs. The VPP participates in the electricity and hydrogen energy markets.

As we can observe, most of the RT decision-support optimization tools exploit MPC frameworks to optimize the operation of DMERs according to the most accurate data in RT. These frameworks allow aggregators to minimize their costs as they reduce imbalances between RT delivery and DA market commitments. They also increase the reliability of the market services offered by aggregators which is important in the market context.

The RT decision-support optimization tools from [108][109][112][144][105][111] are network-free. As we have seen in the literature for DA algorithms, the lack of observability in the energy networks can make the market services offered in the DA market to not be delivered. Taking this into account, different works developed network-secure (from the electricity network perspective) RT optimization approaches. These models can be centralized [160] or distributed [107][45].

Regarding centralized models, in [160], a bi-level model is proposed to trade in RT markets by scheduling DR portfolios. The upper-level optimizes the bidding strategy to minimize costs and considers the constraints of a DC power flow. The lower-level controls resources to minimize costs during the RT phase and considers the constraints of an AC power flow.

In relation to distributed models, the authors in [107] presented a network-secure co-optimization framework to participate in RT markets. This framework enables the optimization of consumers' resources to participate in energy and reserve markets while ensuring the secure operation of electricity networks. This approach is based on the ADMM, which coordinates the consumers' actions with the electricity grid on a receding horizon. In [45], the authors also developed an optimization approach based on the ADMM. In this approach, the aggregators participate in RT markets and negotiate with DSOs to calculate MV-LV network-secure bids. This allows aggregators and DSOs to evaluate the network feasibility of the bids at multiple voltage levels. In [161], the authors developed a distributed approach by dividing the problem into aggregator and electricity network subproblems, which are sequentially solved. In this work, the aggregators participate in the RT energy and FCAS markets and the model considers the electricity network constraints.

Again, it is important to note that distributed approaches have the benefits of ensuring data privacy and relaxing the computational needs to solve these problems in relation to centralized approaches.

Table 2.5 presents the RT control strategies identified in this subsection. It identifies the bidding strategy used (centralized or distributed), the energy and reserve market considered, the region of the markets and case study, and if the model considered network constraints.

Table 2.5 - Real-time control strategies.

Paper	Bidding strategy	Markets	Region	Network observability
[108][109][112]	Centralized	Energy	Europe	-
[144][105][111]	Centralized	Energy Secondary reserves	Europe	-
[158]	Centralized	Energy Gas	Europe	-
[159]	Centralized	Energy Hydrogen	Australia	-
[160]	Centralized	Energy	-	Electricity
[107][45]	Distributed	Energy Secondary reserves	Australia	Electricity
[161]	Distributed	Energy FCAS	Australia	Electricity

2.5. Final remarks

DR is an important mechanism that can help to mitigate the bad effects of the integration of RES. To enhance DR, the different energy markets must be well designed with sufficient incentives for prosumers to accept to participate in these programs and allow aggregators to execute their functions to their fullest capabilities. Some of the energy markets presented in this chapter already have proper mechanisms for DR such as the electricity markets in Australia, through its Wholesale Demand Response Mechanism, or in the US. Nonetheless, some regions still need more clarification on the regulation concerning the role that aggregators may have in managing DR programs.

This chapter also presented different real case studies for the application of aggregators or VPPs. Through these case studies, it is possible to conclude that aggregators can bring economic benefits to prosumers and even to other network agents, like DSOs or TSOs.

Aggregators need decision-support optimization tools to transform the flexibility of DMERs into multi-energy services, which can be traded into multi-energy markets, such as electricity (energy and reserves), natural gas, green hydrogen, and carbon markets. In this context, aggregators rely on two groups of optimization algorithms: 1) bidding optimization algorithms to compute bids for day-head markets; and 2) RT optimization algorithms to ensure the reliable delivery of the bids in RT. The first group of optimization algorithms is rich in the literature. The second group of optimization algorithms is not so common in the literature.

The works described in this chapter, together with other studies not covered here, have provided valuable contributions to the formulation of algorithms to optimize DMERs for market participation. However, there are still some gaps in the literature that should be filled. For example, an integrated approach to support the participation of an aggregator in multi-energy markets (including electricity, natural gas, green hydrogen, and carbon markets) considering the non-linear constraints of electricity, gas, and heat networks is still lacking in the literature. Moreover, to our best knowledge, none of the studies in the literature proposes a RT optimization algorithm to safely deliver multi-energy services traded by aggregators in electricity (energy and reserves), natural gas, green hydrogen, and carbon markets. More specifically, none of the works considers the RT optimization of aggregators considering electricity, gas, and heat networks and a portfolio of associated DMERs. The joint consideration of all these technologies and system constraints yields several benefits, in particular, the increase of flexibility and security of the energy system and an overall reduction of energy costs.

This way, in this thesis we propose to fill those gaps by developing a set of frameworks and tools for the DA bidding optimization and RT optimization stages. The innovative feature of these new tools are the following:

- Participation of an aggregator of MES in DA electricity (energy and secondary reserve), natural gas, green hydrogen, and carbon markets;
- It computes multi-energy (electricity, natural gas, green hydrogen, and CO2) bids and delivers multi-energy market services considering the constraints of electricity, gas (with blending of natural gas and hydrogen), and heat networks. This decreases the risk of the aggregator violating the constraints of the multi-energy networks in RT, reducing consequently possible energy imbalances and reserve shortages due to network violations;

- It exploits distributed optimization (i.e. ADMM) to preserve the independent roles of energy operators and the data privacy of the aggregator and networks' resources. In addition, it makes it possible to solve a large-scale problem in a time-effective manner by decomposing the original problem into smaller sub-problems.

The following chapter presents the aggregator's frameworks developed for aggregators of MES to participate in the DA and RT multi-energy markets stages.

Chapter 3
The multi-energy aggregator's framework

3.1. Introduction

In this chapter, we describe the framework for a multi-energy aggregator to participate in electricity, natural gas, green hydrogen, and carbon markets. We also detail the relevant interactions of the aggregator with TSOs, DSOs, market operators, and prosumers with multi-energy resources. This chapter is divided into the following sections:

- Section 3.2 presents the aggregator's framework. It provides a general description of the framework and describes in detail the architecture of the aggregator's business model;
- Section 3.3 presents the aggregator's interactions with energy markets. It provides a detailed description of the interactions with the electricity, natural gas, green hydrogen, and carbon markets. It also presents the chronological actions of the aggregator in the markets. Finally, the energy markets settlement is presented;
- Section 3.4 presents the aggregator's interactions with the electricity, gas, and heat DSOs;
- Finally, section 3.5 presents the aggregator's interactions with prosumers.

3.2. Aggregator's description

The novel aggregators' framework proposed in this thesis considers the participation of aggregators in multi-energy markets. This framework aims at expanding the roles of both the aggregator and DSOs to make energy systems more secure and cost-effective. This section presents not only the architecture developed but also the related business model.

3.2.1. General description

The aggregator of prosumers participates in the DA and RT electricity (energy and reserves), natural gas, green hydrogen, and carbon markets. To participate in these markets, the aggregator's actions are divided into three main stages:

- **Day-ahead** – the main tasks in this stage are the calculation of multi-energy bids and their submission to the respective DA market. To complete these tasks, the aggregator needs to interact with DSOs, the electricity TSO, and market operators. This stage can start several days before (D-N) and go up to the day before (D-1) of the operating day (D);

- **Real-time** – the main task in this stage is the delivery of the multi-energy services traded in the DA markets during the operating day (D). To complete this task, the aggregator needs to interact with DSOs, the electricity TSO, and prosumers;

- **Settlement** – the main task in this stage is to settle energy and services transactions. To complete this task, the aggregator needs to interact with market operators and the electricity and gas TSOs. This stage can start hours or days after the operating day (D+1).

Figure 3.1 presents the three stages of the aggregator when participating in multi-energy markets.

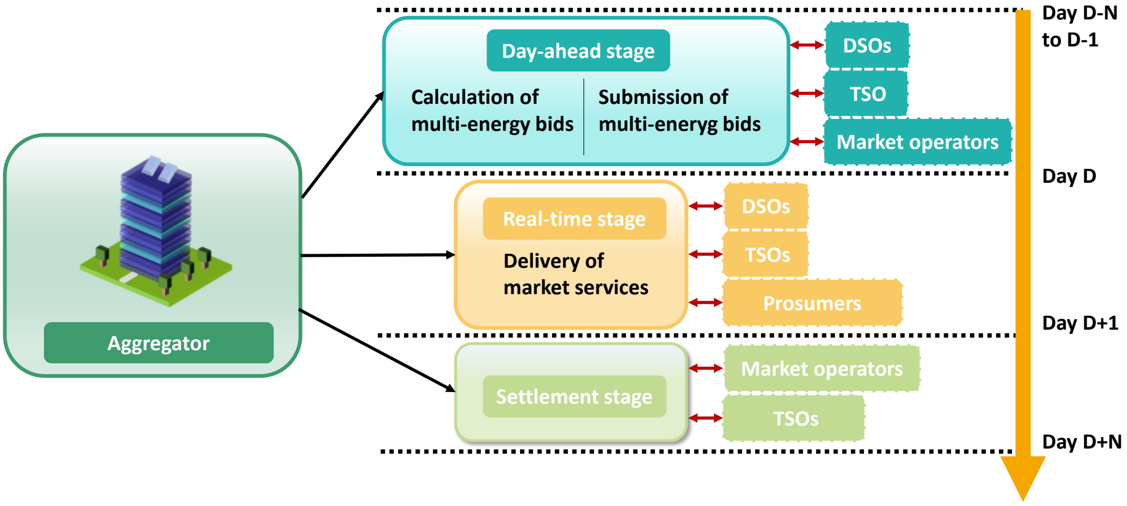

Figure 3.1 - Aggregator's stages.

3.2.2. Business model

The aggregator of prosumers participates in the DA and RT electricity (energy and reserves), natural gas, green hydrogen, and carbon markets. It acts as a retailer, buying energy, and as a generator, selling energy. It also acts as a price-taker submitting bids without affecting the market's clearing prices. This way, the aggregator only defines the quantities to buy or sell in the markets.

The aggregator buys the following services:

- **Electrical energy –** the aggregator buys electricity to satisfy prosumers' electricity hourly needs. It submits hourly electricity bids to the DA electrical energy market and in RT it seeks to comply with the energy traded in the DA markets;

- **Natural gas -** the aggregator buys natural gas to satisfy prosumers' daily needs. It submits daily natural gas bids to the DA natural gas market and in RT it seeks to comply with the energy traded in the DA markets;

- **Carbon allowances –** the aggregator buys allowances to cover prosumers' daily carbon emissions. It submits daily carbon bids to the carbon market and in RT it seeks to comply with the allowances traded in the markets;

- **Water –** the aggregator buys water to produce hydrogen with the P2G. In the DA stage, it estimates the necessary water to be bought and in RT it complies with the actual consumption needs;

- **Guarantees of origin –** the aggregator buys GOs to ensure that all the hydrogen produced uses electricity from RES[3]. In the DA stage, it estimates the necessary GOs to be bought and in RT it complies with the actual needs.

The products that the aggregator sells are:

- **Electrical energy –** the aggregator sells the excess of electricity produced from prosumers' resources. It submits hourly electrical energy bids to the DA electrical energy market and in RT it seeks to comply with the energy traded in the DA markets;

- **Secondary reserves –** the aggregator submits hourly secondary reserve bids to the DA secondary reserve markets. These bids can be upward (reduce load or increase generation) or downward (increase load or reduce generation) bids. In RT, the aggregator must activate the secondary reserve traded in the DA markets according to the AGC signal received from the TSO. The aggregator is paid for both the traded secondary reserves in the DA market and the actual activated reserve in RT;

- **Green hydrogen –** the aggregator sells the excess of green hydrogen produced by prosumers. It submits daily green hydrogen bids to the DA green hydrogen market and in RT it seeks to comply with the energy traded in the DA markets;

- **Oxygen –** the aggregator sells oxygen, which is a byproduct from the production of hydrogen with the P2G. In the DA stage, it estimates the necessary oxygen to be sold and in RT it sells the actual available quantities.

The electrical energy bids are divided into supply and demand bids, which result from the net-load of consumption and generation.

The aggregator's portfolio is managed in a short-term and RT horizon. The short-term horizon represents the management of resources for up to 24h of the following day. This allows the aggregator to optimize its portfolio for the participation in the DA markets. The RT horizon represents the management of resources in the range of seconds to minutes ahead. This allows the aggregator to optimize its portfolio to deliver the energy and secondary reserve services traded in the DA markets in RT.

The aggregator also has the option to deliver flexibility services directly to TSOs or DSOs. Nonetheless, this feature is not explored in this thesis.

3.2.3. Architecture

This subsection presents the architecture framework developed in this work. This architecture defines the interactions between the different parties participating in the energy and reserve

[3] It is assumed that the principle of additionality is ensured.

markets. It is based on a traditional architecture of aggregators although it considers new features that will benefit the operation of energy systems and the aggregator's economic value.

The aggregator interacts with downstream actors (prosumers) and with upstream actors, such as: electricity, gas, and district heating DSOs, electricity TSO and with the electricity, natural gas, green hydrogen, and carbon market operators. Figure 3.2 presents the aggregator's architecture.

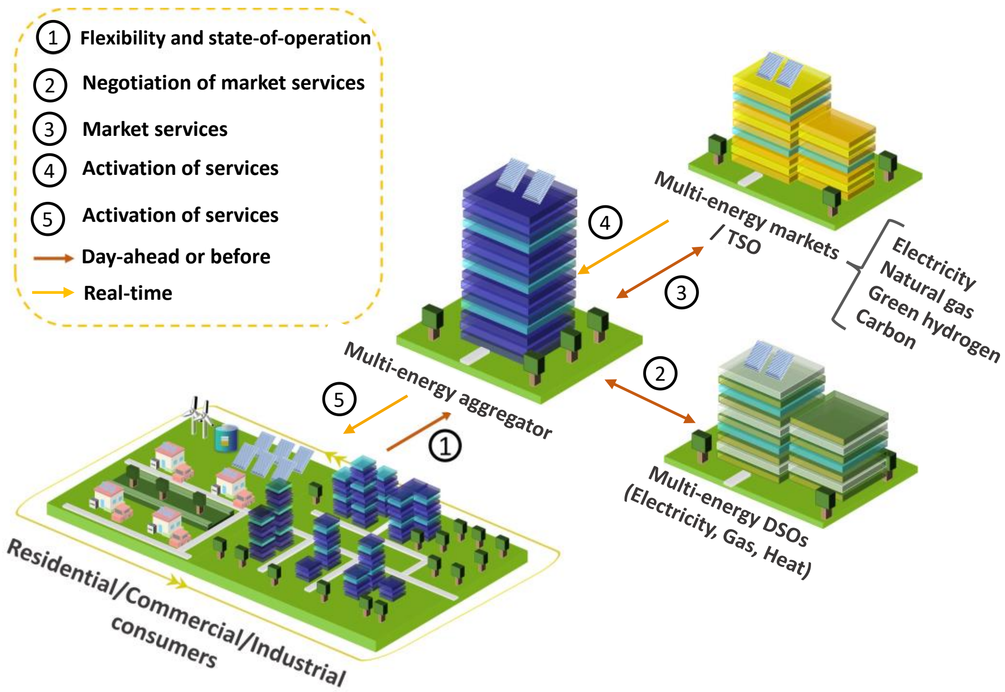

Figure 3.2 - Aggregator's architecture.

Market operators are responsible for managing energy markets. In the DA phase, the aggregator submits energy and secondary reserve bids to the respective market operator. After the market clearing, market operators communicate the accepted offers.

The interactions with prosumers are made through an EMS installed on each prosumer's premises. The aggregator interacts with prosumers in the DA and RT phase. In the DA phase, the interactions are made by the aggregator to get information about the resources' state to optimize its participation in energy markets. In the RT phase, the aggregator interacts with prosumers by communicating control set-points to activate the delivery of market services traded in the DA phase. The aggregator is able to communicate control signals to the EMS in order to change the power consumed/deployed by resources.

The aggregator also compensates prosumers for the flexibility provided. There are several business model options to be explored between aggregators and prosumers, as seen in Chapter 2. Nonetheless, this issue is not addressed in this thesis.

A new feature of the proposed architecture is the interactions between the aggregator and the DSOs. The DSOs are responsible for securely operating the energy networks. As seen in Chapter

2, this task can be challenging depending on the regulatory context. The DSO may not have proper solutions to interact with the other energy agents to operate its network in an optimized and secured manner. In this framework, the aggregator negotiates with the DSOs of the electricity, gas, and district heating networks in the bidding optimization and delivery of services phases, in order to compute network-feasible bids. This means that the DA bids submitted to the DA markets and the delivery of market services in RT do not violate any network constraint. This framework can be integrated into the actual Iberian TSO coordination scheme and adopted in most of the electricity market frameworks worldwide.

This feature can bring benefits to the operation of energy networks, particularly at the reliability and quality-of-service levels. The activities of the DSO will be facilitated as it will have some level of control over the resources connected to the distribution networks, even though indirectly. This way, it can prevent the malfunction of energy networks in advance, avoiding the incurrence of higher costs. Moreover, the aggregator himself may benefit economically from this feature, as will be demonstrated later in this work. The interactions between the aggregator and the DSO will be better detailed and explored in section 0.

The electricity TSO validates the electrical energy bids and buys secondary reserve band (upward and downward) from the DA secondary reserve market for frequency control purposes (demand-supply balance). To activate the band during the RT stage, the TSO interacts with the aggregator through an AGC signal. This signal indicates the power set-points of the aggregator. The aggregator is responsible for following the TSO set-points by changing the control set-points of resources.

The market settlement occurs days after the delivery of the services. Both energy market operators and TSOs confirm the energy exchanges occurred and settle with the aggregator the market transitions. The aggregator has to pay for the energy consumed and be remunerated for the energy and reserve services sold.

A more detailed analysis of the interactions between the aggregator and the energy markets (section 3.3), DSOs (section 0), and prosumers (section 3.5) is presented in the following subsections.

3.3. Interactions of the aggregator with electricity, natural gas, green hydrogen, and carbon markets

The multi-energy aggregator participates in the DA and RT electricity, natural gas, green hydrogen, and carbon markets of the Iberian Peninsula (Portugal and Spain). The electricity markets include the energy and secondary reserve markets.

In the DA stage, the aggregator submits bids into the markets. In this stage, the aggregator behaves as a price-taker: it offers supply (electricity) and secondary reserve bids at floor-prices; and demand (electricity), natural gas, hydrogen, and CO_2 bids at cap-prices. This way, the aggregator ensures that all offers submitted to the market are accepted. In the RT stage, the aggregator delivers the multi-energy services traded in the DA markets.

The following subsections describe the market frameworks, the chronological steps, and the market settlement mechanisms.

3.3.1. Description of the markets

The aggregator participates in the energy and secondary reserve markets present in the Iberian Peninsula. This subsection presents the description of these markets. Nonetheless, it is important to note that the framework developed can be easily modified, with only some small changes, so that it is correctly adapted to other energy markets worldwide, such as the ones from Europe, the USA, or Australia.

3.3.1.1. Electricity markets

The multi-energy aggregator participates in the energy and secondary reserves electricity markets. The DA energy market is a two-side auction, where market participants can trade for energy for the 24h of the next day. Aggregators submit bids indicating the hourly quantity (MWh) and price (€/MWh). The market operator collects the bids and submits them to EUPHEMIA, the European market-clearing platform (presented in Chapter 2). Besides the bids from auctions, EUPHEMIA [19] also considers bilateral contracts. Afterwards, the bids and bilateral contracts are cleared so that the social welfare is maximized and the power flows in the transmission interconnectors of the European control areas do not exceed the capacity limits [20]. Then, the TSO of each control area performs congestion management to calculate viable energy schedules, considering the transmission network constraints of their own area. When transmission network problems occur, the TSO can activate market-based (e.g. market-splitting) or technical-based (e.g. changing transform taps) mechanisms to solve those problems.

In the secondary reserve market, market participants trade upward and downward reserves that later are activated by the AGC. These bids are presented between 19h and 19h45. The TSO buys secondary reserve under the form of band (MW), taking into account the constraints of the transmission network of its control area [28]. They are remunerated in the form of availability (€/MW) and utilization (€/MWh). The price of band availability is set by the secondary reserve market, while the price of utilization is defined by the tertiary reserve market [21].

In the RT stage, the aggregator dispatches its resources according to the energy and secondary reserves traded in the DA markets. Days after the delivery, the aggregator settles the transactions with market operators and TSOs.

3.3.1.2. Natural gas market

The aggregator participates in the DA daily session of the natural gas market. It submits simple bids including price (€/MWh) and daily quantity (MWh/day) of natural gas. The natural gas market operator collects all the bids and clears the market. The clearing price is calculated according to the intersection point between the aggregated curves of supply and demand. Then, market agents send information related with the quantity and direction of the flow of natural gas to the gas TSO. Finally, the TSO validates the bids according to the technical constraints of the transmission gas network [63].

3.3.1.3. Green hydrogen market

Currently, there is no green hydrogen market implemented or fully developed in the Iberian Peninsula, nor in any other country worldwide. Nonetheless, in this thesis, we assume the presence of a green hydrogen market, with a similar structure as the natural gas market. This way, the aggregator can sell green hydrogen by submitting selling bids to the market indicating the price (€/MWh) and daily quantity (€/MWh) to be sold. As the green hydrogen sold in this market is injected into the gas network, the gas TSO needs to validate these bids, as it does for the natural gas market bids. The role of the TSO is very important in this case as the mixture of natural gas with green hydrogen can affect the high heating value (or upper heating value) of the natural gas, which is usually regulated by pre-established quality-of-service standards.

Moreover, the aggregator can purchase GOs to ensure that all the green hydrogen produced is provided by RES[4].

3.3.1.4. EU carbon market

The EU carbon market is an auction-based market occurring three times per week. GHG emitters can buy carbon allowances (in tonnes of CO_2) to cover their yearly emissions. Bidders submit offers to buy a specific number of allowances at a given price (€/tCO_2). Some installations receive free allowances (calculated through benchmarking [162]) for the production of energy or one of its byproducts. The list of these installations can be found in [162]. CHPs are included in this list, receiving free allowances for the heat produced, although they still need to buy allowances for the electricity generated.

3.3.2. Chronological steps of the aggregator

The chronological steps of the aggregator in the four DA energy markets, based on the current wholesale market rules, are presented in Figure 3.3.

[4] It is assumed that the principle of additionality is ensured.

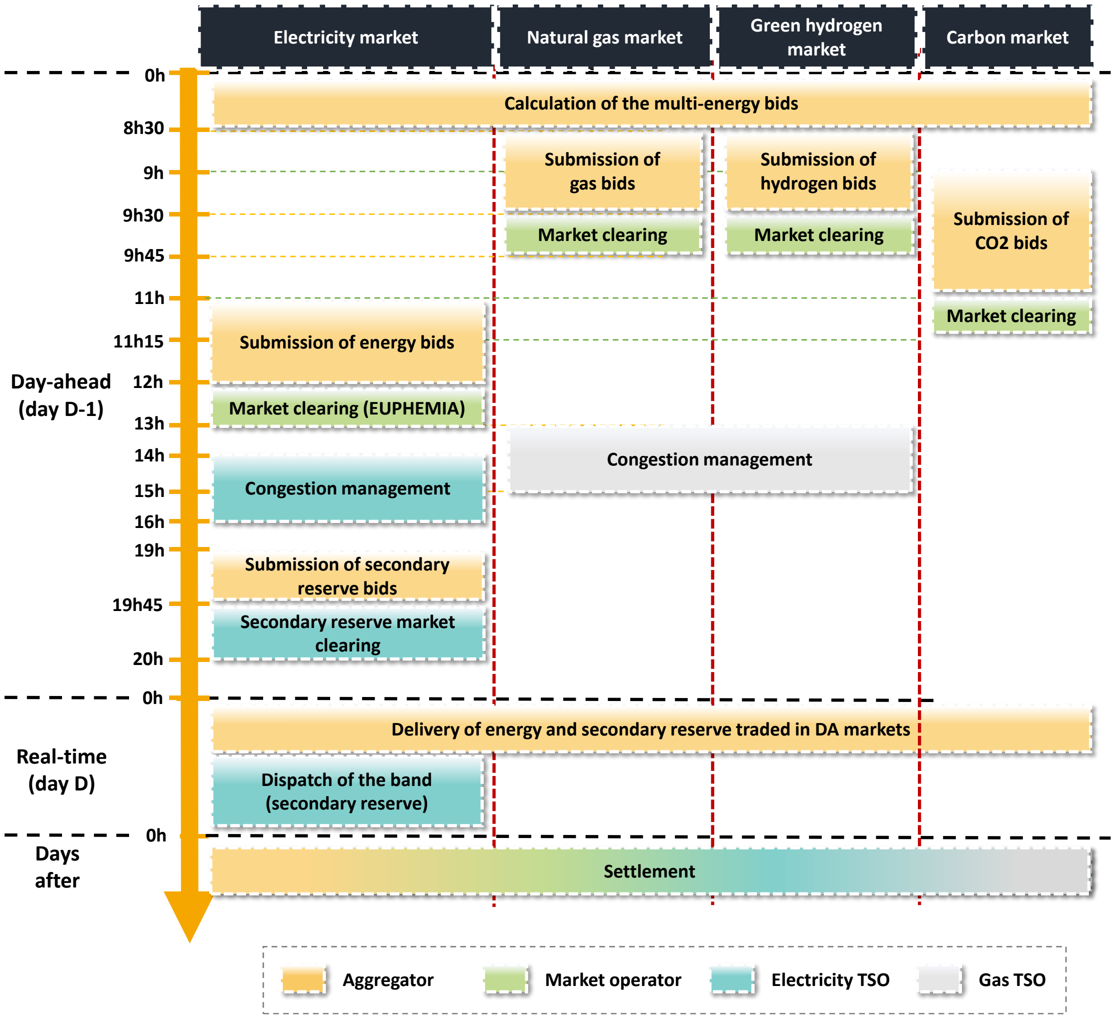

Figure 3.3 – Sequential steps of the aggregator in the electricity, natural gas, green hydrogen, and carbon markets.

As the first step of the DA stage (D-1), the aggregator computes the multi-energy bids: electrical (energy and secondary reserve), natural gas, green hydrogen, and CO_2 bids. After, the aggregator submits the bids to the respective markets. The bids must be submitted according to the schedules of the electricity (between 11h-12h for energy, and 10h-19h45 for secondary reserves), natural gas (8h30-9h30 [26]), green hydrogen (8h30-9h30), and carbon (9h-11h) markets.

In the RT stage (day D), the aggregator delivers the multi-energy market services traded in the DA markets.

3.3.3. Information chain

The information exchange between the aggregator, prosumers, energy markets, and TSOs in the DA stage is presented in Figure 3.4 and are the following:

1. The aggregator calculates DA multi-energy bids while negotiating with the electricity, gas, and heat DSOs;

2. The aggregator submits natural gas, green hydrogen, and carbon energy bids to the respective DA markets;

3. Natural gas, green hydrogen, and carbon markets are cleared;

4. The aggregator submits electrical energy bids to the DA electrical energy markets;

5. The electrical energy market is cleared through EUPHEMIA;

6. The gas TSO performs a congestion management;

7. The gas and green hydrogen market operators communicate the viable energy schedules (MWh) and clearing prices (€/MWh) to the aggregator. The carbon market operator also communicates the carbon clearing prices (€/tCO_2) to the aggregator;

8. The electricity TSO performs a congestion management of the power networks;

9. The electricity market operator communicates viable energy schedules (MWh) and clearing prices (€/MWh) to the aggregator;

10. The aggregator submits secondary reserve bids to the DA secondary reserve markets;

11. The secondary reserve market is cleared with the participation of the electricity TSO;

12. The market operator communicates the cleared band offers (MW) and clearing prices (€/MW) to the aggregator;

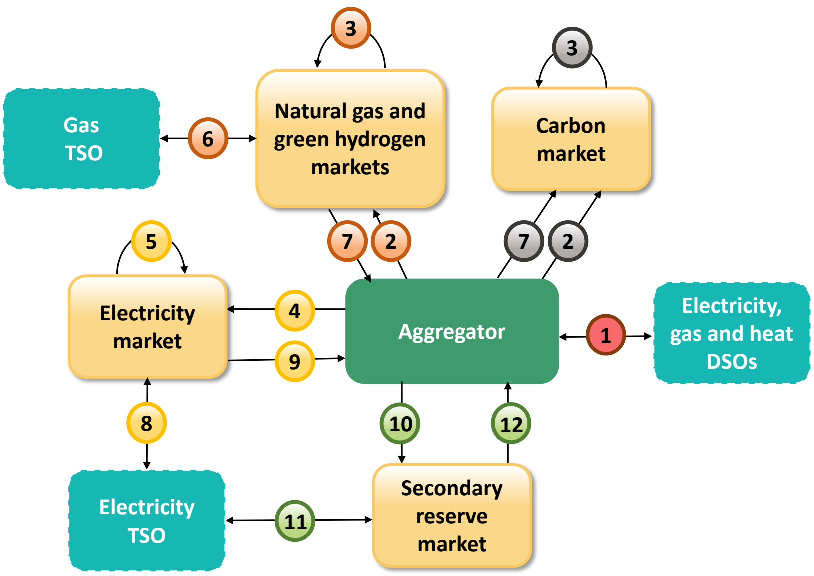

Figure 3.4 - Day-ahead stage flow of information.

The flow of information in RT are presented in Figure 3.5 the following:

13. The aggregator communicates with the prosumers about the most recent state-of-operation of the resources and prosumer's preferences;

14. The electricity TSO communicates with the aggregator through the AGC to activate the bands offered in the DA markets;

15. The aggregator calculates the control set-points of the prosumer's resources considering the AGC signal;

16. The aggregator communicates the control set-points to the prosumers.

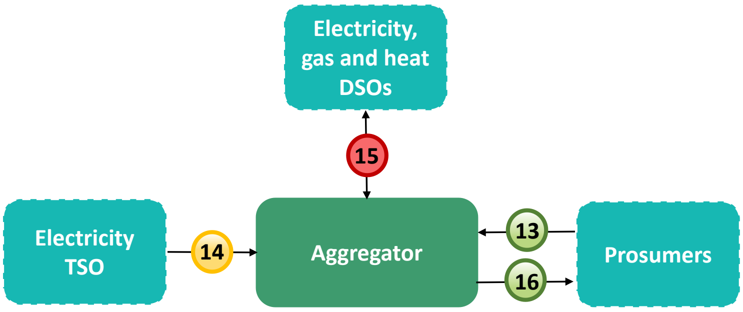

Figure 3.5 - Real-time stage flow of information.

3.3.4. Settlement

The net-cost of the aggregator is presented in equations (3.1)-(3.7). Equation (3.1) is divided into 6 terms. The first term (3.2) represents the costs of buying and selling electricity in the DA markets, selling secondary reserve band (upward and downward) in the DA markets, activating secondary reserves in RT, imbalance costs related with inequalities in DA commitments and RT realizations, and the penalties for the band not supplied. The second (3.3), fourth (3.5), and sixth (3.7) terms represent the costs of buying natural gas, water, and carbon allowances in the DA markets and respective imbalance costs in RT. The third (3.4) and fifth (3.6) terms represent the costs of selling green hydrogen and oxygen in the DA markets and respective imbalance costs in RT. Negative values are revenues and positive values are costs.

$$Settlement = f^{G} + f^{H_2} + f^{H_2 0} + f^{0_2} + f^{C} + \sum_{t \in T} f_t^E \tag{3.1}$$

$$\begin{aligned} f_t^E = {} & \lambda_t^E P_t^{E,DA} \Delta t - \lambda_t^B \left(U_t^{E,DA} + D_t^{E,DA}\right) + \left(\lambda_t^{D,RT} D_t^{E,RT} - \lambda_t^{U,RT} U_t^{E,RT}\right) \Delta t \\ & + \left(\lambda_t^{E,-} \Delta P_t^{E,-} - \lambda_t^{E,+} \Delta P_t^{E,+}\right) \Delta t + \lambda_t^{B,-} \left(\Delta U_t^E + \Delta D_t^E\right) \Delta t \end{aligned} \tag{3.2}$$

$$f^{G} = \lambda^{G,DA} P^{G,DA} \Delta t + \lambda^{G,RT} \left(\Delta P^{G,-} - \Delta P^{G,+}\right) \Delta t \tag{3.3}$$

$$f^{H_2} = -\lambda^{H_2,DA} P^{P2G,H_2,DA} \Delta t + \lambda^{H_2,RT} \left(\Delta P^{P2G,H_2,-} - \Delta P^{P2G,H_2,+}\right) \Delta t \tag{3.4}$$

$$f^{H_2 0} = \lambda^{H_2 0} \left(P^{P2G,E,DA} + \Delta P^{P2G,E,-} - \Delta P^{P2G,E,+}\right) c^{H_2 O} \Delta t \tag{3.5}$$

$$f^{0_2} = \lambda^{0_2} \left(-P^{P2G,E,DA} + \Delta P^{P2G,E,+} - \Delta P^{P2G,E,-}\right) c^{O_2} \Delta t \tag{3.6}$$

$$f^{C} = \lambda^{CO_2} \left(P^{C,DA} + \Delta P^{C,-} - \Delta P^{C,+}\right) c^{CO_2,G} \Delta t \tag{3.7}$$

Table 3.1 presents a description of the variables of the settlement function.

Table 3.1 - Variables of the settlement function.

Variable	Description	Unit

$\boldsymbol{P_{j,t}^{E,DA}}$	Electricity consumption (positive) or generation (negative) calculated in the day-ahead phase	MW
$\boldsymbol{U_t^{E,DA}}, \boldsymbol{D_t^{E,DA}}$	Upward and downward secondary reserve bids	MW
$\boldsymbol{D_t^{E,RT}}, \boldsymbol{U_t^{E,RT}}$	Upward and downward activated secondary reserves	MW
$\boldsymbol{P^{G,DA}}$	Gas consumption calculated in the day-ahead phase	MW
$\boldsymbol{P^{P2G,Hy,DA}}, \boldsymbol{P^{P2G,E,DA}}$	Hydrogen production and electricity consumption by the P2G calculated in the day-ahead phase	MW
$\boldsymbol{P^{C,DA}}$	Carbon allowances calculated during the day-ahead phase	MW
$\Delta\boldsymbol{P_t^{E,-}}, \Delta\boldsymbol{P_t^{E,+}}$	Negative and positive electricity imbalances between DA market commitments and RT realizations	MW
$\Delta\boldsymbol{U_t^{E}}, \Delta\boldsymbol{D_t^{E}}$	Upward and downward secondary reserves imbalances between DA market commitments and RT realizations	MW
$\Delta\boldsymbol{P^{G,-}}, \Delta\boldsymbol{P^{G,+}}$	Negative and positive natural gas imbalances between DA market commitments and RT realizations	MW
$\Delta\boldsymbol{P^{P2G,H_2,-}}, \Delta\boldsymbol{P^{P2G,H_2,+}}$	Negative and positive hydrogen production imbalances by the P2G between DA market commitments and RT realizations	MW
$\Delta\boldsymbol{P^{P2G,E,-}}, \Delta\boldsymbol{P^{P2G,E,+}}$	Negative and positive electricity consumption imbalances by the P2G between DA market commitments and RT realizations	MW
$\Delta\boldsymbol{P^{C,-}}, \Delta\boldsymbol{P^{C,+}}$	Negative and positive carbon allowances imbalances between DA market commitments and RT realizations	MW

Table 3.2 presents a description and the type of each parameter used in this subsection.

Table 3.2 – Parameters of the settlement function.

Parameter	**Description**	**Unit**
$\boldsymbol{\alpha^{CO_2,G}}$	Conversion factor for carbon	–
$\boldsymbol{c^{H_2O}}$	Converstion factor for water	L/MW
$\boldsymbol{c^{O_2}}$	Converstion factor for oxigen	kg/MW
$\boldsymbol{\lambda_t^{E}}, \boldsymbol{\lambda_t^{G,DA}}$ and $\boldsymbol{\lambda^{H_2,DA}}$	Electricity, natural gas and hydrogen energy prices forecasted in the day-ahead phase	$€/MWh$
$\boldsymbol{\lambda_t^{B}}$	Secondary reserve band price	$€/MW$
$\boldsymbol{\lambda_t^{D,RT}}$ and $\boldsymbol{\lambda_t^{U,RT}}$	Downward and upward tertiary reserve prices	$€/MWh$
$\boldsymbol{\lambda_t^{E,-}}, \boldsymbol{\lambda_t^{E,+}}$	Electricity negative and positive imbalance prices	€/MWh
$\boldsymbol{\lambda_t^{B,-}}$	Secondary reserve imbalance penalty	€/MWh
$\boldsymbol{\lambda_t^{G,RT}}$ and $\boldsymbol{\lambda^{H_2,RT}}$	Natural gas and hydrogen energy prices in the real-time phase	$€/MWh$
$\boldsymbol{\lambda^{H_2O}}$	Water prices	$€/L$
$\boldsymbol{\lambda^{O_2}}$	Oxygen prices	$€/kg$
$\boldsymbol{\lambda^{CO_2}}$	Carbon prices	$€/tCO_2$

3.4. Aggregator's interactions with electricity, gas, and heat DSOs

Nowadays, within European current rules, energy markets do not include the participation of DSOs. This means that the feasibility of the aggregator's bids in the distribution network is not checked by DSOs in the DA and RT stages. These bids may end up causing network problems.

This thesis presents a solution to overcome this issue by proposing a framework that considers a negotiation between the aggregator and the DSOs of the electricity, gas, and heat networks. This negotiation occurs both in the DA stage (in the calculation of multi-energy bids phase), producing network-secure DA bids, and in the RT stage, ensuring the network-secure delivery of market services.

This negotiation benefits both the aggregator and DSOs. Without any negotiation or other similar mechanism, the aggregator would offer DA bids and deliver market services without a proper check of their network feasibility. This could create scenarios where the delivery of traded services would cause distribution network problems. To overcome these problems, some of the aggregator's DMERs could end up disconnected from the energy networks. Consequently, the aggregator would not be able to fully deliver the traded market services. In this case, the aggregator would incur in high monetary fines and could even be expelled from participating in energy markets due to consecutive underperformance. By negotiating with the DSOs, the aggregator ensures the network feasibility of the DA bids and market services delivered. It can thus fully deliver the services traded in the DA markets and avoid monetary fines, improving its economic performance. This step also benefits DSOs as it facilitates distribution network operation, contributing to reducing costs and increasing the overall system reliability.

The algorithm used for the negotiation strategy between the aggregator and DSOs is described in detail in the following subsection.

3.4.1. Negotiation algorithm

The negotiation algorithm is based on the ADMM. The ADMM is an algorithm capable of solving convex optimization problems by decomposing them into smaller problems easier to solve. As introduced by S. Boyd et al. in [163]:

"It takes the form of a decomposition-coordination procedure, in which the solutions to small local subproblems are coordinated to find a solution to a large global problem. ADMM can be viewed as an attempt to blend the benefits of dual decomposition and augmented Lagrangian methods for constrained optimization.".

Recently, this algorithm has been used in several areas of expertise including the energy field. This subsection explains how the ADMM algorithm is applied and formulated in our problem, enabling negotiations between aggregators and DSOs. It is important to note that this algorithm is applied in both the DA and RT stages. In the DA stage, the aggregator and the DSO negotiate the bids to be submitted to the markets. In the RT stage, they negotiate the multi-energy market services to be delivered. Although the DA and RT problems are different, the application of the ADMM is the same and it is presented in the following paragraphs.

The generic formulation of the multi-energy and network-secure optimization problem is given by (3.8)-(3.11). The objective function (3.8) minimizes the net cost of participating in the DA electricity, gas, green hydrogen, and carbon markets or the net-cost of delivering the multi-energy services traded in DA markets. Let X be the aggregator's internal variables and P^E, P^G, P^H be the power exchanged between the aggregator and each energy-vector DSO. Equation (3.9) is the aggregator's constraints. Equation (3.10) is the DSO's constraints, where $\widehat{P^d}$ is the duplicated variables of P^d, and Y^d is the internal variables of each DSO. Constraint (3.11) was added to the problem to enable the decomposition of the centralized problem into independent aggregator and DSOs sub-problems.

$$min\ f(P^E, P^G, P^H, X) \tag{3.8}$$

$$h(P^E, P^G, P^H, X) \leq 0 \tag{3.9}$$

$$g^d\left(\hat{P}^d,\, Y^d\right) \leq 0,\ \forall\, d\ \in \{E, G, H\} \tag{3.10}$$

$$P^d - \hat{P}^d = 0, \qquad \forall\, d\ \in \{E, G, H\} \tag{3.11}$$

We use the ADMM to decompose the problem (3.8)-(3.11) into aggregators and DSOs sub-problems. This decomposition enables the aggregator and DSOs to solve their bidding/delivery and multi-energy network sub-problems independently without putting at risk the data privacy of each agent. In addition, the decomposition of (3.8)-(3.11) makes the problem easier to solve since it is divided into smaller and independent aggregator and DSOs sub-problems.

The sub-problem of the aggregator is given by (3.12) and (3.13).

$$min\ f(P^E, P^G, P^H, X) + \sum_{d \in \{E,G,H\}} \mathcal{L}^d(P^d, \hat{P}^{d,k}, \pi^{d,k}) \tag{3.12}$$

$$h(P^E, P^G, P^H, X) \leq 0 \tag{3.13}$$

The network sub-problem of each energy DSO d is given by (3.14) and (3.15).

$$\min\ \mathcal{L}^d(P^{d,k+1}, \hat{P}^d, \pi^{d,k}) \tag{3.14}$$

$$g\left(\hat{P}^d, Y^d\right) \leq 0 \tag{3.15}$$

Equation (3.16) represents the penalty term of the augmented Lagrangian applied to constraint (3.11). π is a vector with dual variables and ρ is a penalty scalar.

$$\mathcal{L}^d(P^d, \widehat{P^d}, \pi^d) = {\pi^d}^{\mathrm{T}}\left(P^d - \widehat{P^d}\right) + \frac{\rho}{2}\left\|P^d - \widehat{P^d}\right\|_2^2 \tag{3.16}$$

ADMM solves the optimization problems (3.12)-(3.13) and (3.14)-(3.15) iteratively until convergence is reached. The steps of each iteration k of the ADMM are presented in Figure 3.6 and described below:

1. The aggregator runs the optimization problem (3.12)-(3.13) and computes the bids by holding $\boldsymbol{\widehat{P}^{d,k}}, \boldsymbol{\pi^{d,k}}$ constant at $\boldsymbol{k^{th}}$ values. Values of $\boldsymbol{P^{d}}$ are obtained and communicated to the independent platform5;

2. Each DSO runs its respective optimization problem from (3.14)-(3.15) and solves it by holding $\boldsymbol{P^{d,k+1}}$, $\boldsymbol{\pi^{d,k}}$ constant. Values of $\boldsymbol{\widehat{P}^{d}}$ are obtained and communicated to the independent platform. The electricity DSO runs an AC optimal power flow and obtains the values of $\boldsymbol{\widehat{P}^{E}}$; the gas DSO runs a non-linear steady state gas flow and obtains the values of $\boldsymbol{\widehat{P}^{G}}$ and the heat DSO runs a non-linear heat flow and obtains the values of $\boldsymbol{\widehat{P}^{H}}$.

3. An independent platform performs different actions. First, it updates the dual variables $\boldsymbol{\pi}$ using (3.17). Then, it checks for convergence with (3.18) and (3.19). If the convergence criteria are satisfied the algorithm stops, otherwise continues and updates ρ using a tuning strategy [39]. Finally, it communicates the updated dual variables and goes back to step 1.

Equation (3.17) updates the dual variables π.

$$\pi^{d,k+1} = \pi^{d,k} + \rho\left(P^{d,k+1} - \hat{P}^{d,k+1}\right) \tag{3.17}$$

The stop criteria are defined by equations (3.18) and (3.19), where ϵ^{abs} is the absolute tolerance and a is the size of the primal and dual residuals as they are part of $\mathbb{R}^{a}$ [163]. Equation (3.18) represents the violation of constraint (3.11). Equation (3.19) represents the violation of the Karush-Kuhn-Tucker stationarity constraint.

$$\left\|\left(P^{d,k+1} - \hat{P}^{d,k+1}\right)^{T}\right\|_{2} \leq \epsilon^{Abs}\sqrt{a} \tag{3.18}$$

$$\left\|\rho\left(\hat{P}^{d,k+1} - P^{d,k+1}\right)^{T}\right\|_{2} \leq \epsilon^{Abs}\sqrt{a} \tag{3.19}$$

The network-secure optimization problem is formulated for a single aggregator but it can be extended to multiple aggregators without requiring any changes in the distributed formulation of the problem, as described in [150]. However, the aim of the paper is not to study the dynamics between multiple aggregators and DSOs, thus, and for sake of simplicity, it was decided to only consider a single aggregator.

[5] An independent platform, managed by an authorized third-party entity, is used to preserve the data privacy of the aggregator and DSOs since the platform communicates to the aggregator and DSOs only the information that they require to solve their optimization sub-problems. It is worth mentioning that this third-party agent/platform also has been adopted by other researchers in similar contexts (e.g. [187]).

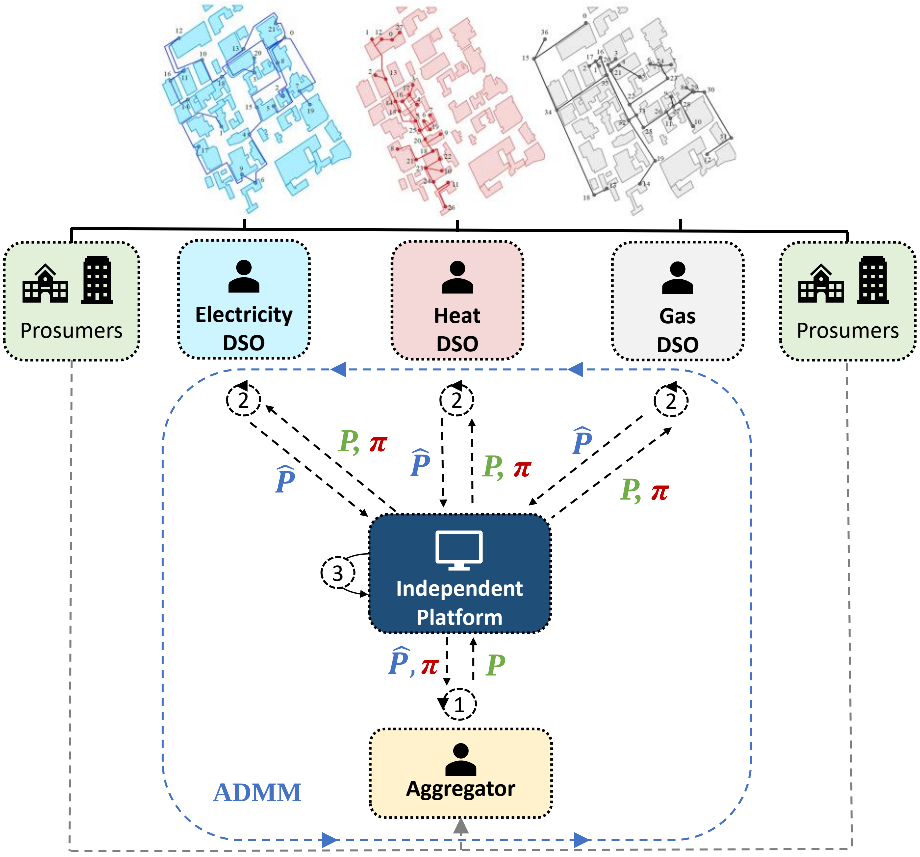

Figure 3.6 - ADMM algorithm.

3.5. Aggregator's interactions with prosumers

The aggregator manages and exploits the flexibility of prosumer's DMERs located in the electricity, gas, and heat distribution networks. This is done through DR programs agreed with prosumers upon a remuneration strategy. Nonetheless, the remuneration schemes are not addressed in this thesis.

As previously mentioned, the communications with prosumers and their DMERs are done through an EMS. The communications between the EMS and aggregator are bidirectional. This means that the aggregator sends control set-points to the EMS which sequentially sends them to the DMERs. The control set-points can be in the form of power or temperature. On the other hand, the DMERs send their current metering and state-of-operation which sequentially is sent to the aggregator. The state-of-operation indicates the state-of-charge (SOC) or room temperature.

Prosumers are able to set their individual preferences and visualize all relevant information about the management of their resources and market participation in the EMS. Prosumers' preferences are related with acceptable temperature ranges of rooms or with EVs necessities.

EMS also gathers information about consumption habits comprising human behavior patterns and typical daily routines. This information is relevant for the aggregator in order to forecast prosumers' electrical, natural gas, and heat energy needs. This way, EMSs include forecasting algorithms capable of forecasting the necessary information while securing its data privacy. Nonetheless, this forecasting algorithm is outside the scope of this work.

3.5.1. Prosumers distributed multi-energy resources and loads

The aggregator can manage a vast range of DMERs. All DMERs are flexible resources and include HPs, PV systems, ESSs, EVs, CHPs, thermal loads, and hydrogen technologies (e.g. P2Gs, HSSs, FCs. and fuel stations). The HPs, thermal loads, and P2Gs are sources of demand flexibility; ESSs, EVs, and HSSs are sources of demand and generation flexibility; CHPs, FCs, and PV systems are sources of generation flexibility. To be a source of demand flexibility means being able to increase or decrease consumption. In contrast, to be a source of generation flexibility means to be able to increase or decrease generation. Thermal loads can be supplied by HPs installed at the prosumer's premises or by the district heating.

Prosumers also have inflexible electricity, gas, and heat loads that are supplied by the aggregator.

Table 3.3 presents the characteristics of DMERS. Figure 3.7 presents a general scheme of the connection between DMERs and energy networks.

Table 3.3 – DMERs characteristics.

Resource	Energy input	Energy output	Physical and technical characteristics	Flexibility
HP/Thermal loads	Electricity	Heat	Efficiency Maximum power Minimum and maximum temperature (preferences) Thermal resistance (building) Thermal capacitance (building) Thermal constant (building) Heat gains and losses (building) Outside temperature	Demand
PV	-	Electricity	Efficiency Maximum power	Generation
ESS	Electricity	Electricity	Charging and discharging efficiency Minimum and maximum state-of-charge Maximum charging/discharging power	Demand Generation
EVs	Electricity	Electricity	Charging and discharging efficiency Minimum and maximum state-of-charge Maximum charging/discharging power	Demand Generation
CHP	Natural gas	Electricity Heat	Efficiency Maximum power	Generation

Electrolyzer	Electricity	Hydrogen	Efficiency Maximum power	Demand Generation
Fuel cell	Hydrogen	Electricity	Efficiency Maximum power	Generation
HSS	Hydrogen	Hydrogen	Battery capacity Maximum and minimum SOC Charging and discharging power values Charging and discharging efficiencies	Demand Generation

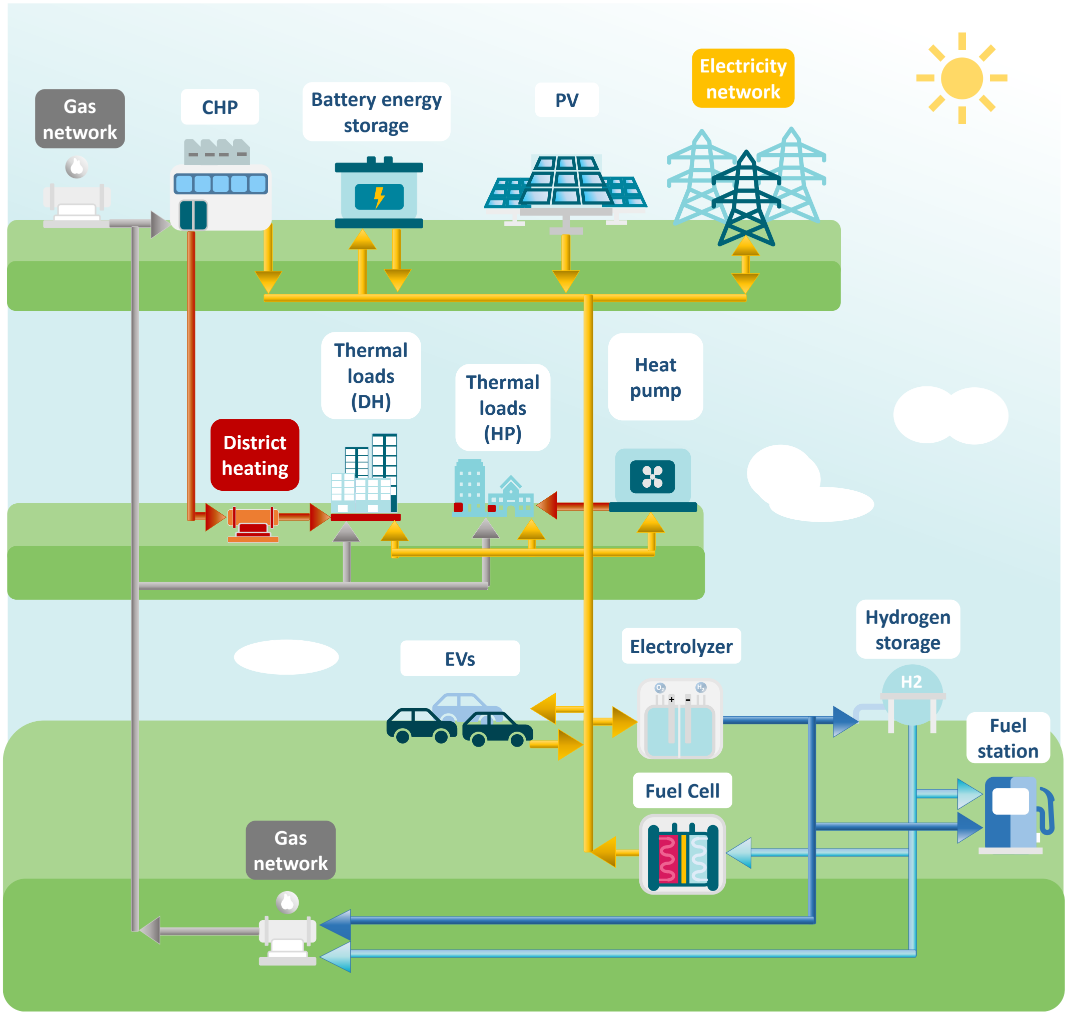

Figure 3.7 – General scheme of the connection between DMERs and energy networks.

3.6. Final remarks

This chapter presents the framework developed in this thesis. The framework adopts a hierarchical control architecture where the aggregator is able to control the prosumers' DMERs, including HPs, EVs, PVs, ESSs, CHPs, P2Gs, FCs, and HSSs. All the interactions between aggregators, DSOs, TSOs, and prosumers are described and detailed. By using this framework, the aggregators are able to participate in multi-energy markets (electricity (energy and reserves), natural gas, green hydrogen, and carbon). It allows aggregators to negotiate with DSOs in order to calculate multi-energy market bids and to deliver multi-energy market services in a secure way from the point-of-view of the electricity, gas, and heat networks. This framework also allows the preservation of the independence of roles and data privacy of the prosumers and network operators. Moreover, it takes into account the prosumers' preferences in both DA and RT market phases.

The following chapters present the optimization tools to support aggregators' participation in the DA (Chapter 4) and RT (Chapter 5) phases.

Chapter 4
Day-ahead network-secure optimization framework

4.1. Introduction

The bidding framework developed in this thesis considers the network-secure participation of aggregators of prosumers in DA multi-energy markets. This way, the aggregator participates in the DA electricity (energy and reserves), natural gas, green hydrogen, and carbon markets. This bidding framework includes negotiations between aggregators and electricity, heat, and gas DSOs. This is done to make the bids network-secure, so they do not violate any network constraints. As explained in Chapter 3, this strategy is a distributed approach based on the ADMM. This way, the bids are computed to satisfy the constraints of multi-energy markets, DMERs, and multi-energy networks. The newly developed framework can be easily integrated into the centralized market coordination mechanism, which is the most common coordination mechanism worldwide. Figure 4.1 presents the scheme of the DA network-secure bidding optimization framework.

This chapter presents the mathematical formulation of the bidding strategy's mentioned above and is divided as follows:

- Section 4.2 presents the formulation of the aggregator subproblem, i.e. the bidding optimization model;
- Section 4.3 presents the formulation of the DSO subproblem, i.e. the multi-energy flow optimization models;
- Section 4.4 presents the case study used to analyze the framework developed;
- Section 4.5 presents the results obtained and the analysis of the newly developed framework;
- Section 4.6 presents the conclusions of this chapter.

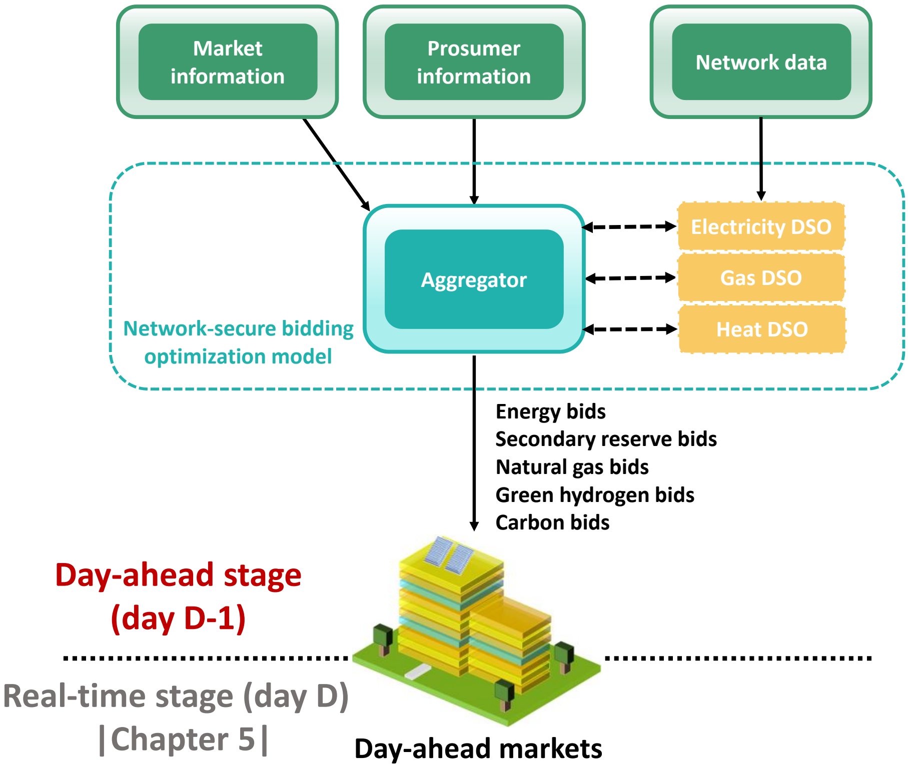

Figure 4.1 - Day-ahead network-secure bidding optimization framework scheme.

4.2. Aggregator's sub-problem: bidding optimization model

This section presents the bidding optimization model used by the aggregator to compute electricity (energy and secondary reserve), gas, green hydrogen, and CO_2 bids. It is important to note that the optimization model (3.12) and (3.13) introduced in Chapter 3 is detailed and represented here by (4.1)-(4.91). In addition, the bidding model computes scenarios of operation for the electricity, gas, and heat networks, i.e. bid delivery scenarios. Some information used in this model is forecasted while other is fixed. This is stated in the following sub-sections. The optimization problem is decomposed by time-step $t \in T$ for an horizon of 24h.

4.2.1. Objective function

The objective function (4.1) minimizes the net cost of the aggregator trading electricity, gas, green hydrogen, and CO_2 in the DA electricity (energy and secondary market), gas, green hydrogen, and carbon markets. The objective function (4.1) is divided into 9 terms. The first term (4.2) is the net cost of buying and selling energy and secondary reserve in the electricity markets. The second term (4.3) is the net cost of trading GOs. The third term (4.4) is the net cost of trading gas in the gas market. The fourth (4.5), fifth (4.6) and sixth (4.7) terms are the cost of selling hydrogen in the green hydrogen market, selling oxygen, and buying water, respectively. The seventh (4.8) and eighth (4.9) terms are the cost of buying CO_2 allowances in the carbon market. These two terms penalize the CO_2 emitted by the CHPs during the generation of electricity and heat. The last term (4.10) is the penalty term of the augmented Lagrangian and penalizes violations in electricity, gas, and heat networks.

$$min \sum_{t\in T}\left[\sum_{v\in\{E,\mathrm{GO},G,\mathrm{H}_2,H_2O,O_2,C\}} f_t^v + \sum_{d\in\{E,G,H,Hy\}}\sum_{s\in\{En,U,D\}}\sum_{n\in N^d}\mathcal{L}_{s,n,t}^d\right] + f^{CFA} \tag{4.1}$$

$$f_t^E = \lambda_t^E \cdot E_t^E \Delta t - \lambda_t^B (U_t^E + D_t^E) + (\lambda_t^{D,E} \cdot \phi_t^D \cdot D_t^E - \lambda_t^{U,E} \cdot \phi_t^U \cdot U_t^E)\Delta t \tag{4.2}$$

$$f_t^{GO} = \lambda_t^{GO} (\sum_{j\in J}\left(P_{j,t}^{P2G,E} - P_{j,t}^{PV}\right)\Delta t \tag{4.3}$$

$$f_t^G = \lambda_t^G \cdot E_t^G \Delta t + (\lambda_t^{U,G} \cdot \phi_t^U \cdot U_t^G - \lambda_t^{D,G} \cdot \phi_t^D \cdot D_t^G)\Delta t \tag{4.4}$$

$$f_t^{H_2} = -\lambda_t^{H_2} \cdot E_t^{H_2}\Delta t + \left(\lambda_t^{U,H_2} \cdot \phi_t^U \cdot U_t^{H_2} - \lambda_t^{D,H_2} \cdot \phi_t^D \cdot D_t^{H_2}\right)\Delta t \tag{4.5}$$

$$f_t^{H_2O} = \lambda_t^{H_2O} (\sum_{j\in J}\left(P_{j,t}^{P2G,E} + D_{j,t}^{P2G,E}\phi_t^D - U_{j,t}^{P2G,E} \cdot \phi_t^U\right)c^{H_2O}\,\Delta t \tag{4.6}$$

$$f_t^{O_2} = -\lambda_t^{O_2}\sum_{j\in J}\left(P_{j,t}^{P2G,E} + D_{j,t}^{P2G,E} \cdot \phi_t^D - U_{j,t}^{P2G,E} \cdot \phi_t^U\right)c^{O2}\,\Delta t \tag{4.7}$$

$$f_t^C = \lambda^{CO_2}\sum_{j\in J_n}\left(P_{j,t}^{CHP,E} + U_{j,t}^{CHP,E} \cdot \phi_t^U - D_{j,t}^{CHP,E} \cdot \phi_t^D\right)\alpha^{CO_2,G}\Delta t \tag{4.8}$$

$$f^{CFA} = \lambda^{CO_2} \cdot \mathrm{A}^{+,CO_2} \tag{4.9}$$

$$\mathcal{L}_{s,n,t}^d = \pi_{s,n,t}^d\left(P_{s,n,t}^d - \hat{P}_{s,n,t}^d\right) + \frac{\rho}{2}\left(P_{s,n,t}^d - \hat{P}_{s,n,t}^d\right)^2 \tag{4.10}$$

Table 4.1 presents a description of the variables of the objective function.

Table 4.1 - Variables of the objective function.

Variable	Description	Unit
$\boldsymbol{D_{j,t}^{CHP,E}}$, $\boldsymbol{D_t^G}$, $\boldsymbol{D_t^{H_2}}$, $\boldsymbol{D_{j,t}^{P2G,E}}$	Downward CHPs (electrical generation), natural gas, hydrogen, and P2G imbalances generated due to the expected activation of secondary reserves	MW
$\boldsymbol{D_t^E}$, $\boldsymbol{U_t^E}$	Upward and downward band bids	MW
$\boldsymbol{E_t^E}$	Consumption (positive) or generation (negative) electrical bids	MW
$\boldsymbol{E_t^G}$	Natural gas bids	MW
$\boldsymbol{E_t^{H_2}}$	Hydrogen bids	MW
$\boldsymbol{P_{j,t}^{CHP,E}}$	Power generated by CHPs	MW
$\boldsymbol{P_{j,t}^{P2G,E}}$	Electricity consumed by the P2G	MW
$\boldsymbol{P_{j,t}^{PV}}$	Electricity generated by PVs	MW
$\boldsymbol{U_{j,t}^{CHP,E}}$, $\boldsymbol{U_t^G}$, $\boldsymbol{U_t^{H_2}}$, $\boldsymbol{U_{j,t}^{P2G,E}}$	Upward CHPs (electrical generation), natural gas, hydrogen, and P2G imbalances generated due to the expected activation of secondary reserves	MW

Table 4.2 presents a description and the type of each parameter used in this subsection. All costs $\boldsymbol{\lambda_t^E}$, $\boldsymbol{\lambda_t^G}$, $\boldsymbol{\lambda^{H_2}}$, $\boldsymbol{\lambda^{CO_2}}$, $\boldsymbol{\lambda^{H_2O}}$, $\boldsymbol{\lambda^{O_2}}$, $\boldsymbol{\lambda_t^{GO}}$, $\boldsymbol{\lambda_t^B}$, $\boldsymbol{\lambda_t^{D,E}}$ and $\boldsymbol{\lambda_t^{U,E}}$, and mobilization ratios $\boldsymbol{\phi_t^D}$ and $\boldsymbol{\phi_t^U}$ are parameters forecasted by the aggregator. The conversion factor $\boldsymbol{\alpha^{CO_2,G}}$, $\boldsymbol{c^{H_2O}}$and $\boldsymbol{c^{O_2}}$ is a fixed value.

Table 4.2 – Parameters of the energy markets.

Parameter	Description	Unit	Type
$\boldsymbol{\alpha^{CO_2,G}}$	Conversion factor for carbon	–	Fixed
$\boldsymbol{c^{H_2O}}$	Converstion factor for water	L/MW	Fixed
$\boldsymbol{c^{O_2}}$	Converstion factor for oxygen	kg/MW	Fixed
$\boldsymbol{\lambda_t^B}$	Secondary reserve band price	$€/MW$	Forecasted
$\boldsymbol{\lambda^{CO_2}}$	Carbon allowances price	$€/tCO2$	Forecasted
$\boldsymbol{\lambda_t^{D,E}}$ and $\boldsymbol{\lambda_t^{U,E}}$	Downward and upward tertiary reserve prices	$€/MWh$	Forecasted
$\boldsymbol{\lambda_t^E}$, $\boldsymbol{\lambda_t^G}$ and $\boldsymbol{\lambda^{H_2}}$	Electricity, natural gas and hydrogen energy prices	$€/MWh$	Forecasted
$\boldsymbol{\lambda_t^{GO}}$	Guarantees of origin prices	€/MWh	Forecasted
$\boldsymbol{\lambda^{H_2O}}$	Water prices	$€/L$	Forecasted
$\boldsymbol{\lambda^{O_2}}$	Oxygen prices	$€/kg$	Forecasted
$\boldsymbol{\phi_t^D}$ and $\boldsymbol{\phi_t^U}$	Downward and upward ratio	–	Forecasted

4.2.2. Market constraints

Constraint (4.11) defines that the secondary reserve band must be 2/3 for upward and 1/3 for downward, according to the rules of the secondary reserve market of the MIBEL [101].

$$U_t^E = 2.D_t^E, \forall\, t \in T \tag{4.11}$$

Constraints (4.12) and (4.13) define the CO_2 allowances that the aggregator has to buy due to the heat generated by the CHPs.

$$\begin{aligned} \mathrm{A}^{+,CO_2} - \mathrm{A}^{-,CO_2} = &\sum_{t\in T}\sum_{j\in J_n}[(P_{j,t}^{CHP,H} + U_{j,t}^{CHP,H}\cdot\phi_t^U \;-\; D_{j,t}^{CHP,H}\phi_t^D)\alpha^{CO_2,G}\cdot\Delta t] \\ &- FA^{CO_2} \end{aligned} \tag{4.12}$$

$$\mathrm{A}^{+,CO_2}, \mathrm{A}^{-,CO_2} \geq 0 \tag{4.13}$$

Table 4.3 presents the variables for market constraints.

Table 4.3 - Variables for market constraints.

Variable	Description	Unit
$\boldsymbol{D_{j,t}^{CHP,H}}$, $\boldsymbol{U_{j,t}^{CHP,H}}$	Downward and upward heat imbalances generated by CHPs due to the expected activation of secondary reserves	MW
$\boldsymbol{P_{j,t}^{CHP,H}}$	Heat generated by CHPs	MW

Table 4.4 presents the parameters of the market constraints. The free carbon allowances FA^{CO_2} and the conversion factor $\alpha^{CO_2,G}$ are fixed parameters. The free carbon allowances are calculated by the aggregator, which is explained in Annex A.

Table 4.4 – Parameters for market constraints.

Parameter	Description	Unit	Type
$\boldsymbol{FA^{CO_2}}$	Free carbon allowances	–	Fixed
$\boldsymbol{\alpha^{CO_2,G}}$	Conversion factor to convert MWh of natural gas to tonnes of CO_2	CO_2/MWh	Fixed

4.2.3. Bidding constraints

Constraints (4.14)-(4.16) define the electricity (demand and supply), gas, and hydrogen bids.

$$E_t^E = \sum_{n \in N^E} P_{n,t}^E , \qquad \forall\, t \in T \tag{4.14}$$

$$E_t^G = \sum_{n \in N^G} P_{n,t}^G , \qquad \forall\, t \in T \tag{4.15}$$

$$E_t^{H_2} = \sum_{n \in N^{Hy}} P_{n,t}^{H_2} , \qquad \forall\, t \in T \tag{4.16}$$

Constraints (4.17) and (4.18) define the upward and downward secondary reserve bids. They include the flexibility provided by ESSs, PV systems, HPs, EVs, CHPs, P2Gs, and FCs.

$$U_t^E = \sum_{j \in J_n} \left(U_{j,t}^{Sto,+} + U_{j,t}^{Sto,-} + U_{j,t}^{PV} + U_{j,t}^{HP} + U_{j,t}^{EV,+} + U_{j,t}^{EV,-} + U_{j,t}^{CHP,E} + U_{j,t}^{P2G,E} + U_{j,t}^{FC,E} \right), \forall\, n \in N^E, t \in T \tag{4.17}$$

$$D_t^E = \sum_{j \in J_n} \left(D_{j,t}^{Sto,+} + D_{j,t}^{Sto,-} + D_{j,t}^{PV} + D_{j,t}^{HP} + D_{j,t}^{EV,+} + D_{j,t}^{EV,-} + D_{j,t}^{CHP,E} + D_{j,t}^{P2G,E} + D_{j,t}^{FC,E} \right), \forall\, n \in N^E t \in T \tag{4.18}$$

Constraints (4.19) and (4.20) define gas imbalances generated due to the expected activation of secondary reserve provided by CHPs.

$$U_t^G = \sum_{j \in J_n} \left(U_{j,t}^{CHP,G} \right), \qquad \forall\, n \in N^G, t \in T \tag{4.19}$$

$$D_t^G = \sum_{j \in J_n} \left(D_{j,t}^{CHP,G} \right), \qquad \forall\, n \in N^G, t \in T \tag{4.20}$$

Constraints (4.21) and (4.22) define hydrogen imbalances due to the expected activation of secondary reserve provided by P2Gs.

$$U_t^{H_2} = \sum_{j \in J_n} \left(U_{j,t}^{P2G \to Net,H_2} \right), \qquad \forall\, n \in N^{Hy}, t \in T \tag{4.21}$$

$$D_t^{H_2} = \sum_{j \in J_n} \left(D_{j,t}^{P2G \rightarrow Net,H_2} \right), \qquad \forall\, n \in N^{Hy}, t \in T \tag{4.22}$$

Table 4.5 presents the variables for bidding constraints.

Table 4.5 – Variables for bidding constraints.

Variable	Description	Unit
$\boldsymbol{D_{j,t}^{CHP,G}}, \boldsymbol{D_{j,t}^{EV,+}}, \boldsymbol{D_{j,t}^{EV,-}}, \boldsymbol{D_{j,t}^{FC,E}}, \boldsymbol{D_{j,t}^{HP}}, \boldsymbol{D_{j,t}^{PV}}, \boldsymbol{D_{j,t}^{P2G \rightarrow Net,H_2}}, \boldsymbol{D_{j,t}^{Sto.+}}, \boldsymbol{D_{j,t}^{Sto,-}}$	Downward CHP (natural gas consumption), electric vehicle, fuel cell, heat pump, PV, electrolyzer (hydrogen injection), and energy storage system imbalances generated due to the expected activation of secondary reserves	MW
$\boldsymbol{P_{n,t}^{E}}$	Electricity consumed (positive) or generated (negative)	MW
$\boldsymbol{P_{n,t}^{G}}$	Natural gas consumption	MW
$\boldsymbol{P_{n,t}^{H_2}}$	Hydrogen generation	MW
$\boldsymbol{U_{j,t}^{CHP,G}}, \boldsymbol{U_{j,t}^{EV,+}}, \boldsymbol{U_{j,t}^{EV,-}}, \boldsymbol{U_{j,t}^{FC,E}}, \boldsymbol{U_{j,t}^{HP}}, \boldsymbol{U_{j,t}^{PV}}, \boldsymbol{U_{j,t}^{P2G \rightarrow Net,H_2}}, \boldsymbol{U_{j,t}^{Sto.+}}, \boldsymbol{U_{j,t}^{Sto,-}}$	Upward CHP (natural gas consumption), electric vehicle, fuel cell, heat pump, PV, electrolyzer (hydrogen injection), and energy storage system imbalances generated due to the expected activation of secondary reserves	MW

4.2.4. Delivery scenario constraints

Delivery scenarios define possible exchanges of power between aggregators' clients and energy networks. The DSOs use these scenarios to evaluate the network feasibility of aggregator's offers. The network sub-problem (3.14) and (3.15) are solved for each DSO and for each delivery scenario. The delivery scenarios are divided by energy vectors. The electricity scenarios include the delivery of energy (4.23), and the activation of upward (4.27) and downward (4.28) secondary reserves in RT. The gas scenarios include the delivery of gas (4.24) and the gas imbalances (4.29)-(4.30) generated in RT due to the activation of secondary reserve provided by CHPs. The heat scenarios include the delivery of heat (4.25) and the heat imbalances (4.31)-(4.32) generated in RT due to the activation of secondary reserve provided by CHPs. The hydrogen scenarios include the delivery of hydrogen (4.26) and the hydrogen imbalances (4.33)-(4.34) generated in RT due to the activation of secondary reserve provided by P2Gs.

Constraint (4.23) defines the scenario of electricity delivery, which results from the sum of the electricity consumed by inflexible loads, HPs, ESSs, EVs, and P2Gs and electricity generated by ESSs, PV systems, EVs, CHPs, and the FCs.

$$\begin{aligned} P_{n,t}^{E} = \sum\nolimits_{j \in J_n} (&P_{j,t}^{IL,E} + P_{j,t}^{HP} + P_{j,t}^{\mathrm{Sto,E.+}} - P_{j,t}^{\mathrm{Sto,E,-}} - P_{jt}^{PV} + \mathrm{P}_{j,t}^{\mathrm{EV,+}} - \mathrm{P}_{j,t}^{\mathrm{EV,-}} + P_{j,t}^{CHP,E} \\ &+ P_{j,t}^{P2G,E} - P_{j,t}^{FC,E}), \qquad \forall\, n \in N^{E}, t \in T \end{aligned} \tag{4.23}$$

Constraint (4.24) defines the scenario of gas delivery, which results from the sum of the gas consumed by the inflexible loads and CHPs connected to the district heating.

$$P_{n,t}^{G} = \sum\nolimits_{j\in J_n} (P_{j,t}^{IL,G} + P_{j,t}^{CHP,G}), \qquad \forall\, n \in N^G,\;\; t \in T \qquad (4.24)$$

Constraint (4.25) defines the scenario of heat delivery, which results from the sum of the heat consumed by the inflexible and flexible heating loads connected to the district heating and the heat generated by CHPs.

$$P_{n,t}^{H} = \sum\nolimits_{j\in J_n} (P_{j,t}^{IL,H} + P_{j,t}^{DH} - P_{j,t}^{CHP,H}), \qquad \forall\, n \in N^H,\;\; t \in T \qquad (4.25)$$

Constraint (4.26) defines the scenario of hydrogen delivery, which results from the sum of the hydrogen injected by the P2G and the HSS into the gas network.

$$P_{n,t}^{H_2} = \sum\nolimits_{j\in J_n} (P_{j,t}^{P2G\rightarrow Net,H_2,} + P_{j,t}^{Sto\rightarrow Net,H_2}), \qquad \forall\, n \in N^{H_2},\;\; t \in T \qquad (4.26)$$

Constraint (4.27) defines the scenario of upward band activation in RT. It considers the sum of the upward flexibility of HPs, ESSs, PV systems, and CHPs. Constraint (4.28) defines the scenario of downward band activation in RT. It considers the sum of the downward flexibility of HPs, ESSs, PV systems, EVs, CHPs, P2Gs, and FCs.

$$P_{n,t}^{U,E} = P_{n,t}^{E} - \sum\nolimits_{j\in J_n}\big(U_{j,t}^{HP} + U_{j,t}^{Sto,+} + U_{j,t}^{Sto,E,-} + U_{j,t}^{PV} + U_{j,t}^{EV,+} + U_{j,t}^{EV,E,-} + U_{j,t}^{CHP,E} + U_{j,t}^{P2G,E} + U_{j,t}^{FC,E}\big), \qquad \forall\, n \in N^E, t \in T \qquad (4.27)$$

$$P_{n,t}^{D,E} = P_{n,t}^{E} + \sum\nolimits_{j\in J_n}\big(D_{j,t}^{HP} + D_{j,t}^{Sto,+} + D_{j,t}^{Sto,E,-} + D_{j,t}^{PV} + D_{j,t}^{EV,+} + D_{j,t}^{EV,E,-} + D_{j,t}^{CHP,E} + D_{j,t}^{P2G,E} + D_{j,t}^{FC,E}\big), \qquad \forall\, n \in N^E, t \in T \qquad (4.28)$$

Constraints (4.29) and (4.30) define the scenarios of gas imbalances generated by the activation of upward and downward band reserves in RT. The gas imbalances are defined in (4.19) and (4.20) and result from the behavior of the CHPs.

$$P_{n,t}^{U,G} = P_{n,t}^{G} + \sum\nolimits_{j\in J_n}\big(U_{j,t}^{CHP,G}\big), \qquad \forall\, n \in N^G, t \in T \qquad (4.29)$$

$$P_{n,t}^{D,G} = P_{n,t}^{G} - \sum\nolimits_{j\in J_n}\big(D_{j,t}^{CHP,G}\big), \qquad \forall\, n \in N^G, t \in T \qquad (4.30)$$

Constraints (4.31) and (4.32) define the scenarios of heat imbalances generated by the activation of upward and downward band reserves in RT. The heat imbalances result from the behavior of the district heating and CHPs.

$$P_{n,t}^{U,H} = P_{n,t}^{H} - \sum\nolimits_{j\in J_n}\big(U_{j,t}^{DH} + U_{j,t}^{CHP,H}\big), \qquad \forall\, n \in N^H, t \in T \qquad (4.31)$$

$$P_{n,t}^{D,H} = P_{n,t}^{H} - \sum\nolimits_{j\in J_n}\big(D_{j,t}^{DH} + D_{j,t}^{CHP,H}\big), \qquad \forall n \in N^H, t \in T \qquad (4.32)$$

Constraints (4.33) and (4.34) define the scenarios of hydrogen imbalances generated by the activation of upward and downward band reserves in RT. The hydrogen imbalances are defined in (4.21) and (4.22) and result from the behavior of the P2Gs.

$$P_{n,t}^{U,H_2} = P_{n,t}^{H_2} - \sum\nolimits_{j\in J_n}\left(U_{j,t}^{P2G\rightarrow Net,H_2}\right), \qquad \forall\, n \in N^{H_2}, t \in T \qquad (4.33)$$

$$P_{n,t}^{D,H_2} = P_{n,t}^{H_2} + \sum_{j\in J_n}\left(D_{j,t}^{P2G\rightarrow Net,H_2}\right), \qquad \forall\, n \in N^{H_2}, t \in T \qquad (4.34)$$

Table 4.6 presents the variables for the delivery scenarios' constraints.

Table 4.6 – Variables for delivery scenarios constraints.

Variable	Description	Unit
$D_{j,t}^{DH}, U_{j,t}^{DH}$	Downward and upward DH imbalances generated due to the expected activation of secondary reserves	MW
$P_{j,t}^{CHP,G}, P_{j,t}^{IL,G}$	Natural gas consumption from CHPs and inflexible loads	MW
$P_{n,t}^{D,E}, P_{n,t}^{U,E}$	Scenarios of electricity imbalances generated by the activation of downward and upward band reserves in real-time	MW
$P_{n,t}^{D,G}, P_{n,t}^{U,G}$	Scenarios of natural gas imbalances generated by the activation of downward and upward band reserves in real-time	MW
$P_{n,t}^{D,H}, P_{n,t}^{U,H}$	Scenarios of heat imbalances generated by the activation of downward and upward band reserves in real-time	MW
$P_{n,t}^{D,H_2}, P_{n,t}^{U,H_2}$	Scenarios of hydrogen imbalances generated by the activation of downward and upward band reserves in real-time	MW
$P_{j,t}^{DH}, P_{j,t}^{IL,H}$	Heat consumption from district heating loads and inflexible loads	MW
$P_{j,t}^{EV,+}, P_{j,t}^{HP}, P_{j,t}^{IL,E}, P_{j,t}^{Sto,E,+}$,	Electricity consumption from electric vehicles, heat pumps, inflexible loads, and battery storage systems	MW
$P_{j,t}^{EV,-}, P_{j,t}^{FC,E}, P_{j,t}^{Sto,E,-}$	Electricity generation from electric vehicles, fuel cells, and energy storage systems	MW
$P_{n,t}^{H}$	Heat consumption	MW
$P_{j,t}^{P2G\rightarrow Net,H_2}$, $P_{j,t}^{Sto\rightarrow Net,H_2}$	Hydrogen injected into the network from P2Gs and hydrogen storage systems	MW

4.2.5. DMER constraints

This section presents the models developed for the HPs, district heating flexible loads, PVs, ESSs, EVs, CHPs, P2Gs, HSSs, FCs, and fuel stations.

4.2.5.1. Heat pumps

Figure 4.2 presents an HP scheme. HPs consume electricity (inputs) to produce heat (outputs).

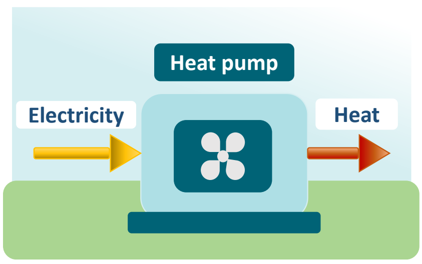

Figure 4.2 - Heat pump scheme (inputs: electricity, outputs: heat).

The HPs are modeled by equations (4.35)-(4.44). Constraint (4.35) defines the minimum and maximum power limits. Constraints (4.36)-(4.38) define the limits of the upward and downward bands. Constraints (4.39)-(4.41) define the temperature in each delivery scenario (energy (4.23), upward (4.27), and downward (4.28) band activations). Constraints (4.42)-(4.44) model the comfort levels of the occupants. The comfort levels are defined by prosumers who set a range of acceptable temperatures in the rooms for each hour.

$$\underline{P_j^{HP}} \leq P_{j,t}^{HP} \leq \overline{P_j^{HP}}, \qquad \forall\ j \in J,\ \ t \in T \tag{4.35}$$

$$U_{j,t}^{HP} \leq\ P_{j,t}^{HP} - \underline{P_j^{HP}}, \qquad \forall\ j \in J,\ \ t \in T \tag{4.36}$$

$$D_{j,t}^{HP} \leq \overline{P_j^{HP}} -\ P_{j,t}^{HP}, \qquad \forall\ j \in J,\ \ t \in T \tag{4.37}$$

$$D_{j,t}^{HP}, U_{j,t}^{HP} \geq 0, \qquad \forall\ j \in J,\ \ t \in T \tag{4.38}$$

$$\theta_{j,t+1}^{E} = \beta_j \cdot \theta_{j,t}^{E} + (1-\beta_j)\left[\theta_{j,t}^{O} + R_j\left(\eta_j^{HP} \cdot P_{j,t}^{HP}\right)\right] +\ \vartheta_{j,t}, \qquad \forall\ j \in J,\ \ t \in T \tag{4.39}$$

$$\theta_{j,t+1}^{U} = \beta_j \cdot \theta_{j,t}^{U} + (1-\beta_j)\left[\theta_{j,t}^{O} + R_j\left(\eta_j^{HP} \cdot P_{j,t}^{HP} - \eta_j^{HP} \cdot U_{j,t}^{HP}\right)\right] +\ \vartheta_{j,t}, \forall\ j \in J\ , t \in T \tag{4.40}$$

$$\theta_{j,t+1}^{D} = \beta_j \cdot \theta_{j,t}^{D} + (1-\beta_j)\left[\theta_{j,t}^{O} + R_j\left(\eta_j^{HP} \cdot P_{j,t}^{HP} + \eta_j^{HP} \cdot D_{j,t}^{HP}\right)\right] +\ \vartheta_{j,t}, \forall\ j \in J\ , t \in T \tag{4.41}$$

$$\underline{\theta_j} \leq \theta_{j,t+1}^{E} \leq \overline{\theta_j}, \qquad \forall\ j \in J,\ \ t \in T \tag{4.42}$$

$$\underline{\theta_j} \leq \theta_{j,t+1}^{U} \leq \overline{\theta_j}, \qquad \forall\ j \in J,\ \ t \in T \tag{4.43}$$

$$\underline{\theta_j} \leq \theta_{j,t+1}^{D} \leq \overline{\theta_j}, \qquad \forall\ j \in J,\ \ t \in T \tag{4.44}$$

Table 4.7 presents the variables for HPs' constraints.

Table 4.7 - Variables for heat pump constraints.

Variable	Description	Unit
$\boldsymbol{\theta_{j,t}^{D}}, \boldsymbol{\theta_{j,t}^{U}}$	Downward and upward temperature imbalances generated due to the expected activation of secondary reserves	C^o
$\boldsymbol{\theta_{j,t}^{E}}$	Temperature of the building	C^o

The HP parameters are presented in Table 4.8. The minimum and maximum power ($\underline{P_{j,t}^{HP}}$ and $\overline{P_{j,t}^{HP}}$) and efficiency (η_j^{HP}) are parameters provided by the manufacturing company. The minimum and maximum temperature ($\underline{\theta_j}$ and $\overline{\theta_j}$) of the spaces are defined by the prosumers and communicated by the EMS. The thermal resistance (R_j) and capacitance (C_j) are physical characteristics of the buildings and they can be calculated by the aggregator using estimation techniques [164][165]. The thermal constant is calculated using equation (4.45). The outside temperature ($\theta_{j,t}^{O}$) can be forecasted by the aggregator himself or by contracting a weather service provider. Heat gains and losses ($\vartheta_{j,t}$)result from solar radiation, loads, or human activity, and they can be estimated by the aggregator.

$$\beta = \frac{\Delta t}{CR} \tag{4.45}$$

Table 4.8 – Parameters of heat pumps and thermal loads.

Parameter	Name	Unit	Type
$\boldsymbol{C_j}$	Thermal capacitance	$MWh/ºC$	Fixed
$\underline{\boldsymbol{P_j^{HP}}}$ and $\overline{\boldsymbol{P_j^{HP}}}$	Minimum and maximum power	MW	Fixed
$\boldsymbol{R_j}$	Thermal resistance	$ºC/MW$	Fixed
$\boldsymbol{\beta_j}$	Thermal constant	–	Fixed
$\boldsymbol{\eta_j^{HP}}$	Efficiency	–	Fixed
$\underline{\boldsymbol{\theta}}_j$ and $\overline{\boldsymbol{\theta}}_j$	Minimum and maximum temperature	$ºC$	Fixed
$\boldsymbol{\theta_{j,t}^{O}}$	Outside temperature	$ºC$	Forecasted
$\boldsymbol{\vartheta_{j,t}}$	Heat gains and losses	$ºC$	Forecasted

4.2.5.2. District heating flexible loads

The district heating flexible loads are modelled by the same equations of the HPs (4.35)-(4.44). However, instead of modelling the electric power variables $\{P_{j,t}^{HP}, D_{j,t}^{HP}, U_{j,t}^{HP}\}$, here we model the thermal variables $\{P_{j,t}^{DH}, D_{j,t}^{DH}, U_{j,t}^{DH}\}$ in constraints (4.35)-(4.44).

4.2.5.3. PV systems

Figure 4.3 presents a PV scheme. PV systems generate electricity, and so, their outputs are electricity.

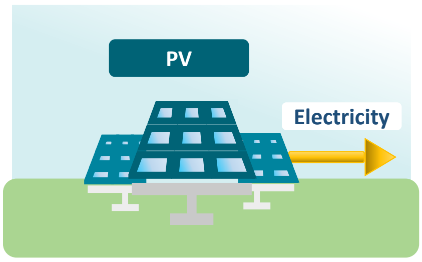

Figure 4.3 - PV scheme (outputs: electricity).

Constraint (4.46) defines the maximum power output of the PV system. The parameter $\overline{P_j^{PV}}$ is the forecasted generation. Constraints (4.47) and (4.48) define the band limits.

$$0 \leq P_{j,t}^{PV} \leq \overline{P_j^{PV}}, \qquad \forall \quad j \in J, \quad t \in T \tag{4.46}$$

$$0 \leq U_{j,t}^{PV} \leq \overline{P_j^{PV}} - P_{j,t}^{PV}, \qquad \forall \quad j \in J, \quad t \in T \tag{4.47}$$

$$0 \leq D_{j,t}^{PV} \leq P_{j,t}^{PV}, \qquad \forall \; j \in J, \;\; t \in T \qquad (4.48)$$

Table 4.9 presents the parameters of PVs. The aggregator can forecast the PV generation ($\overline{P_j^{PV}}$) or contract a weather service provider to get those values.

Table 4.9 – Parameters of PVs.

Parameter	Name	Unit	Type
$\overline{P_j^{PV}}$	Forecasted generation	MW	Forecasted

4.2.5.4. Energy storage system constraints

Figure 4.4 present an ESS scheme. ESSs can store electricity and they are charged and discharged with electricity (inputs and outputs).

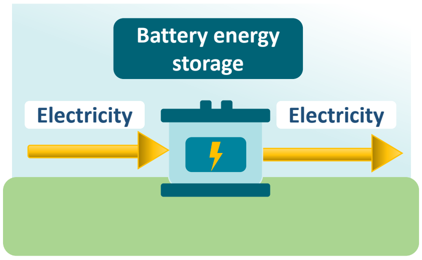

Figure 4.4 – Energy storage system scheme (inputs: electricity, outputs: electricity).

The operation of the ESS units is defined by constraints (4.49)-(4.64). Constraints (4.49) and (4.50) define the SOC and its limits. Constraints (4.51)-(4.53) set the range of the charging and discharging power. Constraint (4.54) ensures that the SOC at the end of the day is equal to the initial SOC.

$$SOC_{j,t+1}^{Sto,E} = SOC_{j,t}^{Sto,E} + \left(P_{j,t}^{Sto,E,+} \cdot \eta_j^{Sto,E} - \frac{P_{j,t}^{Sto,E,-}}{\eta_j^{Sto,E}} \right) \Delta t, \qquad \forall \, j \in J, \;\; t \in T \qquad (4.49)$$

$$\underline{SOC_j^{Sto,E}} \leq SOC_{j,t+1}^{Sto,E} \leq \overline{SOC_j^{Sto,E}}, \qquad \forall \, j \in J, \;\; t \in T \qquad (4.50)$$

$$0 \leq P_{j,t}^{Sto,E,-} + \dot{P}_{j,t}^{Sto,E,-} \leq \left(1 - b_{j,t}^{Sto,E}\right) \overline{P_j^{Sto,E,-}}, \qquad \forall \, j \in J, \;\; t \in T \qquad (4.51)$$

$$0 \leq P_{j,t}^{Sto,E,+} + \dot{P}_{j,t}^{Sto,E,+} \leq b_{j,t}^{Sto,E} \cdot \overline{P_j^{Sto,E,+}}, \qquad \forall \, j \in J, \;\; t \in T \qquad (4.52)$$

$$P_{j,t}^{Sto,E,-}, \dot{P}_{j,t}^{Sto,E,-}, P_{j,t}^{Sto,E,+}, \dot{P}_{j,t}^{Sto,E,+} \geq 0, \qquad \forall \, j \in J, \;\; t \in T \qquad (4.53)$$

$$SOC_{j,0}^{Sto,E} = SOC_{j,-1}^{Sto,E}, \qquad \forall \, j \in J \qquad (4.54)$$

Constraints (4.55) and (4.56) limit the upward band while constraints (4.57) and (4.58) limit the downward band. Constraints (4.59) and (4.60) guarantee that the storage only supplies upward and downward bands if the SOC is within the limits. Constraints (4.61)-(4.64) ensure that the storage has enough capacity to compensate for the activation of upward and downward bands [150].

$$0 \leq U_{j,t}^{Sto,E,-} \leq \overline{P_{J}^{Sto,E,-}} - P_{j,t}^{Sto,E,-}, \qquad \forall\, j \in J,\ \ t \in T \tag{4.55}$$

$$0 \leq U_{j,t}^{Sto,E,+} \leq P_{j,t}^{Sto,E,+}, \qquad \forall\, j \in J,\ \ t \in T \tag{4.56}$$

$$0 \leq D_{j,t}^{Sto,E,+} \leq \overline{P_{J}^{Sto,E,+}} - P_{j,t}^{Sto,E,+}, \qquad \forall\, j \in J,\ \ t \in T \tag{4.57}$$

$$0 \leq D_{j,t}^{Sto,E,-} \leq P_{j,t}^{Sto,E,-}, \qquad \forall\, j \in J,\ \ t \in T \tag{4.58}$$

$$\left(\frac{U_{j,t}^{Sto,E,-}}{\eta_{j}^{Sto,E}} + U_{j,t}^{Sto,E,+} \cdot \eta_{j}^{Sto,E}\right)\Delta t \leq SOC_{j,t+1}^{Sto,E} - \underline{SOC_{j}^{Sto,E}}, \qquad \forall\, j \in J,\ \ t \in T \tag{4.59}$$

$$\left(\frac{D_{j,t}^{Sto,E,-}}{\eta_{j}^{Sto,E}} + D_{j,t}^{Sto,E,+} \cdot \eta_{j}^{Sto,E}\right)\Delta t \leq \overline{SOC_{j}^{Sto,E}} - SOC_{j,t+1}^{Sto,E}, \qquad \forall\, j \in J,\ \ t \in T \tag{4.60}$$

$$U_{j,t}^{Sto,E,+} + U_{j,t}^{Sto,E,-} + D_{j,t}^{Sto,E,+} + D_{j,t}^{Sto,E,-} \leq \dot{P}_{J,t+1}^{Sto,E,+} + \dot{P}_{J,t+1}^{Sto,E,-}, \qquad \forall\, j \in J,\ \ t \in T \tag{4.61}$$

$$U_{j,t}^{Sto,E,+} + U_{j,t}^{Sto,E,-} + D_{j,t}^{Sto,E,+} + D_{j,t}^{Sto,E,-} \leq \dot{b}_{j,t}^{Sto,E} \cdot M, \qquad \forall\, j \in J,\ \ t \in T \tag{4.62}$$

$$\dot{P}_{J,t}^{Sto,E,+} + \dot{P}_{J,t}^{Sto,E,-} \leq \left(1 - \dot{b}_{j,t}^{Sto,E}\right)M, \qquad \forall\, j \in J,\ \ t \in T \tag{4.63}$$

$$U_{j,-1}^{Sto,E,+}, U_{j,-1}^{Sto,E,-}, D_{j,-1}^{Sto,E,+}, D_{j,-1}^{Sto,E,-} = 0, \qquad \forall\, j \in J \tag{4.64}$$

Table 4.10 presents the variables for ESSs constraints.

Table 4.10 - Variables for energy storage systems constraints.

Variable	Description	Unit
$\boldsymbol{b_{j,t}^{Sto,E}}$	Binary variable indicating the charging (1) or discharging (0) mode	-
$\boldsymbol{\dot{b}_{j,t}^{Sto,E}}$	Binary variable indicating if there is availability for offering upward and downward reserves	-
$\boldsymbol{\dot{P}_{J,t}^{Sto,E,+}}, \boldsymbol{\dot{P}_{J,t}^{Sto,E,-}}$	Availability for charging and discharging	MW
$\boldsymbol{SOC_{j,t}^{Sto,E}}$	State-of-charge of the energy storage system	MWh

Table 4.11 presents the parameters of the ESSs. The charging and discharging efficiency, minimum and maximum SOC, and maximum charging/discharging power are parameters provided by the manufacturing company. The initial SOC is communicated by the EMS.

Table 4.11 – Parameters of energy storage systems.

Parameter	Name	Unit	Type
$\boldsymbol{\overline{P_{J}^{Sto,E}}}$	Maximum charging/discharging power	MW	Fixed
$\boldsymbol{SOC_{j,0}^{Sto,E}}$	Initial state-of-charge	MWh	Fixed

$\underline{\boldsymbol{SOC}_j^{\mathrm{Sto,E}}}$ and $\overline{\boldsymbol{SOC}_j^{\mathrm{Sto,E}}}$	Minimum and maximum state-of-charge	MWh	Fixed
$\boldsymbol{\eta}_j^{Sto,E,+}$ and $\boldsymbol{\eta}_j^{\mathrm{Sto,E,-}}$	Charging and discharging efficiency	–	Fixed

4.2.5.5. Electric vehicles

Figure 4.5 presents an EV scheme. As well as ESSs, EVs can store energy, and they are charged and discharged with electricity (inputs and outputs). We assume that EVs have vehicle to grid (V2G) capabilities, i.e. they can inject electricity into the electricity network and offer market services. The modeling of EVs considers the time of arrival and departure, and a predefined SOC at the time of arrival and departure.

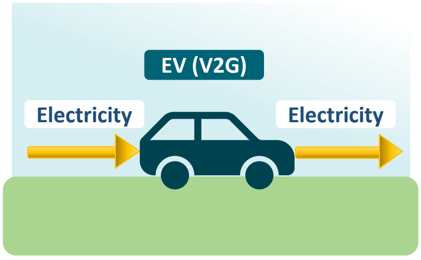

Figure 4.5 – Electric vehicle with V2G capabilities scheme (inputs: electricity, outputs: electricity).

The operation of electric vehicles is defined by constraints (4.65)-(4.81). Constraints (4.65) and (4.66) define the SOC of EVs and its limits. Constraints (4.67)-(4.69) set the range of the charging and discharging power. Constraint (4.70) sets the SOC at the time of arrival. Constraint (4.71) ensures that the predefined SOC at the time of departure is guaranteed.

$$SOC_{j,t+1}^{EV,E} = SOC_{j,t}^{EV,E} + \left(P_{j,t}^{EV,E,+} \cdot \eta_j^{EV,E} - \frac{P_{j,t}^{EV,E,-}}{\eta_j^{EV,E}}\right)\Delta t, \qquad \forall\, j \in J,\;\; t \in T \qquad (4.65)$$

$$\underline{SOC_j^{EV,E}} \le SOC_{j,t+1}^{EV,E} \le \overline{SOC_j^{EV,E}}, \qquad \forall\, j \in J,\;\; t \in T \qquad (4.66)$$

$$0 \le P_{j,t}^{EV,E,-} + P_{j,t}^{E\dot{V},E,-} \le \left(1 - b_{j,t}^{EV,E}\right)\overline{P_j^{EV,E,-}}, \qquad \forall\, j \in J,\;\; t \in T_j^{EV} \qquad (4.67)$$

$$0 \le P_{j,t}^{EV,E,+} + P_{j,t}^{E\dot{V},E,+} \le b_{j,t}^{EV,E} \cdot \overline{P_j^{EV,E,+}}, \qquad \forall\, j \in J,\;\; t \in T \qquad (4.68)$$

$$P_{j,t}^{EV,E,-}, P_{j,t}^{E\dot{V},E,-}, P_{j,t}^{EV,E,+}, P_{j,t}^{E\dot{V},E,+} \ge 0, \qquad \forall\, j \in J,\;\; t \in T \qquad (4.69)$$

$$SOC_{j,\mathrm{t}_j^{\mathrm{AR}}}^{EV,E} = SOC_j^{EV,AR}, \qquad \forall\, j \in J \qquad (4.70)$$

$$SOC_{j,\mathrm{t}_j^{\mathrm{DE}}}^{EV} \ge SOC_j^{EV,DE}, \qquad \forall\, j \in J \qquad (4.71)$$

Constraints (4.72)-(4.75) limit the upward and downward bands of EVs. Constraints (4.76) and (4.77) guarantee that EVs only supply upward and downward bands if the SOC is within the limits. Constraints (4.78)-(4.81) ensure that each EV has enough capacity to compensate for the activation of upward and downward bands [150].

$$0 \leq U_{j,t}^{EV,E,-} \leq \overline{P_J^{EV,E,-}} - P_{j,t}^{EV,E,-}, \qquad \forall\, j \in J,\ \ t \in T \qquad (4.72)$$

$$0 \leq U_{j,t}^{EV,E,+} \leq P_{j,t}^{EV,E,+}, \qquad \forall\, j \in J,\ \ t \in T \qquad (4.73)$$

$$0 \leq D_{j,t}^{EV,E,+} \leq \overline{P_J^{EV,E,+}} - P_{j,t}^{EV,E,+}, \qquad \forall\, j \in J,\ \ t \in T \qquad (4.74)$$

$$0 \leq D_{j,t}^{EV,E,-} \leq P_{j,t}^{EV,E,-}, \qquad \forall\, j \in J,\ \ t \in T \qquad (4.75)$$

$$\left(\frac{U_{j,t}^{EV,E,-}}{\eta_j^{EV,E}} + U_{j,t}^{EV,E,+} \cdot \eta_j^{EV,E}\right)\Delta t \leq SOC_{j,t+1}^{EV,E} - \underline{SOC_j^{EV,E}}, \qquad \forall\, j \in J,\ \ t \in T \qquad (4.76)$$

$$\left(\frac{D_{j,t}^{EV,E,-}}{\eta_j^{EV,E}} + D_{j,t}^{EV,E,+} \cdot \eta_j^{EV,E}\right)\Delta t \leq \overline{SOC_j^{EV,E}} - SOC_{j,t+1}^{EV,E}, \qquad \forall\, j \in J,\ \ t \in T \qquad (4.77)$$

$$U_{j,-1}^{EV,E,+}, U_{j,-1}^{EV,E,-}, D_{j,-1}^{EV,E,+}, D_{j,-1}^{EV,E,-} = 0, \qquad \forall\, j \in J \qquad (4.78)$$

$$U_{j,t}^{EV,E,+} + U_{j,t}^{EV,E,-} + D_{j,t}^{EV,E,+} + D_{j,t}^{EV,E,-} \leq P_{J,t+1}^{E\dot{V},E,+} + P_{J,t+1}^{E\dot{V},E,-}, \qquad \forall\, j \in J,\ \ t \in T \qquad (4.79)$$

$$U_{j,t}^{EV,E,+} + U_{j,t}^{EV,E,-} + D_{j,t}^{EV,E,+} + D_{j,t}^{EV,E,-} \leq \dot{b}_{j,t}^{EV,E} \cdot M, \qquad \forall\, j \in J,\ \ t \in T \qquad (4.80)$$

$$P_{J,t}^{E\dot{V},E,+} + P_{J,t}^{E\dot{V},E,-} \leq \left(1 - \dot{b}_{j,t}^{EV,E}\right) \cdot M, \qquad \forall\, j \in J,\ \ t \in T \qquad (4.81)$$

Table 4.12 presents the variables for EVs constraints.

Table 4.12 - Variables for electric vehicles' constraints.

Variable	Description	Unit
$\boldsymbol{b_{j,t}^{EV,E}}$	Binary variable indicating the charging (1) or discharging (0) mode	-
$\boldsymbol{\dot{b}_{j,t}^{EV,E}}$	Binary variable indicating if there is space for offering upward and downward reserves	-
$\boldsymbol{P_{J,t+1}^{E\dot{V},E,+}}, \boldsymbol{P_{J,t+1}^{E\dot{V},E,-}}$	Electricity space for charging and discharging	MW
$\boldsymbol{SOC_{j,t}^{EV,E}}$	State-of-charge of the electric vehicles	MWh

Table 4.13 presents the EVs parameters. Charging and discharging efficiency, minimum, and maximum SOC, and maximum charging/discharging power are provided by the manufacturing company. The SOC at the time of arrival and departure, and the time of arrival and departure are forecasted by the aggregator.

Table 4.13 – Parameters of electric vehicles.

Parameter	Name	Unit	Type
$\overline{\boldsymbol{P_J^{EV}}}$	Maximum charging/discharging power	MW	Fixed
$\boldsymbol{SOC_j^{EV,AR}}, \boldsymbol{SOC_j^{EV,DE}}$	State-of-charge at time of arrival and departure	MWh	Forecasted
$\underline{\boldsymbol{SOC_j^{EV}}}$ and $\overline{\boldsymbol{SOC_j^{EV}}}$	Minimum and maximum state-of-charge	MWh	Fixed
$\boldsymbol{t_j^{AR}}, \boldsymbol{t_j^{DE}}$	Time of arrival and departure	–	Forecasted

$\boldsymbol{\eta_j^{EV,+}}$ and $\boldsymbol{\eta_j^{EV,-}}$	Charging and discharging efficiency	–	Fixed

4.2.5.6. District heating CHPs

Figure 4.6 presents a CHP scheme. CHPs consume natural gas (inputs) to produce heat and electricity (outputs).

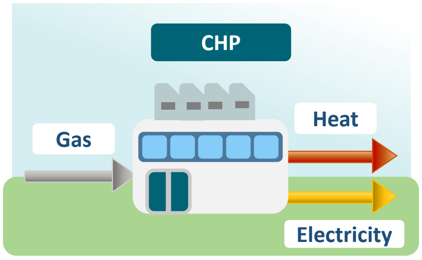

Figure 4.6 – CHP scheme (inputs: gas, outputs: heat and electricity).

Constraints (4.82)-(4.91) model the CHPs connected to the district heating. Constraint (4.82) sets the gas consumption range. Constraints (4.83) and (4.84) define the electricity and heat generated by the CHPs. Constraints (4.85)-(4.90) define the electricity, gas, and heat flexibilities of the CHPs to provide upward and downward reserve bands.

$$\underline{P_j^{CHP,G}} \le P_{j,t}^{CHP,G} \le \overline{P_j^{CHP,G}}, \qquad \forall\ j \in J,\ \ t \in T \quad (4.82)$$

$$P_{j,t}^{CHP,E} = \eta_j^{CHP,E} \cdot P_{j,t}^{CHP,G}, \qquad \forall\ j \in J,\ \ t \in T \quad (4.83)$$

$$P_{j,t}^{CHP,H} = \eta_j^{CHP,H} \cdot P_{j,t}^{CHP,G}, \qquad \forall\ j \in J,\ \ t \in T \quad (4.84)$$

$$0 \le U_{j,t}^{CHP,G} \le \overline{P_j^{CHP,G}} - P_{j,t}^{CHP,G}, \qquad \forall\ j \in J,\ \ t \in T \quad (4.85)$$

$$U_{j,t}^{CHP,E} = \eta_j^{CHP,E} \cdot U_{j,t}^{CHP,G}, \qquad \forall\ j \in J,\ \ t \in T \quad (4.86)$$

$$U_{j,t}^{CHP,H} = \eta_j^{CHP,H} \cdot U_{j,t}^{CHP,G}, \qquad \forall\ j \in J,\ \ t \in T \quad (4.87)$$

$$0 \le D_{j,t}^{CHP,G} \le P_{j,t}^{CHP,G} - \underline{P_j^{CHP,G}}\ , \qquad \forall\ j \in J,\ \ t \in T \quad (4.88)$$

$$D_{j,t}^{CHP,E} = \eta_j^{CHP,E} \cdot D_{j,t}^{CHP,G}, \qquad \forall\ j \in J,\ \ t \in T \quad (4.89)$$

$$D_{j,t}^{CHP,H} = \eta_j^{CHP,H} \cdot D_{j,t}^{CHP,G}, \qquad \forall\ j \in J,\ \ t \in T \quad (4.90)$$

CHPs have a slower response than other electric resources and they are only able to provide 100% of their power within 60 s [166]. Constraint (4.91) limits the response of the CHPs to a fraction of its maximum power. This ensures that the CHPs can deliver the reserves traded in the secondary reserve market. Secondary reserve markets typically require full activations at fast response times.

$$U_{j,t}^{CHP,G}, D_{j,t}^{CHP,G} \leq \mu^{CHP} \cdot \overline{P_j^{CHP,G}}, \qquad \forall\ j \in J,\ \ t \in T \qquad (4.91)$$

Table 4.14 presents the parameters of CHPs. The maximum and minimum gas power ($\underline{P_j^{CHP,G}}$ and $\overline{P_j^{CHP,G}}$) and efficiency of converting natural gas to electricity and heat ($\eta_j^{CHP,E}$ and $\eta_j^{CHP,H}$) are provided by the manufacturing company. The CHP participation factor[6] (μ^{CHP}) is defined by the aggregator.

Table 4.14 – Parameters of CHPs.

Parameter	Name	Unit	Type
$\underline{\boldsymbol{P_j^{CHP,G}}}$ and $\overline{\boldsymbol{P_j^{CHP,G}}}$	Maximum and minimum gas power	MW	Fixed
$\boldsymbol{\eta_j^{CHP,E}}$ and $\boldsymbol{\eta_j^{CHP,H}}$	Efficiency of converting natural gas to electricity and heat	–	Fixed
$\boldsymbol{\mu^{CHP}}$	Participation factor	–	Fixed

4.2.5.7. Electrolyzer constraints

Figure 4.7 presents a P2G scheme. P2Gs consume electricity (inputs) to produce hydrogen (outputs).

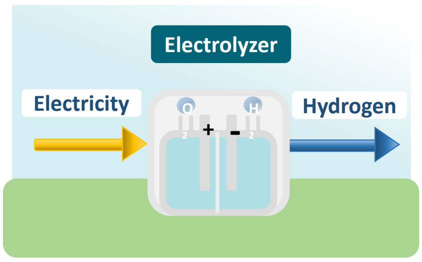

Figure 4.7 – Electrolyzer scheme (inputs: electricity, outputs: hydrogen).

Constraints (4.92)-(4.100) model the P2Gs connected to the electricity network. Constraints (4.92) and (4.93) define the hydrogen produced by the P2Gs. It considers the flow from the P2G to the fuel station, the gas network, and the HSS. The hydrogen flow from the P2G to the FC was not considered as it is an inefficient process that would never be considered by the aggregator. Constraints (4.94)-(4.100) define the limits of the P2Gs: (4.94) for electricity consumption and (4.95)-(4.100) for secondary reserves provision in upward and downward directions. As seen in equations (4.99) and (4.100), the P2G upward and downward secondary reserve provision considers the changes in the hydrogen flow from the P2G to the gas network and the HSS. The sign → represents the power that flows from X to Y. For example, the notation in $P2G \rightarrow Sto, H_2$ represents the hydrogen that flows from the P2G to the HSS.

$$P_{j,t}^{P2G,H_2} = \eta_j^{P2G} \cdot P_{j,t}^{P2G,E}, \qquad \forall\ j \in J,\ \ t \in T \qquad (4.92)$$

[6] The Participation Factor indicates the response fraction of a generator/load power as a response to frequency deviations.

$$P_{j,t}^{P2G,H_2} = P_{j,t}^{P2G\rightarrow HV,H_2} + P_{j,t}^{P2G\rightarrow Net,H_2,} + P_{j,t}^{P2G\rightarrow Sto,H_2}, \qquad \forall\ j \in J,\ \ t \in T \qquad (4.93)$$

$$\underline{P_{j}^{P2G,E}} \leq P_{j,t}^{P2G,E} \leq \overline{P_{j}^{P2G,E}}, \qquad \forall\ j \in J,\ \ t \in T \qquad (4.94)$$

$$U_{j,t}^{P2G,E} \leq\ P_{j,t}^{P2G,E} - \underline{P_{j}^{P2G,E}}, \qquad \forall\ j \in J,\ \ t \in T \qquad (4.95)$$

$$D_{j,t}^{P2G,E} \leq \overline{P_{j}^{P2G,E}} -\ P_{j,t}^{P2G,E}, \qquad \forall\ j \in J,\ \ t \in T \qquad (4.96)$$

$$U_{j,t}^{P2G,H_2} = \eta_{j}^{P2G} \cdot U_{j,t}^{P2G,E}, \qquad \forall\ j \in J,\ \ t \in T \qquad (4.97)$$

$$D_{j,t}^{P2G,H_2} = \eta_{j}^{P2G} \cdot D_{j,t}^{P2G,E}, \qquad \forall\ j \in J,\ \ t \in T \qquad (4.98)$$

$$U_{j,t}^{P2G,H_2} = U_{j,t}^{P2G\rightarrow Net,H_2} + U_{j,t}^{P2G\rightarrow Sto,H_2}, \qquad \forall\ j \in J,\ \ t \in T \qquad (4.99)$$

$$D_{j,t}^{P2G,H_2} = D_{j,t}^{P2G\rightarrow Net,H_2} + D_{j,t}^{P2G\rightarrow Sto,H_2}, \qquad \forall\ j \in J,\ \ t \in T \qquad (4.100)$$

Table 4.15 presents the variables for the P2Gs' constraints.

Table 4.15 - Variables for electrolyzers' constraints.

Variable	Description	Unit
$\boldsymbol{D_{j,t}^{P2G,H_2}}, \boldsymbol{U_{j,t}^{P2G,H_2}}$	Downward and upward hydrogen imbalances from the electrolyzer generated due to the expected activation of secondary reserves	MW
$\boldsymbol{D_{j,t}^{P2G\rightarrow Sto,H_2}}, \boldsymbol{U_{j,t}^{P2G\rightarrow Sto,H_2}}$	Downward and upward hydrogen imbalances from the electrolyzer to the hydrogen storage systems generated due to the expected activation of secondary reserves	MW
$\boldsymbol{P_{j,t}^{P2G,H_2}}$	Hydrogen produced	MW
$\boldsymbol{P_{j,t}^{P2G\rightarrow HV,H_2}}, \boldsymbol{P_{j,t}^{P2G\rightarrow Sto,H_2}}$	Hydrogen going from the electrolyzer to the hydrogen vehicles fuel station and the hydrogen storage systems	MW

The efficiency (η_{j}^{P2G}) and the minimum and maximum power ($\underline{P_{j}^{P2G,E}}$ and $\overline{P_{j}^{P2G,E}}$) are provided by the manufacturer.

Table 4.16 presents the parameters of the P2G. The efficiency (η_{j}^{P2G}) and the minimum and maximum power ($\underline{P_{j}^{P2G,E}}$ and $\overline{P_{j}^{P2G,E}}$) are provided by the manufacturer.

Table 4.16 – Parameters of the electrolyzer.

Parameter	Name	Unit	Type
$\underline{\boldsymbol{P_{j}^{P2G,E}}}$ and $\overline{\boldsymbol{P_{j}^{P2G,E}}}$	Minimum and maximum power	MW	Fixed
$\boldsymbol{\eta_{j}^{P2G}}$	Efficiency of converting electricity into hydrogen	–	Fixed

4.2.5.8. Hydrogen storage system constraints

Figure 4.8 presents a HSS scheme. The HSSs store hydrogen and they are charged and discharged with hydrogen (inputs and outputs).

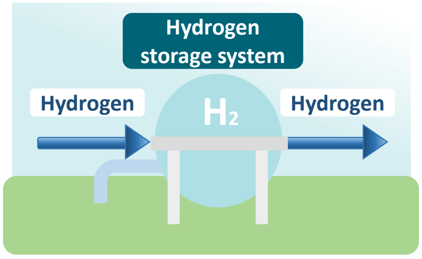

Figure 4.8 – Hydrogen storage scheme (inputs: hydrogen, outputs: hydrogen).

Constraints (4.101)-(4.114) define the operation of HSSs. Constraints (4.101) and (4.102) define the SOC and its limits. Constraints (4.103)-(4.107) set the charging and discharging power and their limits. As seen in equations (4.103) and (4.104), the charging of the HSSs considers the flow from the P2G to the HSS, and the discharging of the HSS considers the flow from the HSS to the fuel station, the gas network, and the FC.

$$SOC_{j,t+1}^{Sto,H_2} = SOC_{j,t}^{Sto,H_2} + \left(P_{j,t}^{Sto,H_2,+} \cdot \eta_j^{Sto,H_2,+} - \frac{P_{j,t}^{Sto,H_2,-}}{\eta_j^{Sto,H_2,-}} \right) \Delta t - \gamma_j \cdot SOC_{j,t}^{Sto,H_2}, \quad \forall \; j \in J, \; t \in T \tag{4.101}$$

$$\underline{SOC_j^{Sto,H_2}} \leq SOC_{j,t}^{Sto,H_2} \leq \overline{SOC_j^{Sto,H_2}}, \qquad \forall \; j \in J, \; t \in T \tag{4.102}$$

$$P_{j,t}^{Sto,H_2,+} = P_{j,t}^{P2G \rightarrow Sto,H_2}, \qquad \forall \; j \in J, \; t \in T \tag{4.103}$$

$$P_{j,t}^{Sto,H_2,-} = P_{j,t}^{Sto \rightarrow HV,H_2} + P_{j,t}^{Sto \rightarrow Net,H_2} + P_{j,t}^{Sto \rightarrow FC,H_2}, \qquad \forall \; j \in J, \; t \in T \tag{4.104}$$

$$\underline{P_j}^{Sto,H_2} \leq b_{j,t}^{Sto,H_2,+} \cdot P_{j,t}^{Sto,H_2,+}, \qquad \forall \; j \in J, \; t \in T \tag{4.105}$$

$$P_{j,t}^{Sto,H_2,-} \leq b_{j,t}^{Sto,H_2,-} \cdot \overline{P_j^{Sto,H_2,-}}, \qquad \forall \; j \in J, \; t \in T \tag{4.106}$$

$$b_{j,t}^{Sto,H_2,+} + b_{j,t}^{Sto,H_2,-} \leq 1, \qquad \forall \; j \in J, \; t \in T \tag{4.107}$$

$$SOC_{j,0}^{Sto,H_2} = SOC_{j,-1}^{Sto,H_2}, \qquad \forall \, j \in J \tag{4.108}$$

Constraints (4.109)-(4.114) define the secondary reserves bands provided by the HSSs. Constraints (4.109)-(4.112) define the power limits, while constraints (4.113) and (4.114) set the energy limits of HSSs.

$$0 \leq D_{j,t}^{P2G \rightarrow Sto,H_2} \leq \overline{P_j^{Sto,H_2}} - P_{j,t}^{Sto,H_2,+}, \qquad \forall \; j \in J, \; t \in T \tag{4.109}$$

$$0 \leq U_{j,t}^{P2G \rightarrow Sto,H_2} \leq P_{j,t}^{Sto,H_2,+}, \qquad \forall \; j \in J, \; t \in T \tag{4.110}$$

$$0 \leq D_{j,t}^{Sto \to FC,H_2} \leq P_{j,t}^{Sto \to FC,H_2}, \qquad \forall\ j \in J,\ \ t \in T \tag{4.111}$$

$$0 \leq U_{j,t}^{Sto \to FC,H_2} \leq \overline{P_j^{Sto,H_2}} - P_{j,t}^{Sto,H_2,-}, \qquad \forall\ j \in J,\ \ t \in T \tag{4.112}$$

$$D_{j,t}^{P2G \to Sto,H_2} + D_{j,t}^{Sto \to FC,H_2} \leq \frac{\overline{SOC_j^{Sto,H_2}} - SOC_{j,t+1}^{Sto,H_2}}{\Delta t}, \qquad \forall\ j \in J,\ \ t \in T \tag{4.113}$$

$$U_{j,t}^{P2G \to Sto,H_2} + U_{j,t}^{Sto \to FC,H_2} \leq \frac{SOC_{j,t+1}^{Sto,H_2} - \underline{SOC_j^{Sto,H_2}}}{\Delta t}, \qquad \forall\ j \in J,\ \ t \in T \tag{4.114}$$

Table 4.17 presents the variables for HSSs constraints.

Table 4.17 - Variables for hydrogen storage system constraints.

Variable	Description	Unit
$\boldsymbol{b_{j,t}^{Sto,H_2,+}}, \boldsymbol{b_{j,t}}^{Sto,H_2,-}$	Binary variable indicating the charging and discharging modes	-
$\boldsymbol{D_{j,t}^{Sto \to FC,H_2}}, \boldsymbol{U_{j,t}^{Sto \to FC,H_2}}$	Downward and upward hydrogen imbalances from the electrolyzer to the fuel cell generated due to the expected activation of secondary reserves	MW
$\boldsymbol{SOC_{j,t}^{Sto,H_2}}$	State-of-charge of the hydrogen storage system	MWh
$\boldsymbol{P_{j,t}^{Sto,H_2,+}}, \boldsymbol{P_{j,t}^{Sto,H_2,-}}$	Hydrogen charging and discharging	MW
$\boldsymbol{P_{j,t}^{Sto \to HV,H_2}}, \boldsymbol{P_{j,t}^{Sto \to FC,H_2}}$	Hydrogen from the hydrogen storage system to the hydrogen vehicle fuel station and fuel cells	MW

Table 4.18 presents the parameters of the HSS. The minimum and maximum SOC, the low heating value, and the maximum charging are parameters provided by the manufacturing company. The initial SOC is communicated by the EMS.

Table 4.18 – Parameters of the hydrogen storage system.

Parameter	Name	Unit	Type
$\boldsymbol{SOC_{j,0}^{Sto,H_2}}$	Initial state-of-charge	MWh	Fixed
$\underline{\boldsymbol{SOC_j^{Sto,H_2}}}$ and $\overline{\boldsymbol{SOC_j^{Sto,H_2}}}$	Minimum and maximum state-of-charge	MWh	Fixed
$\boldsymbol{\gamma_j}$	Discharging rate	$-$	Fixed

4.2.5.9. Fuel cell constraints

Figure 4.9 presents a FC scheme. FCs transform hydrogen (inputs) into electricity (outputs).

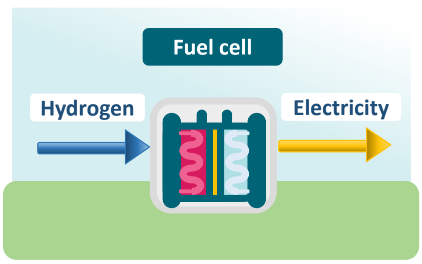

Figure 4.9 – Fuel cell scheme (inputs: hydrogen, outputs: electricity).

Constraints (4.115)-(4.121) define the operation of the FCs. Constraints (4.115) and (4.116) define the electricity produced by the FCs. The remaining constraints (4.117)-(4.121) define the secondary reserves bands provided by the FCs.

$$P_{j,t}^{FC,E} = \eta_j^{FC} \cdot P_{j,t}^{Sto\to FC,H_2}, \quad \forall\ j \in J,\ \ t \in T \tag{4.115}$$

$$0 \le P_{j,t}^{Sto\to FC,H_2} \le b_{j,t}^{Sto,H_2,-} \cdot \overline{P_j^{FC,H_2}}, \quad \forall\ j \in J,\ \ t \in T \tag{4.116}$$

$$U_{j,t}^{Sto\to FC,H_2} \le b_{j,t}^{Sto,H_2,-} \cdot \overline{P_j^{FC,H_2}} - P_{j,t}^{Sto\to FC,H_2}, \quad \forall\ j \in J,\ \ t \in T \tag{4.117}$$

$$D_{j,t}^{Sto\to FC,H_2} \le P_{j,t}^{Sto\to FC,H_2}, \quad \forall\ j \in J,\ \ t \in T \tag{4.118}$$

$$U_{j,t}^{FC,E} = \eta_j^{FC} \cdot U_{j,t}^{Sto\to FC,H_2}, \quad \forall\ j \in J,\ \ t \in T \tag{4.119}$$

$$D_{j,t}^{FC,E} = \eta_j^{FC} \cdot D_{j,t}^{Sto\to FC,H_2}, \quad \forall\ j \in J,\ \ t \in T \tag{4.120}$$

$$D_{j,t}^{FC,E}, U_{j,t}^{FC,E} \ge 0, \quad \forall\ j \in J,\ \ t \in T \tag{4.121}$$

Table 4.19 presents the parameters of the FC. The efficiency of converting hydrogen into electricity, and the maximum power are parameters provided by the manufacturing company.

Table 4.19 – Parameters of the fuel cell.

Parameter	**Name**	**Unit**	**Type**
$\overline{P_j^{FC,H_2}}$	Maximum power	MW	Fixed
η_j^{FC}	Efficiency of converting hydrogen into electricity	–	Fixed

4.2.5.10. Fuel station constraint

Figure 4.10 presents a fuel station scheme and it consumes hydrogen (input).

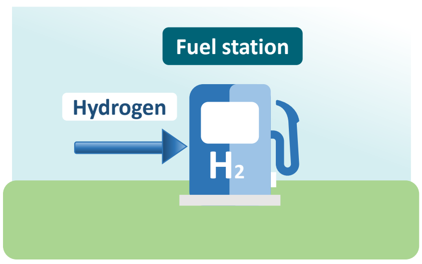

Figure 4.10 – Fuel station scheme (inputs: hydrogen).

Constraint (4.122) ensures that fuel stations supply hydrogen to inflexible loads, such as hydrogen vehicles. Note that the production of green hydrogen[7] to supply fuel stations connected to local hubs is not traded in the market.

$$P_{j,t}^{P2G\rightarrow HV,H_2} + P_{j,t}^{Sto\rightarrow HV,H_2} = P_{j,t}^{HV}, \qquad \forall\, j \in J, t \in T \qquad (4.122)$$

Table 4.20 presents the parameters of the fuel station. The hydrogen load is forecasted by the aggregator.

Table 4.20 – Parameters of the fuel station.

Parameter	Name	Unit	Type
$\boldsymbol{P_{j,t}^{HV}}$	Hydrogen load	MW	Forecasted

4.3. DSO subproblems: multi-energy flow optimization models

This section presents the formulation of the optimization models (3.14) and (3.15) introduced in Chapter 3. These optimization models are multi-energy flow models used by the DSOs to evaluate the network feasibility of the aggregator's offers. The DSOs use the delivery scenarios computed by the aggregator to check if the aggregator's offers violate or not the constraints of the multi-energy networks.

The role of the DSOs in this paper is to ensure multi-energy network security while opening up as much network capacity as possible for the aggregator to bid into the markets. The minimization of the operating costs of the DSOs, such as network losses, is not considered since the operation of the system is defined by the dispatch of the wholesale markets.

4.3.1. Time horizon and delivery scenarios

The optimization problem is decomposed by time-step $t \in T$ and delivery scenarios $s \in \{E, U, D\}$ since there are no coupling constraints between different time-steps and delivery scenarios. In the next subsections, for the sake of readability, the subscripts of time and delivery scenarios are dropped.

4.3.2. Electricity DSO sub-problem

Here, we formulate the optimization problem that the electricity DSO uses to evaluate the feasibility of the aggregator's offers.

4.3.2.1. Objective function

The objective function (4.123) minimizes the augmented Lagrangian penalty terms, which penalize electricity network violations.

[7] As explained in Chapter 3, the aggregator makes sure the hydrogen produced is green by ensuring it is produced using generation from PVs or by buying guarantees of origin when PV generation is not enough to satisfy the electricity consumption of the P2Gs.

$$min \sum_{n \in N^E} \left[\pi_n^E \left(P_n^E - \hat{P}_n^E \right) + \frac{\rho}{2} \left(P_n^E - \hat{P}_n^E \right)^2 \right] \tag{4.123}$$

4.3.2.2. Electricity network constraints

The electricity network is modeled using the non-convex formulation of the branch flow model [167][168]. Constraints (4.124)-(4.127) are the branch power flow equations. Constraints (4.128) and (4.129) set the limits of the square of the voltage and current magnitudes.

$$P_{m,n}^F = \frac{\hat{P}_n^E}{SB} + \sum_{i:n \to i} P_{n,i}^F + r_{m,n} \cdot \ell_{m,n}, \qquad \forall\, (m,n) \in B^E \tag{4.124}$$

$$Q_{m,n}^F = \ Q_n^E + \sum_{i:n \to i} Q_{n,i}^F + x_{m,n} \cdot \ell_{m,n}, \qquad \forall\, (m,n) \in B^E \tag{4.125}$$

$$v_n = v_m - 2\left(r_{m,n} \cdot P_{m,n}^F + x_{m,n} \cdot Q_{m,n}^F\right) + \left(r_{m,n}^2 + x_{m,n}^2\right)\ell_{m,n}, \qquad \forall\, (m,n) \in B^E \tag{4.126}$$

$$\ell_{m,n} \cdot v_m = {P_{m,n}^F}^2 + {Q_{m,n}^F}^2, \qquad \forall\, (m,n) \in B^E \tag{4.127}$$

$$\underline{v_n} \leq v_n \leq \overline{v_n}\,, \qquad \forall\, n \in N^E \tag{4.128}$$

$$0 \leq \ell_{m,n} \leq \overline{\ell_{m,n}}, \qquad \forall\, (m,n) \in B^E \tag{4.129}$$

Table 4.21 presents the variables for the electricity flow model.

Table 4.21 - Variables for the electricity flow model.

Variable	Description	Unit
$\boldsymbol{\ell_{m,n}}$	Square of the current magnitude	$p.u.$
$\boldsymbol{P_{m,n}^F}$	Active power flow	$p.u.$
$\boldsymbol{Q_{m,n}^F}$	Reactive power flow	$p.u.$
$\boldsymbol{v_n}$	Square of the voltage magnitude	$p.u.$

Table 4.22 presents the parameters for the electricity network model.

Table 4.22 – Parameters for the electricity flow model.

Parameter	Name	Unit
$\boldsymbol{\overline{\ell_{m,n}}}$	Maximum current	$p.u.$
$\boldsymbol{r_{m,n}}$	Resistance of lines	$p.u.$
$\boldsymbol{SB}$	Base Power	$p.u.$
$\boldsymbol{\overline{v_n}, \underline{v_n}}$	Maximum and minimum voltage	$p.u.$
$\boldsymbol{x_{m,n}}$	Reactance of lines	$p.u.$

4.3.3. Gas DSO sub-problem

The gas flow optimization problem (4.130)-(4.144) is used by the gas DSO to assure that delivery scenarios of hydrogen and natural gas computed by the aggregator are network-secure.

4.3.3.1. Objective function

The objective function (4.130) minimizes the augmented Lagrangian penalty, which penalizes the calculation of network-secure gas delivery scenarios that deviate from the aggregator's preferences.

$$Min \sum_{d\,\in\,\{GL,H2\}} \left[\sum_{m \in N^d} \pi_m^d \left(P_m^d - \hat{P}_m^d\right) + \frac{\rho}{2}\left(P_m^d - \hat{P}_m^d\right)^2 \right] \tag{4.130}$$

4.3.3.2. Network constraints

Constraints (4.131)-(4.132) define the limits of natural gas injection (4.131) and nodal pressure (4.132).

$$\underline{P_m^{NG}} \leq P_m^{NG} \leq \overline{P_m^{NG}}, \qquad \forall\, m \in N^{NG} \tag{4.131}$$

$$\underline{p_m^G} \leq p_m^G \leq \overline{p_m^G}, \qquad \forall\, m \in N^G \tag{4.132}$$

Constraint (4.133) models the gas balance in each node. Constraints (4.134)-(4.136) define the volumetric flow of natural gas (4.134), hydrogen (4.135), and gas mixture (4.136).

$$q_m^{NG} + \hat{q}_m^{H_2} - \hat{q}_m^G + \sum_{n:n \to m} q_{n,m} - \sum_{n:m \to n} q_{m,n} = 0, \qquad \forall\, m \in N^G \tag{4.133}$$

$$q_m^{NG} = \frac{P_m^{NG}}{c^G}, \qquad \forall\, m \in N^G \tag{4.134}$$

$$\hat{q}_m^{H2} = \frac{\hat{P}_m^{H2}}{c^{H2}}, \qquad \forall\, m \in N^G \tag{4.135}$$

$$\hat{q}_m^G = \frac{\hat{P}_m^G \cdot HHV_m^G}{\left(HHV_m^{Mix}\right)^2 c^G}, \qquad \forall\, m \in N^G \tag{4.136}$$

Constraints (4.137)-(4.140) define the HHV (4.137)-(4.138) and the relative gas density to air (4.139) of the gas mixture of hydrogen with natural gas [169]. Constraint (4.140) defines the fraction of hydrogen in the gas mixture.

$$HHV_m^{mix} = w_m^{H_2} \cdot HHV_m^{H_2} + \left(1 - w_m^{H_2}\right) HHV_m^G, \qquad \forall\, m \in N^G \tag{4.137}$$

$$\underline{HHV^{mix}} \leq HHV_m^{mix} \leq \overline{HHV^{mix}}, \qquad \forall\, m \in N^G \tag{4.138}$$

$$S_m^{mix} = w_m^{H_2} \cdot S_m^{H_2} + \left(1 - w_m^{H_2}\right) S_m^G, \qquad \forall\, m \in N^G \tag{4.139}$$

$$w_m^{H_2} = \frac{\hat{q}_m^{H_2}}{q_m^{NG} + \hat{q}_m^{H_2}}, \qquad \forall\, m \in N^G \tag{4.140}$$

Constraints (4.141)-(4.142) are related with the Wobbe Index (WI) [170] of the gas mixture. These two constraints are used to ensure that the energy output of the gas mixture is acceptable for the end-users and meets established quality of service requirements.

$$WI_m = \frac{HHV_m^{mix}}{\sqrt{S_m^{mix}}}, \qquad \forall\, m \in N^G \tag{4.141}$$

$$\underline{WI} \le WI_m \le \overline{WI}, \qquad \forall\, m \in N^G \tag{4.142}$$

Constraint (4.143) defines the steady-stage gas flow [171]. In this case, the gas flowing into the pipeline is equal to the gas flowing out of the pipeline. Constraint (4.144) defines the resistance coefficient of each pipeline.

$$(p_m^G)^2 - (p_n^G)^2 = K_{m,n}^G \cdot q_{m,n} \left|\left(q_{m,n}\right)^{0.848}\right|, \qquad \forall\ (m,n) \in B^G \tag{4.143}$$

$$K_{m,n}^G = \frac{(p^{G,St})^2\left(S_m^{Mix}\right)^{0.848}\theta^G}{57.3 \times 10^{-8}(\theta^{G,St})^2 143.52} \cdot \frac{L_{m,n}}{\left(\eta_{m,n}\right)^2\left(d_{m,n}\right)^{4.848}}, \qquad \forall\, (m,n) \in B^G \tag{4.144}$$

Table 4.23 presents the variables for the gas flow model.

Table 4.23 - Variables for the gas flow model.

Variable	**Description**	**Unit**
$\boldsymbol{HHV_m^{Mix}}$	Higher heating value of the mixed gases	MJ/m^3
$\boldsymbol{p_m^G}$	Gas pressure	bar
$\boldsymbol{P_m^{NG}}$	Natural gas injection	MW
$\boldsymbol{q_{n,m}, q_m}$	Gas flows	m^3/h
$\boldsymbol{S_m^{mix}}$	Specific gas gravity	$-$
$\boldsymbol{w_m^{H_2}}$	Hydrogen fraction	$-$
$\boldsymbol{WI_m}$	Wobbe index	MJ/m^3

Table 4.24 presents the parameters for the gas flow model.

Table 4.24 – Parameters for the gas flow model.

Parameter	**Name**	**Unit**
$\boldsymbol{c^{H2}, c^G}$	Factor to convert MWh to m^3/h	$\frac{m^3/h}{MWh}$
$\boldsymbol{d_{m,n}}$	Diameter of pipeline	mm
$\boldsymbol{HHV_m^G, HHV_m^{H_2}}$	Higher heating value of natural gas and hydrogen	MJ/m^3
$\boldsymbol{\overline{HHV^{mix}}, \underline{HHV^{mix}}}$	Maximum and minimum higher heating value of the mixed gases	MJ/m^3
$\boldsymbol{K_{m,n}^G}$	Resistance pipeline coefficient	-
$\boldsymbol{L_{m,n}}$	Lenght of pipeline	m

$\boldsymbol{p^{G,St}}$	Pressure of natural gas at standard pressure	bar
$\overline{\boldsymbol{p_m^G}}, \underline{\boldsymbol{p_m^G}}$	Maximum and minimum gas pressure	bar
$\overline{\boldsymbol{P_m^{NG}}}, \underline{\boldsymbol{P_m^{NG}}}$	Maximum and minimum injection of natural gas	MWh
$\overline{\boldsymbol{WI}}, \underline{\boldsymbol{WI}}$	Maximum and minimum Wobbe index	$\mathrm{MJ/m^3}$
$\boldsymbol{\theta^G}, \boldsymbol{\theta^{G,St}}$	Temperature of the gases and standard temperature of natural gas	C^o

4.3.4. Heat DSO sub-problem

Here, we formulate the optimization problem that the heat DSO uses to evaluate the feasibility of the aggregator’s offers.

4.3.4.1. Objective function

The objective function (4.145) minimizes the augmented Lagrangian penalty terms, which penalize heat network violations.

$$min \sum_{n\in N^H}\left[\pi_n^H\left(P_n^H-\hat{P}_n^H\right)+\frac{\rho}{2}\left(P_n^H-\hat{P}_n^H\right)^2\right] \tag{4.145}$$

4.3.4.2. Heat network constraints

Heat networks consist of supply and return networks. Hydraulic and thermal optimizations are performed to calculate the mass flows and temperatures of pipes and nodes. In this model, it was assumed that the temperature of generator supply nodes and load return nodes are defined, as well as the heat power at all nodes, except the slack node.

Hydraulic model

Constraints (4.146) and (4.147) define the conservation of mass and pressure drop. Constraints (4.148)-(4.150) define the pressure and mass flow limits of pipelines and loads/generators [172]. The value of $k_{i,j}$ is calculated as in [173]. To relax the problem, the heat direction flow was initialized for each hour based on the algorithm developed in [174] and remained static for the rest of the iterations.

$$\sum_{j:j\to i} m_{j,i}^a - \sum_{j:i\to j} m_{i,j}^a = A_i^a \cdot mq_i, \qquad \forall\, a \in \{S,R\},\ i \in N^H \tag{4.146}$$

$$p_i^{H,a} - p_j^{H,a} = k_{i,j}^a \cdot m_{i,j}^a\left|m_{i,j}^a\right|, \qquad \forall\, a \in \{S,R\},\ (i,j) \in B^H \tag{4.147}$$

$$\underline{p_i^{H,a}} \le p_i^{H,a} \le \overline{p_i^{H,a}}, \qquad \forall\, a \in \{S,R\},\ i \in N^H \tag{4.148}$$

$$\underline{m_{i,j}^a} \le m_{i,j}^a \le \overline{m_{i,j}^a}, \qquad \forall\, a \in \{S,R\},\ (i,j) \in B^H \tag{4.149}$$

$$\underline{mq_i} \le mq_i \le \overline{mq_i}, \qquad \forall\, i \in N^H \tag{4.150}$$

Thermal model

The thermal model (4.151)-(4.156) is used to determine the temperatures at each network node. Constraint (4.151) is the heat power equation of the loads and generators. The temperature drop constraint (4.152) defines the temperature at the end node of the pipe. Constraints (4.153) and (4.154) set the limits of the temperatures at the end and start nodes of the pipe. Constraint (4.155) defines the conservation of energy. Constraint (4.156) connects equation (4.151) to the remaining constraints of the thermal model by imposing that the temperatures of mass flowing through the node are equal to the temperatures mixed at the node.

$$\hat{P}_i^H = CP \cdot mq_i\left(\theta_i^S - \theta_i^R\right), \qquad \forall\, i \in N^H \tag{4.151}$$

$$\theta_{i,j}^{End,a} = (\theta_{i,j}^{Start,a} - \theta^{Amb})e^{\frac{h \cdot L}{CP \cdot m_{i,j}^a}} + \theta^{Amb}, \qquad \forall\, a \in \{S,R\},\ (i,j) \in B^H \tag{4.152}$$

$$\underline{\theta_{i,j}^{End,a}} \le \theta_{i,j}^{End,a} \le \overline{\theta_{i,j}^{End,a}}, \qquad \forall\, a \in \{S,R\},\ (i,j) \in B^H \tag{4.153}$$

$$\underline{\theta_{i,j}^{Start,a}} \le \theta_{i,j}^{Start,a} \le \overline{\theta_{i,j}^{Start,a}}, \qquad \forall\, a \in \{S,R\},\ (i,j) \in B^H \tag{4.154}$$

$$\sum_{j:j\to i} \theta_{j,i}^{End,a} \cdot m_{j,i}^a = \theta_i^a \sum_{j:i\to j} m_{i,j}^a, \qquad \forall\, a \in \{S,R\},\ \forall\, i \in N^H \tag{4.155}$$

$$\theta_i^a = \theta_{i,j}^{Start,a}, \qquad \forall\, a \in \{S,R\}, \forall\, i \in N^H \tag{4.156}$$

Table 4.25 presents the variables for the heat flow model.

Table 4.25 - Variables for the heat flow model.

Variable	Description	Unit
$\boldsymbol{m_{i,j}^a}$	Mass flows of pipelines	kg/s
$\boldsymbol{mq_i}$	Mass flows of heat loads and generators	kg/s
$\boldsymbol{p_i^{H,a}}$	Pressure of water pipelines	Pa
$\boldsymbol{\theta_{i,j}^{End,a}}, \boldsymbol{\theta_{i,j}^{Start,a}}$	Temperature at the end and the start of a pipeline	C°
$\boldsymbol{\theta_i^R}, \boldsymbol{\theta_i^S}$	Temperature of return (generators) and supply (loads) nodes	C°

Table 4.26 presents the parameters for the heat flow model.

Table 4.26 – Parameters for the heat flow model.

Parameter	Name	Unit
$\boldsymbol{CP}$	Water specific heat (J/kg.oC)	$J/kg.C^o$
$\boldsymbol{h}$	Heat transfer coefficient (W/°C.m)	$W/C^o.m$
$\boldsymbol{k_{i,j}^a}$	Coefficient of pressure loss in water pipelines	–
$\boldsymbol{L}$	Lenght of pipeline	m
$\overline{\boldsymbol{m_{i,j}^a}}, \underline{\boldsymbol{m_{i,j}^a}}$	Maximum and minimum mass flows of pipelines	kg/s

$\overline{mq_i}, \underline{mq_i}$	Maximum and minimum mass flows of heat loads and generators	kg/s
$\overline{p_i^{H,a}}, \underline{p_i^{H,a}}$	Maximum and minimum pressure of water pipelines	Pa
θ^{Amb}	Ambient temperature of pipelines' surroundings	C^o
θ_i^S, θ_i^R	Temperature of supply (generators) and return (loads) nodes	C^o
$\overline{\theta_{i,j}^{End,a}}, \underline{\theta_{i,j}^{End,a}}, \overline{\theta_{i,j}^{Start,a}}, \underline{\theta_{i,j}^{Start,a}}$	Maximum and minimum temperature at the end and start of a pipeline	C^o

4.4. Case study

The proposed multi-energy and network-secure bidding strategy is evaluated using the microgrid from the University of Manchester [175]. The case study's data are presented in Annex A and contain network, DMERs, buildings, market, weather, and inflexible load data. This data can assume the form of point forecasts or actual measurements, as described in Annex A.

4.5. Results

The novel aggregators' framework developed in this thesis considers the participation of aggregators in multi-energy markets.

In this section, we discuss and compare the results computed by three different bidding strategies:

- Multi-energy and network-free (M-NF) strategy: under this strategy, the aggregator manages DMERs and computes bids without considering the constraints of the energy networks;

- Single-energy and network-free (S-NF) strategy: under this strategy, the aggregator only manages single energy-vector resources and computes bids without considering the constraints of the energy networks. This strategy was evaluated using two aggregators, one with only electricity resources, and another with only gas resources;

- Multi-energy and network-secure (M-NS) strategy: under this fully integrated approach, an aggregator manages DMERs and computes network-secure bids.

This section discusses the results obtained for each strategy focusing on the placement of the aggregator's bids (4.5.1), the disaggregated band bids deployed per resource (4.5.2), the impacts of the multi-energy bids in the energy networks (4.5.3), the economic performance (4.5.4), the CO_2 emissions (4.5.5) and finally, the computational performance (4.5.6).

4.5.1. Optimized multi-energy bids

Figure 4.11 presents the electricity (energy and secondary reserve band), gas, hydrogen, CO_2 allowance, and GO bids submitted by the aggregator(s) to the day-ahead markets, under the M-

NF, S-NF, and M-NS strategies. It is important to note that gas, hydrogen, CO_2, and GO bids are presented in the market as daily bids and not hourly bids. The hourly disaggregation presented is only for analysis purposes. Table 4.27 presents the total daily bids under the three scenarios.

The three bidding strategies present similar placement behaviors in the DA energy market (electricity). Demand (positive values) and supply (negative values) bids are mainly influenced by PV production, prices, and heat requirements. The aggregator places most of the supply bids during the period of forecasted PV generation (i.e., during daylight time). On the other hand, the aggregator placed a high quantity of demand bids at the beginning of the day, ie. between 1h and 6h, to benefit from lower prices to heat the buildings.

The three bidding strategies also present some placement similarities in the DA gas market. The gas bids are mainly influenced by prices and heat requirements. Most of the gas was bought to supply the CHPs, which generate heat to satisfy the heat load requirements of the prosumers connected to the heat network. The heat load requirements are stricter between 7h and 18h, which leads the aggregator to buy more gas in the market. During this period, the bids end up following the electricity energy prices as it can profit from the injection of electricity from the CHPs and higher prices. From 0h to 5h and from 21h onwards, the gas bids do not change much, which can suggest that at these hours, the aggregator is only fulfilling gas loads and heat load requirements expected from the CHPs. As the CO_2 allowances bids are directly related to the CHP production, their behavior is very similar to the gas bids.

Table 4.27 - Total daily bids of the three strategies. The differences in percentage are the comparison with the M-NF strategy.

Bids (MW)	M-NF	S-NF		M-NS	
Demand electricity bid	17.3	9.5	-45 %	11.4	-34 %
Supply electricity bid	-21.0	-24.8	+18 %	-18.0	-14 %
Upward bid	34.4	23.2	-33 %	28.9	-16 %
Downward bid	17.2	11.6	-33 %	14.5	-16 %
Gas	90.9	110.4	+21 %	96.0	+6 %
Hydrogen	2.9	0.0	-100 %	1.5	-48 %
CO_2	6.2	7.6	+22 %	6.6	+6 %
Water	5176.1	3475.5	-33 %	4359.3	-16 %
Oxygen	1368.0	918.5	-33 %	1152.1	-16 %
Guarantees of origin	-7.0	-9.7	+38 %	-7.7	+9 %

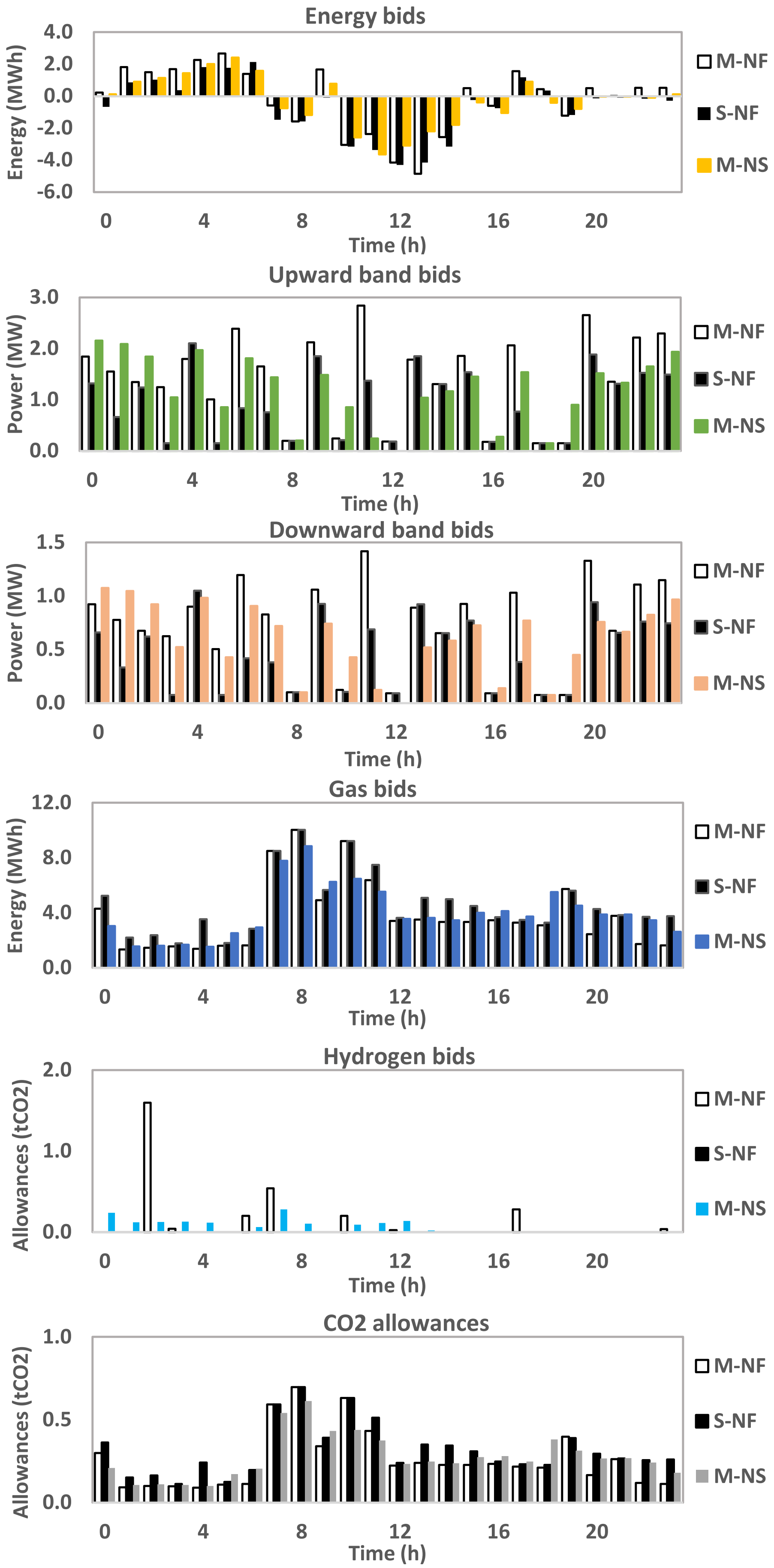
Energy bids
Energy (MWh)
4.0
2.0
0.0
-2.0
-4.0
-6.0
0
4
8
12
16
20
Time (h)
M-NF
S-NF
M-NS
Upward band bids
Power (MW)
3.0
2.0
1.0
0.0
0
4
8
12
16
20
Time (h)
M-NF
S-NF
M-NS
Downward band bids
Power (MW)
1.5
1.0
0.5
0.0
0
4
8
12
16
20
Time (h)
M-NF
S-NF
M-NS
Gas bids
Energy (MWh)
12.0
8.0
4.0
0.0
0
4
8
12
16
20
Time (h)
M-NF
S-NF
M-NS
Hydrogen bids
Allowances (tCO2)
2.0
1.0
0.0
0
4
8
12
16
20
Time (h)
M-NF
S-NF
M-NS
CO2 allowances
Allowances (tCO2)
1.0
0.5
0.0
0
4
8
12
16
20
Time (h)
M-NF
S-NF
M-NS

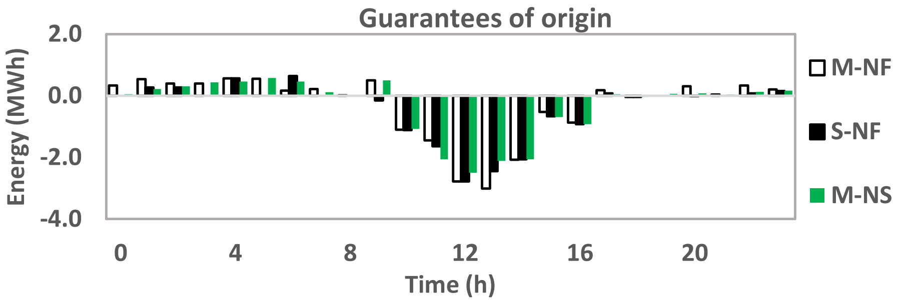

Figure 4.11 – Aggregator’s hourly bids.

The M-NF strategy presented more electricity bids to the DA markets than the M-NS strategy. The electricity bids include energy and secondary reserve bids in both downward and upward directions. The difference in bids indicates that the M-NF may have encountered scenarios with a large injection of electricity (from PV and CHPs) which caused violations of the electricity network constraints. To mitigate this problem, the M-NS strategy reduced the quantities of the bids. The S-NF strategy also presented more total electricity and gas bids to the DA market than the M-NS strategy, which may indicate that the bids placed by this strategy may also have created electricity network problems. In relation to the M-NF strategy, the S-NF scenarios submitted less demand daily energy bids (-45%) and more supply (+18%) and gas (+21%) energy daily bids, while the M-NS strategy submitted less demand (-34%) and supply (-14%) daily energy bids and more gas (+6%) energy daily bids.

In addition, M-NF and S-NF strategies present very different placements of secondary reserve bids in both upward and downward directions. This is related to the fact that the M-NF strategy has more sources of flexibility, which allows it to offer higher upward and downward bids. The S-NF strategy presented fewer upward and downward bids (-33%), as well as the M-NS strategy (-16%).

In relation to the hydrogen bids, the three strategies present very different behaviors among themselves. First, the S-NF strategy did not present any DA hydrogen bid, as it did not see it to be economically advantageous. This is because the electricity cost to produce hydrogen is higher than the profit of injecting that hydrogen into the network. Secondly, the M-NF strategy presents almost two times more total daily bids than the M-NS strategy. Thirdly, the M-NF strategy presents much higher hourly bids than the M-NS strategy (-48%). This difference may indicate that the M-NF strategy encountered scenarios with high injection of hydrogen that ended up violating gas network constraints.

The hourly placement of GO bids is similar among the three cases. The demand for GOs is related with the P2G consumption during times when there is no PV generation, while their supply occurs during the periods of forecasted PV generation. The S-NF (+38%) and M-NS (+9%) strategies presented higher hourly bids than the M-NF strategy.

The oxygen and water bids are related with the hydrogen produced by the P2G which is higher in the M-NF, as it is the strategy with more flexibility.

4.5.2. Disaggregation of the aggregator’s bids per DMER

Figure 4.12 presents the disaggregation of electricity, gas, and hydrogen bids per DMER. Comparing M-NF and S-NF strategies, the energy bids are similar for all the DMERs with a small difference of 6.8 MWh for the CHPs and 4.9 MWh for the P2G. The electricity DMERs HPs, PVs, ESSs, and EVs) provided a total of 19.5 MW and 14.7 MW of upward and downward bands under the M-NF strategy.

In the S-NF strategy, there is a slight decrease in the provision of the upward band bid (-0.1 MW, -1%) and a great decrease in the provision of the downward band bid (-2.1 MW, -37%) by electricity DMERs. This occurs because the electricity aggregator in the S-NF strategy must comply with constraint (4.11)) and can only use electricity DMERs. This way, the aggregator is still able to maximize the provision of upward reserves by electricity DMERs, but it highly decreases its capability to provide downward reserves. In relation to gas DMERs, under the S-NF strategy, it is possible to observe a decrease in the CHPs capacity to provide an upward band bid (-6.6 MW, -50%) and an increase of downward band bid (+6.7 MW, +472%), as they are constrained by restriction (4.11) and other prosumers' constraints. These results allow concluding that a mix of electric and gas DMERs can optimize the capability of each resource in offering reserve band bids.

Comparing M-NF and M-NS strategies, the consumption and supply of electricity are similar for all DMERs except for CHPs, which had an increase in electricity supply (+1.8 MWh), the P2G, which had a decrease of electricity demand (-2.3 MWh) and the EVs, which started supplying electricity in the M-NS strategy. The ESSs, P2Gs, FCs, and EVs had a substantial decrease in the upward band of 1.4 MW (23%), 3.2 MW (26%), 0.3 MW (17%), and 0.25 MW (35%), respectively. The PVs and P2G had a decrease in the downward band of 1.6 MW (52%) and 1.8 MW (18%), respectively, while the CHPs had an increase in the downward band of 0.9 MW (64%). Overall, the M-NS strategy provided the lowest reserve band to counteract the network problems encountered under the M-NF strategy.

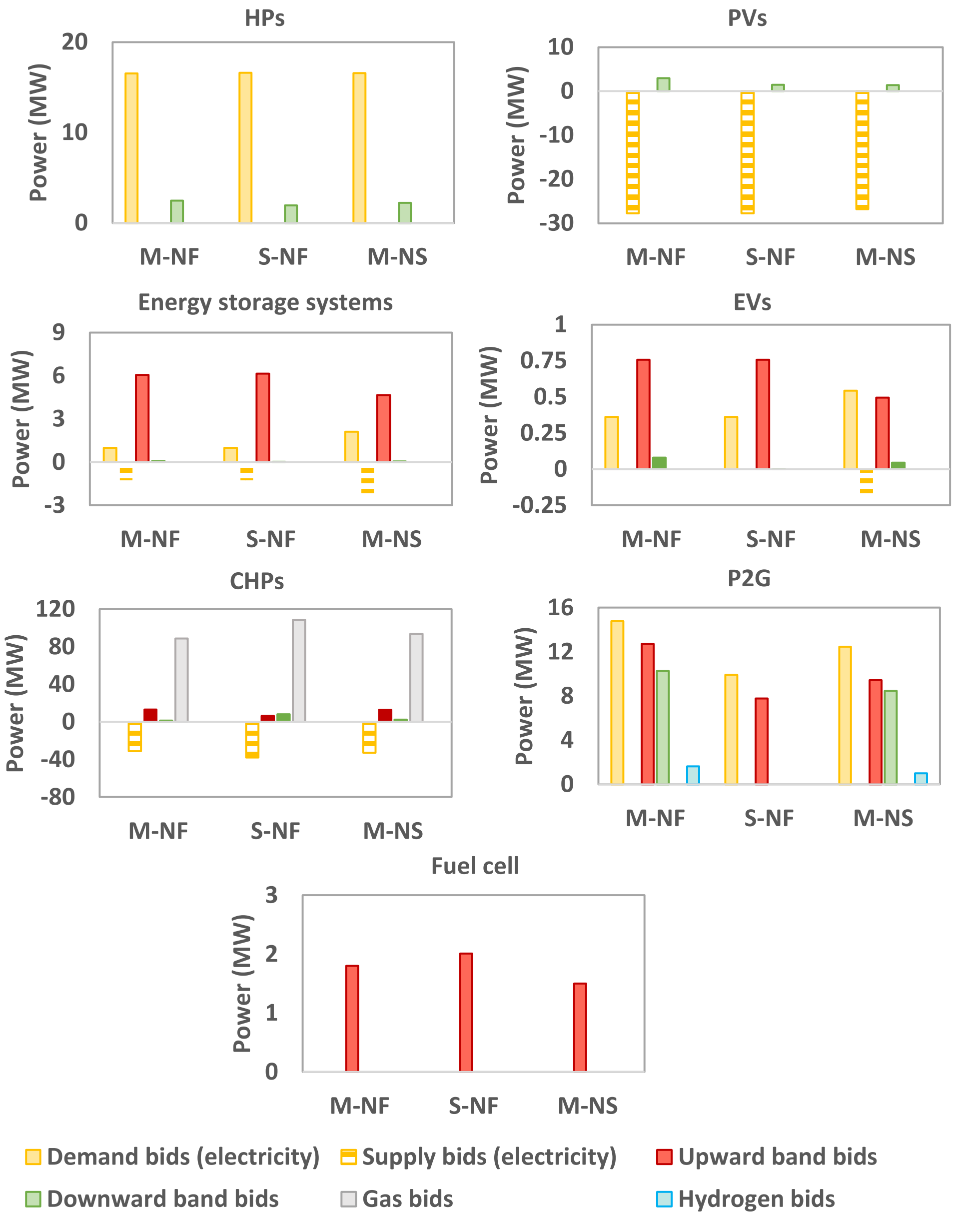

Figure 4.12 - Disaggregation of the electricity (energy and secondary reserve band), gas, and hydrogen bids by DMER.

Figure 4.13 presents the disaggregated energy hourly bids per DMER for each strategy. With the exception of ESSs and EVs, the DMERs have similar results for the three strategies. It is possible to observe that HPs have a high consumption of electricity in the middle of the day, i.e. from 6h to 18h, as the building's temperature restrictions during these hours are stricter. PV systems only provide power during daylight times, as expected. In the M-NF and S-NF strategies, ESSs only consume energy at the beginning of the day, and only inject energy at the end of the day. On the other hand, in the M-NS strategy, ESSs also consume and inject energy in the middle of the day. EVs have the same behavior in the M-NF and S-NF strategies and only consume energy. On the contrary, in the M-NS strategy, EVs also inject energy into the electricity network. Heat production of CHPs is higher from 7h and 18h as the temperature's ranges of its prosumers are stricter and more demanding. The P2G has a similar behavior for the three strategies and injects more hydrogen into the gas network between 0h and 15h, as it makes use of lower energy prices and PV generation during this time.

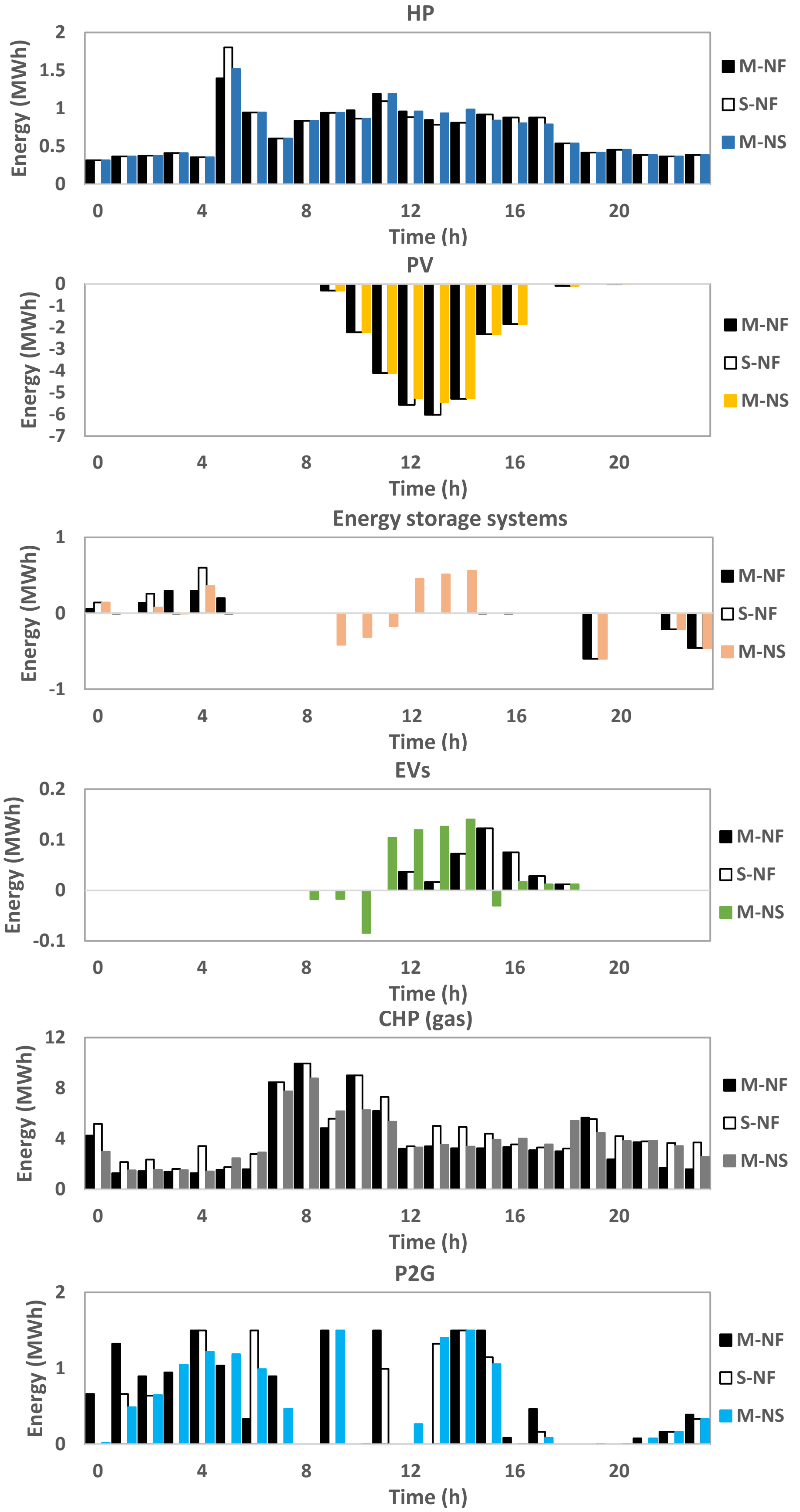

Figure 4.13 - Disaggregation of energy bids per resource for each strategy.

4.5.3. Multi-energy networks

In this section, we evaluate the feasibility of the aggregator's offers in the electricity, gas, and heat networks.

Regarding the electricity network, the voltage results for each strategy are presented in Table 4.28 and Figure 4.14. The voltage limits are [0.95, 1.05] p.u.. We can observe that M-NF and S-NF strategies generated overvoltage problems, which surpassed the limit of 1.05. The maximum values of 1.096 and 1.074 p.u were observed under the M-NF and S-NF strategies for the upward activation scenario. The M-NF strategy also encountered undervoltage problems for the downward activation scenario, reaching the minimum value of 0.947 p.u.. On the contrary, the M-NS strategy did not encounter any voltage problems. It remained between the upper and lower voltage limits. This proves that the M-NS strategy computes network-secure bids from the electricity network perspective.

Table 4.28 - Voltage results for the electricity network.

		Energy scenario	Upward scenario	Downward scenario
Number violations	**M-NF**	5	11	11
	S-NF	4	5	3
	M-NS	0	0	0
Maximum voltage (p.u.)	**M-NF**	1.069	1.096	1.066
	S-NF	1.065	1.074	1.061
	M-NS	1.050	1.050	1.050
Minimum voltage (p.u.)	**M-NF**	0.954	0.985	0.947
	S-NF	0.970	0.973	0.968
	M-NS	0.955	0.984	0.955

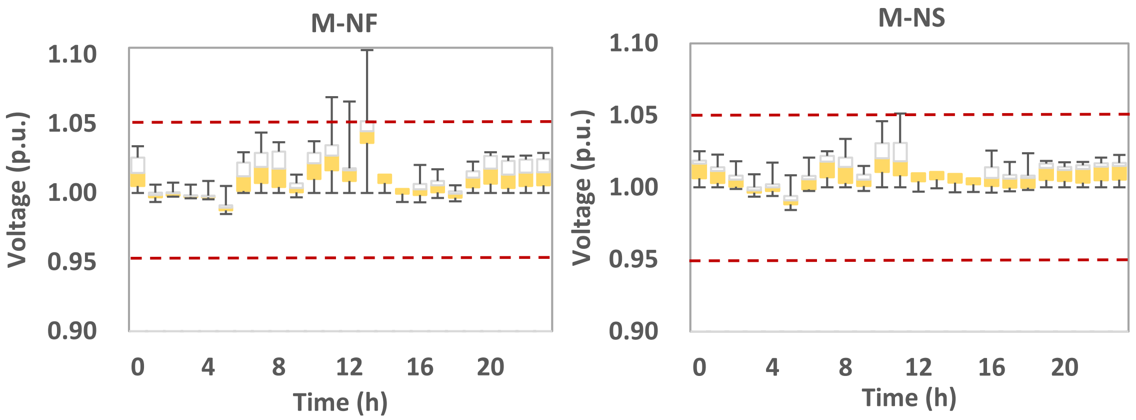

Figure 4.14 - Voltage results for the upward scenario.

The district heating results are presented in Table 4.29 and Figure 4.15. The mass flow limits are [0, 40] kg/s. We can observe that violations of the mass flow occurred in the NF strategies, especially in the upward scenario. Contrarily, the M-NS strategy was able to calculate bids without any network violation. In Figure 4.15, we can observe that the mass flows were almost at their limits but never surpassed them. On the other hand, under the M-NF strategy, the mass flows violated the limits of the heat network between 6h to 10h.

When calculating the bids of the M-NF strategy, the heat losses were not considered as it was assumed that the CHP generation had to be equal to the heat consumption from the district heating. This way, the actual heat to be produced by CHPs will be higher than the one calculated, which will incur in higher costs. For example, in the M-NF strategy, the total heat load is 40 MW for the entire day. The necessary generation to fulfill this load is 42.3 MW, which represents an increase of 2.3 MW (6%). Thus, part of the energy to be bought or sold was not duly distributed and optimized. This problem does not occur in the M-NS strategy, adding another advantage to it.

Table 4.29 - Mass flow results for the district heating network.

		Energy scenario	Upward scenario	Downward scenario
Number violations	**M-NF**	3	9	3
	S-NF	3	6	3
	M-NS	0	0	0
Maximum mass flow (kg/s)	**M-NF**	45.93	45.93	45.93
	S-NF	45.93	45.93	45.93
	M-NS	36.03	40.00	36.03

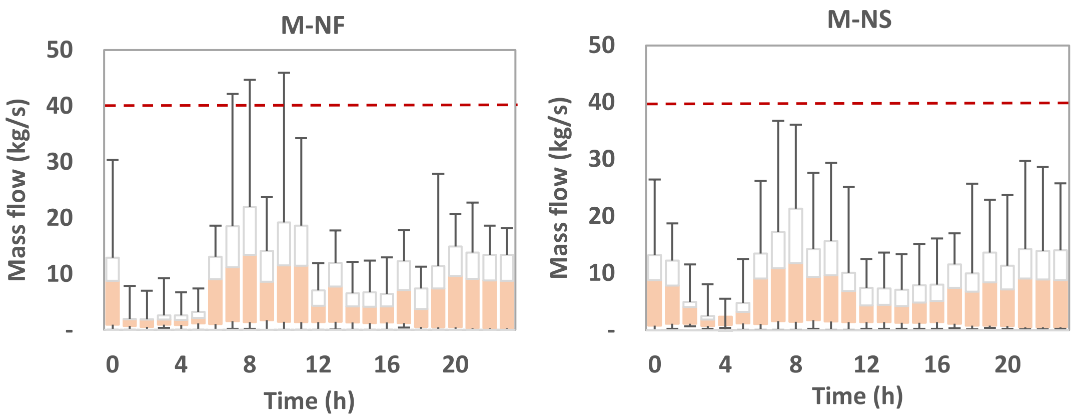

Figure 4.15 - Mass flows for the upward scenarios.

In relation to the gas network, the HHV and WI results are presented in Table 4.30, Table 4.31, and Figure 4.16. The HHV and WI limits are [35.5, 47.8] MJ/m3 and [45.7, 55.9] MJ/m3, respectively. The M-NF strategy encountered problems related with HHV and WI values for the energy, upward, and downward scenarios. The downward scenario presents the highest number of violations for both HHV and WI, as in this scenario the P2G provides downward band by consuming more electricity, which in turn results in producing more hydrogen. Then, this hydrogen can be stored in the HSS or injected into the gas network. This way, due to higher injection rates of hydrogen, there will occur gas network violations. On the other hand, the M-NS strategy did not encounter any problems and it was able to compute network-secure bids from the gas network perspective. The S-NF strategy also did not generate any gas network violation, as there was not any hydrogen injected into the gas network.

Table 4.30 – Higher heating value results for the gas network.

		Energy scenario	Upward scenario	Downward scenario
Number violations	**M-NF**	3	1	12
	S-NF	0	0	0
	M-NS	0	0	0
Maximum HHV (MJ/m^3)	**M-NF**	41	41	41
	S-NF	41	41	41
	M-NS	41	41	41
Minimum HHV (MJ/m^3)	**M-NF**	19.2	22	17.9
	S-NF	41	41	41
	M-NS	35.5	38.1	35.5

Table 4.31 – Wobbe index results for the gas network.

		Energy scenario	Upward scenario	Downward scenario
Number violations	**M-NF**	1	1	3
	S-NF	0	0	0
	M-NS	0	0	0
Maximum WI (MJ/m^3)	**M-NF**	52.8	52.8	52.8
	S-NF	52.8	52.8	52.8
	M-NS	52.8	52.8	52.8
Minimum WI (MJ/m^3)	**M-NF**	43.9	44.5	43.8
	S-NF	52.8	52.8	52.8
	M-NS	50.2	51.4	50.2

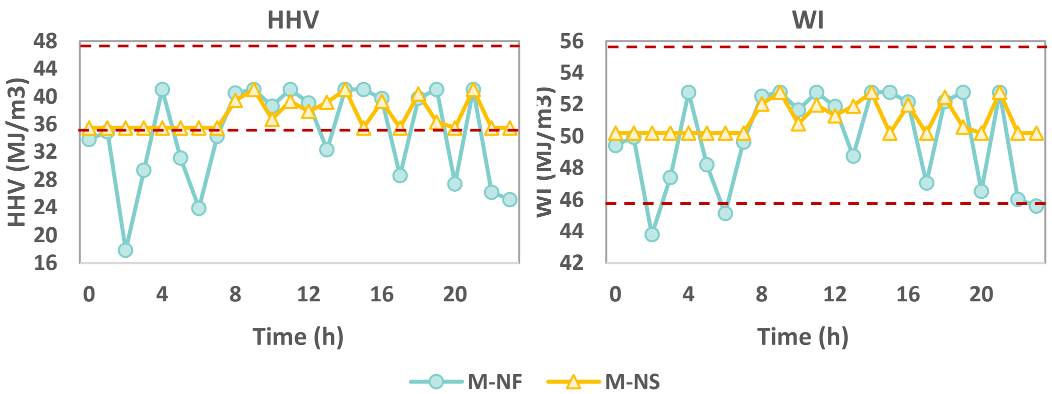

Figure 4.16 – HHV and WI for the downward scenarios.

4.5.4. Economic performance

Table 4.32 presents the cumulative costs obtained for the three bidding strategies. Positive values represent costs and negative values represent income. The costs of the S-NF strategy are the sum of the costs of aggregators 1 and 2. The results in Table 4.32 show that the M-NF strategy produced the most profitable outcome, followed by S-NF and M-NS strategies. It is possible to observe that the costs of gas and carbon increased while the costs of water decreased in the S-NF and M-NS strategies. On the other hand, the profits of electricity energy and GOs increased while the profits of the secondary reserve, hydrogen, and oxygen decreased in the S-NF and M-NS strategies.

The M-NF strategy outperformed the S-NF strategy with 7% lower costs, which allows us to conclude that a multi-energy aggregator exploits better the flexibility of DMERs than single-energy aggregators. Comparing the results of M-NF and M-NS strategies, we conclude that the M-NF strategy is more profitable (with lower 13% costs) since it is not limited by the constraints of the electricity, gas, and heat networks, which prevents the aggregator from using the maximum flexibility of the DMERs.

The M-NF strategy may produce bidding solutions with lower costs. However, these solutions may be network-infeasible, as described in section 4.5.3. These network infeasibilities will end up significantly increasing the costs of the aggregator in RT since he will not be able to deliver the services traded in the day-ahead markets, due to network violations.

Table 4.32 - Costs of each strategy. The percentage indicates the comparison with the M-NF strategy.

Cost (€)	M-NF	S-NF		M-NS	
Electricity - energy	-415	-1006	-142 %	-547	-32 %
Electricity - secondary reserve	-277	-176	+36 %	-244	+12 %
Gas	1272	1545	+21 %	1343	+6 %
Hydrogen	-222	0	+100 %	-115	+48 %
Water	19	13	-33 %	16	-16 %
Oxygen	-0.2	-0.1	+33 %	-0.2	+16 %
Guarantees of origin	-7.0	-9.7	-38 %	-7.7	-9 %
Carbon	303	357	+18 %	317	+5 %
Total	672	723	+7 %	764	+13 %

4.5.5. Carbon allowances

Table 4.33 presents the CO_2 allowances bought by the aggregator due to the electricity and heat generated by CHPs. The results show that the M-NF strategy produces the lowest total CO_2 allowances, followed by M-NS and S-NF strategies. Moreover, the free allowances (calculated in Annex A) were not sufficient to fulfill the needs and only covered 16% to 19% of the total needs.

Table 4.33 – CO_2 allowances of each strategy.

	M-NF	S-NF	M-NS

Electricity (tCO_2)	6.5	7.5	6.8
Heat (tCO_2)	8.4	9.6	8.7
Free allowances (tCO_2)	2.8	2.8	2.8
Total (tCO_2)	12.1	14.3	12.7

4.5.6. Computational performance

The optimization sub-problems of the bidding strategies were implemented in Python 3.7 and solved in an Intel® Core™ i5.8265U CPU @ at 1.6GHz with 8 GB RAM. The aggregator sub-problem is a mixed-integer quadratic program and was solved by the IBM CPLEX v12.9.0 optimizer. The sub-problem of each DSO is a non-linear program and was solved by the interior point optimization (IPOPT) v3.11.1 optimizer.

Table 4.34 presents the execution times and the sizes of the bidding optimization problems, divided by sub-problems. The DSOs' sub-problems result from the decomposition of the multi-temporal and multi-scenario problems into smaller sub-problems, as described in section 4.1. The total size of the M-NS results from the sum of the aggregator sub-problem to all DSOs' sub-problems, representing the equivalent size of the centralized problem. The total time is the execution time of the ADMM.

The optimization bidding times of the M-NF and S-NF strategies were 4.37 and 2.07s (max (2.07, 0.72)), respectively. In relation to the M-NS strategy, if we run in parallel and do not consider communications between the aggregator, DSOs, and the independent platform, an iteration can be run in 15s (14.48 + max (0.04, 0.18, 0.51)). Considering that the ADMM algorithm runs in 117 iterations, it would take 1755s (or approximately 29 minutes) to run the M-NS strategy. It is possible to conclude that the M-NF and S-NF strategies were faster than the M-NS strategy. Nonetheless, any of the three strategies present suitable execution times for the timelines of the electricity, gas, green hydrogen, and carbon markets.

Table 4.34 - Size and execution time of the bidding optimization strategies.

Strategy	Sub-problems	Nº of variables	Nº of constraints	Time (s)
M-NF	**Aggregator**	75 782	102 016	4.37
S-NF	**Aggregator 1**	38 749	59 989	2.07
	Aggregator 2	47 018	51 340	0.72
M-NS	**Aggregator**	74 006	100 192	14.48
	Electricity DSO	10 848	20 496	0.04
	Gas DSO	22 224	64 368	0.18
	Heat DSO	38 448	141 048	0.51
	Total	145 526	326 104	1 755

Convergence of the ADMM under the M-NS strategy

The literature has been proving that the ADMM is globally convergent for convex problems [163]. Nonetheless, recent works [150][176] also show that the ADMM converges for many non-convex problems, as demonstrated here in Figure 4.17. Both primal and dual residuals converged to the stop criteria at iteration 117. The absolute tolerance ϵ^{Abs} was set to 0.001 which corresponds to a stop criterion of 0.082 kW in the case of the primal residual. After iteration 117, it was decided to run the ADMM until iteration 200 in order to check the variation of the aggregator's cost. We observed almost no variation of the aggregator's cost after iteration 117 (0.00014% variation), which demonstrates that the ADMM converged to a stationary solution.

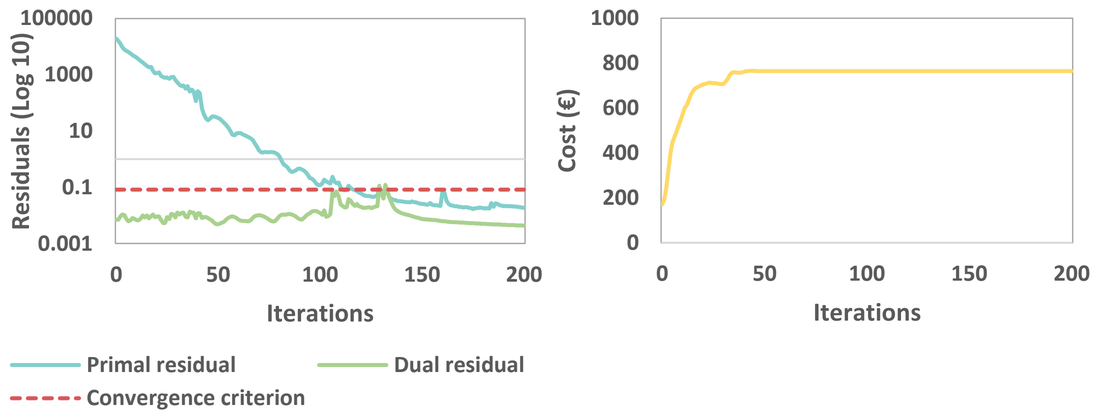

Figure 4.17 - Residuals (left) and aggregator's costs (right).

The choice of the absolute tolerance ϵ^{Abs} impacts the convergence of the ADMM, as illustrated in Figure 4.18. We can observe that the number of iterations increases with the reduction of the absolute tolerances, which impacts similarly the computational times. It is worth mentioning here that the computational time is within suitable execution times for the timelines of the energy markets even for the most conservative absolute tolerance of 0.0001.

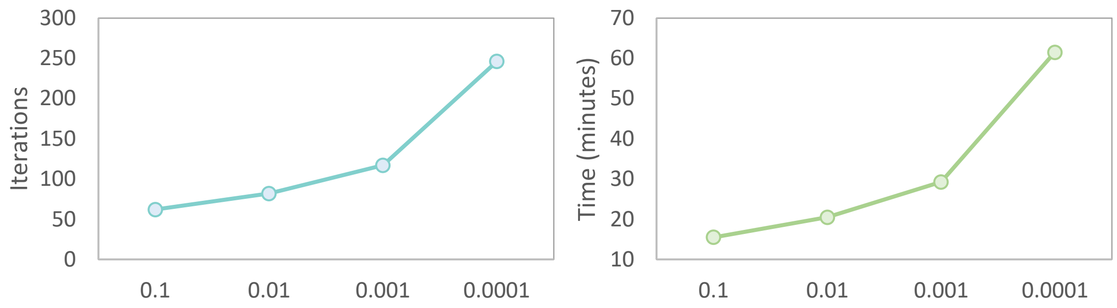

Figure 4.18 - Number of iterations and computational times across different absolute tolerances.

Centralized versus distributed formulation for the M-NS strategy

The centralized formulation of the M-NS strategy assumes the form of a mixed-integer non-linear problem. As reported in Table 4.34, this problem has 103 979 variables and 257 617 constraints. Solving such a large-scale mixed-integer non-linear problem in a reasonable time was not possible using state-of-the-art solvers on a computer with 8 GB RAM. To solve this optimization problem in a reasonable time, it would be necessary to set a time limit and the mixed-integer non-linear solvers would only compute a sub-optimal solution, when possible.

The application of the ADMM made it possible to solve the problem in reasonable computational times. In addition to this computational advantage, the ADMM allows the aggregator and DSOs to preserve their data privacy and ensure a clear separation of their roles by solving the problem in a distributed manner.

4.6. Conclusions

This chapter presents a network-secure bidding framework for multi-energy aggregators to participate in DA electricity (energy and reserves), gas, green hydrogen, and carbon markets. Using a distributed approach based on the ADMM algorithm, the aggregator negotiates with the electricity, gas, and heat DSOs to compute network-secure and multi-energy bids. This approach allows aggregators to preserve their data privacy.

The proposed bidding strategy was benchmarked against two other strategies. The numerical results of these comparisons yielded three main findings.

The first one shows that the proposed strategy counteracts all the operating problems of the electricity, heat, and gas networks and provides network-secure bids. When the aggregator uses the network-free strategies, different network problems occurred in the electricity, district heating, and gas networks. The electrical problems found were related with voltages, the district heating problems were related with mass flows, and the gas problems were related with the HHVs and the WI of the gases. On the other hand, by using the network-secure strategy, the aggregator was able to offer bids that did not violate any of these network constraints, avoiding network problems. This avoids the situation of significantly increasing the aggregator's costs in RT as he would not be able to deliver the services offered in the DA markets due to network violations.

The second finding revealed that the aggregator's costs of trading energy, gas, green hydrogen, GOs, and carbon allowances decreased in the order of 7% when considering a strategy that jointly optimizes MES. This allows us to conclude that a multi-energy aggregator exploits better the flexibility of DMERs than single-energy aggregators.

Finally, the third one confirmed that the execution time of this strategy, although slower than the other strategies studied, is well suited for the timelines of the electricity, gas, green hydrogen, and carbon markets. This indicates that the newly developed strategy can be applied in real scenarios.

Chapter 5 presents a new hierarchical MPC framework to assist multi-energy aggregators in the network-secure delivery of multi-energy services traded in electricity, natural gas, green hydrogen, and carbon markets. It concludes the entire cycle of multi-energy market participation, by addressing the RT phase. It provides clear evidence of the effectiveness of the proposed approach, namely concerning the advantages of considering network-secure bidding methods both in the DA and RT phases.

Chapter 5
Real-time management of distributed multi-energy resources in multi-energy networks

5.1. Introduction

This chapter presents the new hierarchical MPC framework to support aggregators in the RT delivery of network-secure and multi-energy services. The aim is to ensure that aggregators deliver the multi-energy services traded in DA electricity, gas, green hydrogen, and carbon markets. The MPC framework uses the ADMM on a rolling horizon to negotiate the network-secure delivery of multi-energy services between aggregators and multi-energy DSOs. The multi-energy services include electricity (energy and reserves), natural gas, green hydrogen, and carbon allowances, which result from the RT optimization of the multi-energy resources managed by aggregators. Figure 5.1 presents the scheme of the RT network-secure optimization framework.

This work builds upon the framework developed in Chapter 4, extending it and completing the participation cycle of aggregators in multi-energy markets. The framework developed in Chapter 4 is a network-secure bidding optimization framework for the participation of aggregators in multi-energy DA markets. That framework only considers the submission of DA bids by the aggregators, without considering their RT activation. The framework presented in this chapter, concludes the entire cycle of multi-energy market participation, by addressing the RT phase. It provides clear evidence of the effectiveness of the proposed approach, namely concerning the advantages of considering network-secure bidding methods both in the DA and RT phases.

The following sections present the MPC framework formulation and respective results. The sections of this chapter are divided as follows:

- Section 5.2 presents the hierarchical MPC framework;
- Section 5.3 presents the formulation of the aggregator's sub-problem, i.e. the aggregator's RT optimization model;
- Section 5.4 presents the formulation of the DSO's sub-problem, i.e. the DSOs' flow optimization models;
- Section 5.5 presents the case study used to analyze the framework developed;

- Section 5.6 presents the results obtained and the analysis of the newly developed framework;

- Section 5.7 presents the conclusions of this chapter.

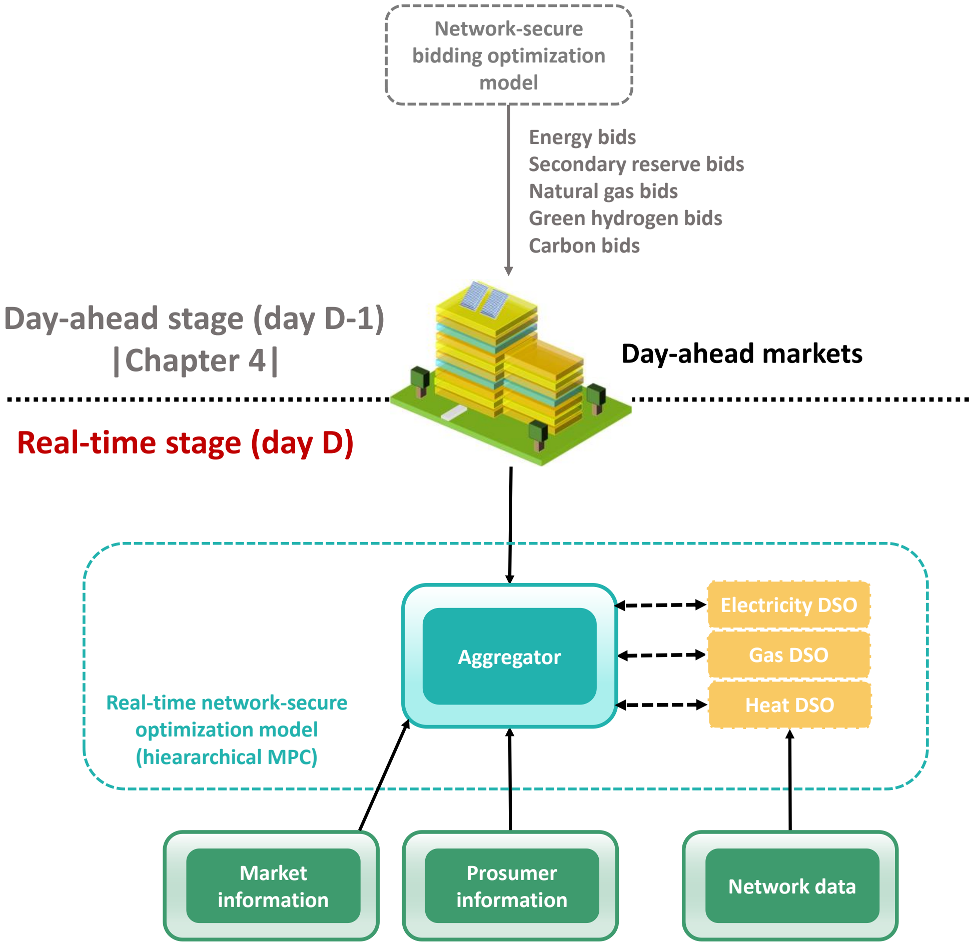

Figure 5.1 - Real-time network-secure optimization scheme.

5.2. Hierarchical model predictive control framework

In this section, we present the hierarchical MPC framework used by the aggregator to safely deliver the multi-energy services (bids) traded in the DA markets. The hierarchical MPC has two levels, as illustrated in Figure 5.2. In the first level, a multi-energy and network-secure optimization model computes network-secure bands and control set-points for the DMERs. The optimization model is solved on a rolling horizon framework, which moves forward in intervals of 1h for a horizon of 24h. In the second level, a controller adjusts the set-points (3) using the bands communicated by level 1 (1) to track the AGC signal (2) communicated by the TSO. The controller runs in cycles of 20s. Subsection 5.2.1 describes the multi-energy and network-secure optimization framework and subsection 5.2.2 describes the controller.

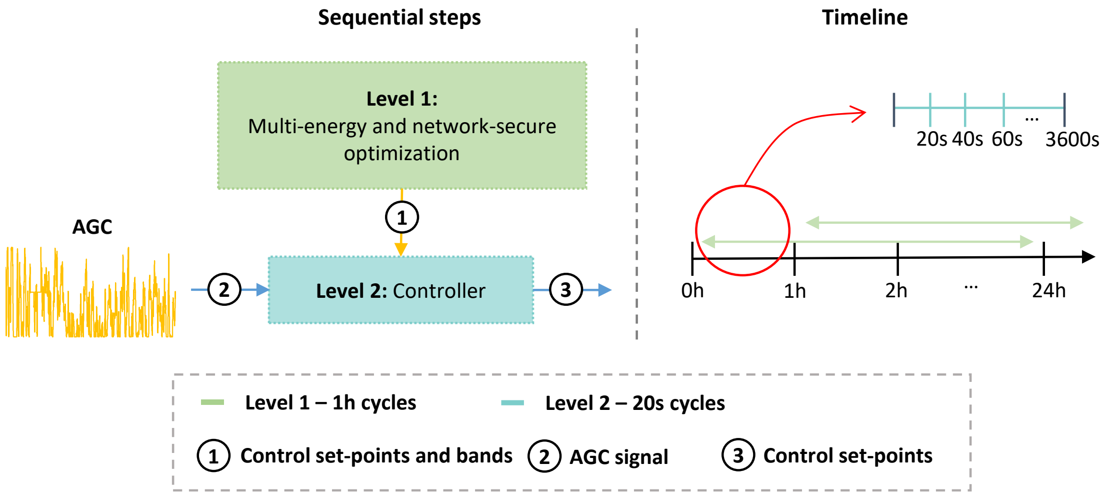

Figure 5.2 - Hierarchical model predictive control framework.

5.2.1. Multi-energy and network-secure optimization

The level 1 of the hierarchical MPC framework is described in detail in Chapter 3. This module computes bands and control set-points considering the constraints of DMERs and electricity, gas and heat networks. The formulation of the optimization subproblem used by the aggregator is presented in section 5.3 and the formulation of the optimization subproblem for each DSO is presented in section 5.4.

5.2.2. Controller

The controller of the aggregator tracks the AGC signal P^{AGC} in order to make the operating point of the aggregator ψ equal to the AGC signal. This is done by adjusting the operating points of the flexible resources P^{v}, i.e. adjusting their consumption and generation.

The operating point of the aggregator is given by equation (5.1) and considers the operating points defined at level 1 and the AGC signal. The operating point of each resource is given by equation (5.2). It considers the operating point of the aggregator and the parameters $\frac{U_{i,t}^{v}}{U_t^{RT}}$ and $\frac{D_{i,t}^{v}}{D_t^{RT}}$, which define the contribution of each resource to the AGC signal.

$$\psi_h = \begin{cases} min\left(P_h^{AGC} - P_t^{E,RT}, U_t^E\right), U^E + D^E > 0 \wedge P_h^{AGC} \geq P_t^{E,RT} \\ min\left(P_t^{E,RT} - P_h^{AGC}, D_t^E\right), U^E + D^E > 0 \wedge P_h^{AGC} < P_t^{E,RT} \\ 0, U_t^E + D_t^E = 0 \end{cases} \tag{5.1}$$

$$P_{i,h}^{v} = \begin{cases} P_{i,t}^{v} + min\ (\psi_h(U_{i,t}^{v}/U_t^E), U_{i,t}^{v}), \psi_h > 0 \wedge P_h^{AGC} \geq P_t^{E,RT} \\ P_{i,t}^{v} - min\ (\psi_h(D_{i,t}^{v}/D_t^E), D_{i,t}^{v}), \psi_h > 0 \wedge P_h^{AGC} < P_t^{E,RT}, \\ P_{i,t}^{v}, \psi_h = 0 \end{cases} \tag{5.2}$$

$$\forall\ v \in \{PV, HP, ESS, EV, CHP, FC, P2G\}, i \in I^{v}$$

5.3. Aggregator subproblem: operational optimization model

This section presents the optimization subproblem used by the aggregator (3.12)-(3.13) (introduced in Chapter 3) to deliver the multi-energy bids traded in DA electricity, natural gas, green hydrogen, and carbon markets. In more detail, the optimization subproblem computes bands, control set-points, and delivery scenarios. Note that the DMERs' constraints are the same as the constraints presented in Chapter 4. They are repeated here to improve readability and facilitate the interpretation of this chapter.

5.3.1. Objective function

The objective function (5.3) minimizes the net-cost of the aggregator dispatching the electricity, natural gas, green hydrogen, and CO_2 traded in the DA electricity (energy and secondary reserves), gas, green hydrogen, and carbon markets. The objective function (5.3) is divided into 8 terms. The first term (5.4) represents the RT electricity costs – it includes the energy imbalance costs, secondary reserves mobilization net-costs, and penalties for not providing secondary reserves. The terms (5.5)-(5.10) represent the imbalance costs between DA commitments and RT deliveries of GOs (5.5), natural gas (5.6), green hydrogen (5.7) and its derivative products (water (5.8) and oxygen (5.9)), and CO2 (5.10). The last term (5.11) represents the penalty term of the augmented Lagrangian, which penalizes the violation of the constraints of the electricity, gas, and heat networks.

$$Min \sum_{t\in T}\left[f_t^E + f_t^{GO} + \sum_{d\in\{E,G,H,H2\}}\sum_{s\in\{En,U,D\}}\sum_{n\in N^d}\mathcal{L}_{n,t}^{s,d}\right] + \sum_{v\in\{G,H2,H2O,O2,C\}} f^v \tag{5.3}$$

$$\begin{aligned} f_t^E = {} & \left(\lambda_t^{E,-}\Delta P_t^{E,-} - \lambda_t^{E,+}\Delta P_t^{E,+}\right)\Delta t + \left(\lambda_t^D \phi_t^D D_t^E - \lambda_t^U \phi_t^U U_t^E\right)\Delta t \\ & + \lambda_t^{B,-}\left(\Delta U_t^E + \Delta D_t^E\right)\Delta t \end{aligned} \tag{5.4}$$

$$f_t^{GO} = \lambda_t^{GO,-}\left(\Delta P_t^{GO,-} - \Delta P_t^{GO,+}\right)\Delta t \tag{5.5}$$

$$f^G = \lambda^{G,-}\left(\Delta P^{G,-} - \Delta P^{G,+}\right)\Delta t \tag{5.6}$$

$$f^{H_2} = \lambda^{H_2,-}\left(\Delta P^{H_2,-} - \Delta P^{H_2,+}\right)\Delta t \tag{5.7}$$

$$f^{H_20} = \lambda^{H_20,-}\left(\Delta P^{P2G,E,-} - \Delta P^{P2G,E,+}\right)c^{H_20}\Delta t \tag{5.8}$$

$$f^{0_2} = \lambda^{0_2,-}\left(\Delta P^{P2G,E,+} - \Delta P^{P2G,E,-}\right)c^{0_2}\Delta t \tag{5.9}$$

$$f^C = \lambda^{CO_2,-}\left(\Delta P^{C,-} - \Delta P^{C,+}\right)\alpha^{CO_2,G}\Delta t \tag{5.10}$$

$$\mathcal{L}_{n,t}^{s,d} = \pi_{n,t}^{s,d}\left(P_{n,t}^{s,d} - \hat{P}_{n,t}^{s,d}\right) + \frac{\rho}{2}\left(P_{n,t}^{s,d} - \hat{P}_{n,t}^{s,d}\right)^2 \tag{5.11}$$

Table 5.1 presents a description of the variables of the objective function.

Table 5.1 - Variables of the objective function.

Variable	Description	Unit
$\boldsymbol{D_t^E}, \boldsymbol{U_t^E}$	Upward and downward electricity reserve bids	MW
$\Delta\boldsymbol{P^{C,+}}, \Delta\boldsymbol{P_t^{E,+}}, \Delta\boldsymbol{P^{G,+}}, \Delta\boldsymbol{P_t^{GO,+}}, \Delta\boldsymbol{P^{H_2,+}}, \Delta\boldsymbol{P^{P2G,E,+}}$	Positive carbon, electricity, natural gas, guarantee of origins, hydrogen, and the electrolyzer imbalances	MW
$\Delta\boldsymbol{P^{C,-}}, \Delta\boldsymbol{P_t^{E,-}}, \Delta\boldsymbol{P^{G,-}}, \Delta\boldsymbol{P_t^{GO,-}}, \Delta\boldsymbol{P^{H_2,-}}, \Delta\boldsymbol{P^{P2G,E,-}}$	Negative carbon, electricity, natural gas, guarantee of origins, hydrogen, and the electrolyzer imbalances	MW
$\Delta\boldsymbol{U_t^E} + \Delta\boldsymbol{D_t^E}$		

Table 5.2 presents a description and the type of each parameters used in this subsection. All costs $\lambda_t^{B,-}, \lambda^{CO_2,-}, \lambda^{G,-}, \lambda_t^{GO,-}, \lambda^{H_2,-}, \lambda^{H_20,-}, \lambda^{0_2,-}, \lambda_t^D, \lambda_t^U, \lambda_t^{E,-}$, and $\lambda_t^{E,+}$ and mobilization ratios ϕ_t^D *and* ϕ_t^U are parameters forecasted by the aggregator. The conversion factor c^{H_20}, c^{0_2} and $\alpha^{CO_2,G}$ are fixed values.

Table 5.2 – Parameters of the objective function.

Parameter	Description	Unit	Type
$\boldsymbol{c^{H_20}}$	Water coefficient	L/MWh	Fixed
$\boldsymbol{c^{0_2}}$	Oxygen coefficient	kg/MWh	Fixed
$\boldsymbol{\alpha^{CO_2,G}}$	Conversion factor for carbon	$-$	Fixed
$\boldsymbol{\lambda_t^{B,-}}$	Penalty cost for band not supplied	$€/MWh$	Forecasted
$\boldsymbol{\lambda^{CO_2,-}}, \boldsymbol{\lambda^{G,-}}, \boldsymbol{\lambda_t^{GO,-}}, , \boldsymbol{\lambda^{H_2,-}}, \boldsymbol{\lambda^{H_20,-}}, \boldsymbol{\lambda^{0_2,-}}$	Carbon, natural gas, guarantee of origin, green hydrogen, water, and oxygen imbalance prices	$€/MWh$	Forecasted
$\boldsymbol{\lambda_t^D}, \boldsymbol{\lambda_t^U}$	Downward and upward tertiary reserve prices	$€/MWh$	Forecasted
$\boldsymbol{\lambda_t^{E,-}}, \boldsymbol{\lambda_t^{E,+}}$	Negative and positive electricity imbalance prices	$€/MWh$	Forecasted
$\boldsymbol{\phi_t^D}, \boldsymbol{\phi_t^U}$	Downward and upward mobilization ratios	$€/MWh$	Forecasted

5.3.2. Multi-energy service constraints

Constraints (5.12)-(5.14) define the electricity (demand and supply), natural gas, and green hydrogen to be delivered in RT. Constraints (5.15) and (5.16) define the upward and downward secondary reserves to be delivered in RT. They include the flexibility provided by ESSs, PV systems, HPs, CHPs, P2Gs, and FCs.

$$P_t^{E,RT} = \sum_{n \in N^E} P_{n,t}^E, \qquad \forall\, t \in T \tag{5.12}$$

$$P_t^{G,RT} = \sum_{n \in N^{GL}} P_{n,t}^G, \qquad \forall\, t \in T \tag{5.13}$$

$$P_t^{H_2,RT} = \sum_{n \in N^{H2}} P_{n,t}^{H_2}, \qquad \forall\, t \in T \tag{5.14}$$

$$U_t^E = \sum_{j\in J}\left(U_{j,t}^{Sto,+} + U_{j,t}^{Sto,-} + U_{j,t}^{PV} + U_{j,t}^{HP} + U_{j,t}^{CHP,E} + U_{j,t}^{P2G,E} + U_{j,t}^{FC,E}\right), \quad \forall\, t \in T \qquad (5.15)$$

$$D_t^E = \sum_{j\in J}\left(D_{j,t}^{Sto,+} + D_{j,t}^{Sto,-} + D_{j,t}^{PV} + D_{j,t}^{HP} + D_{j,t}^{CHP,E} + D_{j,t}^{P2G,E} + D_{j,t}^{FC,E}\right), \quad \forall\, t \in T \qquad (5.16)$$

Constraints (5.17) and (5.18) define natural gas imbalances caused by the expected activation of secondary reserves provided by CHPs. Constraints (5.19) and (5.20) define green hydrogen imbalances caused by the expected activation of secondary reserves provided by P2Gs.

$$U_t^G = \sum_{j\in J} U_{j,t}^{CHP,G}, \qquad \forall\, t \in T \qquad (5.17)$$

$$D_t^G = \sum_{j\in J} D_{j,t}^{CHP,G}, \qquad \forall\, t \in T \qquad (5.18)$$

$$U_t^{H_2} = \sum_{j\in J} U_{j,t}^{P2G,Net,H_2}, \qquad \forall\, t \in T \qquad (5.19)$$

$$D_t^{H_2} = \sum_{j\in J} D_{j,t}^{P2G,Net,H_2}, \qquad \forall\, t \in T \qquad (5.20)$$

Table 5.3 presents a description of the variables of the multi-energy services' constraints.

Table 5.3 - Variables of the multi-energy services' constraints.

Variable	Description	Unit
$\boldsymbol{D_{j,t}^{CHP,E}}, \boldsymbol{D_{j,t}^{CHP,G}}, \boldsymbol{D_{j,t}^{EV}}, \boldsymbol{D_{j,t}^{FC,E}}, \boldsymbol{D_{j,t}^{HP}}, \boldsymbol{D_{j,t}^{PV}}, \boldsymbol{D_{j,t}^{P2G,E}}, \boldsymbol{D_{j,t}^{P2G,Net,H_2}}, \boldsymbol{D_{j,t}^{Sto,+}}, \boldsymbol{D_{j,t}^{Sto,-}}$,	Downward CHP (natural gas and electricity consumption), electric vehicle, fuel cell, heat pump, PV, electrolyzer (electricity consumption and hydrogen injection), and energy storage system imbalances generated due to the expected activation of secondary reserves	MW
$\boldsymbol{D_t^G}, \boldsymbol{D_t^{H_2}}$	Downward natural gas, and green hydrogen imbalances generated due to the expected activation of secondary reserves	MW
$\boldsymbol{P_{n,t}^E}, \boldsymbol{P_t^{E,RT}}, \boldsymbol{P_{n,t}^G}, \boldsymbol{P_t^{G,RT}}, \boldsymbol{P_{n,t}^{H_2}}, \boldsymbol{P_t^{H_2,RT}}$	Electricity, natural gas, and green hydrogen delivery in real-time	MW
$\boldsymbol{U_{j,t}^{CHP,E}}, \boldsymbol{U_{j,t}^{CHP,G}}, \boldsymbol{U_{j,t}^{EV}}, \boldsymbol{U_{j,t}^{FC,E}}, \boldsymbol{U_{j,t}^{HP}}, \boldsymbol{U_{j,t}^{PV}}, \boldsymbol{U_{j,t}^{P2G,E}}, \boldsymbol{U_{j,t}^{P2G,Net,H_2}}, \boldsymbol{U_{j,t}^{Sto,+}}, \boldsymbol{U_{j,t}^{Sto,-}}$	Upward CHP (natural gas and electricity consumption), electric vehicle, fuel cell, heat pump, PV, electrolyzer (electricity consumption and hydrogen injection), and energy storage system imbalances generated due to the expected activation of secondary reserves	MW
$\boldsymbol{U_t^G}, \boldsymbol{U_t^{H_2}}$	Upward electricity, natural gas, and green hydrogen imbalances generated due to the expected activation of secondary reserves	MW

5.3.3. Imbalance constraints

Constraints (5.21)-(5.26) define imbalances between DA market commitments and RT expected realizations. In more detail, constraints (5.21)-(5.22) define hourly imbalances of electricity and GOs, and constraints (5.23)-(5.26) define daily imbalances of natural gas (5.23), green hydrogen (5.24)-(5.25), and CO_2 (5.26).

$$\Delta P_t^{E,-} - \Delta P_t^{E,+} = P_t^{E,RT} - P_t^{E,DA}, \qquad \forall\, t \in T \qquad (5.21)$$

$$\Delta P_t^{GO,-} - \Delta P_t^{GO,+} = P_t^{GO,RT} - P_t^{GO,DA}, \qquad \forall\, t \in T \qquad (5.22)$$

$$\Delta P^{G,-} - \Delta P^{G,+} = \sum\nolimits_{t\in T}\left(P_t^{G,RT} + \phi_t^U U_t^G - \phi_t^D D_t^G\right) - P^{G,DA} \qquad (5.23)$$

$$\Delta P^{H_2,+} - \Delta P^{H_2,-} = \sum\nolimits_{t\in T}\left(P_t^{H_2,RT} + \phi_t^D D_t^{H_2} - \phi_t^U U_t^{H_2}\right) - P^{H2,DA} \qquad (5.24)$$

$$\Delta P^{P2G,E,-} - \Delta P^{P2G,E,+} = \sum\nolimits_{j\in J}\sum\nolimits_{t\in T}\left(P_{j,t}^{P2G,E} + \phi_t^D D_{j,t}^{P2G,E} - \phi_t^U U_{j,t}^{P2G,E}\right) - P^{P2G,E,DA} \qquad (5.25)$$

$$\Delta P^{C,-} - \Delta P^{C,+} = \frac{A^{+,CO_2}}{c^{CO_2,G}\Delta t} + \sum\nolimits_{j\in J}\sum\nolimits_{t\in T}\left(P_{j,t}^{CHP,E} + U_{j,t}^{CHP,E}\phi_t^U - D_{j,t}^{CHP,E}\phi_t^D\right) - P^{C,DA} \qquad (5.26)$$

$$\Delta P_t^{E,-}, \Delta P_t^{E,+}, \Delta P_t^{GO,-}, \Delta P_t^{GO,+}, \geq 0, \qquad \forall\, t \in T \qquad (5.27)$$

$$\Delta P^{G,-}, \Delta P^{G,+}, \Delta P^{H_2,-}, \Delta P^{H_2,+}, \Delta P^{P2G,E,-}, \Delta P^{P2G,E,+}, \Delta P^{C,-}, \Delta P^{C,+} \geq 0 \qquad (5.28)$$

Constraints (5.29) and (5.30) ensure that the aggregator only provides secondary reserves when electricity imbalances are not expected to occur. Constraints (5.31) and (5.32) define the secondary reserves band not supplied.

$$\Delta P_t^{E,-} + \Delta P_t^{E,+} \leq (1 - b_t^E)M, \qquad \forall\, t \in T \qquad (5.29)$$

$$D_t^E + U_t^E \leq b_t^E(D_t^{E,DA} + U_t^{E,DA}), \qquad \forall\, t \in T \qquad (5.30)$$

$$\Delta D_t^E = D_t^{E,DA} - D_t^E, \qquad \forall\, t \in T \qquad (5.31)$$

$$\Delta U_t^E = U_t^{E,DA} - U_t^E, \qquad \forall\, t \in T \qquad (5.32)$$

$$D_t^E, U_t^E, \Delta D_t^E, \Delta U_t^E \geq 0, \qquad \forall\, t \in T \qquad (5.33)$$

Table 5.4 presents a description of the variables of the imbalance constraints.

Table 5.4 - Variables of the imbalance constraints.

Variable	Description	Unit
$\boldsymbol{P_t^{GO,RT}}$	Guarantees of origin delivery in real-time	MW
$\boldsymbol{P_{j,t}^{CHP,E}}, \boldsymbol{P_{j,t}^{P2G,E}}$	Electricity consumption by CHPs and electrolyzers	MW

Table 5.5 presents a description and the type of each parameter used in this subsection. All DA energy $P_t^{E,DA}$, $\boldsymbol{P^{G,DA}}, \boldsymbol{P_t^{GO,DA}}, P^{H2,DA}, P^{C,DA}$ and reserve $D_t^{E,DA}, U_t^{E,DA}$ bids and the electrolyzer electricity consumption $P^{P2G,E,DA}$ are fixed parameters.

Table 5.5 – Parameters of the imbalance constraints.

Parameter	Description	Unit	Type
$\boldsymbol{D_t^{E,DA}}, \boldsymbol{U_t^{E,DA}}$	Day-ahead electricity downward and upward bids	MW	Fixed
$\boldsymbol{P_t^{E,DA}}, \boldsymbol{P^{G,DA}}, \boldsymbol{P_t^{GO,DA}}, \boldsymbol{P^{H2,DA}}, \boldsymbol{P^{C,DA}}$	Day-ahead electricity, natural gas, guarantees of origin, green hydrogen, and carbon bids	MW	Fixed

$\boldsymbol{P^{P2G,E,DA}}$	Day-ahead electrolyzer electricity consumption	MW	Fixed

5.3.4. Market regulation constraints

The rules of the secondary reserves market (in the Portuguese control area) define that upward and downward bands should be 2/3 and 1/3 of the total band, as represented by constraint (5.34) [101].

$$U_t^E = 2.D_t^E, \qquad \forall\, t \in T \qquad (5.34)$$

Constraint (5.35) defines the CO_2 allowances to cover the electricity generated by the CHPs. Note that CHPs receive free allowances for the heat produced, although they still need to buy CO_2 allowances for the electricity generated.

$$A^{+,CO_2} - A^{-,CO_2} = \sum_{t\in T}\sum_{j\in J}[(P_{j,t}^{CHP,H} + U_{j,t}^{CHP,H}\phi_t^U - D_{j,t}^{CHP,H}\phi_t^D)c^{CO_2,G}\Delta t] - FA^{CO_2} \qquad (5.35)$$

$$A^{+,CO_2}, A^{-,CO_2} \geq 0 \qquad (5.36)$$

Constraint (5.37) defines the GOs bought and sold by the aggregator. The aggregator buys when the renewable energy resources managed by it do not produce enough electricity to certify the hydrogen produced by the P2G as green. The aggregator sells when the opposite happens.

$$P_t^{GO,RT} = \sum_{j\in J} P_{j,t}^{P2G,E} - \sum_{j\in J} P_{jt}^{PV} + \sum_{j\in J}\left(D_{j,t}^{P2G,E} + D_{j,t}^{PV}\right)\phi_t^D - \sum_{j\in J}\left(U_{j,t}^{P2G,E} + U_{j,t}^{PV}\right)\phi_t^U, \qquad \forall \quad t \in T \qquad (5.37)$$

Table 5.6 presents a description of the variables of the market regulation constraints.

Table 5.6 - Variables of the market regulation constraints.

Variable	Description	Unit
$\boldsymbol{P_{j,t}^{CHP,H}}$	Heat production by the CHP	MW
$\boldsymbol{P_{jt}^{PV}}$	Electricity generation by the PV system	MW
$\boldsymbol{D_{j,t}^{CHP,H}}, \boldsymbol{U_{j,t}^{CHP,H}}$	Downward and upward CHP (heat production) imbalances generated due to the expected activation of secondary reserves	MW

Table 5.7 presents the parameters of market regulations constraints. The free carbon allowances FA^{CO_2} is a fixed parameter.

Table 5.7 – Parameters of the energy markets.

Parameter	Description	Unit	Type
$\boldsymbol{FA^{CO_2}}$	Free carbon allowances	MW	Fixed

5.3.5. Delivery scenario constraints

Delivery scenarios define possible exchanges of power between the aggregator and multi-energy networks (or multi-energy DSOs). In the ADMM negotiation, they are used by the DSOs to check for network violations caused by the delivery of aggregator services. The network sub-problems (3.14) and (3.15) are solved for each DSO and each delivery scenario.

We model twelve delivery scenarios. The first six scenarios model the delivery of services traded in the DA markets, such as electricity (5.38), natural gas (5.39), heat (5.40), hydrogen (5.41), and secondary reserves (5.42)-(5.43). The last six scenarios model imbalances in heat (5.44)-(5.45) and gas (5.46)-(5.49) networks caused by the activation of secondary reserves.

Constraint (5.38) defines the electricity delivery scenario, which results from the electricity consumed by ESSs, HPs, inflexible loads, and P2Gs, and electricity generated by CHPs, ESSs, PV systems, and FCs.

$$P_{n,t}^{E} = \sum\nolimits_{j\in J_n} (P_{j,t}^{Sto,+} + P_{j,t}^{EV,+} + P_{j,t}^{HP} + P_{j,t}^{IL,E} + P_{j,t}^{P2G,E} - P_{j,t}^{CHP,E} - P_{j,t}^{Sto,-} - P_{j,t}^{EV,-} - P_{jt}^{PV} - P_{j,t}^{FC,E}), \ \ \forall\, n \in N^E, \quad t \in T \tag{5.38}$$

Constraint (5.39) defines the gas delivery scenario, which results from the gas consumed by CHPs and inflexible loads.

$$P_{n,t}^{GL} = \sum\nolimits_{j\in J_n} (P_{j,t}^{CHP,G} + P_{j,t}^{IL,G})\,, \forall\, n \in N^{GL}, \quad t \in T \tag{5.39}$$

Constraint (5.40) defines the heat delivery scenario, which results from the heat consumed by flexible and inflexible heating loads connected to the district heating, and the heat generated by CHPs.

$$P_{n,t}^{H} = \sum\nolimits_{j\in J_n} (P_{j,t}^{DH} + P_{j,t}^{IL,H} - P_{j,t}^{CHP,H}), \forall\, n \in N^{H}, \quad t \in T \tag{5.40}$$

Constraint (5.41) defines the hydrogen delivery scenario, which results from the hydrogen injected into the gas network by hydrogen technologies.

$$P_{n,t}^{H_2} = \sum\nolimits_{j\in J_n} (P_{j,t}^{P2G\to Net,H_2} + P_{j,t}^{Sto\to Net,H_2})\,, \forall\, n \in N^{H_2}, \quad t \in T \tag{5.41}$$

Constraints (5.42) and (5.43) define the secondary reserves delivery scenarios in both upward (5.42) and downward (5.43) directions. They are provided by CHPs, ESSs, FCs, HPs, PV systems, and P2Gs.

$$P_{n,t}^{U,E} = P_{n,t}^{E} - \sum\nolimits_{j\in J_n} \big(U_{j,t}^{CHP,E} + U_{j,t}^{Sto,+} + U_{j,t}^{Sto,-} + U_{j,t}^{FC,E} + U_{j,t}^{HP} + U_{j,t}^{PV} + U_{j,t}^{P2G,E}\big), \ \ \forall\, n \in N^E, \quad t \in T \tag{5.42}$$

$$P_{n,t}^{D,E} = P_{n,t}^{E} + \sum\nolimits_{j\in J_n} \big(D_{j,t}^{CHP,E} + D_{j,t}^{Sto,+} + D_{j,t}^{Sto,-} + D_{j,t}^{FC,E} + D_{j,t}^{HP} + D_{j,t}^{PV} + D_{j,t}^{P2G,E}\big), \ \ \forall\, n \in N^E, \quad t \in T \tag{5.43}$$

Constraints (5.44) and (5.45) define the scenarios of heat imbalances caused by the possible activation of the secondary reserves provided by district heating loads and CHPs.

$$P_{n,t}^{U,H} = P_{n,t}^{H} - \sum_{j\in J_n}\left(U_{j,t}^{DH} + U_{j,t}^{CHP,H}\right), \quad \forall\, n \in N^H, \qquad t \in T \tag{5.44}$$

$$P_{n,t}^{D,H} = P_{n,t}^{H} - \sum_{j\in J_n}\left(D_{j,t}^{DH} + D_{j,t}^{CHP,H}\right), \quad \forall n \in N^H, \qquad t \in T \tag{5.45}$$

Constraints (5.46) and (5.47) define the scenarios of gas imbalances caused by the possible activation of the secondary reserves provided by CHPs.

$$P_{n,t}^{U,G} = P_{n,t}^{G} + \sum_{j\in J_n}\left(U_{j,t}^{CHP,G}\right), \quad \forall\, n \in N^{GL}, \qquad t \in T \tag{5.46}$$

$$P_{n,t}^{D,G} = P_{n,t}^{G} - \sum_{j\in J_n}\left(D_{j,t}^{CHP,G}\right), \quad \forall\, n \in N^{GL}, \qquad t \in T \tag{5.47}$$

Constraints (5.48) and (5.49) define the scenarios of hydrogen imbalances caused by the possible activation of the secondary reserves provided by P2Gs.

$$P_{n,t}^{U,H_2} = P_{n,t}^{H_2} - \sum_{j\in J_n}\left(U_{j,t}^{P2G,Net,H_2}\right), \quad \forall\, n \in N^{H_2}, \qquad t \in T \tag{5.48}$$

$$P_{n,t}^{D,H_2} = P_{n,t}^{H_2} + \sum_{j\in J_n}\left(D_{j,t}^{P2G,Net,H_2}\right), \quad \forall\, n \in N^{H_2}, \qquad t \in T \tag{5.49}$$

Table 5.8 presents the variables for the delivery scenarios' constraints.

Table 5.8 – Variables for delivery scenarios constraints.

Variable	**Description**	**Unit**
$\boldsymbol{D_{j,t}^{DH}}, \boldsymbol{U_{j,t}^{DH}}$	Downward and upward DH imbalances generated due to the expected activation of secondary reserves	MW
$\boldsymbol{P_{j,t}^{CHP,G}}, \boldsymbol{P_{j,t}^{IL,G}}$	Natural gas consumption from CHPs and inflexible loads	MW
$\boldsymbol{P_{n,t}^{D,E}}, \boldsymbol{P_{n,t}^{U,E}}$	Scenarios of electricity imbalances generated by the activation of downward and upward band reserves in real-time	MW
$\boldsymbol{P_{n,t}^{D,G}}, \boldsymbol{P_{n,t}^{U,G}}$	Scenarios of natural gas imbalances generated by the activation of downward and upward band reserves in real-time	MW
$\boldsymbol{P_{n,t}^{D,H}}, \boldsymbol{P_{n,t}^{U,H}}$	Scenarios of heat imbalances generated by the activation of downward and upward band reserves in real-time	MW
$\boldsymbol{P_{n,t}^{D,H_2}}, \boldsymbol{P_{n,t}^{U,H_2}}$	Scenarios of hydrogen imbalances generated by the activation of downward and upward band reserves in real-time	MW
$\boldsymbol{P_{j,t}^{DH}}, \boldsymbol{P_{j,t}^{IL,H}}$	Heat consumption from district heating loads and inflexible loads	MW
$\mathbf{P_{j,t}^{EV,+}}, \boldsymbol{P_{j,t}^{HP}}, \boldsymbol{P_{j,t}^{IL,E}}, \boldsymbol{P_{j,t}^{Sto,E,+}}$,	Electricity consumption from electric vehicles, heat pumps, inflexible loads, and energy storage systems	MW
$\mathbf{P_{j,t}^{EV,-}}, \boldsymbol{P_{j,t}^{FC,E}}, \boldsymbol{P_{j,t}^{Sto,E,-}}$	Electricity generation from electric vehicles, fuel cells, and energy storage systems	MW
$\boldsymbol{P_{n,t}^{H}}$	Heat consumption	MW
$\boldsymbol{P_{j,t}^{P2G\rightarrow Net,H_2}}$, $\boldsymbol{P_{j,t}^{Sto\rightarrow Net,H_2}}$	Hydrogen injected into the network from P2Gs and hydrogen storage systems	MW

5.3.6. Distributed multi-energy resource constraints

The framework developed considers PVs, ESSs, CHPs, HPs, district heating loads, and hydrogen technologies as DMERs. The next subsection details the constraints of these technologies.

5.3.6.1. Heat pumps

Figure 5.3 presents an HP scheme. HPs consume electricity (inputs) to produce heat (outputs).

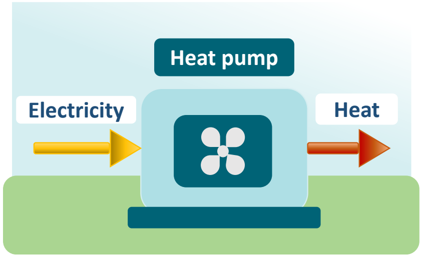

Figure 5.3 - Heat pump scheme (inputs: electricity, outputs: heat).

The HPs are modeled by equations (5.50)-(5.59). Constraint (5.50) defines the minimum and maximum power limits. Constraints (5.51)-(5.53) define the limits of the upward and downward bands. Constraints (5.54)-(5.56) define the temperature in each delivery scenario (energy (5.38), upward (5.42), and downward (5.43) band activations). Constraints (5.57)-(5.59) model the comfort levels of the occupants. The comfort levels are defined by prosumers who set a range of acceptable temperatures in the rooms for each hour.

$$\underline{P_j^{HP}} \leq P_{j,t}^{HP} \leq \overline{P_j^{HP}}, \qquad \forall\ j \in J,\ \ t \in T \tag{5.50}$$

$$U_{j,t}^{HP} \leq\ P_{j,t}^{HP} - \underline{P_j^{HP}}, \qquad \forall\ j \in J,\ \ t \in T \tag{5.51}$$

$$D_{j,t}^{HP} \leq \overline{P_j^{HP}} -\ P_{j,t}^{HP}, \qquad \forall\ j \in J,\ \ t \in T \tag{5.52}$$

$$D_{j,t}^{HP}, U_{j,t}^{HP}\ \geq 0, \qquad \forall\ j \in J,\ \ t \in T \tag{5.53}$$

$$\theta_{j,t+1}^{E} = \beta_j \cdot \theta_{j,t}^{E} + (1-\beta_j)[\theta_{j,t}^{O} + R_j(\eta_j^{HP} \cdot P_{j,t}^{HP})] +\ \vartheta_{j,t}, \qquad \forall\ j \in J,\ \ t \in T \tag{5.54}$$

$$\theta_{j,t+1}^{U} = \beta_j \cdot \theta_{j,t}^{U} + (1-\beta_j)[\theta_{j,t}^{O} + R_j(\eta_j^{HP} \cdot P_{j,t}^{HP} - \eta_j^{HP} \cdot U_{j,t}^{HP})] +\ \vartheta_{j,t}, \forall\, j \in J\,, t \in T \tag{5.55}$$

$$\theta_{j,t+1}^{D} = \beta_j \cdot \theta_{j,t}^{D} + (1-\beta_j)[\theta_{j,t}^{O} + R_j(\eta_j^{HP} \cdot P_{j,t}^{HP} + \eta_j^{HP} \cdot D_{j,t}^{HP})] +\ \vartheta_{j,t}, \forall\, j \in J\,, t \in T \tag{5.56}$$

$$\underline{\theta_j} \leq \theta_{j,t+1}^{E} \leq \overline{\theta_j}, \qquad \forall\ j \in J,\ \ t \in T \tag{5.57}$$

$$\underline{\theta_j} \leq \theta_{j,t+1}^{U} \leq \overline{\theta_j}, \qquad \forall\ j \in J,\ \ t \in T \tag{5.58}$$

$$\underline{\theta_j} \leq \theta_{j,t+1}^{D} \leq \overline{\theta_j}, \qquad \forall\ j \in J,\ \ t \in T \tag{5.59}$$

Table 5.9 presents the variables for HPs' constraints.

Table 5.9 - Variables for heat pump constraints.

Variable	Description	Unit
$\boldsymbol{\theta^{D}_{j,t}}, \boldsymbol{\theta^{U}_{j,t}}$	Downward and upward temperature imbalances generated due to the expected activation of secondary reserves	C^{o}
$\boldsymbol{\theta^{E}_{j,t}}$	Temperature of the building	C^{o}

The HP parameters are presented in Table 5.10. The minimum and maximum power ($\underline{P^{HP}_{j,t}}$ and $\overline{P^{HP}_{j,t}}$) and efficiency (η^{HP}_{j}) are parameters provided by the manufacturing company. The minimum and maximum temperature ($\underline{\theta}_{j}$ and $\overline{\theta}_{j}$) of the spaces are defined by the prosumers and communicated by the EMS. The thermal resistance (R_j) and capacitance (C_j) are physical characteristics of the buildings and they can be calculated by the aggregator using estimation techniques [164][165]. The thermal constant is calculated using equation (5.60). The outside temperature ($\theta^{O}_{j,t}$) can be forecasted by the aggregator himself or by contracting a weather service provider. Heat gains and losses ($\vartheta_{j,t}$)result from solar radiation, loads, or human activity, and they can be estimated by the aggregator.

$$\beta = \frac{\Delta t}{CR} \tag{5.60}$$

Table 5.10 – Parameters of heat pumps and thermal loads.

Parameter	Name	Unit	Type
$\boldsymbol{C_j}$	Thermal capacitance	$MWh/ºC$	Fixed
$\underline{\boldsymbol{P^{HP}_{j}}}$ and $\overline{\boldsymbol{P^{HP}_{j}}}$	Minimum and maximum power	MW	Fixed
$\boldsymbol{R_j}$	Thermal resistance	$ºC/MW$	Fixed
$\boldsymbol{\beta_j}$	Thermal constant	$-$	Fixed
$\boldsymbol{\eta^{HP}_{j}}$	Efficiency	$-$	Fixed
$\underline{\boldsymbol{\theta}}_{j}$ and $\overline{\boldsymbol{\theta}}_{j}$	Minimum and maximum temperature	$ºC$	Fixed
$\boldsymbol{\theta^{O}_{j,t}}$	Outside temperature	$ºC$	Forecasted
$\boldsymbol{\vartheta_{j,t}}$	Heat gains and losses	$ºC$	Forecasted

5.3.6.2. District heating flexible loads

The district heating flexible loads are modelled by the same equations of the HPs (5.50)-(5.59). However, instead of modelling the electric power variables $\{P^{HP}_{j,t}, D^{HP}_{j,t}, U^{HP}_{j,t}\}$, here we model the thermal variables $\{P^{DH}_{j,t}, D^{DH}_{j,t}, U^{DH}_{j,t}\}$ in constraints (5.50)-(5.59).

5.3.6.3. PV systems

Figure 5.4 presents a PV scheme. PV systems generate electricity, and so, their outputs are electricity.

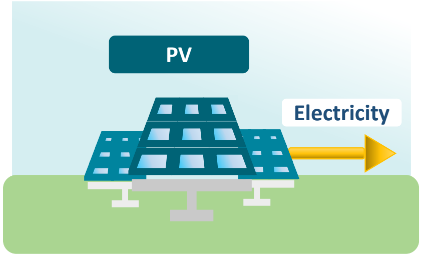

Figure 5.4 - PV scheme (outputs: electricity).

Constraint (5.61) defines the maximum power output of the PV system. The parameter $\overline{P_j^{PV}}$ is the forecasted generation. Constraints (5.62) and (5.63) define the band limits.

$$0 \leq P_{j,t}^{PV} \leq \overline{P_j^{PV}}, \qquad \forall\ j \in J,\ t \in T \tag{5.61}$$

$$0 \leq U_{j,t}^{PV} \leq \overline{P_j^{PV}} - P_{j,t}^{PV}, \qquad \forall\ j \in J,\ t \in T \tag{5.62}$$

$$0 \leq D_{j,t}^{PV} \leq P_{j,t}^{PV}, \qquad \forall\ j \in J,\ t \in T \tag{5.63}$$

Table 5.11 presents the parameters of PVs. The aggregator can forecast the PV generation ($\overline{P_j^{PV}}$) or contract a weather service provider to get those values.

Table 5.11 – Parameters of PVs.

Parameter	Name	Unit	Type
$\overline{\boldsymbol{P_j^{PV}}}$	Forecasted generation	MW	Forecasted

5.3.6.4. Energy storage system constraints

Figure 5.5 presents an ESS scheme. ESSs can store electricity and they are charged and discharged with electricity (inputs and outputs).

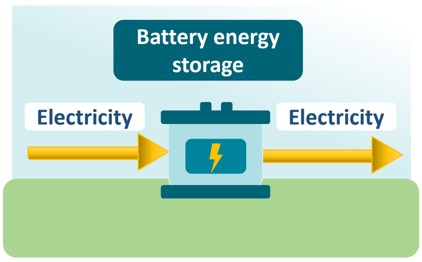

Figure 5.5 – Energy storage system scheme (inputs: electricity, outputs: electricity).

The operation of the ESS units is defined by constraints (5.64)-(5.79). Constraints (5.64) and (5.65) define the SOC and its limits. Constraints (5.66)-(5.68) set the range of the charging and discharging power. Constraint (5.69) ensures that the SOC at the end of the day is equal to the initial SOC.

$$SOC_{j,t+1}^{Sto,E} = SOC_{j,t}^{Sto,E} + \left(P_{j,t}^{Sto,E,+} \cdot \eta_j^{Sto,E} - \frac{P_{j,t}^{Sto,E,-}}{\eta_j^{Sto,E}}\right)\Delta t, \quad \forall\, j \in J,\ t \in T \tag{5.64}$$

$$\underline{SOC_j^{Sto,E}} \leq SOC_{j,t+1}^{Sto,E} \leq \overline{SOC_j^{Sto,E}}, \quad \forall\, j \in J,\ t \in T \tag{5.65}$$

$$0 \leq P_{j,t}^{Sto,E,-} + \dot{P}_{j,t}^{Sto,E,-} \leq \left(1 - b_{j,t}^{Sto,E}\right)\overline{P_j^{Sto,E,-}}, \quad \forall\, j \in J,\ t \in T \tag{5.66}$$

$$0 \leq P_{j,t}^{Sto,E,+} + \dot{P}_{j,t}^{Sto,E,+} \leq b_{j,t}^{Sto,E} \cdot \overline{P_j^{Sto,E,+}}, \quad \forall\, j \in J,\ t \in T \tag{5.67}$$

$$P_{j,t}^{Sto,E,-}, \dot{P}_{j,t}^{Sto,E,-}, P_{j,t}^{Sto,E,+}, \dot{P}_{j,t}^{Sto,E,+} \geq 0, \quad \forall\, j \in J,\ t \in T \tag{5.68}$$

$$SOC_{j,0}^{Sto,E} = SOC_{j,-1}^{Sto,E}, \quad \forall\, j \in J \tag{5.69}$$

Constraints (5.70) and (5.71) limit the upward band while constraints (5.72) and (5.73) limit the downward band. Constraints (5.74) and (5.75) guarantee that the storage only supply upward and downward bands if the SOC is within the limits. Constraints (5.76)-(5.79) ensure that the storage has enough capacity to compensate for the activation of upward and downward bands [150].

$$0 \leq U_{j,t}^{Sto,E,-} \leq \overline{P_j^{Sto,E,-}} - P_{j,t}^{Sto,E,-}, \quad \forall\, j \in J,\ t \in T \tag{5.70}$$

$$0 \leq U_{j,t}^{Sto,E,+} \leq P_{j,t}^{Sto,E,+}, \quad \forall\, j \in J,\ t \in T \tag{5.71}$$

$$0 \leq D_{j,t}^{Sto,E,+} \leq \overline{P_j^{Sto,E,+}} - P_{j,t}^{Sto,E,+}, \quad \forall\, j \in J,\ t \in T \tag{5.72}$$

$$0 \leq D_{j,t}^{Sto,E,-} \leq P_{j,t}^{Sto,E,-}, \quad \forall\, j \in J,\ t \in T \tag{5.73}$$

$$\left(\frac{U_{j,t}^{Sto,E,-}}{\eta_j^{Sto,E}} + U_{j,t}^{Sto,E,+} \cdot \eta_j^{Sto,E}\right)\Delta t \leq SOC_{j,t+1}^{Sto,E} - \underline{SOC_j^{Sto,E}}, \quad \forall\, j \in J,\ t \in T \tag{5.74}$$

$$\left(\frac{D_{j,t}^{Sto,E,-}}{\eta_j^{Sto,E}} + D_{j,t}^{Sto,E,+} \cdot \eta_j^{Sto,E}\right)\Delta t \leq \overline{SOC_j^{Sto,E}} - SOC_{j,t+1}^{Sto,E}, \quad \forall\, j \in J,\ t \in T \tag{5.75}$$

$$U_{j,t}^{Sto,E,+} + U_{j,t}^{Sto,E,-} + D_{j,t}^{Sto,E,+} + D_{j,t}^{Sto,E,-} \leq \dot{P}_{j,t+1}^{Sto,E,+} + \dot{P}_{j,t+1}^{Sto,E,-}, \quad \forall\, j \in J,\ t \in T \tag{5.76}$$

$$U_{j,t}^{Sto,E,+} + U_{j,t}^{Sto,E,-} + D_{j,t}^{Sto,E,+} + D_{j,t}^{Sto,E,-} \leq \dot{b}_{j,t}^{Sto,E} \cdot M, \quad \forall\, j \in J,\ t \in T \tag{5.77}$$

$$\dot{P}_{j,t}^{Sto,E,+} + \dot{P}_{j,t}^{Sto,E,-} \leq \left(1 - \dot{b}_{j,t}^{Sto,E}\right)M, \quad \forall\, j \in J,\ t \in T \tag{5.78}$$

$$U_{j,-1}^{Sto,E,+}, U_{j,-1}^{Sto,E,-}, D_{j,-1}^{Sto,E,+}, D_{j,-1}^{Sto,E,-} = 0, \quad \forall\, j \in J \tag{5.79}$$

Table 5.12 presents the variables for ESSs constraints.

Table 5.12 - Variables for energy storage systems constraints.

Variable	Description	Unit
$\boldsymbol{b}^{Sto,E}_{j,t}$	Binary variable indicating the charging (1) or discharging (0) mode	-
$\dot{\boldsymbol{b}}^{Sto,E}_{j,t}$	Binary variable indicating if there is space for offering upward and downward reserves	-
$\dot{\boldsymbol{P}}^{Sto,E,+}_{j,t}, \dot{\boldsymbol{P}}^{Sto,E,-}_{j,t}$	Electricity space for charging and discharging	MW
$\boldsymbol{SOC}^{Sto,E}_{j,t}$	State-of-charge of the energy storage system	MWh

Table 5.13 presents the parameters of the ESSs. The charging and discharging efficiency, minimum and maximum SOC, and maximum charging/discharging power are parameters provided by the manufacturing company. The initial SOC is communicated by the EMS.

Table 5.13 – Parameters of energy storage systems.

Parameter	Name	Unit	Type
$\overline{\boldsymbol{P}}^{Sto,E}_{j}$	Maximum charging/discharging power	MW	Fixed
$\boldsymbol{SOC}^{Sto,E}_{j,0}$	Initial state-of-charge	MWh	Fixed
$\underline{\boldsymbol{SOC}}^{Sto,E}_{j}$ and $\overline{\boldsymbol{SOC}}^{Sto,E}_{j}$	Minimum and maximum state-of-charge	MWh	Fixed
$\boldsymbol{\eta}^{Sto,E,+}_{j}$ and $\boldsymbol{\eta}^{Sto,E,-}_{j}$	Charging and discharging efficiency	$-$	Fixed

5.3.6.5. Electric vehicles

Figure 5.6 presents an EV scheme. As well as ESSs, EVs can store energy, and they are charged and discharged with electricity (inputs and outputs). We assume that EVs have vehicle to grid (V2G) capabilities, i.e. they can inject electricity into the electricity network and offer market services. The modeling of EVs considers a time of arrival and departure, and a predefined SOC at the time of arrival and departure.

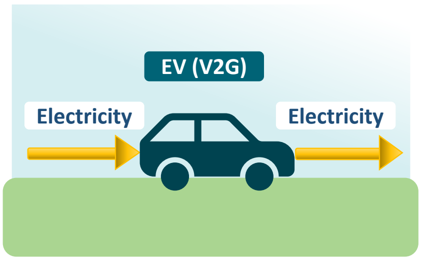

Figure 5.6 – Electric vehicle with V2G capabilities scheme (inputs: electricity, outputs: electricity).

The operation of EVs is defined by constraints (5.80)-(5.96). Constraints (5.80) and (5.81) define the SOC of EVs and its limits. Constraints (5.82) and (5.84) set the range of the charging and discharging power. Constraint (5.85) sets the SOC at the time of arrival. Constraint (5.86) ensures that the predefined SOC at the time of departure is guaranteed.

$$SOC_{j,t+1}^{EV,E} = SOC_{j,t}^{EV,E} + \left(P_{j,t}^{EV,E,+} \cdot \eta_j^{EV,E} - \frac{P_{j,t}^{EV,E,-}}{\eta_j^{EV,E}}\right)\Delta t, \qquad \forall\, j \in J,\;\; t \in T \tag{5.80}$$

$$\underline{SOC_j^{EV,E}} \le SOC_{j,t+1}^{EV,E} \le \overline{SOC_j^{EV,E}}, \qquad \forall\, j \in J,\;\; t \in T \tag{5.81}$$

$$0 \le P_{j,t}^{EV,E,-} + P_{j,t}^{E\dot{V},E,-} \le \left(1 - b_{j,t}^{EV,E}\right)\overline{P_j^{EV,E,-}}, \qquad \forall\, j \in J,\;\; t \in T_j^{EV} \tag{5.82}$$

$$0 \le P_{j,t}^{EV,E,+} + P_{j,t}^{E\dot{V},E,+} \le b_{j,t}^{EV,E} \cdot \overline{P_j^{EV,E,+}}, \qquad \forall\, j \in J,\;\; t \in T \tag{5.83}$$

$$P_{j,t}^{EV,E,-}, P_{j,t}^{E\dot{V},E,-}, P_{j,t}^{EV,E,+}, P_{j,t}^{E\dot{V},E,+} \ge 0, \qquad \forall\, j \in J,\;\; t \in T \tag{5.84}$$

$$SOC_{j,\mathrm{t}_j^{\mathrm{AR}}}^{EV,E} = SOC_j^{EV,AR}, \qquad \forall\, j \in J \tag{5.85}$$

$$SOC_{j,\mathrm{t}_j^{\mathrm{DE}}}^{EV} \ge SOC_j^{EV,DE}, \qquad \forall\, j \in J \tag{5.86}$$

Constraints (5.87)-(5.90) limit the upward and downward bands of EVs. Constraints (5.91) and (5.92) guarantee that EVs only supply upward and downward bands if the SOC is within the limits. Constraints (5.93)-(5.96) ensure that each EV has enough capacity to compensate the activation of upward and downward bands [150].

$$0 \le U_{j,t}^{EV,E,-} \le \overline{P_j^{EV,E,-}} - P_{j,t}^{EV,E,-}, \qquad \forall\, j \in J,\;\; t \in T \tag{5.87}$$

$$0 \le U_{j,t}^{EV,E,+} \le P_{j,t}^{EV,E,+}, \qquad \forall\, j \in J,\;\; t \in T \tag{5.88}$$

$$0 \le D_{j,t}^{EV,E,+} \le \overline{P_j^{EV,E,+}} - P_{j,t}^{EV,E,+}, \qquad \forall\, j \in J,\;\; t \in T \tag{5.89}$$

$$0 \le D_{j,t}^{EV,E,-} \le P_{j,t}^{EV,E,-}, \qquad \forall\, j \in J,\;\; t \in T \tag{5.90}$$

$$\left(\frac{U_{j,t}^{EV,E,-}}{\eta_j^{EV,E}} + U_{j,t}^{EV,E,+} \cdot \eta_j^{EV,E}\right)\Delta t \le SOC_{j,t+1}^{EV,E} - \underline{SOC_j^{EV,E}}, \qquad \forall\, j \in J,\;\; t \in T \tag{5.91}$$

$$\left(\frac{D_{j,t}^{EV,E,-}}{\eta_j^{EV,E}} + D_{j,t}^{EV,E,+} \cdot \eta_j^{EV,E}\right)\Delta t \le \overline{SOC_j^{EV,E}} - SOC_{j,t+1}^{EV,E}, \qquad \forall\, j \in J,\;\; t \in T \tag{5.92}$$

$$U_{j,-1}^{EV,E,+}, U_{j,-1}^{EV,E,-}, D_{j,-1}^{EV,E,+}, D_{j,-1}^{EV,E,-} = 0, \qquad \forall\, j \in J \tag{5.93}$$

$$U_{j,t}^{EV,E,+} + U_{j,t}^{EV,E,-} + D_{j,t}^{EV,E,+} + D_{j,t}^{EV,E,-} \le P_{j,t+1}^{E\dot{V},E,+} + P_{j,t+1}^{E\dot{V},E,-}, \qquad \forall\, j \in J,\;\; t \in T \tag{5.94}$$

$$U_{j,t}^{EV,E,+} + U_{j,t}^{EV,E,-} + D_{j,t}^{EV,E,+} + D_{j,t}^{EV,E,-} \le \dot{b}_{j,t}^{EV,E} \cdot M, \qquad \forall\, j \in J,\;\; t \in T \tag{5.95}$$

$$P_{j,t}^{E\dot{V},E,+} + P_{j,t}^{E\dot{V},E,-} \le \left(1 - \dot{b}_{j,t}^{EV,E}\right) \cdot M, \qquad \forall\, j \in J,\;\; t \in T \tag{5.96}$$

Table 5.14 presents the variables for EVs' constraints.

Table 5.14 - Variables for electric vehicles' constraints.

Variable	Description	Unit
$\boldsymbol{b_{j,t}^{EV,E}}$	Binary variable indicating the charging (1) or discharging (0) mode	-
$\boldsymbol{\dot{b}_{j,t}^{EV,E}}$	Binary variable indicating if there is space for offering upward and downward reserves	-
$\boldsymbol{P_{j,t+1}^{E\dot{V},E,+}}$, $\boldsymbol{P_{j,t+1}^{E\dot{V},E,-}}$	Electricity space for charging and discharging	MW
$\boldsymbol{SOC_{j,t}^{EV,E}}$	State-of-charge of the electric vehicles	MWh

Table 5.15 presents the EVs' parameters. Charging and discharging efficiency, minimum, and maximum SOC, and maximum charging/discharging power are provided by the manufacturing company. The state-of-charge at the time of arrival and departure, and the time of arrival and departure are communicated by the EMS when the EV is plugged-in. The prosumers define the time of departure and SOC at the time of departure.

Table 5.15 – Parameters of electric vehicles.

Parameter	Name	Unit	Type
$\overline{\boldsymbol{P_j^{EV}}}$	Maximum charging/discharging power	MW	Fixed
$\boldsymbol{SOC_j^{EV,AR}}, \boldsymbol{SOC_j^{EV,DE}}$	State-of-charge at time of arrival and departure	MWh	Forecasted
$\underline{\boldsymbol{SOC_j^{EV}}}$ and $\overline{\boldsymbol{SOC_j^{EV}}}$	Minimum and maximum state-of-charge	MWh	Fixed
$\boldsymbol{t_j^{AR}}, \boldsymbol{t_j^{DE}}$	Time of arrival and departure	$-$	Forecasted
$\boldsymbol{\eta_j^{EV,+}}$ and $\boldsymbol{\eta_j^{EV,-}}$	Charging and discharging efficiency	$-$	Fixed

5.3.6.6. District heating CHPs

Figure 5.7 presents a CHP scheme. CHPs consume natural gas (inputs) to produce heat and electricity (outputs).

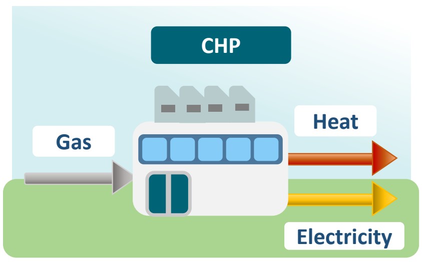

Figure 5.7 – CHP scheme (inputs: gas, outputs: heat and electricity).

Constraints (5.97)-(5.106) model the CHPs connected to the district heating. Constraint (5.97) sets the gas consumption range. Constraints (5.98) and (5.99) define the electricity and heat generated by the CHPs. Constraints (5.100)-(5.105) define the electricity, gas, and heat flexibilities of the CHPs to provide upward and downward reserve bands.

$$\underline{P_j^{CHP,G}} \leq P_{j,t}^{CHP,G} \leq \overline{P_j^{CHP,G}}, \qquad \forall\ j \in J,\ \ t \in T \quad (5.97)$$

$$P_{j,t}^{CHP,E} = \eta_j^{CHP,E} \cdot P_{j,t}^{CHP,G}, \qquad \forall\ j \in J,\ \ t \in T \quad (5.98)$$

$$P_{j,t}^{CHP,H} = \eta_j^{CHP,H} \cdot P_{j,t}^{CHP,G}, \qquad \forall\ j \in J,\ \ t \in T \quad (5.99)$$

$$0 \leq U_{j,t}^{CHP,G} \leq \overline{P_j^{CHP,G}} - P_{j,t}^{CHP,G}, \qquad \forall\ j \in J,\ \ t \in T \quad (5.100)$$

$$U_{j,t}^{CHP,E} = \eta_j^{CHP,E} \cdot U_{j,t}^{CHP,G}, \qquad \forall\ j \in J,\ \ t \in T \quad (5.101)$$

$$U_{j,t}^{CHP,H} = \eta_j^{CHP,H} \cdot U_{j,t}^{CHP,G}, \qquad \forall\ j \in J,\ \ t \in T \quad (5.102)$$

$$0 \leq D_{j,t}^{CHP,G} \leq P_{j,t}^{CHP,G} - \underline{P_j^{CHP,G}}\ , \qquad \forall\ j \in J,\ \ t \in T \quad (5.103)$$

$$D_{j,t}^{CHP,E} = \eta_j^{CHP,E} \cdot D_{j,t}^{CHP,G}, \qquad \forall\ j \in J,\ \ t \in T \quad (5.104)$$

$$D_{j,t}^{CHP,H} = \eta_j^{CHP,H} \cdot D_{j,t}^{CHP,G}, \qquad \forall\ j \in J,\ \ t \in T \quad (5.105)$$

CHPs have a slower response than other electric resources and they are only able to provide 100% of their power within 60 s [166]. Constraint (5.106) limits the response of the CHPs to a fraction of its maximum power. This ensures that the CHPs can deliver the reserves traded in the secondary reserve market. Secondary reserve markets typically require full activations at fast response times.

$$U_{j,t}^{CHP,G}, D_{j,t}^{CHP,G} \leq \mu^{CHP} \cdot \overline{P_j^{CHP,G}}, \qquad \forall\ j \in J,\ \ t \in T \quad (5.106)$$

Table 5.16 presents the parameters of CHPs. The maximum and minimum gas power ($\underline{P_j^{CHP,G}}$ and $\overline{P_j^{CHP,G}}$) and efficiency of converting natural gas to electricity and heat ($\eta_j^{CHP,E}$ and $\eta_j^{CHP,H}$) are provided by the manufacturing company. The CHP participation factor[8] (μ^{CHP}) is defined by the aggregator.

Table 5.16 – Parameters of CHPs.

Parameter	Name	Unit	Type
$\underline{\boldsymbol{P_j^{CHP,G}}}$ and $\overline{\boldsymbol{P_j^{CHP,G}}}$	Maximum and minimum gas power	MW	Fixed
$\boldsymbol{\eta_j^{CHP,E}}$ and $\boldsymbol{\eta_j^{CHP,H}}$	Efficiency of converting natural gas to electricity and heat	–	Fixed
$\boldsymbol{\mu^{CHP}}$	Participation factor	–	Fixed

5.3.6.7. Electrolyzer constraints

[8] The Participation Factor indicates the response fraction of a generator/load power as a response to frequency deviations.

Figure 5.8 presents a P2G scheme. P2Gs consume electricity (inputs) to produce hydrogen (outputs).

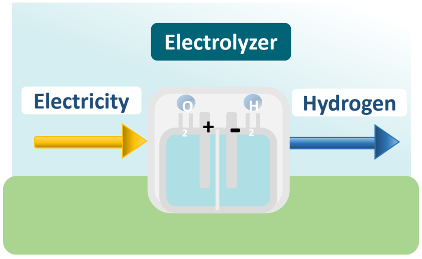

Figure 5.8 – Electrolyzer scheme (inputs: electricity, outputs: hydrogen).

Constraints (5.107)-(5.115) model the P2Gs connected to the electricity network. Constraints (5.107) and (5.108) define the hydrogen produced by the P2Gs. It considers the flow from the P2G to the fuel station, the gas network, and the HSS. The hydrogen flow from the P2G to the fuel cell was not considered as it is an inefficient process that would never be considered by the aggregator. Constraints (5.109)-(5.115) define the limits of the P2Gs: (5.109) for electricity consumption and (5.110)-(5.115) for secondary reserves provision in upward and downward directions. As seen in equations (5.114) and (5.115), the P2G upward and downward secondary reserve provision considers the changes in the hydrogen flow from the P2G to the gas network and the HSS. The sign $\rightarrow$ represents the power that flows from X to Y. For example, the notation in $P2G \rightarrow Sto, H_2$ represents the hydrogen that flows from the P2G to the HSS.

$$P_{j,t}^{P2G,H_2} = \eta_j^{P2G} \cdot P_{j,t}^{P2G,E}, \qquad \forall\ j \in J,\ \ t \in T \tag{5.107}$$

$$P_{j,t}^{P2G,H_2} = P_{j,t}^{P2G\rightarrow HV,H_2} + P_{j,t}^{P2G\rightarrow Net,H_2,} + P_{j,t}^{P2G\rightarrow Sto,H_2}, \qquad \forall\ j \in J,\ \ t \in T \tag{5.108}$$

$$\underline{P_j^{P2G,E}} \leq P_{j,t}^{P2G,E} \leq \overline{P_j^{P2G,E}}, \qquad \forall\ j \in J,\ \ t \in T \tag{5.109}$$

$$U_{j,t}^{P2G,E} \leq P_{j,t}^{P2G,E} - \underline{P_j^{P2G,E}}, \qquad \forall\ j \in J,\ \ t \in T \tag{5.110}$$

$$D_{j,t}^{P2G,E} \leq \overline{P_j^{P2G,E}} - P_{j,t}^{P2G,E}, \qquad \forall\ j \in J,\ \ t \in T \tag{5.111}$$

$$U_{j,t}^{P2G,H_2} = \eta_j^{P2G} \cdot U_{j,t}^{P2G,E}, \qquad \forall\ j \in J,\ \ t \in T \tag{5.112}$$

$$D_{j,t}^{P2G,H_2} = \eta_j^{P2G} \cdot D_{j,t}^{P2G,E}, \qquad \forall\ j \in J,\ \ t \in T \tag{5.113}$$

$$U_{j,t}^{P2G,H_2} = U_{j,t}^{P2G\rightarrow Net,H_2} + U_{j,t}^{P2G\rightarrow Sto,H_2}, \qquad \forall\ j \in J,\ \ t \in T \tag{5.114}$$

$$D_{j,t}^{P2G,H_2} = D_{j,t}^{P2G\rightarrow Net,H_2} + D_{j,t}^{P2G\rightarrow Sto,H_2}, \qquad \forall\ j \in J,\ \ t \in T \tag{5.115}$$

Table 5.17 presents the variables for the P2Gs' constraints.

Table 5.17 - Variables for electrolyzers' constraints.

Variable	Description	Unit
$\boldsymbol{D_{j,t}^{P2G,H_2}}, \boldsymbol{U_{j,t}^{P2G,H_2}}$	Downward and upward hydrogen imbalances from the electrolyzer generated due to the expected activation of secondary reserves	MW
$\boldsymbol{D_{j,t}^{P2G \to Sto,H_2}}, \boldsymbol{U_{j,t}^{P2G \to Sto,H_2}}$	Downward and upward hydrogen imbalances from the electrolyzer to the hydrogen storage systems generated due to the expected activation of secondary reserves	MW
$\boldsymbol{P_{j,t}^{P2G,H_2}}$	Hydrogen produced	MW
$\boldsymbol{P_{j,t}^{P2G \to HV,H_2}}, \boldsymbol{P_{j,t}^{P2G \to Sto,H_2}}$	Hydrogen going from the electrolyzer to the hydrogen vehicles fuel station and the hydrogen storage systems	MW

The efficiency (η_j^{P2G}) and the minimum and maximum power ($\underline{P_j^{P2G,E}}$ and $\overline{P_j^{P2G,E}}$) are provided by the manufacturer.

Table 4.16 presents the parameters of the P2G. The efficiency (η_j^{P2G}) and the minimum and maximum power ($\underline{P_j^{P2G,E}}$ and $\overline{P_j^{P2G,E}}$) are provided by the manufacturer.

Table 5.18 – Parameters of the electrolyzer.

Parameter	Name	Unit	Type
$\boldsymbol{\underline{P_j^{P2G,E}}}$ and $\boldsymbol{\overline{P_j^{P2G,E}}}$	Minimum and maximum power	MW	Fixed
$\boldsymbol{\eta_j^{P2G}}$	Efficiency of converting electricity into hydrogen	$-$	Fixed

5.3.6.8. Hydrogen storage system constraints

Figure 5.9 presents a HSS scheme. The HSSs store hydrogen and they are charged and discharged with hydrogen (inputs and outputs).

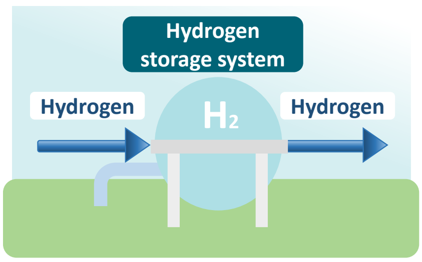

Figure 5.9 – Hydrogen storage scheme (inputs: hydrogen, outputs: hydrogen).

Constraints (5.116)-(5.129) define the operation of HSSs. Constraints (5.116) and (5.117) define the SOC and its limits. Constraints (5.118)-(5.122) set the charging and discharging power and their limits. As seen in equations (5.118) and (5.119), the charging of the HSSs considers the flow from the P2G to the HSS, and the discharging of the HSS considers the flow from the HSS to the fuel station, the gas network, and the FC.

$$SOC_{j,t+1}^{Sto,H_2} = SOC_{j,t}^{Sto,H_2} + \left(P_{j,t}^{Sto,H_2,+} \cdot \eta_j^{Sto,H_2,+} - \frac{P_{j,t}^{Sto,H_2,-}}{\eta_j^{Sto,H_2,-}}\right)\Delta t - \gamma_j \cdot SOC_{j,t}^{Sto,H_2}, \quad \forall \ j \in J,\ t \in T \tag{5.116}$$

$$\underline{SOC_j^{Sto,H_2}} \leq SOC_{j,t}^{Sto,H_2} \leq \overline{SOC_j^{Sto,H_2}}, \quad \forall \ j \in J,\ t \in T \tag{5.117}$$

$$P_{j,t}^{Sto,H_2,+} = P_{j,t}^{P2G\rightarrow Sto,H_2}, \quad \forall \ j \in J,\ t \in T \tag{5.118}$$

$$P_{j,t}^{Sto,H_2,-} = P_{j,t}^{Sto\rightarrow HV,H_2} + P_{j,t}^{Sto\rightarrow Net,H_2} + P_{j,t}^{Sto\rightarrow FC,H_2}, \quad \forall \ j \in J,\ t \in T \tag{5.119}$$

$$\underline{P_j}^{Sto,H_2} \leq b_{j,t}^{Sto,H_2,+} \cdot P_{j,t}^{Sto,H_2,+}, \quad \forall \ j \in J,\ t \in T \tag{5.120}$$

$$P_{j,t}^{Sto,H_2,-} \leq b_{j,t}^{Sto,H_2,-} \cdot \overline{P_j^{Sto,H_2,-}}, \quad \forall \ j \in J,\ t \in T \tag{5.121}$$

$$b_{j,t}^{Sto,H_2,+} + b_{j,t}{}^{Sto,H_2,-} \leq 1, \quad \forall \ j \in J,\ t \in T \tag{5.122}$$

$$SOC_{j,0}^{Sto,H_2} = SOC_{j,-1}^{Sto,H_2}, \quad \forall\, j \in J \tag{5.123}$$

Constraints (5.124)-(5.129) define the secondary reserve bands provided by the HSSs. Constraints (5.124)-(5.127) define the power limits, while constraints (5.128) and (5.129) set the energy limits of HSSs.

$$0 \leq D_{j,t}^{P2G\rightarrow Sto,H_2} \leq \overline{P_j^{Sto,H_2}} - P_{j,t}^{Sto,H_2,+}, \quad \forall \ j \in J,\ t \in T \tag{5.124}$$

$$0 \leq U_{j,t}^{P2G\rightarrow Sto,H_2} \leq P_{j,t}^{Sto,H_2,+}, \quad \forall \ j \in J,\ t \in T \tag{5.125}$$

$$0 \leq D_{j,t}^{Sto\rightarrow FC,H_2} \leq P_{j,t}^{Sto\rightarrow FC,H_2}, \quad \forall \ j \in J,\ t \in T \tag{5.126}$$

$$0 \leq U_{j,t}^{Sto\rightarrow FC,H_2} \leq \overline{P_j^{Sto,H_2}} - P_{j,t}^{Sto,H_2,-}, \quad \forall \ j \in J,\ t \in T \tag{5.127}$$

$$D_{j,t}^{P2G\rightarrow Sto,H_2} + D_{j,t}^{Sto\rightarrow FC,H_2} \leq \frac{\overline{SOC_j^{Sto,H_2}} - SOC_{j,t+1}^{Sto,H_2}}{\Delta t}, \quad \forall \ j \in J,\ t \in T \tag{5.128}$$

$$U_{j,t}^{P2G\rightarrow Sto,H_2} + U_{j,t}^{Sto\rightarrow FC,H_2} \leq \frac{SOC_{j,t+1}^{Sto,H_2} - \underline{SOC_j^{Sto,H_2}}}{\Delta t}, \quad \forall \ j \in J,\ t \in T \tag{5.129}$$

Table 5.19 presents the variables for HSSs constraints.

Table 5.19 - Variables for hydrogen storage system constraints.

Variable	Description	Unit
$b_{j,t}^{Sto,H_2,+}$, $b_{j,t}^{Sto,H_2,-}$	Binary variable indicating the charging and discharging modes	-
$D_{j,t}^{Sto\rightarrow FC,H_2}$, $U_{j,t}^{Sto\rightarrow FC,H_2}$	Downward and upward hydrogen imbalances from the electrolyzer to the fuel cell generated due to the expected activation of secondary reserves	MW
$SOC_{j,t}^{Sto,H_2}$	State-of-charge of the hydrogen storage system	MWh
$P_{j,t}^{Sto,H_2,+}$, $P_{j,t}^{Sto,H_2,-}$	Hydrogen charging and discharging	MW
$P_{j,t}^{Sto\rightarrow HV,H_2}$, $P_{j,t}^{Sto\rightarrow FC,H_2}$	Hydrogen from the hydrogen storage system to the hydrogen vehicle fuel station and fuel cells	MW

Table 5.20 presents the parameters of the HSS. The minimum and maximum SOC, the low heating value, and the maximum charging are parameters provided by the manufacturing company. The initial SOC is communicated by the EMS.

Table 5.20 – Parameters of the hydrogen storage system.

Parameter	Name	Unit	Type
$SOC_{j,0}^{Sto,H_2}$	Initial state-of-charge	MWh	Fixed
$\underline{SOC_j^{Sto,H_2}}$ and $\overline{SOC_j^{Sto,H_2}}$	Minimum and maximum state-of-charge	MWh	Fixed
γ_j	Discharging rate	–	Fixed

5.3.6.9. Fuel cell constraints

Figure 5.10 presents a FC scheme. FCs transform hydrogen (inputs) into electricity (outputs).

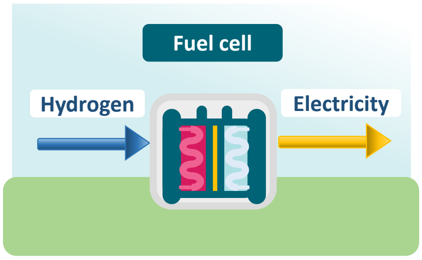

Figure 5.10 – Fuel cell scheme (inputs: hydrogen, outputs: electricity).

Constraints (5.130)-(5.136) define the operation of the FCs. Constraints (5.130) and (5.131) define the electricity produced by the FCs. The remaining constraints (5.132)-(5.136) define the secondary reserves bands provided by the FCs.

$$P_{j,t}^{FC,E} = \eta_j^{FC} \cdot P_{j,t}^{Sto\rightarrow FC,H_2}, \qquad \forall\ j \in J,\ \ t \in T \tag{5.130}$$

$$0 \leq P_{j,t}^{Sto\rightarrow FC,H_2} \leq b_{j,t}^{Sto,H_2,-} \cdot \overline{P_j^{FC,H_2}}, \qquad \forall\ j \in J,\ \ t \in T \tag{5.131}$$

$$U_{j,t}^{Sto\rightarrow FC,H_2} \leq b_{j,t}^{Sto,H_2,-} \cdot \overline{P_j^{FC,H_2}} - P_{j,t}^{Sto\rightarrow FC,H_2}, \qquad \forall\ j \in J,\ \ t \in T \tag{5.132}$$

$$D_{j,t}^{Sto\rightarrow FC,H_2} \leq P_{j,t}^{Sto\rightarrow FC,H_2}, \qquad \forall\ j \in J,\ \ t \in T \qquad (5.133)$$

$$U_{j,t}^{FC,E} = \eta_j^{FC} \cdot U_{j,t}^{Sto\rightarrow FC,H_2}, \qquad \forall\ j \in J,\ \ t \in T \qquad (5.134)$$

$$D_{j,t}^{FC,E} = \eta_j^{FC} \cdot D_{j,t}^{Sto\rightarrow FC,H_2}, \qquad \forall\ j \in J,\ \ t \in T \qquad (5.135)$$

$$D_{j,t}^{FC,E}, U_{j,t}^{FC,E} \geq 0, \qquad \forall\ j \in J,\ \ t \in T \qquad (5.136)$$

Table 5.21 presents the parameters of the FC. The efficiency of converting hydrogen into electricity, and the maximum power are parameters provided by the manufacturing company.

Table 5.21 – Parameters of the fuel cell.

Parameter	Name	Unit	Type
$\overline{\boldsymbol{P}_j^{FC,H_2}}$	Maximum power	MW	Fixed
$\boldsymbol{\eta}_j^{FC}$	Efficiency of converting hydrogen into electricity	–	Fixed

5.3.6.10. Fuel station constraint

Figure 5.11 presents a fuel station scheme and it consumes hydrogen (input).

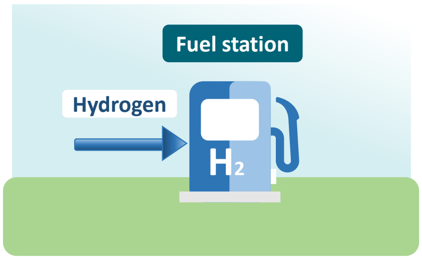

Figure 5.11 – Fuel station scheme (inputs: hydrogen).

Constraint (5.137) ensures that fuel stations supply hydrogen to inflexible loads, such as hydrogen vehicles. Note that the production of green hydrogen to supply fuel stations connected to local hubs is not traded in the market.

$$P_{j,t}^{P2G\rightarrow HV,H_2} + P_{j,t}^{Sto\rightarrow HV,H_2} = P_{j,t}^{HV}, \qquad \forall\, j \in J, t \in T \qquad (5.137)$$

Table 5.22 presents the parameters of the fuel station. The hydrogen load is forecasted by the aggregator.

Table 5.22 – Parameters of the fuel station.

Parameter	Name	Unit	Type
$\boldsymbol{P}_{j,t}^{HV}$	Hydrogen load	MW	Forecasted

5.4. Distribution system operator subproblems: multi-energy flow optimization models

This section presents the multi-energy flow optimization models (3.14) and (3.15) used by the DSOs to evaluate the network feasibility of the multi-energy market services expected to be delivered by the aggregator. The DSOs use the delivery scenarios computed by the aggregator to check if the aggregator's offers violate or not the constraints of the multi-energy networks. Again, these constraints are the same as the constraints presented in Chapter 4. They are repeated here to improve readability and facilitate the interpretation of this chapter.

The role of the DSOs in this paper is to ensure multi-energy network security while opening up as much network capacity as possible for the aggregator to bid into the markets. The minimization of the operating costs of the DSOs, such as network losses, is not considered since the operation of the system is defined by the dispatch of the wholesale markets.

5.4.1. Time horizon and delivery scenarios

The optimization problem is decomposed by time-step $t \in T$ and delivery scenarios $s \in \{E, U, D\}$ because there are no coupling constraints between different time-steps and delivery scenarios. In the next subsections, for the sake of readability, we drop the subscripts of time and delivery scenarios.

5.4.2. Electricity DSO sub-problem

Here, we formulate the optimization problem that the electricity DSO uses to evaluate the feasibility of the aggregator's offers.

5.4.2.1. Objective function

The objective function (5.138) minimizes the augmented Lagrangian penalty terms, which penalize electricity network violations.

$$min \sum_{n \in N^E} \left[\pi_n^E\left(P_n^E - \hat{P}_n^E\right) + \frac{\rho}{2}\left(P_n^E - \hat{P}_n^E\right)^2\right] \tag{5.138}$$

5.4.2.2. Electricity network constraints

The electricity network is modeled using the non-convex formulation of the branch flow model [167][168]. Constraints (5.139)-(5.142) are the branch power flow equations. Constraints (5.143) and (5.144) set the limits of the square of the voltage and current magnitudes.

$$P_{m,n}^F = \frac{\hat{P}_n^E}{SB} + \sum_{i:n \to i} P_{n,i}^F + r_{m,n} \cdot \ell_{m,n}, \qquad \forall\ (m,n) \in B^E \tag{5.139}$$

$$Q_{m,n}^F = Q_n^E + \sum_{i:n \to i} Q_{n,i}^F + x_{m,n} \cdot \ell_{m,n}, \qquad \forall\ (m,n) \in B^E \tag{5.140}$$

$$v_n = v_m - 2\left(r_{m,n} \cdot P_{m,n}^F + x_{m,n} \cdot Q_{m,n}^F\right) + \left(r_{m,n}^2 + x_{m,n}^2\right)\ell_{m,n}, \qquad \forall\, (m,n) \in B^E \quad (5.141)$$

$$\ell_{m,n} \cdot v_m = {P_{m,n}^F}^2 + {Q_{m,n}^F}^2, \qquad \forall\, (m,n) \in B^E \quad (5.142)$$

$$\underline{v_n} \leq v_n \leq \overline{v_n}\,, \qquad \forall\, n \in N^E \quad (5.143)$$

$$0 \leq \ell_{m,n} \leq \overline{\ell_{m,n}}, \qquad \forall\, (m,n) \in B^E \quad (5.144)$$

Table 5.23 presents the variables for the electricity flow model.

Table 5.23 - Variables for the electricity flow model.

Variable	Description	Unit
$\boldsymbol{\ell_{m,n}}$	Square of the current magnitude	$p.u.$
$\boldsymbol{P_{m,n}^F}$	Active power flow	$p.u.$
$\boldsymbol{Q_{m,n}^F}$	Reactive power flow	$p.u.$
$\boldsymbol{v_n}$	Square of the voltage magnitude	$p.u.$

Table 5.24 presents the parameters for the electricity network model.

Table 5.24 – Parameters for the electricity flow model.

Parameter	Name	Unit
$\boldsymbol{\overline{\ell_{m,n}}}$	Maximum current	$p.u.$
$\boldsymbol{r_{m,n}}$	Resistance of lines	$p.u.$
$\boldsymbol{SB}$	Base Power	$p.u.$
$\boldsymbol{\overline{v_n}, \underline{v_n}}$	Maximum and minimum voltage	$p.u.$
$\boldsymbol{x_{m,n}}$	Reactance of lines	$p.u.$

5.4.3. Gas DSO sub-problem

The gas flow optimization problem (5.145)-(5.159) is used by the gas DSO to assure that delivery scenarios of hydrogen and natural gas computed by the aggregator are network-secure.

5.4.3.1. Objective function

The objective function (5.145) minimizes the augmented Lagrangian penalty, which penalizes the calculation of network-secure gas delivery scenarios that deviate from the aggregator's preferences.

$$Min \sum_{d\,\in\,\{GL,H2\}} \left[\sum_{m \in N^d} \pi_m^d\left(P_m^d - \hat{P}_m^d\right) + \frac{\rho}{2}\left(P_m^d - \hat{P}_m^d\right)^2\right] \quad (5.145)$$

5.4.3.2. Network constraints

Constraints (5.146) and (5.147) define the limits of natural gas injection and nodal pressure, respectively.

$$\underline{P_m^{NG}} \leq P_m^{NG} \leq \overline{P_m^{NG}}, \qquad \forall\, m \in N^{NG} \qquad (5.146)$$

$$\underline{p_m^{G}} \leq p_m^{G} \leq \overline{p_m^{G}}, \qquad \forall\, m \in N^{G} \qquad (5.147)$$

Constraint (5.148) models the gas balance in each node. Constraints (5.149)-(5.151) define the volumetric flow of natural gas (5.149), hydrogen (5.150), and gas mixture (5.151).

$$q_m^{NG} + \hat{q}_m^{H_2} - \hat{q}_m^{G} + \sum_{n:n\rightarrow m} q_{n,m} - \sum_{n:m\rightarrow n} q_{m,n} = 0, \qquad \forall\, m \in N^{G} \qquad (5.148)$$

$$q_m^{NG} = \frac{P_m^{NG}}{c^G}, \qquad \forall\, m \in N^{G} \qquad (5.149)$$

$$\hat{q}_m^{H_2} = \frac{\hat{P}_m^{H_2}}{c^{H_2}}, \qquad \forall\, m \in N^{G} \qquad (5.150)$$

$$\hat{q}_m^{G} = \frac{\hat{P}_m^{G} \cdot HHV_m^{G}}{\left(HHV_m^{Mix}\right)^2 c^G}, \qquad \forall\, m \in N^{G} \qquad (5.151)$$

Constraints (5.152)-(5.155) define the HHV (5.152)-(5.153) and the relative gas density to air (5.154) of the gas mixture of hydrogen with natural gas [169]. Constraint (5.155) defines the fraction of hydrogen in the gas mixture.

$$HHV_m^{mix} = w_m^{H_2} \cdot HHV_m^{H_2} + \left(1 - w_m^{H_2}\right) HHV_m^{G}, \qquad \forall\, m \in N^{G} \qquad (5.152)$$

$$\underline{HHV^{mix}} \leq HHV_m^{mix} \leq \overline{HHV^{mix}}, \qquad \forall\, m \in N^{G} \qquad (5.153)$$

$$S_m^{mix} = w_m^{H_2} \cdot S_m^{H_2} + \left(1 - w_m^{H_2}\right) S_m^{G}, \qquad \forall\, m \in N^{G} \qquad (5.154)$$

$$w_m^{H_2} = \frac{\hat{q}_m^{H_2}}{q_m^{NG} + \hat{q}_m^{H_2}}, \qquad \forall\, m \in N^{G} \qquad (5.155)$$

Constraints (5.156)-(5.157) are related with the WI [170] of the gas mixture. These two constraints are used to ensure that the energy output of the gas mixture is acceptable for the end-users and meets established quality of service requirements.

$$WI_m = \frac{HHV_m^{mix}}{\sqrt{S_m^{mix}}}, \qquad \forall\, m \in N^{G} \qquad (5.156)$$

$$\underline{WI} \leq WI_m \leq \overline{WI}, \qquad \forall\, m \in N^{G} \qquad (5.157)$$

Constraint (5.158) defines the steady-stage gas flow [171]. In this case, the gas flowing into the pipeline is equal to the gas flowing out of the pipeline. Constraint (5.159) defines the resistance coefficient of each pipeline.

$$(p_m^G)^2 - (p_n^G)^2 = K_{m,n}^G \cdot q_{m,n} \left|(q_{m,n})^{0.848}\right|, \qquad \forall\ (m,n) \in B^G \tag{5.158}$$

$$K_{m,n}^G = \frac{(p^{G,St})^2 (S_m^{Mix})^{0.848} \theta^G}{57.3 \times 10^{-8} (\theta^{G,St})^2 143.52} \cdot \frac{L_{m,n}}{(\eta_{m,n})^2 (d_{m,n})^{4.848}}, \qquad \forall\ (m,n) \in B^G \tag{5.159}$$

Table 5.25 presents the variables for the gas flow model.

Table 5.25 - Variables for the gas flow model.

Variable	Description	Unit
$\boldsymbol{HHV_m^{Mix}}$	Higher heating value of the mixed gases	MJ/m^3
$\boldsymbol{p_m^G}$	Gas pressure	bar
$\boldsymbol{P_m^{NG}}$	Natural gas injection	MW
$\boldsymbol{q_{n,m}, q_m}$	Gas flows	m^3/h
$\boldsymbol{S_m^{mix}}$	Specific gas gravity	$-$
$\boldsymbol{w_m^{H_2}}$	Hydrogen fraction	$-$
$\boldsymbol{WI_m}$	Wobbe index	MJ/m^3

Table 5.26 presents the parameters for the gas flow model.

Table 5.26 – Parameters for the gas flow model.

Parameter	Name	Unit
$\boldsymbol{c^{H2}, c^G}$	Factor to convert MWh to m^3/h	$\frac{m^3/h}{MWh}$
$\boldsymbol{d_{m,n}}$	Diameter of pipeline	mm
$\boldsymbol{HHV_m^G, HHV_m^{H_2}}$	Higher heating value of natural gas and hydrogen	MJ/m^3
$\boldsymbol{\overline{HHV^{mix}}, \underline{HHV^{mix}}}$	Maximum and minimum higher heating value of the mixed gases	MJ/m^3
$\boldsymbol{K_{m,n}^G}$	Resistance pipeline coefficient	$-$
$\boldsymbol{L_{m,n}}$	Lenght of pipeline	m
$\boldsymbol{p^{G,St}}$	Pressure of natural gas at standard pressure	bar
$\boldsymbol{\overline{p_m^G}, \underline{p_m^G}}$	Maximum and minimum gas pressure	bar
$\boldsymbol{\overline{P_m^{NG}}, \underline{P_m^{NG}}}$	Maximum and minimum injection of natural gas	MWh
$\boldsymbol{\overline{WI}, \underline{WI}}$	Maximum and minimum Wobbe index	$\mathrm{MJ/m^3}$
$\boldsymbol{\theta^G, \theta^{G,St}}$	Temperature of the gases and standard temperature of natural gas	C^o

5.4.4. Heat DSO sub-problem

Here, we formulate the optimization problem that the heat DSO uses to evaluate the feasibility of the aggregator’s offers.

5.4.4.1. Objective function

The objective function (5.160) minimizes the augmented Lagrangian penalty terms, which penalize heat network violations.

$$min \sum_{n \in N^H} \left[\pi_n^H \left(P_n^H - \hat{P}_n^H \right) + \frac{\rho}{2} \left(P_n^H - \hat{P}_n^H \right)^2 \right] \quad (5.160)$$

5.4.4.2. Heat network constraints

Heat networks consist of supply and return networks. Hydraulic and thermal optimizations are performed to calculate the mass flows and temperatures of pipes and nodes. In this model, it was assumed that the temperature of generator supply nodes and load return nodes are defined, as well as the heat power at all nodes, except the slack node.

Hydraulic model

Constraints (5.161) and (5.162) define the conservation of mass and pressure drop. Constraints (5.163)-(5.165) define the pressure and mass flow limits of pipelines and loads/generators [172]. The value of $k_{i,j}$ is calculated as in [173]. To relax the problem, the heat direction flow was initialized for each hour based on the algorithm developed in [174] and remained static for the rest of the iterations.

$$\sum_{j:j\to i} m_{j,i}^a - \sum_{j:i\to j} m_{i,j}^a = A_i^a \cdot mq_i, \qquad \forall\, a \in \{S,R\},\ i \in N^H \quad (5.161)$$

$$p_i^{H,a} - p_j^{H,a} = k_{i,j}^a \cdot m_{i,j}^a \left| m_{i,j}^a \right|, \qquad \forall\, a \in \{S,R\},\ (i,j) \in B^H \quad (5.162)$$

$$\underline{p_i^{H,a}} \le p_i^{H,a} \le \overline{p_i^{H,a}}, \qquad \forall\, a \in \{S,R\},\ i \in N^H \quad (5.163)$$

$$\underline{m_{i,j}^a} \le m_{i,j}^a \le \overline{m_{i,j}^a}, \qquad \forall\, a \in \{S,R\},\ (i,j) \in B^H \quad (5.164)$$

$$\underline{mq_i} \le mq_i \le \overline{mq_i}, \qquad \forall\, i \in N^H \quad (5.165)$$

Thermal model

The thermal model (5.166)-(5.171) is used to determine the temperatures at each network node. Constraint (5.166) is the heat power equation of the loads and generators. The temperature drop constraint (5.167) defines the temperature at the end node of the pipe. Constraints (5.168) and (5.169) set the limits of the temperatures at the end and start nodes of the pipe. Constraint (5.170) defines the conservation of energy. Constraint (5.171) connects equation (5.166) to the remaining constraints of the thermal model by imposing that the temperatures of mass flowing through the node are equal to the temperatures mixed at the node.

$$\hat{P}_i^H = CP \cdot mq_i \left(\theta_i^S - \theta_i^R \right), \qquad \forall\, i \in N^H \quad (5.166)$$

$$\theta_{i,j}^{End,a} = (\theta_{i,j}^{Start,a} - \theta^{Amb}) e^{\frac{h \cdot L}{CP \cdot m_{i,j}^a}} + \theta^{Amb}, \qquad \forall\, a \in \{S,R\},\ (i,j) \in B^H \quad (5.167)$$

$$\underline{\theta_{i,j}^{End,a}} \leq \theta_{i,j}^{End,a} \leq \overline{\theta_{i,j}^{End,a}}, \qquad \forall\, a \in \{S,R\},\ \ (i,j) \in B^H \qquad (5.168)$$

$$\underline{\theta_{i,j}^{Start,a}} \leq \theta_{i,j}^{Start,a} \leq \overline{\theta_{i,j}^{Start,a}}, \qquad \forall\, a \in \{S,R\},\ \ (i,j) \in B^H \qquad (5.169)$$

$$\sum_{j:j\rightarrow i} \theta_{j,i}^{End,a} \cdot m_{j,i}^{a} = \theta_{i}^{a} \sum_{j:i\rightarrow j} m_{i,j}^{a}, \qquad \forall\, a \in \{S,R\},\ \forall\, i\ \in N^H \qquad (5.170)$$

$$\theta_{i}^{a} = \theta_{i,j}^{Start,a}, \qquad \forall\, a \in \{S,R\}, \forall\, i\ \in N^H \qquad (5.171)$$

Table 5.27 presents the variables for the heat flow model.

Table 5.27 - Variables for the heat flow model.

Variable	Description	Unit
$\boldsymbol{m_{i,j}^{a}}$	Mass flows of pipelines	kg/s
$\boldsymbol{mq_{i}}$	Mass flows of heat loads and generators	kg/s
$\boldsymbol{p_{i}^{H,a}}$	Pressure of water pipelines	Pa
$\boldsymbol{\theta_{i,j}^{End,a}}, \boldsymbol{\theta_{i,j}^{Start,a}}$	Temperature at the end and start of a pipeline	C°
$\boldsymbol{\theta_{i}^{R}}, \boldsymbol{\theta_{i}^{S}}$	Temperature of return (generators) and supply (loads) nodes	C°

Table 5.28 presents the parameters for the heat flow model.

Table 5.28 – Parameters for the heat flow model.

Parameter	Name	Unit
$\boldsymbol{CP}$	Water specific heat (J/kg.oC)	$J/kg.C^{o}$
$\boldsymbol{h}$	Heat transfer coefficient (W/°C.m)	$W/C^{o}.m$
$\boldsymbol{k_{i,j}^{a}}$	Coefficient of pressure loss in water pipelines	$-$
$\boldsymbol{L}$	Lenght of pipeline	m
$\overline{\boldsymbol{m_{i,j}^{a}}}, \underline{\boldsymbol{m_{i,j}^{a}}}$	Maximum and minimum mass flows of pipelines	kg/s
$\overline{\boldsymbol{mq_{i}}}, \underline{\boldsymbol{mq_{i}}}$	Maximum and minimum mass flows of heat loads and generators	kg/s
$\overline{\boldsymbol{p_{i}^{H,a}}}, \underline{\boldsymbol{p_{i}^{H,a}}}$	Maximum and minimum pressure of water pipelines	Pa
$\boldsymbol{\theta^{Amb}}$	Ambient temperature of pipelines' surroundings	C^{o}
$\boldsymbol{\theta_{i}^{S}}, \boldsymbol{\theta_{i}^{R}}$	Temperature of supply (generators) and return (loads) nodes	C^{o}
$\overline{\boldsymbol{\theta_{i,j}^{End,a}}}, \underline{\boldsymbol{\theta_{i,j}^{End,a}}}$, $\overline{\boldsymbol{\theta_{i,j}^{Start,a}}}, \underline{\boldsymbol{\theta_{i,j}^{Start,a}}}$	Maximum and minimum temperature at the end and start of a pipeline	C^{o}

5.5. Case study

The proposed multi-energy and network-secure bidding strategy is evaluated using the microgrid from the University of Manchester [175]. The case study's data are presented in Annex

A and contains network, DMERs, buildings, market, weather, and inflexible load data. This data can assume the form of point forecasts or actual measurements.

5.6. Results

In this section, we discuss the economic, network, and computational performances of different combinations of DA and RT optimization strategies. The DA and RT optimization strategies vary on the level of multi-energy network observability. The combinations of DA and RT optimization strategies are the following:

1. Day-ahead network-free and RT network-free (NF-NF): the aggregator performs day-ahead and RT optimizations using network-free approaches, which do not consider the constraints of the multi-energy networks of the DSOs;

2. Day-ahead network-free and RT network-secure (NF-NS): the aggregator performs day-ahead optimization without considering multi-energy network constraints, and RT optimization considering multi-energy network constraints;

3. Day-ahead network-secure and RT network-free (NS-NF): the aggregator performs day-ahead optimization considering multi-energy network constraints, and RT optimization without considering multi-energy network constraints;

4. Day-ahead network-secure and RT network-secure (NS-NS): the aggregator performs day-ahead and RT optimizations considering multi-energy network constraints. Note that the RT network-secure strategy corresponds to the new hierarchical MPC proposed in this paper.

This subsection presents and discusses the performance of the DA and RT optimization strategies. It reports and discusses the RT imbalances (5.6.2), secondary reserves (5.6.3), AGC signal activation (5.6.4), multi-energy network (5.6.5), computational results (5.6.6), and the combined DA and RT results (5.6.7). We discuss these results by the combination of two DA strategies (NF and NS) with two RT strategies (NF and NS).

5.6.1. Day-ahead results

The aggregator participates in the DA electricity (energy and secondary reserve), natural gas, green hydrogen, and carbon markets, as described in Chapter 3. The aggregator computes bids using a bidding optimization framework, which can be network-free (NF) or network-secure (NS). These two bidding optimization frameworks are described and discussed in detail in Chapter 3.

This subsection aims to discuss the DA bidding results, which are used as inputs of the hierarchical MPC framework proposed in this paper to perform RT optimization.

The results of Figure 5.12 and Table 5.29 show that NF and NS strategies result in the computation of different hourly and daily bids. These differences are caused by the imposition of the multi-energy networks' constraints. It means that the bids computed by NF are network-infeasible and could not be delivered since they would cause violations of the networks' constraints. The following subsections discuss the impact of these two DA bidding strategies on the RT performance of the aggregator.

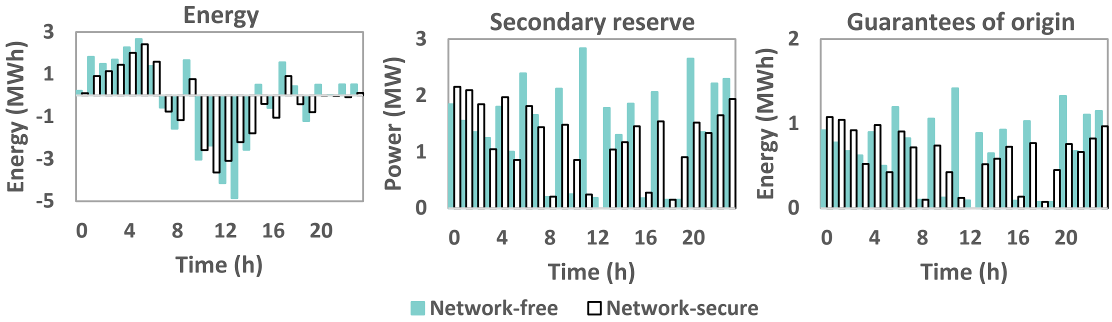

Figure 5.12 - Day-ahead hourly electricity (energy and reserves) and guarantees of origin bids. Positive values are reserves and buying bids of energy and guarantees of origin. Negative values are selling bids of energy and guarantees of origin. Secondary reserves are divided into 2/3 upward and 1/3 downward.

Table 5.29 – Day-ahead daily bids. Positive values are buying quantities. Negative values are selling quantities.

	NF strategy	NS strategy
Natural gas (MWh)	90.9	96.0
Green hydrogen (MWh)	2.9	1.5
Water (L)	5 176	3 476
Oxygen (kg)	1 368	919
CO_2 (tCO_2)	6.2	6.6

5.6.2. Imbalance results

Imbalances are deviations between DA commitments and RT realizations. These imbalances represent an extra cost for the aggregator, which tries to minimize it in RT. In this subsection, we discuss the imbalances produced by the combined DA and RT strategies mentioned previously: NF-NF; NS-NF; NF-NS; and NS-NS.

Figure 5.13 and Table 5.30 show that the NF-NF strategy produced hourly imbalances of GOs, and daily imbalances of natural gas, green hydrogen, water, oxygen, and CO_2. However, these imbalances are network-free, meaning that they can be network-infeasible, as it will be shown in subsection 5.6.5. These network violations may eventually lead to the unpredictable disconnection of DMERs and prosumers from the networks, which makes it very difficult to estimate the expected network-secure imbalances in this case.

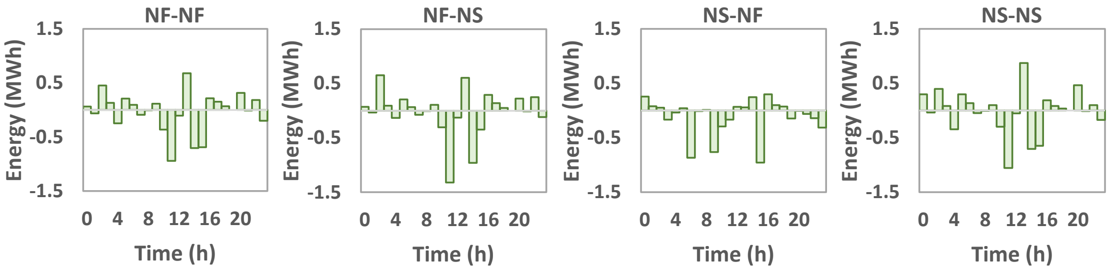

Figure 5.13 - Guarantees of origin imbalances. Positive and negative values are positive[9] and negative[10] imbalances.

Table 5.30 – Daily imbalances. Positive and negative values are positive and negative imbalances.

	NF-NF strategy	NF-NS strategy	NS-NF strategy	NS-NS strategy
Electricity (MWh)	0	0	0	0
Natural gas (MWh)	9.5	20.4	8.6	14.1
Green hydrogen (MWh)	-2.5	-2.0	-2.4	-2.0
Water (L)	-372.7	-547.3	-268.8	-611.7
Oxygen (kg)	98.5	144.6	71.0	161.7
CO_2 (tCO_2)	2.3	4.5	2.1	3.2
Guarantees of origin (MWh)	-0.7	0	-2.6	0

Similar to NF-NF, the NS-NF strategy also produced hourly imbalances of GOs, and daily imbalances of natural gas, green hydrogen, water, oxygen, and CO_2. As it is network-free in RT, it allows the aggregator's assets scheduling in a way that leads to the violation of technical limits in one or more of the networks considered. However, this option may produce imbalances that create network problems, as discussed previously. If we compare these results to those of the other 3 strategies, we can observe that the NS-NF strategy produces the lowest daily imbalances.

The NF-NS strategy produced the highest daily imbalances of natural gas, green hydrogen, water, oxygen, and CO_2. In addition, it was the only strategy to produce imbalances of secondary reserves, as illustrated in Figure 5.14. This happens because the aggregator computes bids without considering multi-energy network constraints, and delivers them considering multi-energy network constraints. The imposition of multi-energy network constraints in the RT stage makes it impossible to deliver all the network-free bids computed in the DA.

[9] A positive imbalance represents an excess buying position or a shortage selling position of the aggregator in real-time compared to the day-ahead.

[10] A negative imbalance represents a shortage buying position or an excess selling position of the aggregator in real-time compared to the day-ahead.

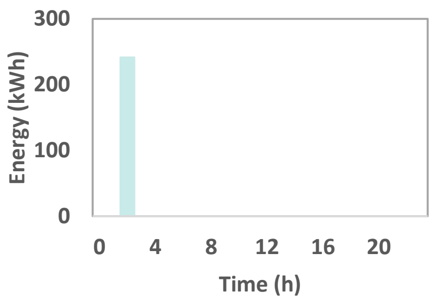

Figure 5.14 – Secondary reserves not supplied for the NF-NS strategy.

Finally, the NS-NS strategy produced lower daily and hourly imbalances than the NF-NS strategy. This is because, in the DA phase, it preemptively prevented some imbalances from occurring due to network violations by using a network-secure strategy to compute the DA bids. In relation to the NF-NF and NS-NF strategies, the NS-NS strategy has more imbalances as it prevented the delivery of multi-energy services that violated network constraints. These imbalance results demonstrate that considering multi-energy network constraints in DA and RT stages reduces imbalances, and at the same time ensures multi-energy network security.

5.6.3. Secondary reserves results

This section analyzes the electrical upward and downward reserves activated. Figure 5.15 and Table 5.31 present the reserves activated along the 24h period and daily totals for the NF-NF, NF-NS, and NS-NF cases, respectively. The NF-NF and NF-NS cases have the same DA bids and so, the reserves activated are very similar. The only difference is at 2h, as the NF-NS strategy produced imbalances of secondary reserves, as previously seen. The NS-NF and NS-NS did not produce any imbalance and they have the same behavior in terms of activated reserves. The NF-NF and NF-NS strategies had more daily upward (+0.9 MW and +0.6 MW) and downward (+0.2 MW) reserves activated than the NS-NF and NS-NS strategies. This occurs in part because they initially submitted higher DA bids to the secondary reserve market.

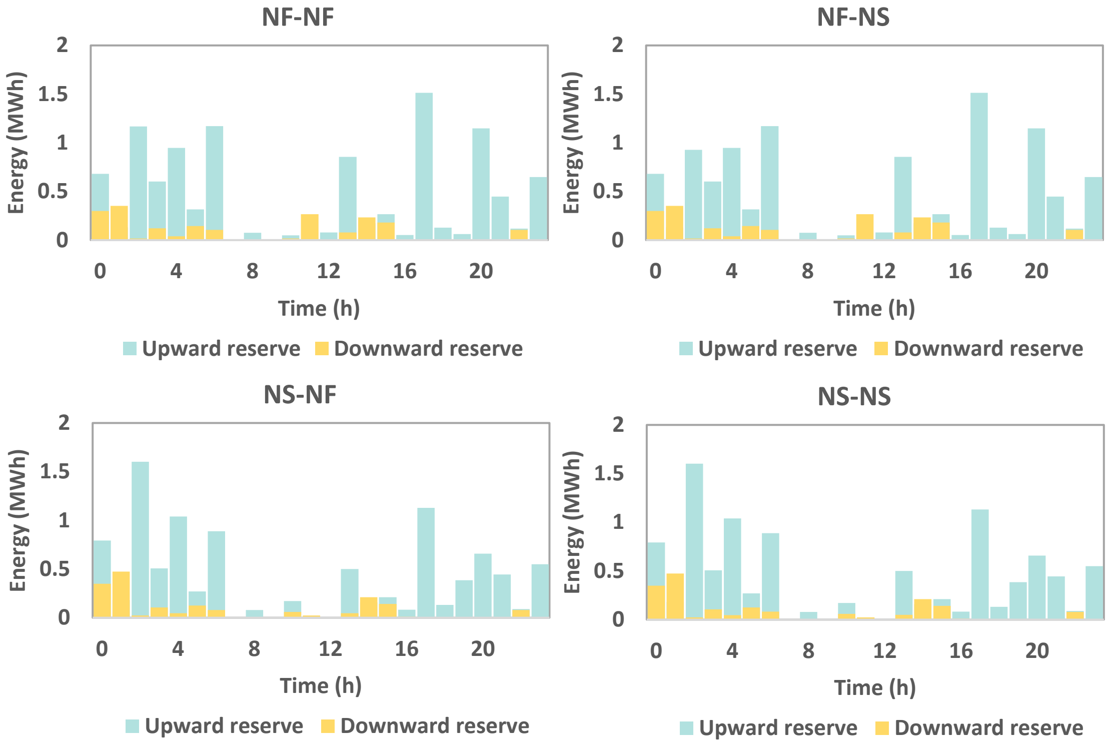

Figure 5.15 – Hourly activated upward and downward secondary reserves.

Table 5.31 - Daily upward and downward reserves activated.

	NF-NF strategy	NF-NS strategy	NS-NF strategy	NS-NS strategy
Upward reserve	10.7	10.4	9.8	9.8
Downward reserve	2.0	2.0	1.8	1.8
Total	12.6	12.4	11.6	11.6

5.6.4. AGC signal activation results

Figure 5.16 presents the tracking of the AGC signal during the day for each case study. The power deployed represents the actual power provided by the aggregator in RT. It is possible to observe that NF-NF has a behavior similar to NF-NS and NS-NF has a similar behavior to NS-NS, due to their DA bidding strategies. The power deployed by the aggregator was able to follow the AGC signal in NF-NF, NS-NF, and NS-NS. In NF-NS, as we have concluded before, the aggregator was not able to provide all the requested reserve services. Thus, it was not able to fully follow the AGC signal (e.g. 2h).

This behavior is seen more clearly in Figure 5.17 where it is presented the tracking of AGC signal from 2h to 4h for the NF-NF and NF-NS strategies. At 2h, the aggregator could not comply with the upward reserve bid offered in the DA markets. As the AGC signal is calculated according to the DA reserve bids, it requested more reserves than the aggregator could offer in RT. This way, the aggregator ended up not following the AGC signal. On the other hand, at 3h there was not any secondary reserve imbalance, and the aggregator was able to satisfy the requested power from the AGC.

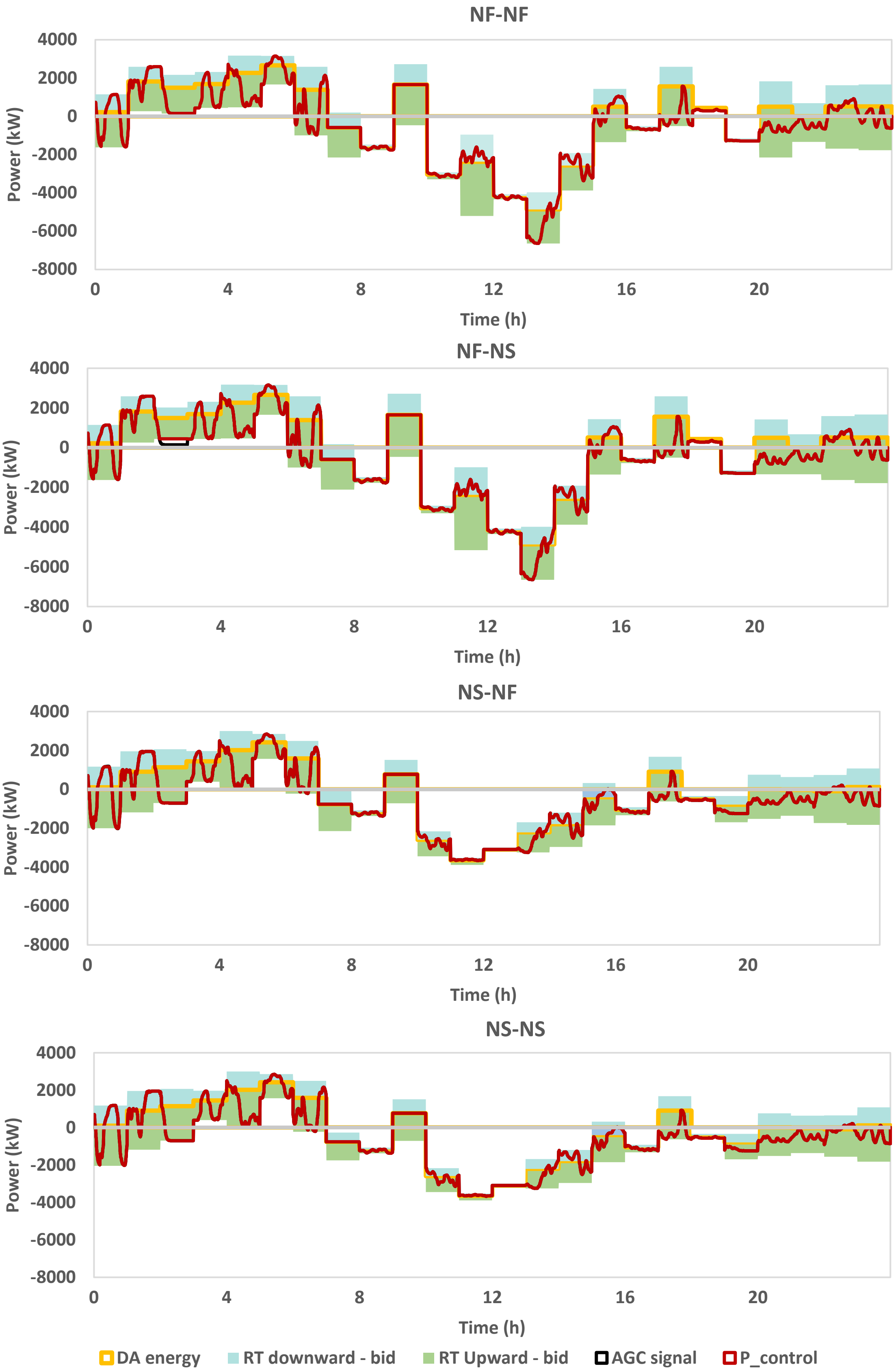

Figure 5.16 - Automatic generation control signal during the day for the four strategies.

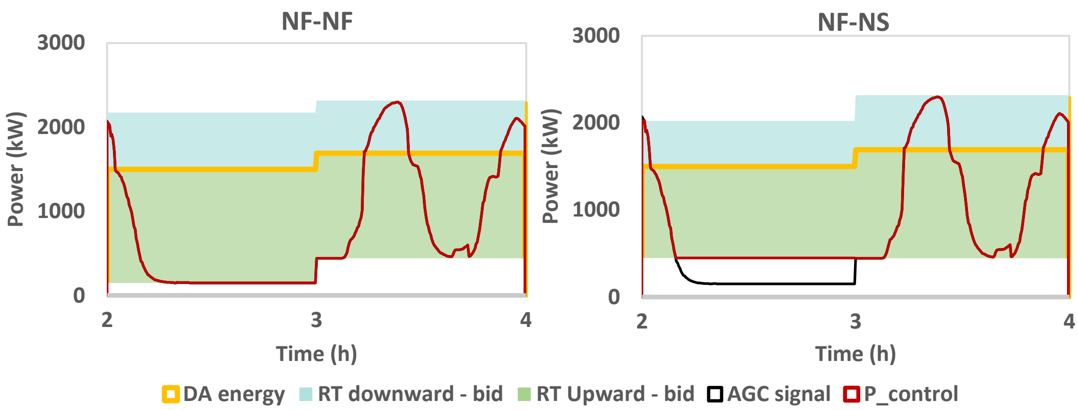

Figure 5.17 – Automatic generation control signal for cases NF-NF and NF-NS between 2h and 4h.

5.6.5. Multi-energy network results

This section illustrates the network problems caused by the four strategies when the three delivery scenarios $s \in \{E, U, D\}$ are simulated across the electricity, gas, and heat networks.

The electricity problems are related to voltage violations. Figure 5.18 presents the voltage results obtained for the four strategies for the upward scenario along the day. Table 5.32 presents the daily number of voltage problems and their maximum and minimum values for the four strategies for each scenario $s \in \{E, U, D\}$. These results show that the NF-NF and NS-NF strategies caused multiple problems. The NF-NF strategy caused a total of 61 voltage violations while the NS-NF strategy caused 30. The upward scenarios had more problems and caused more severe voltage violations than the energy and downward scenarios, as more electricity is being injected and causes a raise in voltages.

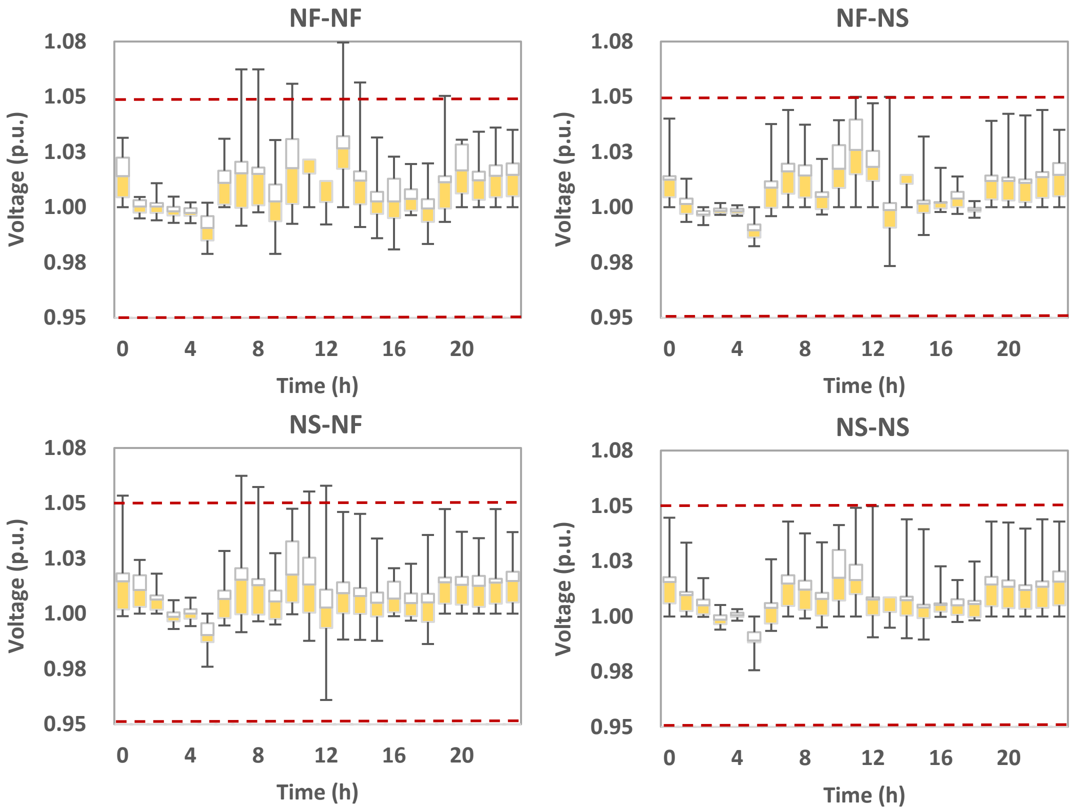

Figure 5.18 - Voltage results for the four strategies for the upward scenario.

Table 5.32 - Voltage results for the four strategies.

		Energy	Upward	Downward
	Number	12	29	20
Free-Free	**Minimum (p.u.)**	0.95	0.98	0.95
	Maximum (p.u.)	1.07	1.07	1.06
	Number	0	0	0
Free-Secure	**Minimum (p.u.)**	0.99	0.96	0.97
	Maximum (p.u.)	1.04	1.01	1
	Number	6	14	10
Secure-Free	**Minimum (p.u.)**	0.95	0.96	0.95
	Maximum (p.u.)	1.06	1.06	1.06
	Number	0	0	0
Secure-Secure	**Minimum (p.u.)**	0.99	0.97	0.97
	Maximum (p.u.)	1.04	1.03	1.02

The heat network problems are related to mass flow violations. Figure 5.19 presents the mass flow results obtained for the four strategies for the upward scenario along the day. Table 5.33 presents the daily number of mass flow problems and their maximum and minimum values for the four strategies for each scenario $s \in \{E, U, D\}$. The NF-NF strategy caused a total of 14 problems while the NS-NF strategy caused a total of 11 problems. Comparing the two strategies, NF-NF had 3 more problems than the NS-NF strategy. Concerning the severity of technical problems, the upward scenarios caused more severe violations compared to the energy and downward scenarios.

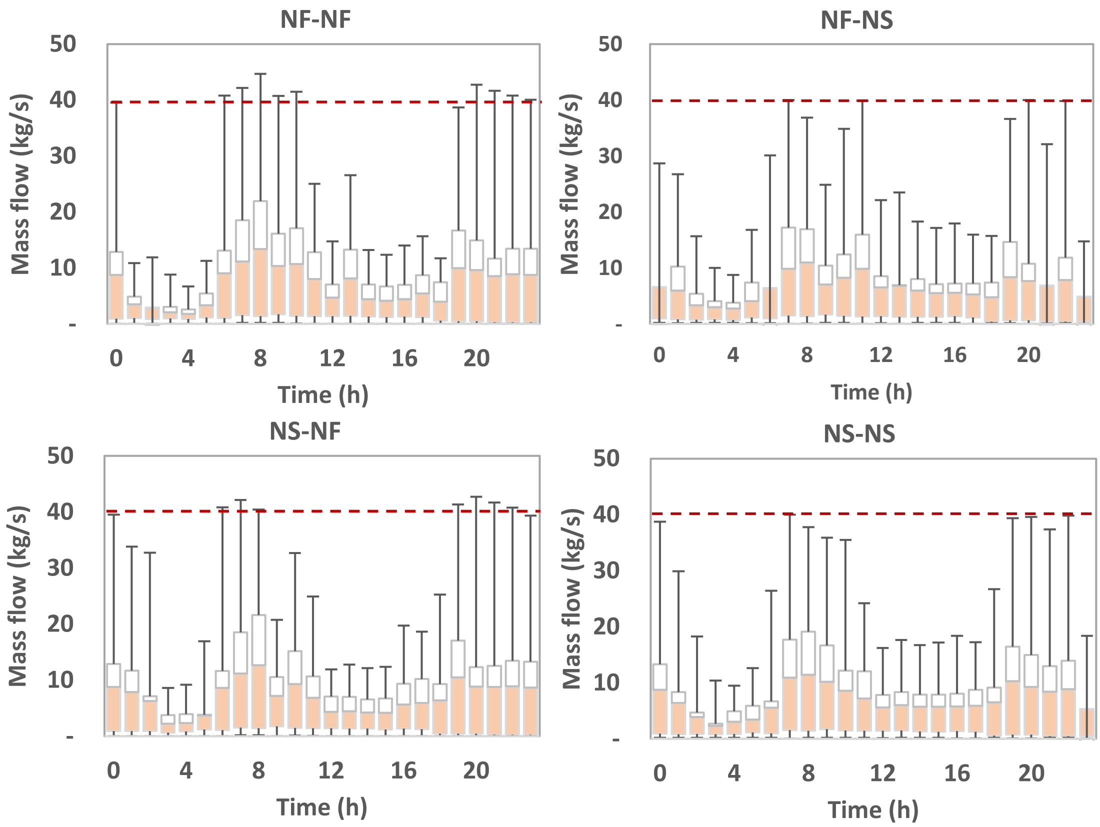

Figure 5.19 – Mass flow results for the four strategies for the upward scenario.

Table 5.33 - Mass flow results for the four strategies.

		Energy	Upward	Downward
	Number	3	8	3
Free-Free	**Minimum (kg/s)**	0.00	1.00	2.00
	Maximum (kg/s)	43.90	45.42	43.90
	Number	0	0	0
Free-Secure	**Minimum (kg/s)**	0.00	0.00	0.00
	Maximum (kg/s)	35.30	26.74	35.30
	Number	2	7	2
Secure-Free	**Minimum (kg/s)**	0.00	0.00	0.00
	Maximum (kg/s)	42.97	42.73	42.97
	Number	0	0	0
Secure-Secure	**Minimum (kg/s)**	0.00	0.00	0.00
	Maximum (kg/s)	38.75	29.91	38.75

The gas network problems are related to WI and HHV violations. Figure 5.20 and Figure 5.21 presents the HHV and WI results obtained for the four strategies for the upward scenario along the day. Table 5.34 and Table 5.35 present the daily number of HVV and WI problems and their maximum and minimum values for the four strategies for each scenario $s \in \{E, U, D\}$. The NF-NF strategy caused a total of 29 HHV and 4 WI problems while the NS-NF strategy caused a total of 24 HHV and 2 WI problems. The downward scenarios caused more severe HHV and WI violations than the energy and upward scenarios. This occurs because, in the downward scenario, the P2G consumes more electricity, resulting in more hydrogen produced and injected into the gas network. This in turn will cause more network violations.

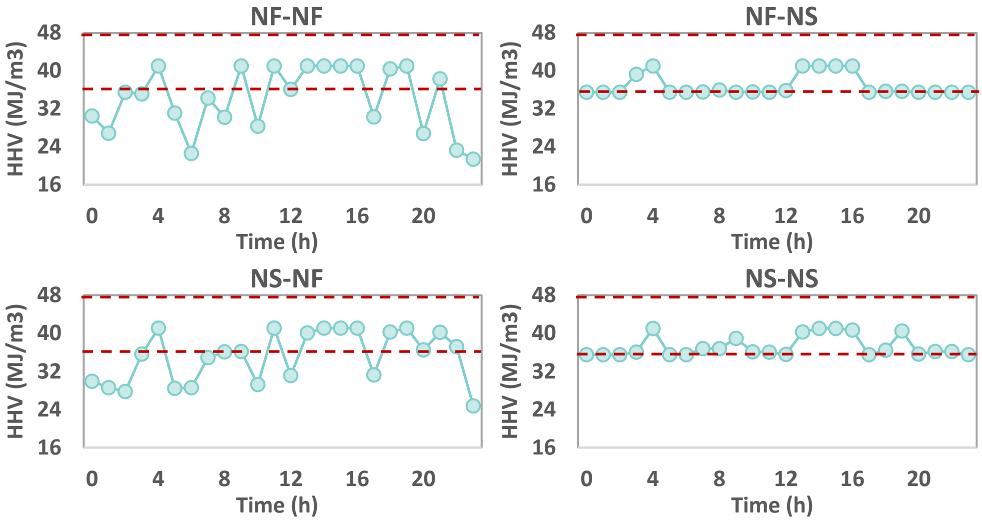

Figure 5.20 - HHV results for the four strategies for the downward scenario.

Table 5.34 - HHV results for the four strategies.

		Energy	Upward	Downward
Free-Free	**Number**	12	5	12
	Minimum (MJ/m3)	21.3	29.2	21.4
	Maximum (MJ/m3)	41.0	41.0	41.0
Free-Secure	**Number**	0	0	0
	Minimum (MJ/m3)	35.5	35.5	35.5
	Maximum (MJ/m3)	41.0	41.0	41.0
Secure-Free	**Number**	10	4	10
	Minimum (MJ/m3)	24.8	30.6	24.8
	Maximum (MJ/m3)	41.0	41.0	41.0
Secure-Secure	**Number**	0	0	0
	Minimum (MJ/m3)	35.5	35.5	35.5
	Maximum (MJ/m3)	41.0	41.0	41.0

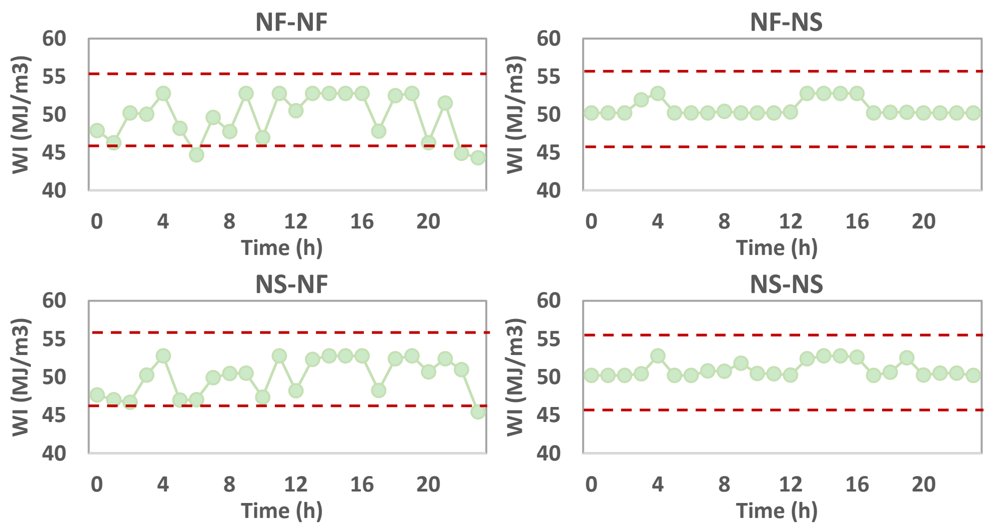

Figure 5.21 - WI results for the four strategies for the downward scenario.

Table 5.35 - WI results for the four strategies.

		Energy	Upward	Downward
Free-Free	**Number**	3	0	1
	Minimum (MJ/m3)	44.3	47.3	44.3
	Maximum (MJ/m3)	52.8	52.8	52.8
Free-Secure	**Number**	0	0	0
	Minimum (MJ/m3)	50.2	50.2	50.2
	Maximum (MJ/m3)	52.8	52.8	52.8
Secure-Free	**Number**	1	0	1
	Minimum (MJ/m3)	45.4	48.0	45.4
	Maximum (MJ/m3)	52.8	52.8	52.8
Secure-Secure	**Number**	0	0	0
	Minimum (MJ/m3)	50.2	50.2	50.2
	Maximum (MJ/m3)	52.8	52.8	52.8

These results show that the NF-NF and NS-NF strategies caused multiple problems in the electricity, heat, and gas networks. On the contrary, the NF-NS and NS-NS strategies did not cause any problems in the electricity, gas, and heat networks, confirming that the consideration of networks' constraints in RT ensures the reliable delivery of market services. Moreover, it can also be concluded that integrating multi-energy networks constraints in the DA stage reduces the number and severity of the technical problems, although it does not ensure security in RT if network constraints are not considered in this stage.

5.6.6. Computational results

The RT strategies use a hierarchical MPC with two levels. Both levels were implemented in Python. The optimization subproblems of the aggregator and DSOs in the first level were implemented in Pyomo and solved by the IBM CPLEX v12.9.0 and IPOPT v3.11.1 optimizers, respectively. The aggregator subproblem is a mixed-integer quadratic program, while the DSOs subproblems are non-linear. The experiments were run on a computer with 8 GB RAM and an Intel® Core™ i5.8265U CPU @ clocked at 1.6GHz.

The optimization subproblems in the first level of the hierarchical MPC are solved every hour. Table 5.36 reports the computational times of these subproblems. As expected, the results show that NF is the fastest approach with a total computational time of 0.96s, followed by the NS with a total computational time of 11.26 min ((3.52 + max(0.05, 0.12, 0.34))*175 ADMM iterations). However, both strategies perform way under the 1 hour requirement. Note that the total computational time of NS results from assuming that aggregator and DSOs subproblems can be solved in parallel.

The controller in the second level of the hierarchical MPC is run every 20s. The execution time of the controller is in the order of milliseconds, far below 20s.

Table 5.36 - Size and execution time of the optimization subproblems in the first level of the hierarchical MPC frameworks.

	Subproblems	Nº of variables	Nº of constraints	Time (s)
NF	**Aggregator**	75 782	102 016	0.98
NS	**Aggregator**	73 089	99 100	3.52
	Electricity DSO	226	427	0.05
	Gas DSO	515	1 023	0.12
	Heat DSO	463	1 341	0.34

It is worth mentioning that the optimization subproblems of the NS strategy were solved using the ADMM, which has recently been proven to converge for convex problems [163], but also for many non-convex problems [177][150][45], such as this one.

5.6.7. Day-ahead and real-time settlement results

Table 5.37 presents the DA, RT, and settlement net-costs. The settlement net-costs result from the sum of the DA and RT net-costs. The equation used to calculate the settlement net-costs is described in Chapter 3.

The results of Table 5.37 show that the NF-NF strategy presents the lowest settlement net-cost of 399€ followed by NS-NF, NS-NS, and NF-NS, with net-cost of 428€, 608€, and 1723€, respectively. The NF-NF strategy presents the lowest settlement net-cost since it does not consider the multi-energy network constraints in the DA and RT optimization phases. However, it does not ensure that bids and services delivered are physically feasible, as discussed before. Therefore, this settlement net-cost is theoretical since the aggregator will not be able to deliver the market services negotiated. Even so, it provides an indication of how much the technical limits of the networks are constraining the profits of the aggregator.

The NS-NF strategy presents the second lowest settlement net-cost. Similarly to NF-NF, it also does not ensure network security in RT, meaning that the delivery of the market services may not be accomplished. As the eventual violation of networks' limits may lead to unpredictable disconnection of DMERs and prosumers, it is impossible to estimate the real network-secure settlement costs of NS-NF and NF-NF. Therefore, these costs are theoretical and can only be used for comparison purposes.

Under RT network-secure conditions, the NS-NS strategy presents the lowest settlement net-cost. This shows that considering multi-energy network constraints in the DA and RT optimization problems significantly reduces the RT net-costs of the aggregator, and consequently its settlement net-costs, while the networks' normal operating conditions are preserved.

Table 5.37 - Settlement net-costs. Positive values are costs, and negative values are revenues.

	Net-cost (€)	NF-NF strategy	NF-NS strategy	NS-NF strategy	NS-NS strategy
DA	**Electricity - Energy**	-415	-415	-547	-547
DA	**Electricity - Band**	-277	-277	-244	-244
DA	**Gas**	1 272	1 272	1 343	1 343
DA	**Hydrogen**	-222	-222	-115	-115
DA	**Water**	19	19	16	16
DA	**Oxygen**	0	0	0	0
DA	**Guarantees of origin**	-7	-7	-8	-8
DA	**CO_2**	303	303	317	317
RT	**Reserve activation**	-535	-530	-470	-470
RT	**Energy imbalance**	0	0	0	0
RT	**Reserve not supplied**	0	1 087	22	0
RT	**Gas imbalance**	160	305	147	221
RT	**Hydrogen imbalance**	41	75	-87	14
RT	**Water imbalance**	-1	-2	-1	-2
RT	**Oxygen imbalance**	0	0	0	0
RT	**Guarantees of origin imbalance**	0	0	-1	0
RT	**CO_2 imbalance**	60	114	55	83
DA + RT	**Settlement**	399	1 723	428	608

5.7. Conclusions

This chapter presents a new hierarchical MPC framework to assist multi-energy aggregators in the network-secure and RT delivery of multi-energy services traded in DA electricity, gas, green hydrogen, and carbon markets. The MPC framework uses the ADMM on a rolling horizon to negotiate the network-secure delivery of multi-energy services between the aggregator and multi-energy DSOs. The multi-energy services include electricity (energy and reserves), natural gas, green hydrogen, and carbon allowances, which result from the RT optimization of the MES managed by the aggregator.

The proposed hierarchical MPC framework was used to conduct a series of studies. The first study discusses and compares the combined performance of DA and RT strategies with different levels of multi-energy network observability. The results of this study allow drawing the following conclusions:

1. Network security is only ensured when the constraints of the multi-energy networks are considered in the RT optimization problem (i.e. in the hierarchical MPC). This means that considering the network constraints only in the DA bidding problem does not guarantee network security;

2. Considering multi-energy network constraints at the DA stage reduces the number of imbalances and the number of network violations in RT;

3. Considering multi-energy network constraints at both DA and RT optimization stages produces the most cost-effective and reliable solution for aggregators since it minimizes settlement net-costs while ensuring multi-energy network security.

The next chapter discusses the economic and environmental aspects of the aggregator's participation in multi-energy markets. For this, two different analyses are performed: one considering different decarbonization policies and another one considering different LCSs.

Chapter 6
Sensitivity studies about economics and sustainability

6.1. Introduction

The previous chapters presented network-secure bidding and RT optimization frameworks for aggregators to participate in multi-energy markets. This chapter discusses the economic and environmental aspects of the aggregator's participation in those markets. For this purpose, two different analyses were made. The first analysis focuses on different decarbonization policies and includes two sensibility studies. These policies consider different carbon and green hydrogen prices. The second analysis focuses on the decarbonization of energy systems through LCSs and includes four different studies. These studies reflect the importance given to the electrification of energy vectors, and to carbon and green hydrogen markets to enhance the sustainability of energy systems. First, carbon markets are an important tool to lower carbon emissions emitted from non-renewable energy generators. Secondly, green hydrogen could be used to replace non-renewable gas or fuels and enhance the decarbonization of certain energy vectors. Moreover, it could help the integration of RES as it can be a means of storing energy. Thirdly, the electrification of the energy vectors based on RES is seen as a possible path to decarbonize most of or even the entire energy system.

These studies were developed using the network-free and network-secure DA bidding optimization frameworks, presented in Chapter 3. This way, besides the analysis of the economic and environmental aspects, the impact of using the network-secure bidding optimization framework developed in this thesis is once again analyzed. Figure 6.1 describes the studies developed in this chapter.

The following sections present the results of the studies developed. The sections of this chapter are divided as follows:

- Section 6.2 presents two sensibility studies covering the impact that carbon prices and green hydrogen policies have on the aggregator's performance;
- Section 6.3 discusses the technical, economic, and environmental impacts of different LCSs from the perspective of the aggregator;
- Section 6.4 presents the conclusions of this chapter.

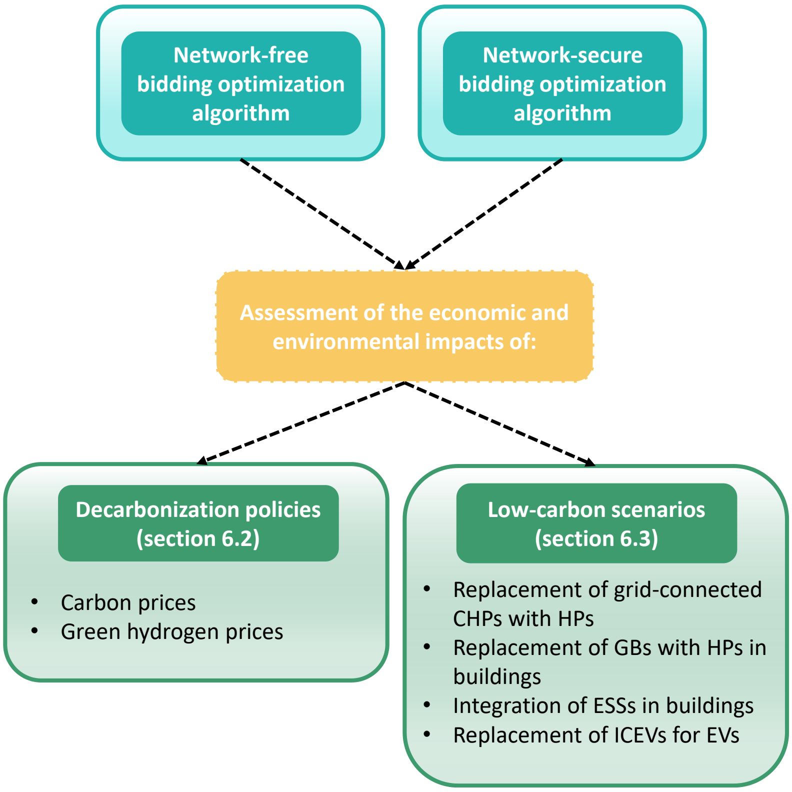

Figure 6.1 – Assessment of the economic and environmental impacts scheme.

6.2. Decarbonization policies

In this section, two sensibility studies are presented related to the economic value of CO_2 emissions (6.2.1) and green hydrogen prices (6.2.2).

6.2.1. Impact of the carbon price on the aggregator performance

The results of Table 6.1 show that increasing the CO_2 price rises the aggregator's costs. If we compare a CO_2 price of 0€/tCO_2 to 25€/tCO_2 (used in the previous sections), we can observe that the net cost increases from 264€ to 672€, representing a 155% rise, when using the network-free framework. The net costs increase even more, from 290€ to 764€, representing a 163% rise, when using the network-secure framework. On the other hand, the increase in the CO_2 price did not have the same impact on the energy and band bids, as shown in Figure 6.2. The energy bids of the CHPs decreased from -31.1 MW to -29.2 MW (-6%), for the network-free framework. The upward bids decreased from 13.8 to 13.1 (-5%), and the downward bids decreased from 1.5 MW to 1.4 MW (-7%). The network-secure framework provided similar bid results. Therefore, CO_2 prices have a significant impact on the aggregator's costs, but they do not significantly impact the operation of the CHPs.

To have a significant impact on the bidding behavior of the CHPs and respective CO_2 emissions, the price would have to increase to more than 400€/tCO_2. This is possible to observe in Figure 6.2, as CHPs' upward band decreased from 14 MW to 5 MW (-64%). This decrease not only significantly impacts the aggregators' total upward bids (-21%), but also the downward bids (-21% as well), as they must comply with constraint (A.1)(A.1). The energy bids of the CHPs were not so affected, as they must satisfy the minimum requirements of the district heating loads.

Table 6.1 - Aggregator costs considering different CO_2 prices. Values in red represent the price difference between the network-secure and network-free bidding optimization framework.

	Price of CO_2 (€/tCO_2)	0	25	100	200	300	400	500
Total cost (€)	Network-free	264	672	1502	2583	3656	4707	5762
	Network-secure	290	764	1679	2820	3805	5039	6143
		+9.8%	+13.7%	+11.8%	+9.2%	+4.1%	+7.1%	+6.6%

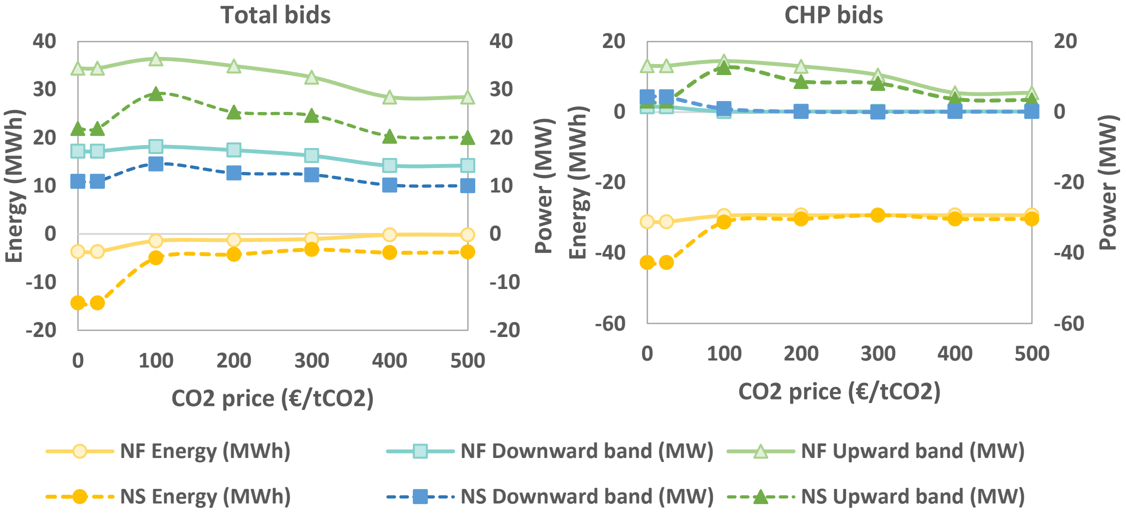

Figure 6.2 - Impact on electricity (energy and reserve) bids considering different CO_2 prices (NF – network-free, NS – network-secure).

From another point of view, it is also possible to conclude that carbon markets may have a negative impact on the provision of secondary reserve since the band bids offered by the aggregator decreased with higher prices. This only occurs if the DMERs used for providing these reserves are affected by the carbon market. Nonetheless, the increase in CO_2 prices rises the operating costs of the CHPs, which may incentivize the adoption of only electricity resources by the aggregator.

Regarding the differences between the network-free and network-secure bidding optimization frameworks, it is possible to observe that they provided different results. These results indicate that the network-secure framework reached network limits. Because of this, the aggregator decreased its downward and upward secondary reserve band offers, as it is possible to observe in Figure 6.2. This, in turn, increased the aggregator's costs up to 13.7%.

6.2.2. Impacts of the aggregator adopting a green hydrogen policy

In this subsection, we analyze the impacts of the multi-energy aggregator adopting a green hydrogen policy under different prices of green hydrogen and CO_2. This analysis covers several aspects, such as the impacts of different prices on the aggregator's economic performance, green hydrogen production, natural gas consumption, CO_2 emissions, and secondary reserves availability.

Figure 6.3 shows that the aggregator cost increases with the increase in CO_2 prices and decreases with the increase of green hydrogen prices. However, the impact of CO_2 prices is significant, while the impact of green hydrogen prices is very small. In sum, the increase in CO_2 prices will increase the economic pressure on aggregators with natural gas resources like CHPs, incentivizing them to replace these technologies with other electricity-powered technologies, like HPs.

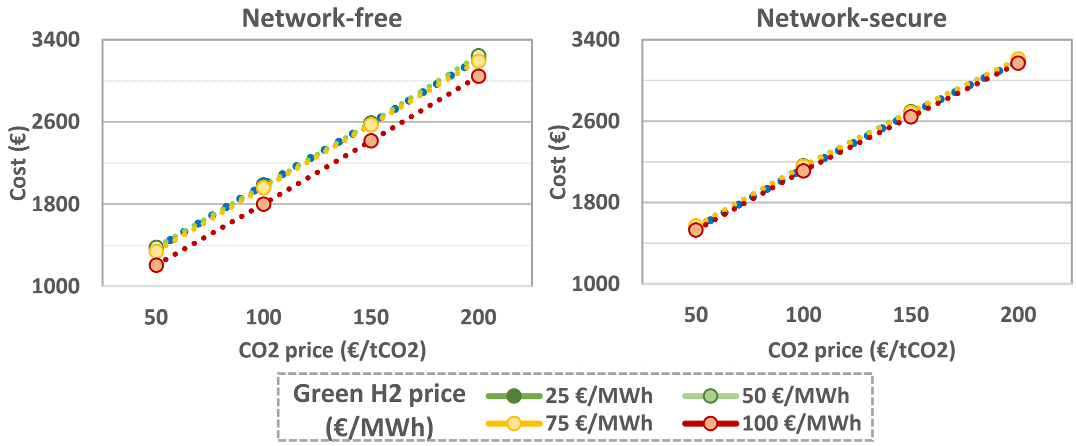

Figure 6.3 – Impacts of CO_2 and green hydrogen prices on the cost of the aggregator.

The prices of CO_2 emissions and green hydrogen also impact the production of green hydrogen, natural gas consumption, and CO_2 emissions of the DMERs managed by the aggregator, as illustrated in Figure 6.4. The production of green hydrogen increases with the increase of its price, namely when they increase from 75 €/MWh to 100 €/MWh. At this point, the injection of green hydrogen into the gas network becomes very attractive. On the other hand, the prices of CO_2 emissions do not impact the production of green hydrogen as much. This shows that injecting green hydrogen into the gas network is only attractive when green hydrogen prices are higher.

The consumption of natural gas decreases with the increase in CO_2 prices, as illustrated in Figure 6.4. In more detail, the increase in CO_2 prices decreases the consumption of natural gas by CHPs, which consume gas to produce heat and carbon-taxed electricity. This is more noticeable when the CO_2 prices increase from 50 €/tCO_2 to 100 €/tCO_2. From 100 €/tCO_2 to 200 €/tCO_2, the room to reduce the consumption of natural gas by CHPs is small. On the other hand, the increase in green hydrogen prices increases the consumption of natural gas. This occurs because it compensates to consume more natural gas in order to ensure the gas quality flowing through the gas network which is affected by the increase in green hydrogen injection.

The CO_2 emissions produced by the consumption of natural gas follow the same trend as natural gas consumption. This shows that a market with high prices of CO_2 allowances and green hydrogen can contribute to significantly reducing the consumption of natural gas and emitted CO_2.

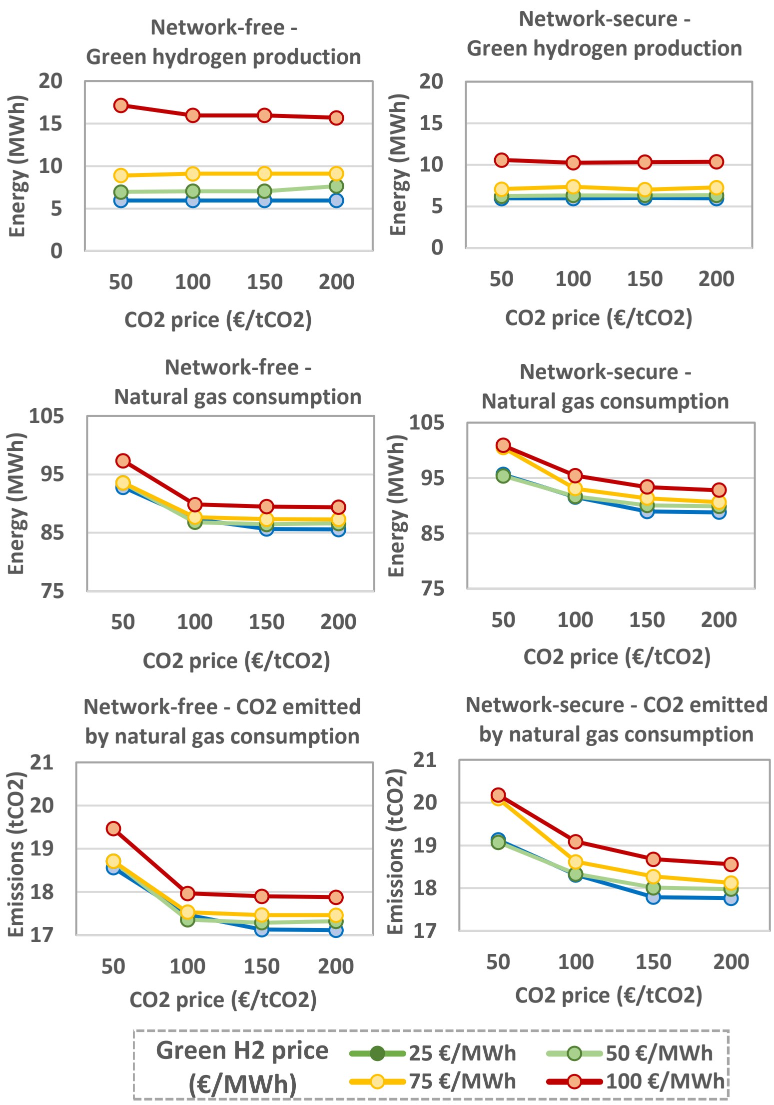

Figure 6.4 – Impacts of CO_2 and green hydrogen prices on hydrogen production, natural gas consumption, and CO_2 emissions.

Another point to analyze in this subsection is the impact of CO_2 and green hydrogen prices in the provision of secondary reserves for the power system operation. Figure 6.5 shows that the provision of secondary reserves by the aggregator increases with the increase of green hydrogen prices and the reduction of CO_2 prices. As mentioned before, high CO_2 prices influence the operation of CHPs and consequently reduce the availability of these resources to provide energy and also secondary reserve services. On the other hand, high green hydrogen prices make hydrogen technologies attractive to provide energy and secondary reserve services. In sum, high CO_2 prices discourage the utilization of technologies powered by natural gas to provide secondary reserves. On the other hand, high green hydrogen prices may attract other technologies to provide this essential power system service.

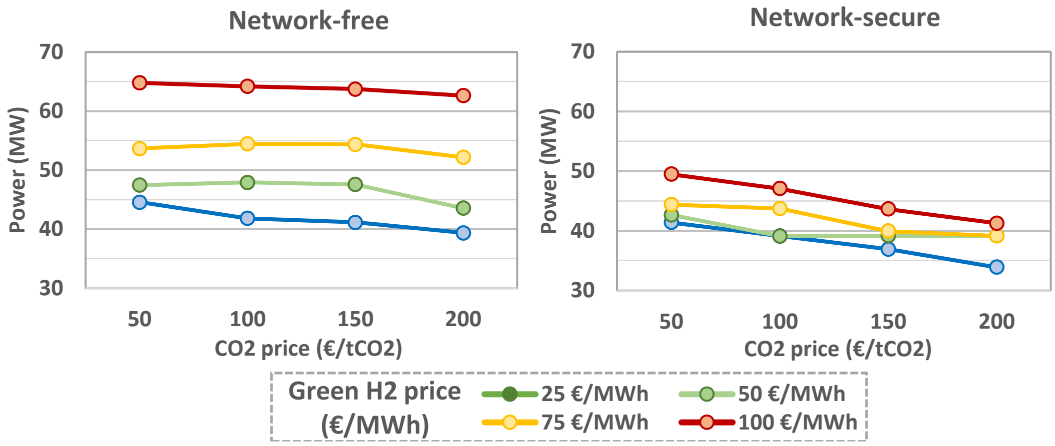

Figure 6.5 - Impacts of CO_2 and green hydrogen prices in the provision of secondary reserves.

Regarding the impact of the network-secure bidding optimization framework, the results show that it changed the aggregator's bids, in relation to the network-free bidding optimization framework. This means that network problems existed when using the network-free bidding optimization framework. In order to counteract those issues, the network-secure framework computed different bids. This is possible to see by analyzing the green hydrogen production and secondary reserve bids. The framework decreased these bids in order to avoid any electricity or gas network problems.

6.3. Decarbonization of energy systems through low-carbon scenarios

This section presents the analysis of four different LCSs related with scenarios of electrification of DMERs and energy vectors:

1. LCS 1 simulates the replacement of grid-connected CHPs with HPs (6.3.1);
2. LCS 2 simulates the replacement of GBs with HPs in buildings (6.3.2);
3. LCS 3 simulates the integration of ESSs in buildings (6.3.3);
4. LCS 4 simulates the replacement of internal combustion engine vehicles (ICEVs) with EVs (6.3.4).

In these four LCSs, it is assessed the environmental, economic, and technical impacts of the two aggregator's frameworks. These LCSs simulate the progressive decarbonization of different economic sectors, following different potential investment pathways defined by decision-makers, and are generally aligned with the European Union's vision and strategy for a carbon-free energy sector [13].

The case studies used in this section have some modifications in relation to the case study used in Chapter 4 and Chapter 5 presented in Annex A. The modifications are related with the installed capacity of CHPs, GBs, HPs, PVs, ESSs, and EVs. The rest of the data (i.e. market data, weather forecasts, network data, and other buildings' characteristics) are kept the same. Each study has its own modifications, and they are identified in each subsection. The installed capacity of PV systems was based on the aggregator's maximum hourly consumption, while the capacity of ESSs was based on the level of PV capacity.

It is important to note that the CO_2 emissions analyzed in the following studies consider the emissions from natural gas consumption and also from electricity consumption from the electricity network. The CO_2 emissions related with the electricity consumed from the network are presented in Annex A. It was assumed that EVs use 20 kWh of electricity for each 100 km and that ICEVs emit 130 g of CO_2 per km. The price of gasoline (without taxes) was set to 0.685 €/L and the consumption of gasoline was set to 6L/100km.

6.3.1. Low-carbon scenario 1: replacement of grid-connected combined heat and power with heat pumps

This LCS presents simulates the replacement of grid-connected CHPs with HPs under different PV penetration levels. There are several differences between these resources. CHPs consume natural gas and produce electricity and heat, while HPs consume electricity and produce heat. As such, CHPs need to be connected to the electricity, gas, and district heating networks, while HPs need to be connected to the electricity and district heating networks. Figure 6.6 illustrates the integration levels of CHPs, HPs and PVs considered in this scenario. The installed capacity of CHPs can be set to 0 or 10 MW, and the installed capacity of HPs can be set to 0 or 2 MW. The installed capacity of PVs varies between 0 and 4 MW. The installed capacity of GBs (in buildings) is 5.5 MW, HPs (in buildings) is 0 MW, ESSs is 0 MWh, and EVs is 1.2 MWh.

The following subsections present the technical, economic, and environmental analysis for this LCS.

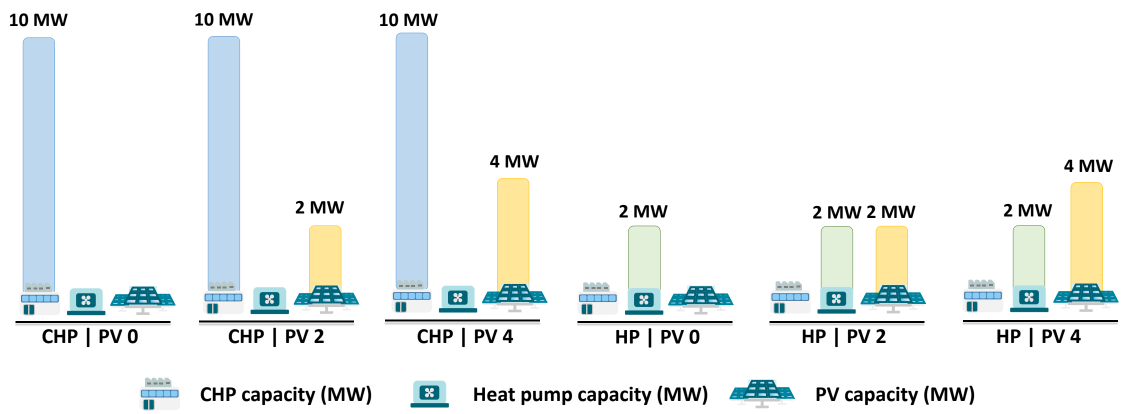

Figure 6.6 - Integration levels of combined heat and power, heat pumps, and PVs for low-carbon scenario 4.

6.3.1.1. Technical analysis

The network-secure framework optimizes multi-energy resources considering the constraints of the electricity, gas, and heat network. This ensures that the dispatch of the multi-energy resources is feasible from the perspective of the networks. On the other hand, the network-free framework does not factor in the constraints of the multi-energy networks, which may result in infeasible dispatch solutions. This difference impacts the economic and environmental performance of network-secure and network-free frameworks in all LCSs.

In this scenario, the network-free framework computes network-infeasible solutions in CHP|PV0, CHP|PV2, CHP|PV4, and HP|PV4 cases. In these cases, we observe violations in the electricity and heat networks caused by the energy services provided by grid-connected CHPs and PVs.

6.3.1.2. Economic analysis

The aggregator's costs for each integration case are illustrated in Figure 6.7. The results show that the network-free outperforms network-secure in almost all integration cases. This happens because network-free does not impose the constraints of multi-energy networks. As a result, the dispatch solutions of network-free are infeasible from the networks' perspective, as discussed before. The results also show that the impact of the network constraints varies according to the integration case. In other words, the cost difference between network-secure and network-free increases with the increase of the installed capacity of PV in both CHP and HP cases. This difference is more noticeable in the CHP case since network-secure reduces the energy services provided by CHPs and PVs to ensure network security.

Finally, the use of HPs increases the aggregator's costs as electricity is more expensive than natural gas in this test case. In the Iberian market, gas generators are typically price-makers, setting the price of electricity above the price of natural gas. The cost increase can reach up to 60% when CHP|PV4 and HP|PV4 are compared (going from 1015€ to 1623€) under the network-secure framework. On the other hand, the increase in PV capacity decreases the costs in both cases (up to 38%) since more electricity is generated locally instead of being bought at market price.

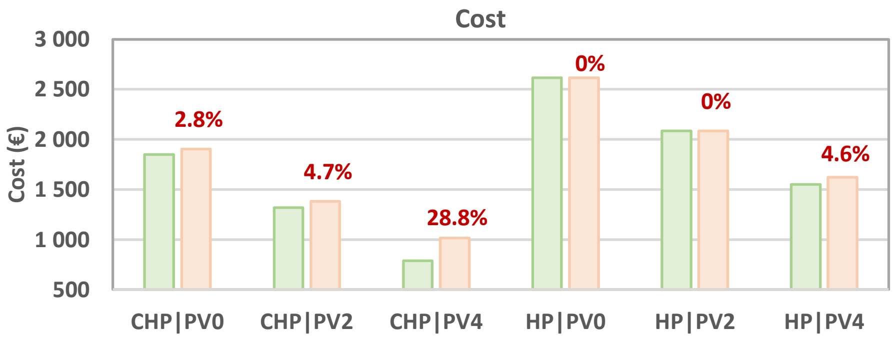

Figure 6.7 – Aggregator's cost in low-carbon scenario 1. The values in red represent the difference between the network-secure and network-free frameworks.

6.3.1.3. Environmental analysis

The CO_2 emissions of the aggregator for each integration case are illustrated in Figure 6.8. The network-secure framework presents lower emission results than the network-free framework in the four cases. In these cases, the network constraints make the network-secure framework decrease the gas consumption of CHPs and decrease the CO_2 emissions.

The results also show that CO_2 emissions are lower in the cases with HPs, as carbon emissions from natural gas consumed by CHPs are higher than the ones from electricity consumed by HPs. This decrease in CO_2 emissions can reach up to 23% when CHP|PV4 and HP|PV4 are compared (going from 32.3 to 25.1 tCO_2) under the network-secure framework. The CO_2 emissions also decrease with the increase of PV capacity, as more electricity is generated locally instead of consumed from the network. Note that a part of the electricity consumed from the network is generated by fossil fuel power plants. This decrease in CO_2 emissions can reach up to 18% when PV0 and PV4 are compared (going from 30.7 to 25.1 tCO_2) under the network-secure framework.

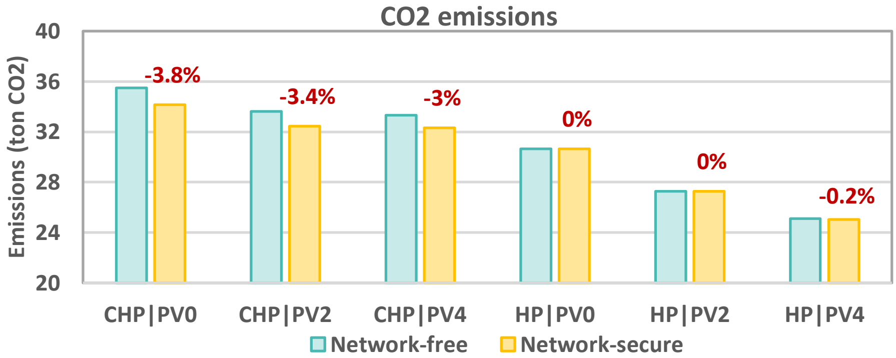

Figure 6.8 – CO_2 emissions in low-carbon scenario 1. The values in red represent the difference between the network-secure and network-free frameworks.

6.3.2. Low-carbon scenario 2: replacement of gas boilers with heat pumps in buildings

This study analyzes different LCSs by comparing the replacement of GBs with HPs in buildings, with different levels of PV penetration. To perform this study, different 6 different integration levels of GBs, HPs, and PVs were considered. Within these scenarios, the installed capacity of GBs can be 0 MW or 5.46 MW, of HPs can be 0 MW or 1.575 MW, and of PVs can be 0 MW, 2 MW or 4 MW. Figure 6.9 presents the integration level of GBs, HPs, and PVs. The installed capacity of district heating' CHPs is 0 MW, district heating HPs is 2 MW, ESSs is 0 MWh, and EVs is 1.2 MWh.

The following subsections present the technical, economic, and environmental analysis for this LCS.

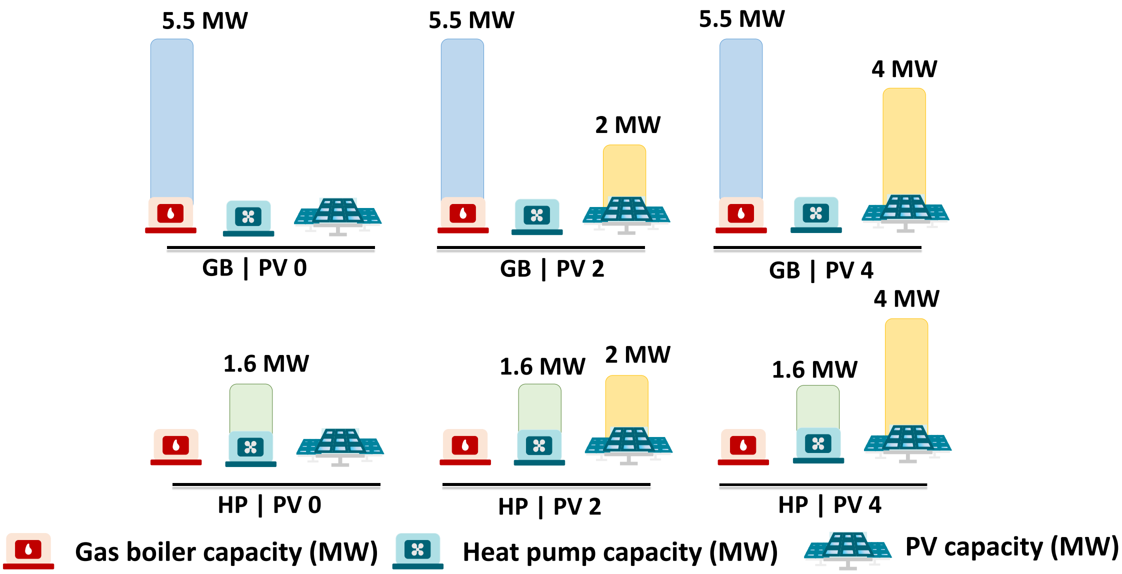

Figure 6.9 – Integration levels of gas boilers, heat pumps, and PVs for low-carbon scenario 2.

6.3.2.1. Technical analysis

The network-free framework computes network-infeasible solutions in GB|PV4 and HP|PV4 cases. In these cases, we observe violations in the electricity network caused by the electricity services provided by PVs.

6.3.2.2. Economic analysis

The costs of the aggregator for each integration case are illustrated in Figure 6.10. The costs of network-secure and network-free only differ in GB|PV4 and HP|PV4 since the network constraints are only active in these two scenarios.

The results also show that the cost increases with the installation of HPs since the electricity consumed by them is more expensive than the gas consumed by the GBs due to the reasons already explained. The cost increase can reach up to 8% when GB|PV4 and HP|PV4 are compared (going from 1623 to 1752€) under the network-secure framework. In addition, the cost also decreases with the increased installation of PVs since more electricity is generated and consumed locally. The decrease in costs can reach up to 37% when HP|PV0 and HP|PV4 are compared (going from 2770 to 1753 €) under the network-secure framework.

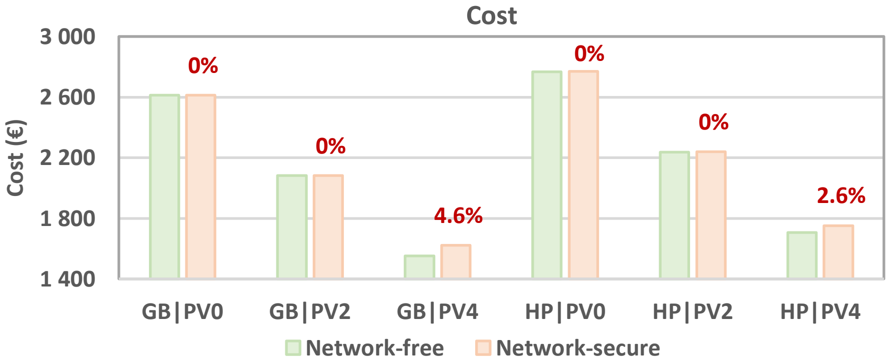

Figure 6.10 – Aggregator's cost in low-carbon scenario 2. The values in red represent the difference between the network-secure and network-free frameworks.

6.3.2.3. Environmental analysis

The CO_2 emissions of the aggregator for each integration case are illustrated in Figure 6.11. Network-secure presents higher emission results than network-free in the two cases since the active network constraints reduce the utilization of PVs.

The results also show that replacing GBs with HPs reduces CO_2 emissions since the gas consumed by the GBs emits more CO_2 than the electricity consumed by the HPs. The decrease in CO_2 emissions can reach up to 39% when GB|PV4 and HP|PV4 are compared (going from 25.1 to 15.4 tCO_2) under the network-secure framework. The case with the lowest CO_2 emissions is HP|PV4, which includes HPs with 4 MW of PVs distributed by the different buildings.

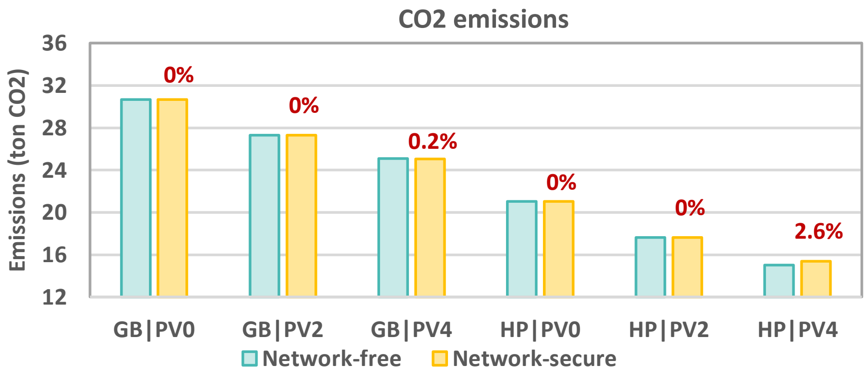

Figure 6.11 – CO_2 emissions in low-carbon scenario 2. The values in red represent the difference between the network-secure and network-free frameworks.

6.3.3. Low-carbon scenario 3: integration of energy storage systems in buildings

This study analyzes a LCS with different levels of PV penetration with and without storage. Different integration levels of ESSs and PVs were considered. The installed capacity of PV can be 0 MW, 2 MW, or 4MW. The installed capacity of ESSs is related with the installed capacity of PVs and can be 5 MWh or 10 MWh. Figure 6.12 presents the different integration levels of PVs and ESSs. The installed capacity of district heating' CHPs is 0 MW, district heating HPs is 2 MW, buildings' GBs is 0 MW, buildings' HPs is 1.575 MW, and EVs is 1.2 MWh.

The following subsections present the technical, economic, and environmental analysis for this LCS.

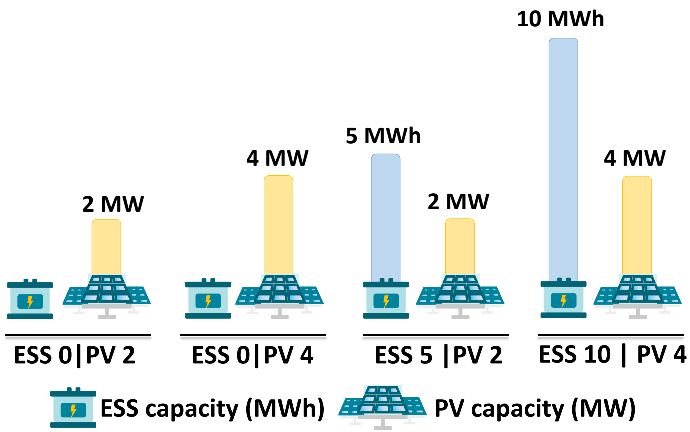

Figure 6.12 – Integration levels of energy storage systems and PVs for low-carbon scenario 3.

6.3.3.1. Technical analysis

Network-free computes network-infeasible solutions in ESS 0|PV4, ESS5|PV2, and ESS10|PV4 cases. In these cases, we observe violations in the electricity network caused by the electricity services provided by PVs and ESSs.

6.3.3.2. Economic analysis

The costs of the aggregator for each integration case are illustrated in Figure 6.13. The costs of network-secure and network-free differ in ESS 0|PV4, ESS5|PV2, and ESS10|PV4, due to the activation of the electricity network constraints.

The results show that the use of ESSs reduces costs since they increase the flexibility to provide services in multiple markets. The costs can decrease up to 31%, as ESS0|PV4 and ESS5|PV4 are compared (going from 1753 to 1215 €) under the network-secure framework.

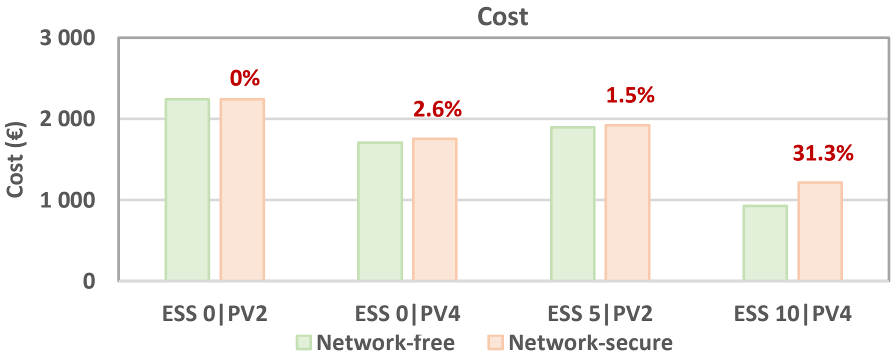

Figure 6.13 – Aggregator's costs in low-carbon scenario 3. The values in red represent the difference between the network-secure and network-free frameworks.

6.3.3.3. Environmental analysis

The CO_2 emissions of the aggregator for each integration case are illustrated in Figure 6.14. Network-secure presents lower emission results than network-free in the two cases with ESSs, because the electricity network constraints reduce the number of charging and discharging cycles of the ESSs, reducing ESS energy losses.

The results also show that the use of ESSs can increase CO_2 emissions. This can be observed if we compare ESS0|PV4 to ESS10|PV4, as emissions increase by 5% (going from 14.4 to 15.2 tCO_2) under the network-secure framework. The increase in CO_2 emissions is related to the fact that the ESSs end up consuming more electricity from the network, at less expensive hours, to store it and then sell it at more expensive hours. This happens because the optimization of the ESSs does not factor in the emission costs of the electricity consumed from the network.

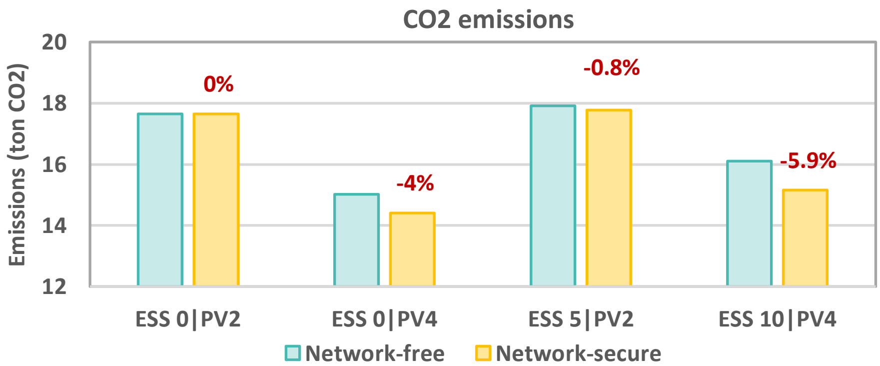

Figure 6.14 – CO_2 emissions in low-carbon scenario 3. The values in red represent the difference between the network-secure and network-free frameworks.

6.3.4. Low-carbon scenario 4: replacement of internal combustion engine vehicles with electric vehicles

This study analyzes a LCS with different levels of EVs' connections. To perform this study, different integration levels of EVs were considered. The installed capacity of EVs per scenario is presented in Figure 6.15 and varies between 1.2 and 3.5 MWh (or between 20 and 60 EVs). The installed capacity of district heating' CHPs is 0 MW, district heating HPs is 2 MW, buildings' GBs is 0 MW, buildings' HPs is 1.575 MW, PVs is 4 MW, and ESSs is 0 MWh.

The following subsections present the technical, economic, and environmental analysis for this LCS.

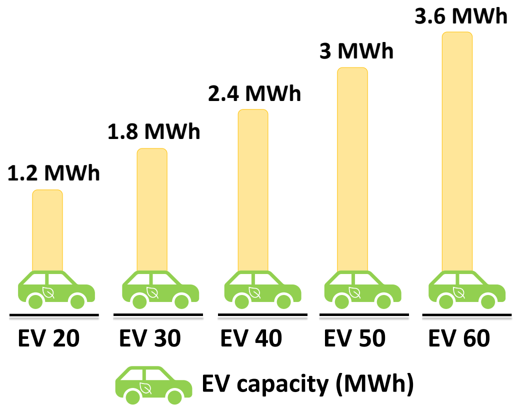

Figure 6.15 – Integration levels of electric vehicles (EV) for low-carbon scenario 4.

Table 6.2 – Integration levels of electric vehicles (EVs) and internal combustion engine vehicles (ICEVs) for low-carbon scenario 4, indicating capacity connected to the network and number of vehicles.

Integration levels	EV (MWh)	Number of EVs	Number of ICEVs
EV20	1.2	20	40
EV30	1.8	30	30
EV40	2.4	40	20
EV50	3	50	10
EV60	3.6	60	0

6.3.4.1. Technical analysis

The network-free framework computes network-infeasible solutions in all EV integration cases. We observe violations in the electricity network caused by the electricity services provided by EVs.

6.3.4.2. Economic analysis

The costs of the aggregator for each integration case are illustrated in Figure 6.16. This LCS considers the costs of buying gasoline for the ICEVs. The costs of network-secure and network-free differ in all integration cases since the electricity network constraints are active in all cases to avoid electricity network violations.

The costs of the aggregator decrease, when the number of EVs increase and the number of ICEVs decrease, because it is more expensive to buy gasoline than electricity in the Iberian market. The costs reduce up to 7% (going from 1896 to 1756 €) when EV20 and EV60 are compared under the network-secure framework.

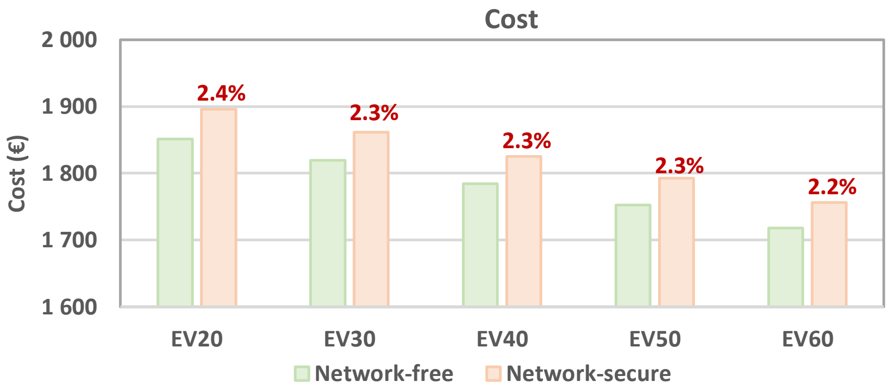

Figure 6.16 – Aggregator's costs in low-carbon scenario 4. The values in red represent the difference between the network-secure and network-free frameworks.

6.3.4.3. Environmental analysis

The CO_2 emissions of the aggregator for each integration case are illustrated in Figure 6.17. Network-secure presents lower emission results than network-free in all cases since it limits the number of charging and discharging cycles of the EVs, reducing energy losses and their associated emissions.

The results also show that the replacement of ICEVs with EVs reduces CO_2 emissions. However, the reduction is not very significant (up to 4.2%) since the electricity consumed by EVs is partially generated by fossil power plants in this test case. In the future, the electricity consumed by EVs is expected to be generated only by carbon-free power plants, which will contribute to further reducing the operating emissions of EVs.

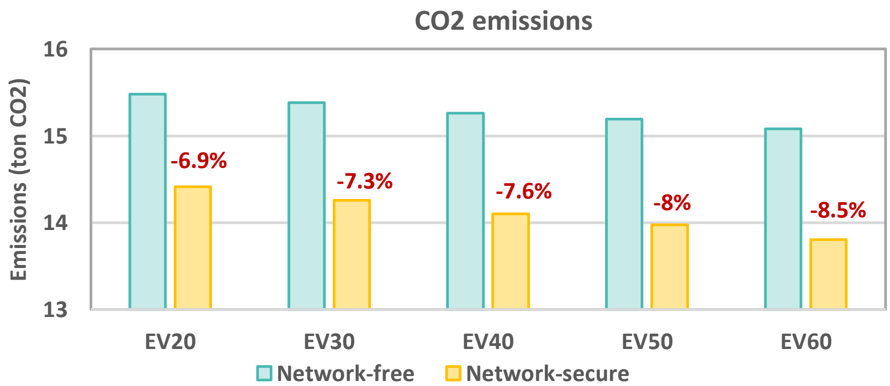

Figure 6.17 – CO_2 emissions in low-carbon scenario 4. The values in red represent the difference between the network-secure and network-free frameworks.

6.4. Conclusions

This chapter studies the economic and environmental impacts of the participation of the aggregator in multi-energy markets. The chapter is divided into two main sections. The first section focuses on the analysis of decarbonization policies. The second section focuses on the analysis of LCSs. The studies presented in this chapter use the network-free and network-secure frameworks described in the previous chapters.

A. Decarbonization policies

From the analysis of the decarbonization policies, several conclusions can be drawn from these case studies:

- Increasing the CO2 prices (from 0 to 25€/tCO2) rises the aggregator's costs. These costs can increase up to 163%. On the other hand, increasing the CO2 prices did not have the same impact on the energy and band bids of CHPs as they only changed up to 6%;
- To have a significant impact on the bidding behavior of the CHPs and respective CO2 emissions, the price would have to increase to more than 400€/tCO2. In this case, CHPs' upward band decreased from 14 MW to 5 MW (-64%) clearly reflecting the impact of CO2 prices;
- It is also possible to conclude that carbon markets may have a negative impact on the provision of secondary reserve since the band bids offered by the aggregator decreased with higher prices. This only occurs if the DMERs used for providing these reserves are affected by the carbon market. Nonetheless, the increase in CO2 prices will increase the economic pressure on aggregators with natural gas resources like CHPs, incentivizing them to replace these technologies with other electricity-powered technologies, like heat pumps;
- Both CO2 emissions and green hydrogen prices impact the production of green hydrogen, natural gas consumption, and CO2 emissions of the DMERs managed by the aggregator;
- The increase in green hydrogen prices increases the injection of green hydrogen into the gas network and consequently reduces the need to consume natural gas. Nonetheless, injecting green hydrogen into the gas network is only attractive when green hydrogen prices are higher;
- A market with high prices of CO2 allowances and green hydrogen can contribute to significantly reducing the consumption of natural gas and emitted CO2;
- The provision of secondary reserves by the aggregator increases with the increase of green hydrogen prices and the reduction of CO2 prices. This way, high green hydrogen prices make hydrogen technologies attractive to provide energy and secondary reserve services;

In sum, high CO_2 prices discourage the utilization of technologies powered by natural gas to provide secondary reserves. On the other hand, high green hydrogen prices may attract other technologies to provide this essential power system service.

B. Low-carbon scenarios

Regarding the studies of the LCSs, it was seen that they result in different economic, environmental, and technical impacts for the aggregator. These impacts are discussed next.

a. LCS 1: replacement of grid-connected CHPs with HPs

The replacement of grid-connected CHPs with HPs increased the operating costs (up to 60%) since the price of electricity is higher than the price of natural gas in the Iberian market. In the Iberian market, gas generators are typically price-makers, setting the price of electricity above the price of natural gas. On the other hand, this replacement reduced the CO_2 emissions (up to 23%) since the gas consumed by CHPs emits more CO_2 than the electricity consumed by HPs.

Network-secure computed network-feasible solutions, while network-free does not. We observed electricity and heat network violations in 4 of the 6 cases analyzed. In these cases, network-secure decreased the natural gas consumption of CHPs, decreasing the CO_2 emissions in comparison to network-free. However, this increased the costs.

In addition, the integration of PVs reduced the costs (up to 38%) since the electricity generated has a zero marginal price. This also decreased CO_2 emissions (up to 18%).

b. LCS 2: replacement of GBs with HPs in buildings

The replacement GBs with HPs in buildings increased the operating costs (up to 8%) since electricity is more expensive than natural gas in the Iberian market. On the other hand, it reduced CO_2 emissions (up to 39%).

Network-free computed network-infeasible solutions in 2 of the 6 cases analyzed. In these two cases, the operation of the PVs caused electricity network violations. As a result, the costs under network-secure increased in these two cases. The emissions also increased since the network constraints imposed by network-secure reduced the utilization of PVs.

c. LCS 3: integration of ESSs in buildings

The integration of ESSs in buildings reduced the cost of the aggregator (up to 31%) since they are used to provide valuable services. On the other hand, the CO_2 emissions increased (up to 5%), because ESSs increased the energy losses in energy arbitrage services. Note that we did not factor in the emission costs of the electricity consumed from the network in the optimization problems.

Network-free computed network-infeasible solutions in 3 of the 4 cases analyzed (2 of the 3 infeasible cases have ESSs). In the 2 ESS cases, the optimization of the ESSs caused electricity network violations. As a result, the costs increased under network-secure to avoid such violations. On the other hand, the emissions decreased as the electricity network constraints reduced the number of charging and discharging cycles of the ESSs and consequently associated energy losses.

d. LCS 4: replacement of ICEVs with EVs

The replacement of ICEVs with EVs reduced the costs (up to 7%) and the CO_2 emissions (up to 4.2%) of the aggregator since the cost of optimizing EVs is lower than the cost of gasoline and the generation of electricity emits less CO_2 than the consumption of gasoline.

Network-free computed network-infeasible solutions in all integration cases. We observed violations in the electricity network caused by the services provided by EVs. To avoid these problems, network-secure constrained the optimization of EVs, reducing the value of the services and increasing the costs of the aggregator. On the other hand, the CO_2 emissions decreased under network-secure, due to the reduction of the charging and discharging cycles of the EVs.

e. Final remarks

The network-secure framework computes network-secure solutions, while network-free does not. This impacts the economic and environmental outputs of the aggregator. In most scenarios, the network-secure framework will increase the costs of the aggregator, when electricity, gas, or heat network constraints are enforced. On the other hand, the CO_2 emissions may increase or decrease, depending on how the network constraints impact the operation of the aggregator.

The following chapter presents the main conclusions of this thesis.

Chapter 7
Conclusion

This chapter presents a summary of the main contributions and findings of this thesis. Furthermore, future perspectives are identified related with further enhancements of the tools developed in this work.

7.1. Main Contributions

The work developed in this thesis addresses an important research gap present in the literature. This gap is related with a lack of optimization tools to allow the secure participation of aggregators of multi-energy systems in multi-energy markets, including in the day-ahead and real-time stages. This is an important subject for the future of energy systems as with the increasing integration of renewable energy sources, new flexibility sources must be exploited. Aggregators can help mitigate these effects as they can provide flexibility services to assist DSOs and TSOs in the secure management of the energy system. This, in turn, can help accelerate the integration of RES and consequently, the decarbonization of the energy system.

The first contribution is the development of an aggregator's framework. This new framework has several new features in relation to the frameworks presented in the literature:

- Enables the participation of aggregators in **multi-energy markets**, including the electricity (energy and secondary reserves), natural gas, green hydrogen, and carbon markets. This framework identifies all the necessary interactions between the aggregator and the different market operators and other market participants;
- Enables the **network-secure** participation of aggregators in multi-energy markets by negotiating network-secure day-ahead bids and real-time realizations between aggregators and multi-energy DSOs The DSOs considered in this framework are the electricity, gas, and heat DSOs. This enables the consideration of the electricity, gas, and heat network constraints in the optimization process. This framework identifies all the necessary interactions and computational processes between the aggregator and the different DSOs;
- Preserves the **independent roles** and **data privacy** of aggregator's clients and DSOs;
- Characterizes the different **distributed multi-energy resources** owned by prosumers. This framework identifies the flexibility services that each DMER is able to offer as well as the necessary interactions with prosumers. The DMERs include HPs, EVs, PVs, ESSs, CHPs, P2G, FCs, and HSSs.

The second contribution is an optimization tool to support the network-secure participation of aggregators of prosumers in day-ahead multi-energy markets. The main features of this tool are the following:

- It supports the participation of an aggregator of multi-energy systems in day-ahead electricity (energy and secondary reserve), natural gas, green hydrogen, and carbon markets;

- It computes multi-energy (electricity, natural gas, green hydrogen, and CO2) bids considering the constraints of electricity, gas, and heat networks. This decreases the risk of the aggregator violating the constraints of the multi-energy networks in real-time, reducing consequently possible energy imbalances and reserve shortages due to network violations;

- It exploits distributed optimization (i.e. ADMM) to preserve the independent roles of energy operators and the data privacy of the aggregator's clients and DSOs. In addition, it makes it possible to solve a complex problem (i.e., a mixed-integer nonlinear problem) in a time-effective manner by decomposing the original problem into smaller sub-problems (e.g., smaller mixed-inter linear problems and nonlinear problems);

- It provides better economic results in relation to other state-of-the-art frameworks and the computational time required by this tool is well suited for the timelines of the electricity, gas, and carbon markets. This is proven by the results obtained.

The third contribution is a hierarchical model predictive control tool to support aggregators in the delivery of network-secure multi-energy services traded in the day-ahead markets. The main features of this tool are the following:

- Ensures that aggregators deliver cost-effectively and safely the multi-energy services traded in day-ahead electricity, gas, green hydrogen, and carbon markets;

- The MPC tool uses the ADMM on a rolling horizon to negotiate the network-secure delivery of multi-energy services between aggregators and multi-energy DSOs. The multi-energy services include electricity (energy and reserves), natural gas, green hydrogen, and carbon allowances, which result from the real-time optimization of the multi-energy resources managed by aggregators;

- It considers the non-convex constraints of electricity, gas (with blending of natural gas and hydrogen), and heat networks. This way, the delivery of multi-energy services does not incur in the violation of networks' constraints and, consequently, it avoids economic penalties for the aggregator for not delivering those multi-energy services.

The fourth contribution is an estimation of the economic impact for an aggregator from using network-secure frameworks over network-free frameworks during the entire cycle of multi-energy market participation, i.e. from day-ahead to real-time. This way, this work provides clear evidence of the effectiveness of the proposed approaches.

This fifth contribution is a discussion about the economic and environmental impacts of different decarbonization policies and scenarios. The decarbonization policies include the consideration of different carbon and green hydrogen prices. The low-carbon scenarios included different levels of electrification of energy vectors considering different installation capacity levels of HPs, PVs, ESSs, and EVs.

In conclusion, the work developed in this thesis helped improve the knowledge about the participation of aggregators in multi-energy markets. It provided new tools and studies that can enhance the development of aggregators and consequently, enhance the active participation of prosumers in the energy sector. It is also important to note that the frameworks developed can be integrated into the actual Iberian transmission system operator coordination scheme and adopted in most of the electricity market frameworks worldwide.

7.2. Main Findings

The analysis of the day-ahead and real-time frameworks allowed me to derive different findings.

Firstly, by analyzing the day-ahead framework, the following conclusions were drawn:

- **Network-free frameworks –** when the aggregator uses the network-free strategies, different network problems occurred in the electricity, heat, and gas networks. The electricity network problems were related with voltages, the heat network problems were related with mass flows, and the gas network problems were related with the higher heating values and the Wobbe index of the gases.

- **Network-secure frameworks –** the network-secure strategy computes bids within the network limits, i.e., network-secure bids. This way, they avoid network problems that could have occurred. This would also avoid the situation of significantly increasing the aggregator's costs in real-time in case of network violations, as he would not be able to deliver the services offered in the day-ahead markets.

- **Economic results -** the aggregator's costs of trading energy, gas, green hydrogen, guarantees of origin, and carbon allowances decreased in the order of 7% when considering a strategy that jointly optimizes multi-energy systems. This allows us to conclude that a multi-energy aggregator exploits better the flexibility of DMERs than single-energy aggregators.

- **Execution times -** the execution time of the network-secure strategy, although slower than the other strategies studied, is well suited for the timelines of the electricity, gas, green hydrogen, and carbon markets. This indicates that the newly developed strategy can be applied in the real world.

Secondly, by analyzing the real-time framework, the following conclusions were derived:

- **Real-time network-secure framework -** Network security is only ensured when the constraints of the multi-energy networks are considered in the real-time optimization problem (i.e., in the hierarchical MPC). This means that considering the network constraints only in the day-ahead bidding problem does not necessarily guarantee network security;
- **Network-secure frameworks in the day-ahead stage –** if a network-secure framework is used in the real-time stage, considering multi-energy network constraints at the day-ahead stage reduces the number of imbalances and the number of network violations in real-time;

- Considering multi-energy network constraints at both day-ahead and real-time optimization stages produces the most cost-effective and reliable solution for aggregators since it minimizes settlement net-costs while ensuring multi-energy network security.

Thirdly, from the analysis of the decarbonization policies, several conclusions were made:

- **Environmental -** Both CO2 emissions and green hydrogen prices impact CO2 emissions of the DMERs managed by the aggregator. A market with high prices of CO2 allowances and green hydrogen can contribute to significantly reducing the consumption of natural gas and emitted CO2;

- **Economic -** Increasing the CO2 prices (from 0 to 25€/tCO2) rises the aggregator's costs. These costs can increase up to 163%;

- **Energy:**

  - To have a significant impact on the bidding behavior of the CHPs, the price would have to increase to more than 400€/tCO_2. In this case, CHPs' upward band decreased from 14 MW to 5 MW (-64%) clearly reflecting the impact of CO_2 prices;
  - Both CO_2 emissions and green hydrogen prices impact the production of natural gas consumption. The increase in green hydrogen prices increases the injection of green hydrogen into the gas network and consequently reduces the need to consume natural gas. Nonetheless, injecting green hydrogen into the gas network is only attractive when green hydrogen prices are high;

- **Secondary reserves:**

  - Carbon markets may have a negative impact on the provision of secondary reserve since the band bids offered by the aggregator decreased with higher prices (e.g. 400€/tCO2). This only occurs if the DMERs used for providing these reserves are affected by the carbon market. Nonetheless, the increase in CO2 prices will increase the economic pressure on aggregators with natural gas resources like CHPs, incentivizing them to replace these technologies with other electricity-powered technologies, like heat pumps;
  - The provision of secondary reserves by the aggregator increases with the increase of green hydrogen prices and the reduction of CO2 prices. This way, high green hydrogen prices make hydrogen technologies attractive to provide energy and secondary reserve services;

In sum, high CO_2 prices discourage the utilization of technologies powered by natural gas to provide secondary reserves. On the other hand, high green hydrogen prices may attract other technologies to provide this essential power system service.

Fourth, regarding the studies of the electrification scenarios, the following conclusions were made:

- **Environmental:**

  - CO_2 emissions decrease in the scenarios with HPs installed instead of CHPs in the district heating. This decrease in CO_2 emissions can reach up to 23%;
  - Increasing the installed capacity of HPs and PVs in buildings decreases CO_2 emissions. HPs have more influence in the decrease in CO_2 emissions than PVs. The decrease in CO_2 emissions by increasing the installed capacity of HPs can reach up to 39%;
  - The use of ESSs increases CO_2 emissions. This happens because the aggregator does not have an economic signal that represents the CO_2 emissions from the electricity consumed from the network. As its optimization is only based on costs, the aggregator is not able to take those emissions into consideration. The increase in CO_2 emissions can reach up to 7%;
  - The replacement of ICEVs with EVs reduced CO_2 emissions (up to 4.2%). Nonetheless, in the future, the electricity consumed by EVs is expected to be generated only by carbon-free power plants, which will contribute to further reducing the operating emissions of EVs.
- **Economic:**
  - The use of HPs instead of CHPs increases aggregators' costs, as electricity is more expensive than natural gas. This increase in costs can reach up to 60%;
  - Aggregator's costs increase with the installation of HPs and decrease with the installation of PVs. This increase can reach up to 8%. The decrease in the aggregator's costs with the installation of PVs can reach up to 37%;
  - The use of ESSs reduces aggregator's costs by up to 31%;
  - By increasing the number of EVs, the costs decrease (up to 7%).

Fifth, when comparing the network-free and network-secure bidding optimization frameworks it was possible to conclude the following:

- The network-secure bidding optimization frameworks increase aggregator's costs in relation to the network-free bidding optimization frameworks as they avoid network problems. This also impacts CO_2 emissions, which usually end up decreasing as the consumption of electricity or natural gas decreases;
- The use of CHPs can cause network problems when using network-free frameworks due to the injection of electricity into the network. Network problems can also occur in scenarios with high penetration of PVs. On the other hand, no problems occurred when using the network-secure framework;
- ESSs can also provoke network violations when using the network-free framework in cases with high injection of electricity into the network;

7.3. Future Perspetives

During the course of the present work, several issues and new ideas not fully addressed in this thesis have arisen. Considering the time constraints, the options made were based on the idea of following the main initial concepts. To further investigate the participation of aggregators in multi-energy markets, the following suggestions for future work are made:

- **Aggregator as price maker –** the aggregator was assumed as a price taker in this thesis. This is a usual assumption in the literature as the aggregator usually does not have control over sufficient resources to have an impact on energy markets. Nonetheless, with the advent of aggregators and the importance given to the demand side and prosumers in the previous years, it is foreseen that the aggregators' portfolio may be extensive enough to impact energy markets. This way, it may be important to consider aggregators as price makers. The day-ahead bidding optimization framework in this thesis should be modified in order to consider this new feature;
- **Modeling uncertainty through stochastic approaches –** the impact of uncertainty in the economic, network, and computational performances of day-ahead and real-time optimization frameworks should also be studied. Modeling uncertainty through stochastic optimization may reduce the settlement cost of the multi-energy aggregator (by 2-3% in [148][154]), but it may also increase the execution time beyond suitable values;
- **Comparison with other distributed methods –** this thesis uses the ADMM model to decompose the mathematical problem. Nonetheless, there are other methods, like sub-gradient methods. This way, a comparison with other distributed methods could provide more insights about the effect of applying distributed methods to the aggregator's problem;
- **Planning of energy systems –** the day-ahead and real-time optimization frameworks can be used in planning tools of energy systems. Usually, planning tools consider two-stage frameworks where one of the stages considers the operation of resources. A new planning tool could be developed where it considers the frameworks developed in this thesis. This way, the benefits of using those frameworks could be incorporated into the planning tool.

Annex A
Case study

This annex presents the case study used to evaluate the strategies presented in Chapter 4 and Chapter 5. It presents the network, DMERs, buildings, market, weather, and inflexible load data.

The data of the case study are divided into static data and variable data. Table A.1 presents the data for the DA and RT stages. The variable data can assume the form of point forecasts or actual values. Both DA and RT optimization frameworks use the same static data that includes network, DMERs, and buildings' characteristics.

The DA and RT phases use variable data consisting of point forecasts of inflexible loads (electricity, natural gas, heat, and hydrogen), weather data (temperature and PV generation), availability and SOC requisites of EVs, and market data. The market data point forecasts differ for each phase:

- In the DA stage, the aggregator forecasts electricity, secondary band, tertiary reserve, natural gas, green hydrogen, CO2, water, oxygen, and GO prices and secondary reserve mobilization ratios;
- In the RT phase, the aggregator forecasts electricity imbalance prices and updates the forecast of tertiary reserve, natural gas, green hydrogen, CO2, water, oxygen, and GO prices and secondary reserve mobilization ratios.

In the RT phase, the aggregator also uses actual values of the activated reserve (AGC signal).

The settlement phase uses variable data consisting of actual values of inflexible loads, weather data (temperature and PV generation), availability and SOC requisites of EVs, and market data (electricity energy, secondary band, tertiary reserve, electricity imbalance, natural gas, green hydrogen, CO_2, water, oxygen, and GO prices and secondary reserve mobilization ratios).

Table A.1 - Fixed and variable data of the day-ahead stages.

	Day-ahead	
Fixed		Network DMERs Buildings characteristics
Variable	**Point forecasts**	Inflexible loads: • Electricity • Natural gas • Heat • Hydrogen Weather data: • Temperature • PV generation Availability and SOC of EVs Market data: • Electricity, secondary band, tertiary reserve, natural gas, green hydrogen, CO_2, water, oxygen, and GO prices Secondary reserve mobilization ratios
	Updated point forecasts	-
	Actual values	-

Table A.2 - Fixed and variable data of the real-time stages.

	Real-time	
Fixed		Network DMERs Buildings characteristics
Variable	**Point forecasts**	Market data: Imbalance prices
	Updated point forecasts	Inflexible loads: • Electricity • Natural gas • Heat • Hydrogen Weather data: • Temperature • PV generation Availability and SOC of EVs Market data: • Tertiary reserve, natural gas, green hydrogen, CO_2, water, oxygen, and GO prices Secondary reserve mobilization ratios
	Actual values	Reserve activation (AGC)

A.1. Network data

The microgrid from the University of Manchester [175] was used, due to the unavailability of a suitable test case in the Iberian peninsula. The microgrid is characterized by electricity, gas, and heat networks, as illustrated in Figure A.1.

The data of the electricity, gas, and heat networks was sourced from [175] and includes the parameters of the networks. Table A.3 presents the electricity network data indicating the resistance R and capacitance C of the lines. Table A.4 presents the length L and diameter d of the gas pipes. Table 3 presents the length, diameter, and heat transfer coefficient of the district heating pipes. All the data described here is static.

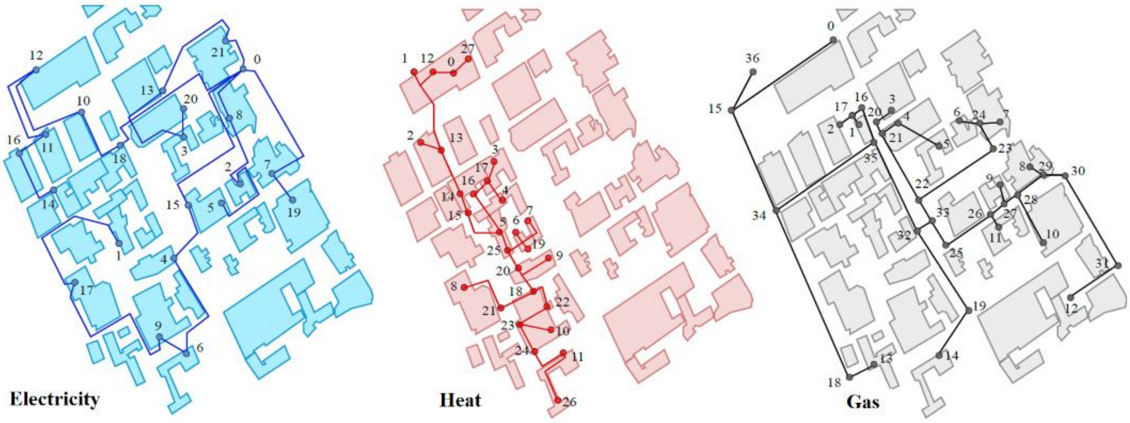

Figure A.1 - Electricity, heat, and gas networks of the study case [175].

Regarding the electricity network, the bounds of the voltages v were fixed at 0.95 and 1.05 p.u., and the voltage in the slack bus 0 was fixed at 1 p.u.. Concerning the heat network, the mass flow limit $\overline{m^a}$ was set at 40 kg/s, the supply temperature θ^S of generators was defined as 85 °C, the outlet temperature θ^R of each load was set at 70 °C and the ambient temperature of the ground θ^{Amb} was defined as 7 °C. At last, it was considered the following gas network parameters: WI bounds of [45.7, 55.9] MJ/m^3 [179]; HHV bounds of [35.5, 47.8] MJ/m^3 [179]; network pressure p^G of 2 bar.

Table A.3 - Electricity network data.

From	To	R (p.u.)	X (p.u.)
22	0	1.8762	2.5212
0	21	1.8762	2.5212
21	13	4.0639	5.4609
13	3	4.0771	5.4787
3	20	0.671	0.9017
0	18	5.1115	6.8685
18	10	2.0305	2.7285
10	12	4.1756	5.6109
12	11	2.7078	3.6386
11	16	0.6274	0.843
16	14	2.1157	2.843
0	15	5.6184	7.5497

15	**4**	2.4066	3.2339
4	**6**	3.54009	4.758
6	**9**	1.3649	1.8341
9	**17**	4.6369	6.2309
17	**1**	4.1682	5.6011
0	**8**	2.0804	2.7956
8	**2**	2.3038	3.0957
2	**5**	2.5241	3.3918
0	**7**	4.6178	6.2052
7	**19**	1.0629	1.4282

Table A.4 - Gas network data.

From	To	Length (m)	Diameter (mm)
0	**15**	240	100
15	**34**	220	100
34	**18**	320	100
18	**13**	90	100
34	**35**	260	100
35	**16**	90	100
16	**17**	20	100
17	**1**	20	500
17	**2**	80	100
35	**32**	160	500
32	**33**	20	500
32	**19**	180	500
19	**14**	110	500
33	**22**	20	500
22	**21**	150	100
21	**4**	30	100
4	**5**	90	100
21	**20**	20	100
20	**3**	20	100
22	**23**	200	100
23	**24**	60	100
24	**6**	20	100
24	**7**	20	500
33	**25**	90	100
25	**26**	130	100
26	**11**	20	500
26	**27**	40	100
27	**9**	20	100
27	**28**	40	100
28	**10**	100	100
28	**29**	40	100
29	**8**	20	100
29	**30**	20	100

30	**31**	200	100
31	**12**	110	100
15	**36**	100	100

Table A.5 - District heating network data.

From	To	Length (m)	Diameter (mm)	Heat transfer coefficient (W/C)
0	**12**	40	219.1	0.455
12	**1**	20	168.3	0.467
12	**13**	70	219.1	0.455
13	**2**	20	139.7	0.367
13	**14**	70	219.1	0.455
14	**15**	70	219.1	0.455
15	**5**	130	219.1	0.455
5	**25**	30	168.3	0.367
5	**16**	80	114.3	0.321
16	**17**	40	76.1	0.278
17	**4**	20	48.3	0.219
17	**3**	40	88.9	0.327
25	**19**	20	60.3	0.236
19	**6**	10	48.3	0.219
19	**7**	30	60.3	0.236
20	**25**	20	168.3	0.367
20	**9**	20	168.3	0.367
18	**20**	40	168.3	0.367
22	**18**	20	168.3	0.367
18	**21**	40	88.9	0.327
21	**8**	40	88.9	0.327
23	**22**	20	168.3	0.367
24	**23**	20	219.1	0.455
23	**10**	40	88.9	0.327
11	**24**	100	219.1	0.455
27	**0**	10	219.1	0.455
26	**11**	10	219.1	0.455

A.2. DMER data

The DMERs can be connected to the electricity, gas, and heat networks. The DMERs connected to the electricity network are HPs, PV systems, ESSs, EVs, CHPs, a P2G, and a FC. The CHPs are also connected to the gas and heat networks, while the P2G and FC are connected to the gas network. The district heating flexible loads are connected to the heat network.

The HPs are connected to the electricity nodes 2, 5, 15, 19 and 20 and buildings 8, 11, 22, 34 and 39. Its parameters are 3.45 of COP η^{HP}, and 750 kW of maximum electric power $\overline{P^{HP}}$.

The PV systems are connected to the electricity nodes 14, 19 and 20 and buildings 3, 7, 12, 14, 24 and 34. The peak power $\overline{P^{PV}}$ of the PV systems ranges from 750 to 1500 kW.

The ESSs are connected to the electricity nodes 5, 9, 15, 18 and 20 and buildings 4, 8, 11, 12, 14, 19, 24, 31, 33 and 34. The parameters of the ESSs are 250 kWh of capacity $\overline{SOC^{Sto,E}}$, 0.9 of efficiency $\eta^{Sto,E}$, and 100 kW of maximum power for charging $\overline{P^{Sto,E,+}}$ and discharging $\overline{P^{Sto,E,-}}$. Their initial SOC $SOC_0^{Sto,E}$ was set to 100 kWh.

The CHPs are connected to the electricity nodes 6 and 12, gas nodes 0 and 14 and heat nodes 26 and 27. The parameters of the CHPs are 10 MW of maximum gas power $P^{CHP,G}$, 0.35 of electricity efficiency $\eta^{CHP,E}$, 0.45 of heat efficiency $\eta^{CHP,H}$, and 1/3 of ramp rate μ^{CHP}.

The district heating flexible loads are connected to the heat nodes 2, 5 and 22 and buildings 2, 13, 15, 25 and 32. The only parameter of the district heating flexible loads is 750 kW of maximum heating power $\overline{P^{DH}}$.

In addition to the mentioned DMERs, a green hydrogen hub is connected to electricity and gas networks at nodes 12 and 0, respectively. The green hydrogen hub has 1 P2G, 1 FC, 1 HSS, 1 fuel station, and 1 PV.

The parameters of the hydrogen technologies are the following: a P2G with a maximum power $\overline{P^{P2G,E}}$ of 1500 kW and an efficiency η^{P2G} of 0.6; HSS with a maximum power $\overline{P^{Sto,H_2}}$ of 1000 kW, a minimum capacity $\underline{SOC^{Sto,H_2}}$of 400 kWh, a maximum capacity $\overline{SOC^{Sto,H_2}}$ of 3200 kWh, and an initial SOC SOC_0^{Sto,H_2} of 1100 kWh; a FC with a maximum power $\overline{P^{FC,H_2}}$ of 250 kW, and an efficiency η^{FC} of 0.6; a fuel station with daily consumption $P^{HV}$of 6000 kg of hydrogen.

Table A.6 presents the main DMERs characteristics. All the data described in here is static.

Table A.6 – DMERs characteristics.

Resource	Efficiency	COP	Maximum power (kW)	Capacity (kWh)	Discharging rate (%)
PV	-	-	750-1500	-	-
ESS	0.9	-	100	250	-
HP	-	3.45	750	-	-
CHP	0.45 (heat) 0.35 (electricity)	-	10 000		-
DH flexible loads	-	-	750	-	-
P2G	0.6	-	1500	-	-
HSS	0.95	-	1 000	3 200	0.02
FC	0.6	-	250	-	-

A.2.1. Electric vehicles

The EVs parameters can be static or variable. The static parameters include the capacity, efficiency, and maximum power for charging and discharging of each EV. The variable parameters include the time of arrival and departure and the SOC at the time of arrival and departure of each EV. They are presented in the form of point forecasts, used in the DA stage, and actual values, used in the RT phase.

There are a total of 20 parking spots for EVs installed in buildings 4 and 11. It was assumed 4 types of EVs, each one with different capacities $\overline{SOC^{EV,E}}$: there are 4 EVs of type 1 (82 kWh), 4 EVs of type 2 (59 kWh), 6 EVs of type 3 (52 kWh), and 6 EVs of type 4 (50 kWh). All EVs have an efficiency η^{EV} of 0.9, and 7 kW of maximum power for charging $\overline{P^{EV,+}}$ and discharging $\overline{P^{EV,-}}$. Table A.7 presents the main EVs characteristics.

Table A.7 – EVs characteristics.

<table>
<tr><th>EV type</th><th>Number of vehicles</th><th>Capacity (kWh)</th><th>Maximum power (kW)</th><th>Efficiency</th></tr>
<tr><td>1</td><td>4</td><td>82</td><td rowspan="4">7</td><td rowspan="4">0.9</td></tr>
<tr><td>2</td><td>4</td><td>59</td></tr>
<tr><td>3</td><td>6</td><td>52</td></tr>
<tr><td>4</td><td>6</td><td>50</td></tr>
</table>

The time of arrival t^{AR} and departure t^{DE} and SOC at time of arrival $SOC^{EV,AR}$ and departure $SOC^{EV,DE}$ of each EV assume the form of point forecasts (DA stage) and actual values (RT stage). The point forecasts were computed using a seasonal naïve forecasting algorithm. Figure A.2 presents the forecasted and actual values for the availability of all EVs, indicating the time of arrival and departure. Figure A.3 presents the forecasted and actual values of EVs requirements for the SOC at time of arrival and departure. Figure A.4 presents the forecasted and actual values of time of arrival and departure and respective SOC requirements for one EV.

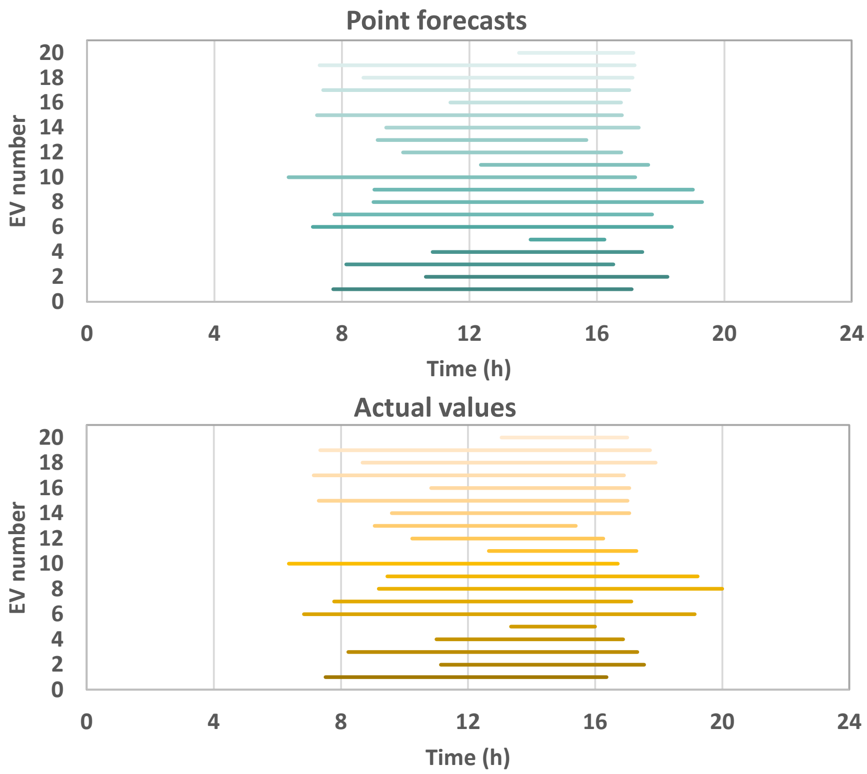

Figure A.2 – Availability of EVs.

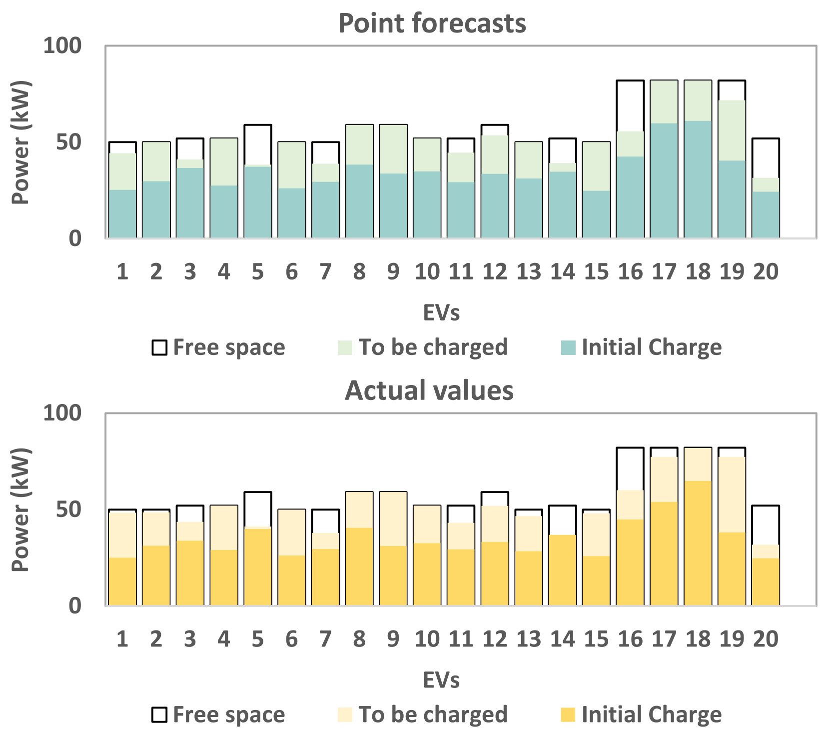

Figure A.3 – EVs initial and final capacity requirements. SOC at the time of arrival is represented by the “Initial charge” series. SOC at the time of departure is represented by the “To be charged” series.

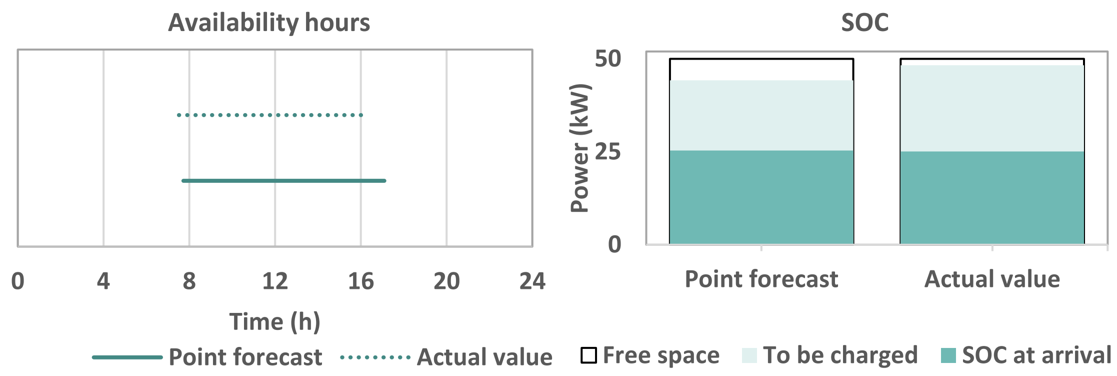

Figure A.4 - Point forecasts and actual values of availability hours and SOC requisites of one vehicle.

A.3. Buildings data

There are 39 buildings in this microgrid and their connection points with the electricity, gas, and district heating networks are presented in Table A.8. All the data described in here is static.

Table A.8. The buildings connected to the HPs and district heating flexible loads are characterized by a β of 0.97 and a R of 0.081 °C/kWh. The comfort range of the users θ^E was set to [19, 23] °C between 7h to 18h, and [16, 26] °C for the rest of the day. All the data described in here is static.

Table A.8 - Buildings connections with electricity, gas and district heating networks.

Building number	Network connection		
	Electricity	Gas	District heating
1	4	32	9
2	10	2	2
3	14	34	4
4	5	-	-
5	7	8	-
6	1	32	6
7	14	34	16
8	12	-	27
9	14	-	15
10	5	11	-
11	6	14	26
12	14	-	-
13	11	2	2
14	14	-	-
15	1	32	5
16	17	-	8
17	13	3	-
18	-	-	-
19	18	35	3
20	12	36	1
21	9	13	24
22	19	10	-
23	16	-	-
24	-	-	-
25	1	32	5
26	12	0	0
27	12	0	0
28	8	6	-
29	9	19	10
30	8	7	-
31	-	12	-
32	4	19	22
33	-	-	-
34	20	4	-
35	18	1	3
36	1	32	7
37	-	-	-
38	3	5	-
39	2	9	-

A.4. Market data

The electricity, natural gas, green hydrogen, and carbon market information is presented in the following subsections.

A.4.1. Electricity market

The electricity market data is divided by type of markets including the energy, secondary and tertiary markets. All electricity prices and reserve activation ratios were calculated using the gradient boosting algorithm [180] through the python package “scikit-learn” [181].

The electricity energy market data includes forecasts and actual values of energy price λ_t^E, and negative $\lambda_t^{E,-}$and positive imbalances $\lambda_t^{E,+}$, as illustrated in Figure A.5. This information was sourced from references [182][183]. During the DA stage, the aggregator forecasts energy prices, while during the RT stage the aggregator forecasts imbalance prices. The settlement phase uses actual values of energy prices and negative and positive imbalances.

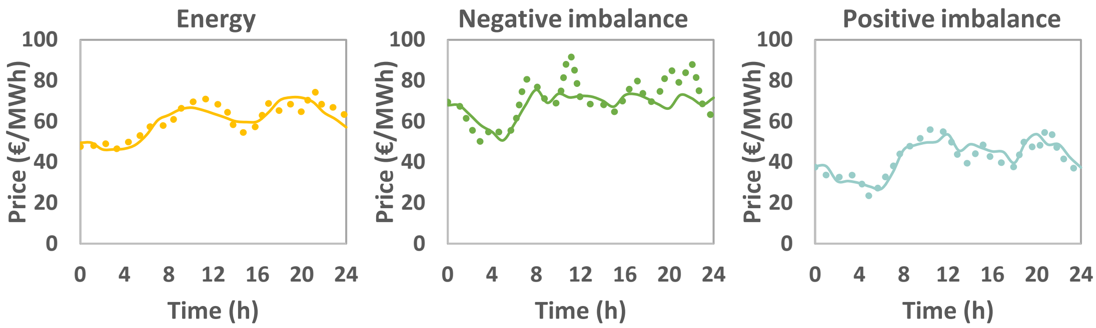

Figure A.5 – Energy market data forecasts (continuous line) and actual values (dashed line).

The electricity secondary market data includes forecasts and actual values of secondary reserve prices λ_t^B (for offering band), ratios of upward ϕ_t^U and downward ϕ_t^D mobilizations, and financial penalties for band not supplied $\lambda_t^{B,-}$[182][183], as illustrated in Figure A.6. It also considers band utilization prices which are represented by the tertiary reserve prices. During the DA stage, the aggregator forecasts the secondary reserve price and the mobilization ratios. During the RT stage, the aggregator updates the forecasts of the mobilization ratios. The settlement phase uses actual values of the secondary reserve band and mobilization ratios. The Portuguese TSO sets the penalty for band not supplied equal to $1.5\lambda_t^B$.

During the RT stage, the secondary band sold in the DA market is dispatched according to the AGC signal sent by the TSO. Figure A.7 presents the AGC signal used in this work with time-steps of 20s and normalized between -1 (upward) and 1 (downward). Positive values represent the activation of the downward reserve band while negative values represent the activation of the upward reserves band.

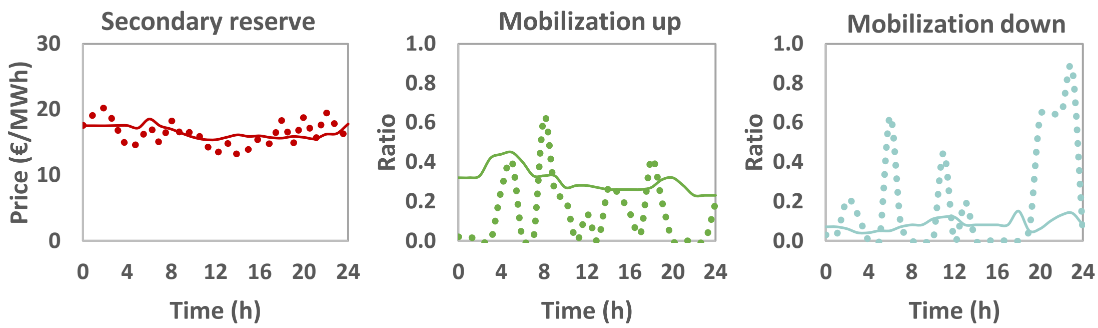

Figure A.6 – Secondary market data forecasts (continuous line) and actual values (dashed line).

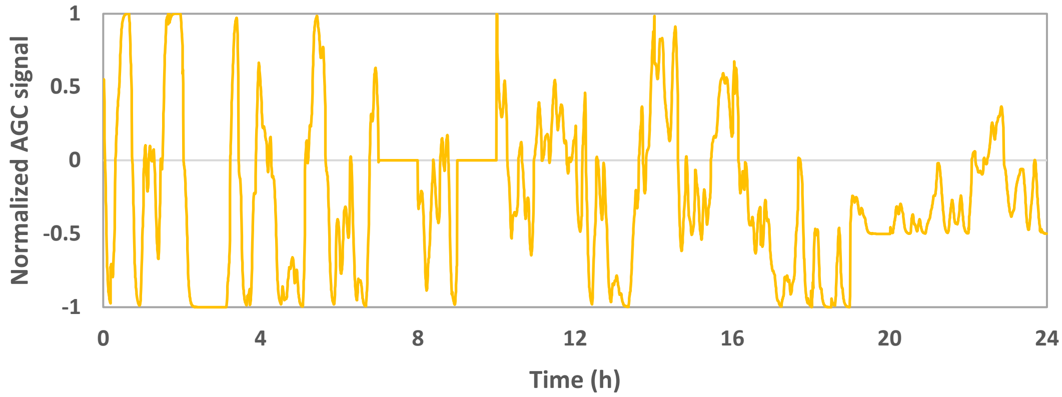

Figure A.7 - Normalized AGC signal.

The electricity tertiary market data includes forecasts of upward $\lambda_t^{U,E}$ and downward $\lambda_t^{D,E}$ tertiary reserve prices as illustrated in Figure A.8 [182][183]. During the DA stage the aggregator forecasts the tertiary reserve prices while during the RT stage it updates those values. The settlement phase uses actual values of tertiary reserve prices.

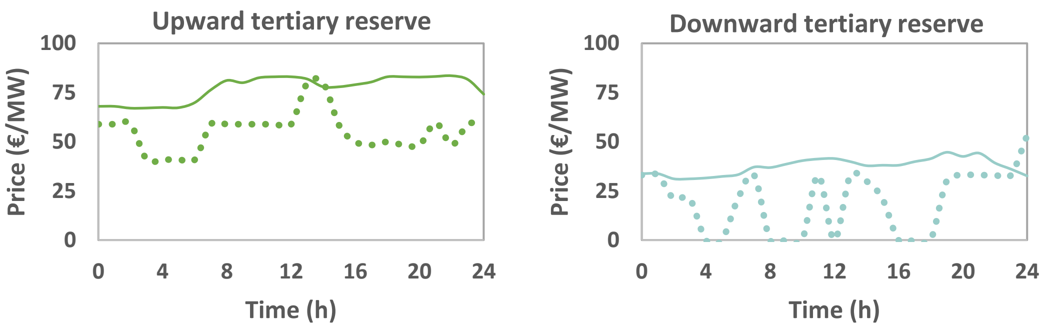

Figure A.8 – Tertiary market data forecasts (continuous line) and actual values (dashed line).

A.4.2. Natural gas and green hydrogen markets

The gas market data includes forecasts of gas price λ_t^{G} (22.96 €/MWh), used during the DA phase, and gas imbalance prices $\lambda_t^{G,-}$ (22.26€/MWh for both directions) [184], used during the RT phase.

The green hydrogen market data includes forecasts of green hydrogen prices $\lambda_t^{H_2}$ (76 €/MWh), used during the DA phase, and green hydrogen imbalance prices $\lambda_t^{H_2,-}$ (73 €/MWh for both direction), used during the RT phase.

The price of water $\lambda_t^{H_2O}$was set to 3.76 €/L, and the price of oxygen $f_t^{O_2}$ was set to 0.15 €/kg. The price of GOs λ_t^{GO} was set to 0.5 €/MWh. These values are static for both the DA and RT phases.

A.4.3. EU ETS market participation

Concerning the participation in the EU ETS market, the aggregator modeled in this work would not qualify to participate in this market as it does not surpass 2500 tonnes of CO_2 emissions in a year. Nonetheless, the model developed here can be applied to aggregators that qualify for it. It was assumed that the aggregator participates together with other entities when buying CO_2 emissions allowances. This allows the aggregator to decrease its market participation costs.

The resources that mandate the participation in the EU ETS market are the CHPs, as they are resources that produce electricity and heat from fuels. In this case, the emissions have to be separated into one part for heat and one part for electricity. As previously explained, electricity generation does not qualify for free allowances but heat generation for district heating does. The free emissions allowances available to the aggregator in this work for the year in study were calculated according to formula (99) [185].

$$FA^{CO_2,year} = HBM \times HAL \times NCL \times CSCF \tag{A.1}$$

HBM is the heat benchmark, which is 62.3 allowances/TJ [162] for heat; HAL is the historical activity level; NCL is the carbon leakage factor which in the case of district heating is 0.3 and CSCF is the cross sector correction factor which is 1 in this case. The total amount of free allowances calculated for the year is 260. Then, considering historical data on heat consumption, the total amount of free allowances was distributed through each day of the year. The value FA^{CO_2} calculated for the day used in this work is 2.8 allowances.

The carbon market also includes the price of CO_2 emission allowances λ^{CO_2} (25 €/tCO_2), and the conversion factor $\alpha^{CO_2,G}$ (0.2).

A.5. Weather and inflexible load data

All the data presented in this subsection is variable data in the form of point forecast and actual values. The point forecasts are used in the DA stage, while the actual values are used in the RT phase. The PV generation $\overline{P^{PV}}$, outside temperature θ^O, and inflexible load (electricity $P^{IL,E}$, gas $P^{IL,G}$, heat $P^{IL,H}$, and hydrogen P^{IL,H_2}) point forecasts and actual values are presented in Figure A.9 and Figure A.10. The point forecasts were computed by the gradient boosting algorithm [180] from the python package "scikit-learn" [181]. The gradient boosting algorithm uses hourly measurements of PV generation and outside temperature from 2 years (2017 and 2018) as inputs for the model to forecast PV generation and outside temperature, respectively. This data and the actual values were collected from the MeteoGalicia website [186]. The input data to forecast the inflexible loads include hourly measurements of the inflexible load collected from the University of Manchester microgrid for a period of 1 year. The actual inflexible loads were also collected from the University Manchester microgrid for the period of 1 day.

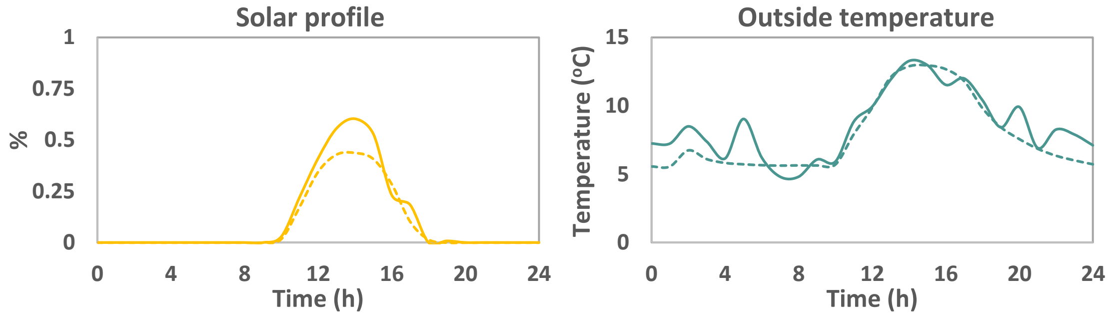

Figure A.9 – Solar profile and outside temperature forecasts (continuous line) and actual values (dashed lines).

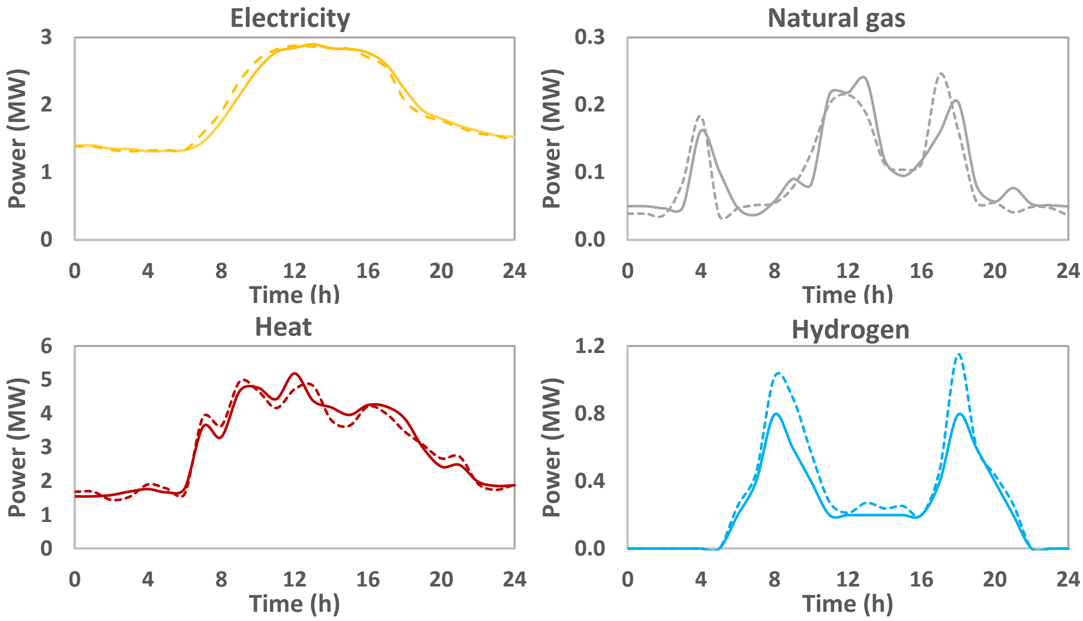

Figure A.10 – Electricity, natural gas, heat, and hydrogen inflexible loads forecasts (continuous line) and actual values (dashed line).

A.6. Carbon emissions

The CO2 emissions associated with the electricity consumed from the network are presented in Figure A.11. These emissions are based on the Portuguese electricity system.

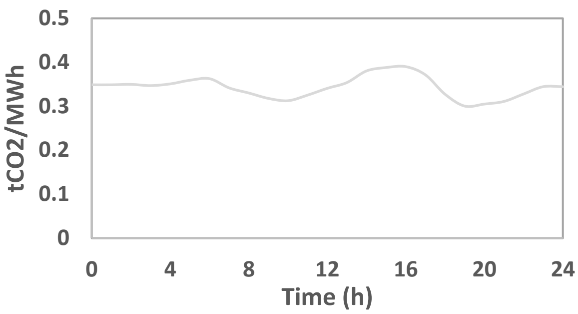

Figure A.11 – CO_2 emissions associated with the electricity consumed from the network.

Bibliography

[1] European Commission, “Communication from the Commission to the European Parliament, the Council, the European Economic and Social Committee and the Committee of the Regions,” 2020.

[2] “Directive 2009/28/EC of the European Parliament and of the Council,” no. 1, Accessed: Nov. 10, 2017. [Online]. Available: http://eur-lex.europa.eu/legal-content/EN/TXT/PDF/?uri=CELEX:32009L0028&from=EN.

[3] European Parliament, “Directive (EU) 2018/2001,” *Off. J. Eur. Union*, 2018.

[4] European Commission, “Directive of the European Parliament and of the Council amending Directive (EU) 2018/2001.”

[5] European Commission, “Renewable energy targets.” https://energy.ec.europa.eu/topics/renewable-energy/renewable-energy-directive-targets-and-rules/renewable-energy-targets_en (accessed Nov. 08, 2022).

[6] European Commission, “Directive of the European Parlinment and of the council on energy efficiency (recast),” 2021, Accessed: Nov. 07, 2022. [Online]. Available: https://www.consilium.europa.eu/media/47296/1011-12-20-euco-conclusions-en.pdf.

[7] European Commission, “REPowerEU: affordable, secure and sustainable energy for Europe.” https://ec.europa.eu/info/strategy/priorities-2019-2024/european-green-deal/repowereu-affordable-secure-and-sustainable-energy-europe_en#relatedlinks (accessed Nov. 07, 2022).

[8] European Commission, “Powering a climate-neutral economy: An EU Strategy for Energy System Integration,” 2020, Accessed: Nov. 08, 2022. [Online]. Available: https://ec.europa.eu/energy/topics/energy-strategy/clean-energy-all-europeans_en.

[9] European Comission, “EU ETS Handbook,” 2015.

[10] European Commission, “EU strategy on energy system integration.” https://energy.ec.europa.eu/topics/energy-systems-integration/eu-strategy-energy-system-integration_en (accessed Nov. 08, 2022).

[11] European Commission, “Markets and consumers.” https://energy.ec.europa.eu/topics/markets-and-consumers_en (accessed Nov. 08, 2022).

[12] European Commission, “Research and technology.” https://energy.ec.europa.eu/topics/research-and-technology_en (accessed Nov. 08, 2022).

[13] European Parliament, “Directive 2012/27/EU of the European Parliament and of the Council on energy efficiency,” *Official Journal of the European Union Directive*, 2012. .

[14] M. O ’malley *et al.*, “Energy Systems Integration: Defining and Describing the Value Proposition,” 2016. doi: 10.2172/1257674.

[15] IEA 2022, "Demand response availability at times of highest flexibility needs and share in total flexibility provision in the Net Zero Scenario, 2020 and 2030 – Charts – Data & Statistics - IEA," *License: CC BY 4.0*. https://www.iea.org/data-and-statistics/charts/demand-response-availability-at-times-of-highest-flexibility-needs-and-share-in-total-flexibility-provision-in-the-net-zero-scenario-2020-and-2030 (accessed Nov. 10, 2022).

[16] IEA, "Demand Response." https://www.iea.org/reports/demand-response (accessed Nov. 10, 2022).

[17] J. P. B. Iria, "Optimal participation of an aggregator of prosumers in the electricity markets," PhD thesis, Faculty of Engineering of the University of Porto, 2019.

[18] Ricardo Bessa, "Methodologies for the Participation of an Electric Vehicles' Aggregator in the Electricity Markets," PhD thesis, Faculty of Engineering of the University of Porto, 2013.

[19] E. SPOT *et al.*, "EUPHEMIA Public Description - PCR Market Coupling Algorithm," Price Coupling of Regions (PCR), 2016.

[20] L. H. Lam, V. Ilea, and C. Bovo, "European day-ahead electricity market coupling: Discussion, modeling, and case study," *Electr. Power Syst. Res.*, vol. 155, pp. 80–92, Feb. 2018, doi: 10.1016/j.epsr.2017.10.003.

[21] A. Pillay, S. Prabhakar Karthikeyan, and D. P. Kothari, "Congestion management in power systems - A review," *Int. J. Electr. Power Energy Syst.*, vol. 70, pp. 83–90, Sep. 2015, doi: 10.1016/j.ijepes.2015.01.022.

[22] Nominated Electricity Market Operator, "NEMOs: Nominated Electricity Market Operators." https://www.nemo-committee.eu/index (accessed Apr. 20, 2022).

[23] A. GmbH, "Cross-Border Intraday (XBID) Project." https://www.amprion.net/Energy-Market/Congestion-Management/Multi-Regional-Coupling-(MRC)-and-Cross-Border-Intraday-(XBID)/Content-Page.html (accessed Jun. 07, 2022).

[24] N. Committee, "Single Intraday Coupling (SIDC)." https://www.nemo-committee.eu/sidc (accessed Jun. 07, 2022).

[25] European Network of Transmission System Operators for Electricity (ENTSO-E), "P1-Policy 1: Load-Frequency Control and Performance [C]," 2009.

[26] European Comission, "Commission Regulation (EU) 2017/1485," *Official Journal of the European Union*, 2017. .

[27] European Network of Transmission System Operators for Electricity (ENTSO-E), "Survey on Ancillary Services Procurement & Balancing market design," 2012.

[28] Entidade Reguladora dos Serviços Energéticos (ERSE), "Manual of procedures for the management of the power system [in Portuguese]," 2020.

[29] M. Rammerstorfer and C. Wagner, "Reforming minute reserve policy in Germany: A step towards efficient markets?," *Energy Policy*, vol. 37, no. 9, pp. 3513–3519, Sep. 2009, doi: 10.1016/J.ENPOL.2009.03.056.

[30] A. Mohammed AL-SAADI, N. Pinho da Silva, R. Pastor, Y. Coa, and G. Luis, "D4.1 –TSO balancing markets requirements for EC flexibility services WP4," Power Flexible Communities (Flexunity), 2020.

[31] European Commission, "Commission Regulation (EU) 2017/2195," 2017. Accessed: Jun. 07, 2022. [Online]. Available: https://eur-lex.europa.eu/legal-

content/EN/TXT/?uri=uriserv:OJ.L_.2017.312.01.0006.01.ENG&toc=OJ:L:2017:312:TOC#d1e2081-6-1.

[32] ETNSO-E, “TERRE.” https://www.entsoe.eu/network_codes/eb/terre/ (accessed Jun. 07, 2022).

[33] ETNSO-E, “Manually Activated Reserves Initiative.” https://www.entsoe.eu/network_codes/eb/mari/ (accessed Jun. 07, 2022).

[34] ETNSO-E, “PICASSO.” https://www.entsoe.eu/network_codes/eb/picasso/ (accessed Jun. 07, 2022).

[35] ETNSO-E, “IGCC Merger.” https://www.entsoe.eu/network_codes/eb/imbalance-netting/ (accessed Jun. 07, 2022).

[36] Federal Energy Regulatory Commission (FERC), “Electric Power Markets.” https://www.ferc.gov/electric-power-markets (accessed May 02, 2022).

[37] E. Ela, M. Milligan, A. Bloom, A. Botterud, A. Townsend, and T. Levin, “Evolution of Wholesale Electricity Market Design with Increasing Levels of Renewable Generation,” no. September, pp. 1–139, 2014, doi: 10.1007/978-0-387-78171-6.

[38] Q. Wang, C. Zhang, Y. Ding, G. Xydis, J. Wang, and J. Østergaard, “Review of real-time electricity markets for integrating Distributed Energy Resources and Demand Response,” *Appl. Energy*, vol. 138, pp. 695–706, Jan. 2015, doi: 10.1016/J.APENERGY.2014.10.048.

[39] A. Botterud, J. Wang, V. Miranda, and R. J. Bessa, “Wind Power Forecasting in U.S. Electricity Markets,” *Electr. J.*, vol. 23, no. 3, pp. 71–82, Apr. 2010, doi: 10.1016/J.TEJ.2010.03.006.

[40] P. González, J. Villar, C. A. Díaz, and F. A. Campos, “Joint energy and reserve markets: Current implementations and modeling trends,” *Electr. Power Syst. Res.*, vol. 109, pp. 101–111, Apr. 2014, doi: 10.1016/J.EPSR.2013.12.013.

[41] Zhi Zhou, Todd Levin, and G. Conzelmann, “Survey of U.S. Ancillary Services Markets Energy Systems Division,” Argonne, IL (United States), 2016.

[42] A. Sadeghi-Mobarakeh and H. Mohsenian-Rad, “Performance Accuracy Scores in CAISO and MISO Regulation Markets: A Comparison Based on Real Data and Mathematical Analysis,” *IEEE Trans. Power Syst.*, vol. 33, no. 3, pp. 3196–3198, May 2018, doi: 10.1109/TPWRS.2018.2816808.

[43] Australian Energy Market Operator (AEMO), “Guide to Ancillary Services in the National Electricity Market,” 2015.

[44] J. Riesz, J. Gilmore, and I. MacGill, “Frequency Control Ancillary Service Market Design: Insights from the Australian National Electricity Market,” *Electr. J.*, vol. 28, no. 3, pp. 86–99, Apr. 2015, doi: 10.1016/J.TEJ.2015.03.006.

[45] J. Iria, P. Scott, A. Attarha, D. Gordon, and E. Franklin, “MV-LV network-secure bidding optimisation of an aggregator of prosumers in real-time energy and reserve markets,” *Energy*, vol. 242, p. 122962, Mar. 2022, doi: 10.1016/J.ENERGY.2021.122962.

[46] F. M. Dikko, “A Study of The Natural Gas Market:’Price Forecast & Measuring Residential Demand’,” PhD Thesis, Faculty of Arts and Social Sciences School of Economics, University of Surrey, 2019.

[47] Keuring van Elektrotechnische Materialen te Arnhem (KEMA) Det Norske Veritas (DNV) and COWI Belgium, “Study on Entry-Exit Regimes in Gas Part A: Implementation of Entry-Exit Systems,” 2013.

[48] European Union Agency for the Cooperation of Energy Regulators (ACER) and Council of European Energy Regulators (CEER), "ACER/CEER Annual Report on the Results of Monitoring the Internal Electricity and Natural Gas Markets in 2020 - Gas Wholesale Markets Volume," 2021.

[49] European Commission, "Third energy package," 2009. https://energy.ec.europa.eu/topics/markets-and-consumers/market-legislation/third-energy-package_en (accessed Apr. 21, 2022).

[50] European Commission, "Clean energy for all Europeans," *Publ. Off. Eur. Union*, 2019, doi: 10.2833/21366.

[51] P. Pozsgai, "Fundamentals of the gas market." Energy Community Secretariat, Accessed: Apr. 22, 2022. [Online]. Available: https://www.energy-community.org/dam/jcr:962ed137-070b-4740-9df3-f80fdea731bd/ECRBREG102018_ECS.pdf.

[52] European Parliament, "Regulation (EC) No 715/2009," *Off. J. Eur. Union*, 2009.

[53] Patrick Heather, "European Traded Gas Hubs: German hubs about to merge," The Oxford Institute for Energy Studies, Oxford, 2021.

[54] Appygas, "appygas | European Gas Market Data Platform | Germany." https://www.appygas.com/ (accessed Apr. 22, 2022).

[55] B. Hiller, T. Koch, L. Schewe, R. Schwarz, and J. Schweiger, "A system to evaluate gas network capacities: Concepts and implementation," *Eur. J. Oper. Res.*, vol. 270, no. 3, pp. 797–808, Nov. 2018, doi: 10.1016/J.EJOR.2018.02.035.

[56] Mercado Ibérico del Gas (MIBGAS), "Rules of the Organized Gas Market (in Portuguese)," Madrid, Spain, 2018.

[57] European Network of Transmission System Operators for Gas (ENTSO-G), "Capacity Allocation Mechanisms Network Code and Guidelines for Congestion Management Procedures," Brussels, Belgium, 2017.

[58] European Commission, "Commission Regulation (EU) No 984/2013," *Off. J. Eur. Union*, 2013.

[59] Mercado Ibérico del Gas (MIBGAS), "MIBGAS Spot | MIBGAS - Iberian Gas Market." https://www.mibgas.es/en/mainmenu/mibgas-spot?menu=1&parent=8#10 (accessed Apr. 22, 2022).

[60] Mercado Ibérico del Gas (MIBGAS), "Rules on the Organized Gas Market," Madrid, Spain, 2018.

[61] Mercado Ibérico del Gas (MIBGAS), "Annex II. Specific Rules On MIBGAS Derivatives Spot," Madrid, Spain, 2022.

[62] Mercado Ibérico del Gas (MIBGAS), "MIBGAS Derivatives Rules," Madrid, Spain, 2022.

[63] Entidade Reguladora dos Serviços Energéticos (ERSE), "Manual of procedures for the access to natural gas infrastructures [in Portuguese]," Lisbon, Portugal, 2017.

[64] Steven Levine, P. Carpenter, and A. Thapa, "Understanding Natural Gas Markets," American Petroleum Institute, 2014.

[65] L. Marks, C. F. Mason, K. Mohlin, and M. Zaragoza-Watkins, "Vertical Market Power in Interconnected Natural Gas and Electricity Markets," *Work. Pap.*, 2017.

[66] Federal Energy Regulatory Commission (FERC), "Order No. 636 - Restructuring of Pipeline Services," 1992. .

[67] M. J. Doane and D. F. Spulber, “Open Access and the Evolution of the U. S. Spot Market for Natural Gas,” *J. Law Econ.*, vol. 37, no. 2, pp. 477–517, Oct. 1994, doi: 10.1086/467321.

[68] A. F. Correljé, “Markets for Natural Gas,” *Encycl. Energy*, pp. 799–808, 2004, doi: 10.1016/B0-12-176480-X/00137-6.

[69] A. Juris, “Development of Competitive Natural Gas Markets in the United States,” *World Bank Gr. - Financ. Priv. Sect. Infrastruct.*, 1998.

[70] International Carbon Action Partnership (ICAP), “Emissions Trading Worlwide - Status Report 2021,” Berlin, Germany, 2021.

[71] California Air Resources Board, “Cap-and-Trade Regulation (Unofficial Electronic Version),” 2019. .

[72] Environmental Defense Fund (EDF) and International Emissions Trading Association (IETA), “California: An Emissions Trading Case Study,” 2018.

[73] Environmental Defense Fund (EDF), Motu Economic and Public Policy Research, and International Emissions Trading Association (IETA), “New Zealand The World’s Carbon Markets: A Case Study Guide for Practitioners,” 2016.

[74] Parliament of New Zealand, “Climate Change Response (Emissions Trading Reform) Amendment Act,” 2019.

[75] European Commission, “A hydrogen strategy for a climate-neutral Europe,” 2020, Accessed: Nov. 08, 2022. [Online]. Available: https://www.eu2018.at/calendar-events/political-events/BMNT-.

[76] European Union, “Key actions of the EU Hydrogen Strategy.” https://energy.ec.europa.eu/topics/energy-systems-integration/hydrogen/key-actions-eu-hydrogen-strategy_en (accessed Nov. 04, 2022).

[77] European Commission, “Regulation of the European Parliament and of the Council on the internal markets for renewable and natural gases and for hydrogen,” 2021.

[78] European Parliament, “Directive 2009/28/EC,” *Off. J. Eur. Union*, 2009.

[79] Australian Government Clean Energy Regulator, “Guarantee of Origin.” http://www.cleanenergyregulator.gov.au/Infohub/Markets/guarantee-of-origin (accessed Apr. 28, 2022).

[80] European Commission, “Communication from the Commission to the European Parliament, the Council, the European Economic and Social Committee and the Committee of the Regions: A hydrogen strategy for a climate-neutral Europe,” Brussels, 2020.

[81] Alberto Pototschnig and European University Institute, “Renewable hydrogen and the ‘additionality’ requirement: why making it more complex than is needed?,” 2021.

[82] H. Gerard, E. I. Rivero Puente, and D. Six, “Coordination between transmission and distribution system operators in the electricity sector: A conceptual framework,” *Util. Policy*, vol. 50, pp. 40–48, Feb. 2018, doi: 10.1016/j.jup.2017.09.011.

[83] M. Grzanic, T. Capuder, H. Pandzic, M. Beus, I. Pavic, and M. Miletic, “D2.4 deliverable - TSO/DSO coordination mechanisms,” Advanced Tools Towards cost-efficient decarbonisation of future reliable Energy SysTems (ATTEST) project, 2020.

[84] R. Silva, E. Alves, R. Ferreira, J. Villar, and C. Gouveia, “Characterization of TSO and DSO grid system services and TSO-DSO basic coordination mechanisms in the current

decarbonization context," *Energies*, vol. 14, no. 15, Aug. 2021, doi: 10.3390/EN14154451.

[85] European Parliament, "Directive (EU) 2019/944," *Off. J. Eur. Union*, 2019.

[86] M. Yazdani-Damavandi, N. Neyestani, M. Shafie-khah, J. Contreras, and J. P. S. Catalao, "Strategic Behavior of Multi-Energy Players in Electricity Markets as Aggregators of Demand Side Resources Using a Bi-Level Approach," *IEEE Trans. Power Syst.*, vol. 33, no. 1, pp. 397–411, Jan. 2018, doi: 10.1109/TPWRS.2017.2688344.

[87] M. Yazdani-Damavandi, N. Neyestani, G. Chicco, M. Shafie-Khah, and J. P. S. Catalão, "Aggregation of Distributed Energy Resources under the Concept of Multienergy Players in Local Energy Systems," *IEEE Trans. Sustain. Energy*, vol. 8, no. 4, pp. 1679–1693, 2017, doi: 10.1109/TSTE.2017.2701836.

[88] N. Neyestani, M. Yazdani-Damavandi, M. Shafie-khah, G. Chicco, and J. P. S. Catalao, "Stochastic Modeling of Multi-Energy Carrier Dependencies in Smart Local Networks with Distributed Energy Resources," *IEEE Trans. Smart Grid*, vol. 6, no. 4, pp. 1748–1762, 2015, doi: 10.1109/TSG.2015.2423552.

[89] M. Aghamohamadi and A. Mahmoudi, "From bidding strategy in smart grid toward integrated bidding strategy in smart multi-energy systems, an adaptive robust solution approach," *Energy*, vol. 183, pp. 75–91, Sep. 2019, doi: 10.1016/J.ENERGY.2019.06.106.

[90] P. Xiao, W. Hu, X. Xu, W. Liu, Q. Huang, and Z. Chen, "Optimal operation of a wind-electrolytic hydrogen storage system in the electricity/hydrogen markets," *Int. J. Hydrogen Energy*, vol. 45, no. 46, pp. 24412–24423, Sep. 2020, doi: 10.1016/J.IJHYDENE.2020.06.302.

[91] European Parliament, "Regulation (EU) 2019/943," *Off. J. Eur. Union*, 2019.

[92] D. Kathan, K. Herzfeld, R. Glick, and J. P. Danly, "Participation of Distributed Energy Resource Aggregations in Markets Operated by Regional Transmission Organizations and Independent System Operators," Federal Energy Regulatory Commission (FERC), Washington, DC, USA, 2020.

[93] Australian Energy Market Operator (AEMO), "Small Generation Aggregators in the NEM," 2021.

[94] Australian Energy Market Commission (AEMC), "National Electricity Amendment (Demand Response Mechanism and Ancillary Services Unbundling) Rule 2016," Sydney, Australia, 2016.

[95] Australian Energy Market Commission (AEMC), "National Electricity Amendment (Wholesale Demand Response Mechanism) Rule 2020," Sydney, Australia, 2020.

[96] Australian Energy Market Commission (AEMC), "National Electricity Amendment (Integrating Energy Storage Systems into the NEM) Rule 2021," Sydney, Australia, 2021.

[97] K. Power, "The Global Virtual Power Plant Solution." https://www.kiwipowered.com/ (accessed Apr. 06, 2022).

[98] Enel X, "Technologies and Innovation for Smart Energy Solutions." https://www.enelx.com/n-a/en (accessed Apr. 06, 2022).

[99] R. Belhomme *et al.*, "Address - Active demand for the smart grids of the future," *IET Semin. Dig.*, vol. 2008, no. 12380, 2008, doi: 10.1049/IC:20080438.

[100] A. Agnetis, G. De Pascale, P. Detti, and A. Vicino, "Load scheduling for household energy consumption optimization," *IEEE Trans. Smart Grid*, vol. 4, no. 4, pp. 2364–2373, Dec.

2013, doi: 10.1109/TSG.2013.2254506.

[101] J. Iria, F. Soares, and M. Matos, "Optimal bidding strategy for an aggregator of prosumers in energy and secondary reserve markets," *Appl. Energy*, vol. 238, pp. 1361–1372, Mar. 2019, doi: 10.1016/J.APENERGY.2019.01.191.

[102] J. P. Iria, F. J. Soares, and M. A. Matos, "Trading Small Prosumers Flexibility in the Energy and Tertiary Reserve Markets," *IEEE Trans. Smart Grid*, pp. 1–1, 2018, doi: 10.1109/TSG.2018.2797001.

[103] E. Vrettos, F. Oldewurtel, and G. Andersson, "Robust Energy-Constrained Frequency Reserves from Aggregations of Commercial Buildings," *IEEE Trans. Power Syst.*, vol. 31, no. 6, pp. 4272–4285, Nov. 2016, doi: 10.1109/TPWRS.2015.2511541.

[104] J. Stede, K. Arnold, C. Dufter, G. Holtz, S. von Roon, and J. C. Richstein, "The role of aggregators in facilitating industrial demand response: Evidence from Germany," *Energy Policy*, vol. 147, p. 111893, Dec. 2020, doi: 10.1016/J.ENPOL.2020.111893.

[105] E. Vrettos and G. Andersson, "Scheduling and Provision of Secondary Frequency Reserves by Aggregations of Commercial Buildings," *IEEE Trans. Sustain. Energy*, vol. 7, no. 2, pp. 850–864, Apr. 2016, doi: 10.1109/TSTE.2015.2497407.

[106] A. Hellmers, M. Zugno, A. Skajaa, and J. M. Morales, "Operational Strategies for a Portfolio of Wind Farms and CHP Plants in a Two-Price Balancing Market," *IEEE Trans. Power Syst.*, vol. 31, no. 3, pp. 2182–2191, May 2016, doi: 10.1109/TPWRS.2015.2439060.

[107] A. Attarha, P. Scott, and S. Thiébaux, "Network-aware co-optimisation of residential DER in energy and FCAS markets," *Electr. Power Syst. Res.*, vol. 189, p. 106730, Dec. 2020, doi: 10.1016/j.epsr.2020.106730.

[108] R. J. Bessa and M. A. Matos, "Global against divided optimization for the participation of an EV aggregator in the day-ahead electricity market. Part I: Theory," *Electr. Power Syst. Res.*, vol. 95, pp. 309–318, Feb. 2013, doi: 10.1016/J.EPSR.2012.08.007.

[109] R. J. Bessa and M. A. Matos, "Global against divided optimization for the participation of an EV aggregator in the day-ahead electricity market. Part II: Numerical analysis," *Electr. Power Syst. Res.*, vol. 95, pp. 309–318, Feb. 2013, doi: 10.1016/J.EPSR.2012.08.013.

[110] Z. Ma, J. Eichman, and J. Kurtz, "Fuel Cell Backup Power Unit Configuration and Electricity Market Participation: A Feasibility Study," National Renewable Energy Laboratory (NREL), Denver, CO, USA, 2017.

[111] J. Iria and F. Soares, "Real-time provision of multiple electricity market products by an aggregator of prosumers," *Appl. Energy*, vol. 255, p. 113792, Dec. 2019, doi: 10.1016/j.apenergy.2019.113792.

[112] Y. Zhou, C. Wang, J. Wu, J. Wang, M. Cheng, and G. Li, "Optimal scheduling of aggregated thermostatically controlled loads with renewable generation in the intraday electricity market," *Appl. Energy*, vol. 188, pp. 456–465, Feb. 2017, doi: 10.1016/J.APENERGY.2016.12.008.

[113] H. Mohsenian-Rad, "Optimal Demand Bidding for Time-Shiftable Loads," *IEEE Trans. Power Syst.*, vol. 30, no. 2, pp. 939–951, Mar. 2015, doi: 10.1109/TPWRS.2014.2338735.

[114] M. Beaudin and H. Zareipour, "Home energy management systems: A review of modelling and complexity," *Renew. Sustain. Energy Rev.*, vol. 45, pp. 318–335, May 2015, doi: 10.1016/J.RSER.2015.01.046.

[115] D. Lee and C. C. Cheng, "Energy savings by energy management systems: A review,"

Renew. Sustain. Energy Rev., vol. 56, pp. 760–777, Apr. 2016, doi: 10.1016/J.RSER.2015.11.067.

[116] EDP, “Re:dy.” https://www.edp.com/en/innovation/redy (accessed Apr. 06, 2022).

[117] IBM, “Telemetry use case: Home energy monitoring and control - IBM Documentation.” https://www.ibm.com/docs/en/ibm-mq/8.0?topic=cases-telemetry-use-case-home-energy-monitoring-control (accessed Apr. 06, 2022).

[118] Samsung, “Samsung SmartThings Energy.” https://www.samsung.com/uk/smartenergy/ (accessed Apr. 06, 2022).

[119] X. He, N. Keyaerts, I. Azevedo, L. Meeus, L. Hancher, and J. M. Glachant, “How to engage consumers in demand response: A contract perspective,” *Util. Policy*, vol. 27, pp. 108–122, Dec. 2013, doi: 10.1016/J.JUP.2013.10.001.

[120] United States (US) Department of Energy, “Benefits of Demand Response in Electricity Markets and Recommendations for Achieving Them. A report to the United States Congress Pursuant to Section 1252 of the Energy Policy Act of 2005,” 2006.

[121] R. Carmichael, R. Gross, R. Hanna, A. Rhodes, and T. Green, “The Demand Response Technology Cluster: Accelerating UK residential consumer engagement with time-of-use tariffs, electric vehicles and smart meters via digital comparison tools,” *Renew. Sustain. Energy Rev.*, vol. 139, p. 110701, Apr. 2021, doi: 10.1016/J.RSER.2020.110701.

[122] International Renewable Energy Agency (IRENA), “Enabling Technologies: Innovation Landscape,” Abu Dhabi, United Arab Emirates, 2019.

[123] D. Kirli *et al.*, “Smart contracts in energy systems: A systematic review of fundamental approaches and implementations,” *Renew. Sustain. Energy Rev.*, vol. 158, p. 112013, Apr. 2022, doi: 10.1016/J.RSER.2021.112013.

[124] S. Burger, J. P. Chaves-Ávila, C. Batlle, and I. J. Pérez-Arriaga, “A review of the value of aggregators in electricity systems,” *Renew. Sustain. Energy Rev.*, vol. 77, pp. 395–405, Sep. 2017, doi: 10.1016/J.RSER.2017.04.014.

[125] M.-K. Codognet, “The shipper as the architect of contractual relations in access to natural gas networks,” *ISNIE 2004, 8th Annu. Conf.*, 2004.

[126] E. Niesten and F. Alkemade, “How is value created and captured in smart grids? A review of the literature and an analysis of pilot projects,” *Renew. Sustain. Energy Rev.*, vol. 53, pp. 629–638, Jan. 2016, doi: 10.1016/J.RSER.2015.08.069.

[127] C. F. Calvillo, A. Sánchez-Miralles, J. Villar, and F. Martín, “Optimal planning and operation of aggregated distributed energy resources with market participation,” *Appl. Energy*, vol. 182, pp. 340–357, Nov. 2016, doi: 10.1016/J.APENERGY.2016.08.117.

[128] C. Defeuilley, “Retail competition in electricity markets,” *Energy Policy*, vol. 37, no. 2, pp. 377–386, Feb. 2009, doi: 10.1016/J.ENPOL.2008.07.025.

[129] S. Chen, Q. Chen, and Y. Xu, “Strategic Bidding and Compensation Mechanism for a Load Aggregator with Direct Thermostat Control Capabilities,” *IEEE Trans. Smart Grid*, vol. 3053, no. c, pp. 1–10, 2016, doi: 10.1109/TSG.2016.2611611.

[130] M. Heleno, M. A. Matos, and J. A. P. Lopes, “A bottom-up approach to leverage the participation of residential aggregators in reserve services markets,” *Electr. Power Syst. Res.*, vol. 136, pp. 425–433, Jul. 2016, doi: 10.1016/J.EPSR.2016.03.025.

[131] Z. Xu, D. S. Callaway, Z. Hu, and Y. Song, “Hierarchical Coordination of Heterogeneous Flexible Loads,” *IEEE Trans. Power Syst.*, vol. 31, no. 6, pp. 4206–4216, Nov. 2016, doi:

10.1109/TPWRS.2016.2516992.

[132] A. Alahäivälä, J. Corbishley, J. Ekström, J. Jokisalo, and M. Lehtonen, “A control framework for the utilization of heating load flexibility in a day-ahead market,” *Electr. Power Syst. Res.*, vol. 145, pp. 44–54, Apr. 2017, doi: 10.1016/J.EPSR.2016.12.019.

[133] K. Poplavskaya and L. de Vries, “Aggregators today and tomorrow From intermediaries to local orchestrators?,” *Behind Beyond M. Digit. Aggregation, Optim. Monet.*, 2020, doi: 10.1016/B978-0-12-819951-0.00005-0.

[134] X. Lu, K. Li, H. Xu, F. Wang, Z. Zhou, and Y. Zhang, “Fundamentals and business model for resource aggregator of demand response in electricity markets,” *Energy*, vol. 204, p. 117885, Aug. 2020, doi: 10.1016/J.ENERGY.2020.117885.

[135] Dirk-Jan Middelkoop, “CrowdNett: The First Dutch Virtual Power Plant of Aggregated Home Batteries.” Amsterdam, Netherlands, 2017.

[136] Sonnen, “sonnenCommunity.” https://sonnengroup.com/sonnencommunity/ (accessed Apr. 08, 2022).

[137] Fluence, “Energy Storage Global Leader | Fluence - A Siemens and AES Company.” https://fluenceenergy.com/ (accessed Apr. 13, 2022).

[138] Ecotricity, “Ecotricity.” https://www.ecotricity.co.uk/ (accessed Apr. 13, 2022).

[139] E2m, “Aggregation & Energy trading - with e2m.” https://www.e2m.energy/en/ (accessed Apr. 13, 2022).

[140] Enel X, “Technologies and Innovation for Smart Energy Solutions.” https://corporate.enelx.com/en (accessed Apr. 13, 2022).

[141] Flexitricity, “Flexitricity.” https://www.flexitricity.com/ (accessed Apr. 13, 2022).

[142] Sunrun, “#1 Residential Solar Panel Company.” https://www.sunrun.com/ (accessed Apr. 13, 2022).

[143] EnergyAustralia, “Demand Response.” https://www.energyaustralia.com.au/industrial-and-commercial/energy-management/demand-response (accessed Apr. 13, 2022).

[144] R. J. Bessa and M. A. Matos, “Optimization Models for EV Aggregator Participation in a Manual Reserve Market,” *IEEE Trans. Power Syst.*, vol. 28, no. 3, pp. 3085–3095, Aug. 2013, doi: 10.1109/TPWRS.2012.2233222.

[145] R. J. Bessa and M. A. Matos, “Optimization models for an EV aggregator selling secondary reserve in the electricity market,” *Electr. Power Syst. Res.*, vol. 106, pp. 36–50, Jan. 2014, doi: 10.1016/j.epsr.2013.08.006.

[146] J. P. Iria and F. Soares, “A cluster-based optimization approach to support the participation of an aggregator of a larger number of prosumers in the day-ahead energy market,” 2018.

[147] J. P. Iria, F. J. Soares, and M. A. Matos, “Trading small prosumers flexibility in the day-ahead energy market,” *IEEE Power Energy Soc. Gen. Meet.*, vol. 2018-January, pp. 1–5, Jan. 2018, doi: 10.1109/PESGM.2017.8274488.

[148] J. Iria, F. Soares, and M. Matos, “Optimal supply and demand bidding strategy for an aggregator of small prosumers,” *Appl. Energy*, vol. 213, pp. 658–669, Mar. 2018, doi: 10.1016/j.apenergy.2017.09.002.

[149] M. Khojasteh, P. Faria, and Z. Vale, “A robust model for aggregated bidding of energy storages and wind resources in the joint energy and reserve markets,” *Energy*, vol. 238, p. 121735, Jan. 2022, doi: 10.1016/J.ENERGY.2021.121735.

[150] J. Iria, P. Scott, and A. Attarha, “Network-constrained bidding optimization strategy for aggregators of prosumers,” *Energy*, vol. 207, p. 118266, Sep. 2020, doi: 10.1016/j.energy.2020.118266.

[151] J. Naughton, H. Wang, S. Riaz, M. Cantoni, and P. Mancarella, “Optimization of multi-energy virtual power plants for providing multiple market and local network services,” *Electr. Power Syst. Res.*, vol. 189, p. 106775, Dec. 2020, doi: 10.1016/j.epsr.2020.106775.

[152] H. Wang, S. Riaz, and P. Mancarella, “Integrated techno-economic modeling, flexibility analysis, and business case assessment of an urban virtual power plant with multi-market co-optimization,” *Appl. Energy*, vol. 259, p. 114142, Feb. 2020, doi: 10.1016/j.apenergy.2019.114142.

[153] K. Steriotis, K. Smpoukis, N. Efthymiopoulos, G. Tsaousoglou, P. Makris, and E. (Manos) M. Varvarigos, “Strategic and network-aware bidding policy for electric utilities through the optimal orchestration of a virtual and heterogeneous flexibility assets’ portfolio,” *Electr. Power Syst. Res.*, vol. 184, p. 106302, Jul. 2020, doi: 10.1016/j.epsr.2020.106302.

[154] J. Iria, A. Coelho, and F. Soares, “Network-secure bidding strategy for aggregators under uncertainty,” *Sustain. Energy, Grids Networks*, vol. 30, p. 100666, Jun. 2022, doi: 10.1016/J.SEGAN.2022.100666.

[155] L. Bobo, A. Venzke, and S. Chatzivasileiadis, “Second-order cone relaxations of the optimal power flow for active distribution grids: Comparison of methods,” *Int. J. Electr. Power Energy Syst.*, vol. 127, p. 106625, May 2021, doi: 10.1016/J.IJEPES.2020.106625.

[156] J. Iria, M. Heleno, and G. Candoso, “Optimal sizing and placement of energy storage systems and on-load tap changer transformers in distribution networks,” *Appl. Energy*, vol. 250, pp. 1147–1157, Sep. 2019, doi: 10.1016/J.APENERGY.2019.04.120.

[157] L. Luo, Z. Wu, W. Gu, H. Huang, S. Gao, and J. Han, “Coordinated allocation of distributed generation resources and electric vehicle charging stations in distribution systems with vehicle-to-grid interaction,” *Energy*, vol. 192, p. 116631, Feb. 2020, doi: 10.1016/j.energy.2019.116631.

[158] J. Zapata Riveros, R. Donceel, J. Van Engeland, and W. D’Haeseleer, “A new approach for near real-time micro-CHP management in the context of power system imbalances – A case study,” *Energy Convers. Manag.*, vol. 89, pp. 270–280, Jan. 2015, doi: 10.1016/J.ENCONMAN.2014.09.076.

[159] R. R. Appino *et al.*, “Energy-based stochastic MPC for integrated electricity-hydrogen VPP in real-time markets,” *Electr. Power Syst. Res.*, vol. 195, p. 106738, Jun. 2021, doi: 10.1016/J.EPSR.2020.106738.

[160] C. Zhang, Q. Wang, J. Wang, M. Korpås, and M. E. Khodayar, “Strategy-making for a proactive distribution company in the real-time market with demand response,” *Appl. Energy*, vol. 181, pp. 540–548, Nov. 2016, doi: 10.1016/J.APENERGY.2016.08.058.

[161] A. Attarha, P. Scott, J. Iria, and S. Thiébaux, “Network-Secure and Price-Elastic Aggregator Bidding in Energy and Reserve Markets,” *IEEE Trans. Smart Grid*, vol. 12, no. 3, 2021, doi: 10.1109/TSG.2021.3049464.

[162] European Commission, “Commission Delegated Regulation (EU) 2019/331,” *Off. J. Eur. Union*, 2018.

[163] S. Boyd *et al.*, “Distributed Optimization and Statistical Learning via the Alternating Direction Method of Multipliers,” *Found. Trends R Mach. Learn.*, vol. 3, no. 1, pp. 1–122, 2010, doi: 10.1561/2200000016.

[164] M. Maasoumy and A. Sangiovanni-Vincentelli, “Total and Peak Energy Consumption Minimization of Building HVAC Systems Using Model Predictive Control,” *IEEE Des. Test Comput.*, vol. 29, no. 4, pp. 26–35, Aug. 2012, doi: 10.1109/MDT.2012.2200871.

[165] P. Radecki and B. Hencey, “Online Building Thermal Parameter Estimation via Unscented Kalman Filtering,” *2012 Am. Control Conf.*, pp. 3056–3062, 2012, doi: 10.1109/acc.2012.6315699.

[166] W. Energy, “Energy Solutions,” 2020.

[167] M. Baran and F. F. Wu, “Optimal sizing of capacitors placed on a radial distribution system,” *IEEE Trans. Power Deliv.*, vol. 4, no. 1, pp. 735–743, 1989, doi: 10.1109/61.19266.

[168] M. E. Baran and F. F. Wu, “Optimal capacitor placement on radial distribution systems,” *IEEE Trans. Power Deliv.*, vol. 4, no. 1, pp. 725–734, 1989, doi: 10.1109/61.19265.

[169] M. Abeysekera, J. Wu, N. Jenkins, and M. Rees, “Steady state analysis of gas networks with distributed injection of alternative gas,” *Appl. Energy*, vol. 164, pp. 991–1002, Feb. 2016, doi: 10.1016/j.apenergy.2015.05.099.

[170] H. de Vries, A. V. Mokhov, and H. B. Levinsky, “The impact of natural gas/hydrogen mixtures on the performance of end-use equipment: Interchangeability analysis for domestic appliances,” *Appl. Energy*, vol. 208, pp. 1007–1019, Dec. 2017, doi: 10.1016/j.apenergy.2017.09.049.

[171] Carlos M. Correa-Posada and P. Sánchez-Martín, “Gas Network Optimization: A comparison of Piecewise Linear Models,” *Lect. Notes Comput. Vis. Biomech.*, vol. 5, pp. 133–159, 2012, doi: 10.1007/978-94-007-4552-0_6.

[172] X. Liu, J. Wu, N. Jenkins, and A. Bagdanavicius, “Combined analysis of electricity and heat networks,” *Appl. Energy*, vol. 162, pp. 1238–1250, Jan. 2016, doi: 10.1016/J.APENERGY.2015.01.102.

[173] M. Pirouti, “Modelling and analysis of a district heating network,” PhD thesis, School of Engineering, Cardiff University, 2013.

[174] Y. Cao, W. Wei, L. Wu, S. Mei, M. Shahidehpour, and Z. Li, “Decentralized Operation of Interdependent Power Distribution Network and District Heating Network: A Market-Driven Approach,” *IEEE Trans. Smart Grid*, vol. 10, no. 5, pp. 5374–5385, Sep. 2018, doi: 10.1109/TSG.2018.2880909.

[175] E. A. M. Cesena, E. Loukarakis, N. Good, and P. Mancarella, “Integrated Electricity-Heat-Gas Systems: Techno-Economic Modeling, Optimization, and Application to Multienergy Districts,” *Proc. IEEE*, pp. 1–19, Jun. 2020, doi: 10.1109/jproc.2020.2989382.

[176] J. S. Rodriguez, B. Nicholson, C. Laird, and V. M. Zavala, “Benchmarking ADMM in nonconvex NLPs,” *Comput. Chem. Eng.*, vol. 119, pp. 315–325, Nov. 2018, doi: 10.1016/j.compchemeng.2018.08.036.

[177] A. Coelho, J. Iria, and F. Soares, “Network-secure bidding optimization of aggregators of multi-energy systems in electricity, gas, and carbon markets,” *Appl. Energy*, vol. 301, p. 117460, Nov. 2021, doi: 10.1016/J.APENERGY.2021.117460.

[178] “ATTEST - Home.” https://attest-project.eu/ (accessed Nov. 06, 2022).

[179] C. Fu, J. Lin, Y. Song, J. Li, and J. Song, “Optimal Operation of an Integrated Energy System Incorporated with HCNG Distribution Networks,” *IEEE Trans. Sustain. Energy*, vol. 11, no. 4, pp. 2141–2151, Oct. 2020, doi: 10.1109/TSTE.2019.2951701.

[180] T. Hastie, R. Tibshirani, and J. Friedman, *The Elements of Statistical Learning - Data Mining, Inference, and Prediction*. 2009.

[181] F. Pedregosa *et al.*, “Scikit-learn: Machine Learning in Python,” *J. Mach. Learn. Res.*, vol. 12, pp. 2825–2830, 2012, doi: 10.1007/s13398-014-0173-7.2.

[182] ENTSO-E, “Transparency Platform.” https://transparency.entsoe.eu/dashboard/show (accessed Nov. 24, 2020).

[183] REN, “SIMEE - Mercado Diário e Intradiário.” https://www.mercado.ren.pt/PT/Electr/InfoMercado/InfOp/MercOmel/Paginas/default.aspx (accessed Nov. 24, 2020).

[184] M.-M. I. de Gás, “Preços diários da MIBGAS.” https://www.mibgas.es/pt/market-results (accessed Nov. 24, 2020).

[185] European Commission, “General Guidance to the allocation methodology,” 2019.

[186] Meteogalicia, “Datos Históricos das redes de estacións.” https://www.meteogalicia.gal/web/inicio.action.

[187] J. Hu, G. Yang, H. W. Bindner, and Y. Xue, “Application of Network-Constrained Transactive Control to Electric Vehicle Charging for Secure Grid Operation,” *IEEE Trans. Sustain. Energy*, vol. 8, no. 2, pp. 505–515, Apr. 2017, doi: 10.1109/TSTE.2016.2608840.